Auburn University

EVALUATION OF FATIGUE CRACKING IN I-65 MOBILE DELTA CROSSING BRIDGES

Volume III: Floortruss-Girder Connections

Project Number ST 2019-16

by

J. Michael Stallings
Thomas E. Cousins
Scott K. Rutland

sponsored by

The State of Alabama Highway Department
Montgomery, Alabama

Highway Research Center
Harbert Engineering Center
Auburn University, Alabama 36849-5337

November 1993

EVALUATION OF FATIGUE CRACKING IN I-65 MOBILE DELTA CROSSING BRIDGES

Volume III
Floortruss-Girder Connections

by

J. Michael Stallings
Thomas E. Cousins
Scott K. Rutland

sponsored by

The State of Alabama Highway Department
Montgomery, Alabama

November 1993

DISCLAIMER

The contents of this report reflect the views of the authors who are responsible for the facts and accuracy of the data presented herein. The contents do not necessarily reflect the official views or policies of the State of Alabama Highway Department or Auburn University. The report does not constitute a standard, specification, or regulation.

ACKNOWLEDGEMENT

The material contained herein was obtained in connection with a research project, "Evaluation of Fatigue Cracking in I-65 Mobile Delta Crossing Bridges" (ST-2019-16), conducted by the Highway Research Center at Auburn University. The research project was sponsored by the State of Alabama Highway Department. The traffic control, test load vehicles, bridge inspection vehicles and operators were provided by the Alabama Highway Department's Ninth Division and Maintenance Bureau. The interest, cooperation, and assistance of many personnel from the Alabama Highway Department is gratefully acknowledged. The assistance of graduate student Brad Christopher during the instrumentation, field testing, and data reduction phases of the project and for his work on numerous figures that appear within this document is also gratefully acknowledged.

TABLE OF CONTENTS

LIST OF TABLES

LIST OF FIGURES

SUMMARY

In early 1991, fatigue cracks were discovered in the connection plate welds of floortruss-girder connections at five different locations away from piers along the steel plate girder spans of the I-65 Mobile Delta Crossing Bridges. The Alabama Highway Department (AHD) was concerned about the potential for fatigue cracking in the two main plate girder webs of these connections. The AHD was also interested in developing a relatively inexpensive retrofit method for the weld cracks that were identified at floortruss-girder connections. Auburn University was contracted to perform field tests to investigate these concerns.

One objective of this research was to use the field testing to evaluate the stress conditions and behavior of a number of cracked and uncracked floortruss-girder connections. Field tests were performed at six different connections at the first and second floortrusses away from pier supports. The connections tested were at 106 in. and 126 in. girder web depths. Preliminary field results indicated extremely high distortion-induced stress ranges in the web gap region. These secondary stress ranges exceeded the fatigue limits estimated for the details and even exceeded the steel yield strength during some tests. These conditions showed a high potential for fatigue cracking in the girder webs.

Based on the preliminary findings, a lengthened web gap retrofit was developed to

provide an inexpensive repair for the weld cracks that had been identified and to provide an effective means of reducing the potential for fatigue cracking in the girder web plate. A total of two retrofits were tested at each of two of the six previously tested connections. Each retrofit consisted of a slot cut into the connection plate that removed a small portion of the connection plate to web fillet welds including the weld cracks. Slot lengths of 6 and 10 in. were chosen for testing, but only the 10 in. slot performed well. The 10 in. slot was judged to be effective at reducing the potential for web cracking through reducing the distortion-induced stress ranges by roughly 70 percent and potentially increasing the fatigue life of the retrofitted connection by a minimum factor of 27. In addition to cutting the slots, bolts were removed from each of the retrofitted connections. Removal of bolts was found not to have a significant effect on the performance of the retrofits.

Based on the test results, the lengthened web gap retrofit was judged to be successful. A 12 in. slot length is recommended for prompt implementation as a preventative maintenance measure at floortruss-girder connections along the 106 in. deep girders. The 12 in. slot is recommended for repairing the connections at locations where weld cracks or distortion-induced web cracking is found in the future.

CHAPTER ONE

INTRODUCTION

BACKGROUND

The I-65 Mobile Delta Crossing Bridges constitute a six mile section (northbound and southbound) of interstate highway over the Mobile River delta plains located approximately 20 miles north of Mobile, Alabama. The bridges consist of three basic types: pre-cast concrete spans, steel plate girder spans, and a steel tied arch span. The steel plate girder spans are made of two main girders which span in the direction of the roadway with transverse members spanning between the girders. The transverse member types vary based on the depth of the main girders and are either floortrusses, built-up floorbeams, or trussed frames (present at pier locations for plate girders with intermediate transverse floortrusses). The bridges were constructed in the early 1980's and were opened to traffic in 1983. A traffic history (total of northbound and southbound vehicles) for the bridges is given in Table 1. The traffic history indicates that approximately 5 million heavy commercial vehicles (3 or more axles) had crossed each bridge span by 1993.

In late 1990, Alabama Highway Department (AHD) bridge inspectors discovered fatigue cracks in the girder webs at floorbeam-girder connections at six locations. All these locations were at pier supports along the steel plate girder spans. An investigation of the

Table 1. Traffic History of the Mobile Delta Crossing Bridges

Year	Average Daily Traffic (ADT)	% (CV) Commercial Vehicles of ADT	Percent Heavy Vehicles of CV	Number Heavy Vehicles
1991	13020	26	85	2877
1990	12220	26	85	2701
1989	11300	28	85	2689
1988	10490	30	85	2675
1987	10150	30	85	2588
1986	9940	30	85	2535
1985	8530	34	85	2465
1984	8410	34	85	2430
1983	8120	35	85	2416

fatigue cracking at the floorbeam-girder connections is reported in Volume I (Stallings et al. 1993) of this project report. In early 1991 fatigue cracks were discovered in welds at five locations not at piers at floortruss-girder connections. The purpose of the project phase reported here was to evaluate the conditions that created the fatigue cracks at the floortruss-girder connections through field tests of the bridges. Based on the results of the field tests, recommendations regarding repair and maintenance of the bridges are made.

BRIDGE DESCRIPTION

The steel plate girder spans of interest in this report are a part of the southbound approach lanes which extend approximately 3400 feet north from the north end of each tied arch span. The structural system at these locations is made of two main plate girders with three continuous intermediate stringers that are supported by transverse floortrusses. These structural components are all made of A588 Grade 50W weathering steel. The reinforced concrete deck was cast on corrugated metal stay-in-place forms that span between the top flanges of the plate girders and intermediate stringers. The top flanges of the main girders and stringers provide support for the concrete deck. The transverse floortrusses are spaced 25 feet on center.

The floortruss-girder connection is composed of a vertical stiffener-connection plate (referred to in the remainder of this report as a connection plate) that is welded to the plate girder web and bottom flange and bolted to the floortruss through a trapezoidal gusset plate (see Figure 1). Vertical bearing stiffeners are welded to the outside web face of the plate girders at pier locations. Vertical intermediate stiffeners are welded to the inside web face

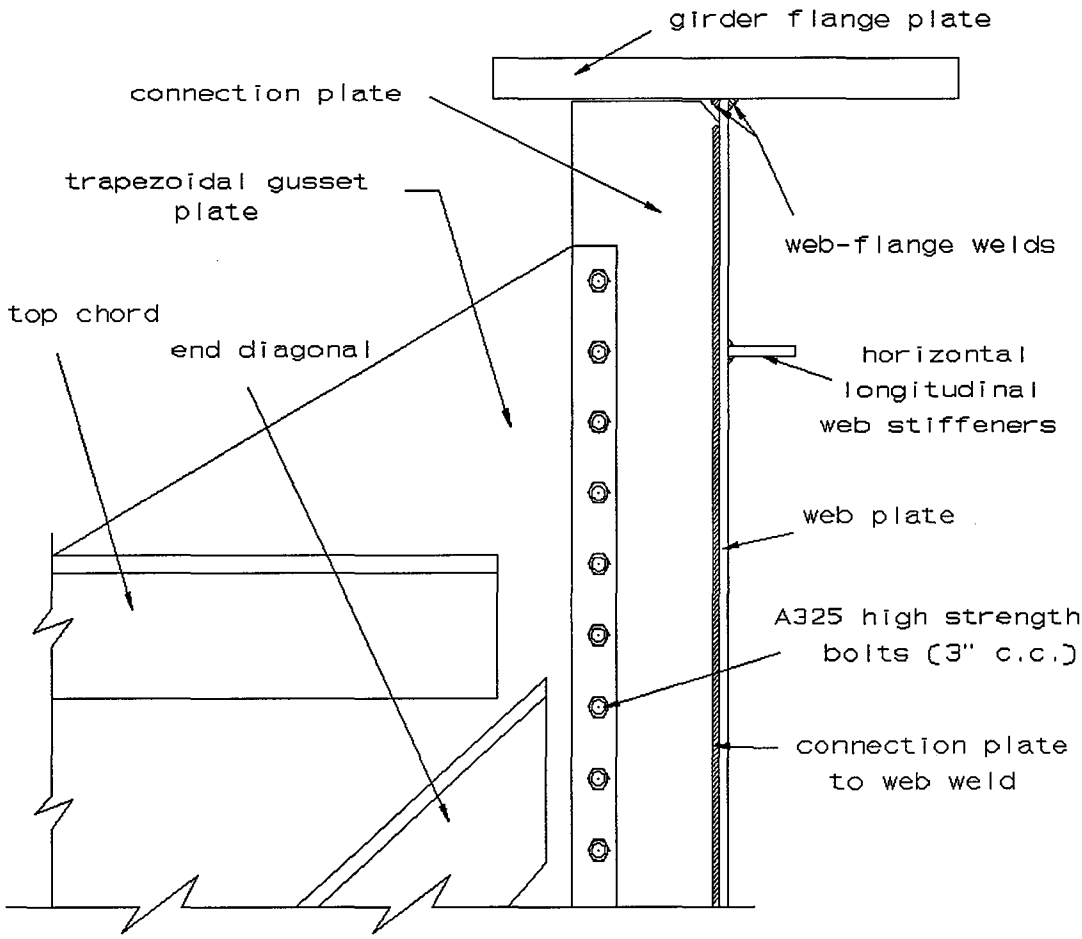

Figure 1. Typical Floortruss-Girder Connection Not at Pier

and run from the bottom to the top girder flange. Horizontal longitudinal web stiffeners are welded to the outside face of the girder web and are spaced approximately 1.5 to 2.5 feet above the bottom flange and below the top flange. A horizontal longitudinal web stiffener is shown in Figure 1, but since it is a structural feature of minor significance it is omitted from all figures that follow. WT-sections which intersect in an "X" configuration between floortrusses provide horizontal cross bracing between the girders near the bottom flange.

The floortruss connection plates are welded to the girder web and the compression flange (bottom flange) and are tight fit to the tension flange (top flange) in the negative moment regions of the main girders near the pier supports. Common bridge engineering practices at the time of the bridge's construction discouraged the welding of stiffeners and connection plates to the main girder tension flanges. Therefore, the connection plate welds to the girder web terminate a short distance from the girder tension flange plate. This web gap region, as it is called, between the bottom of the girder tension flange plate and the top of the connection plate weld, often experiences very high stresses and high stress gradients. Geometrical discontinuities and structural features at the boundaries of this region become points of high stress concentrations.

Since the connection plate to web weld terminates short of the tension flange, the web plate is free to distort out-of-plane (perpendicular to the plane of the web) in the web gap region. Distortion of the web gap is produced by the deflections of the transverse floortruss that subject the top of the connection plate to an inward and downward pull when traffic crosses the floortruss as illustrated in Figure 2.

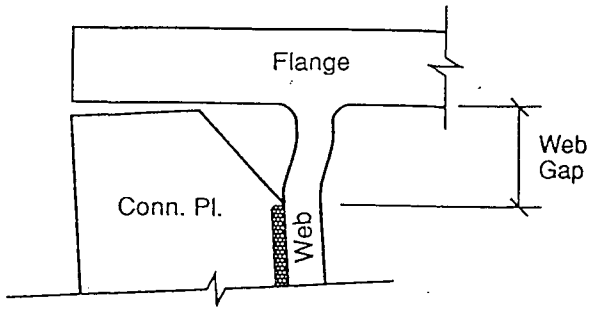

(a)

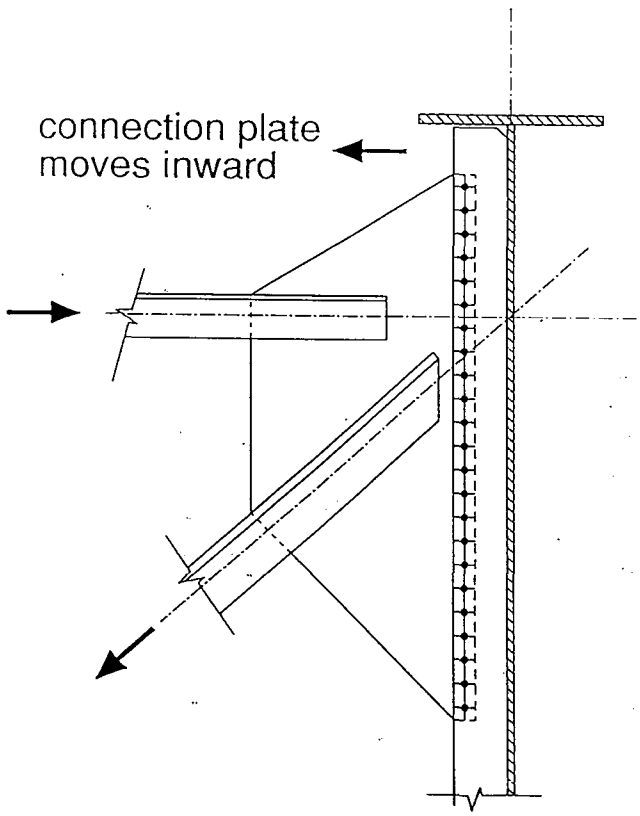

(b)

Figure 2. Illustration of Out-of-Plane Distortion: (a) In the Web Gap Region; (b) Due to Deflections of the Transverse Floortruss

LOCATIONS AND EXTENT OF CRACKING

Fatigue cracks were found by AHD bridge inspectors at the floortruss-girder connection web gaps in the top of the connection plate welds as shown in Figure 3. The cracks had not propagated from the weld throats into the web plate, and therefore, did not pose an immediate threat to the bridge integrity. However, this type of crack is likely to eventually turn and propagate into the girder web. The crack could then turn perpendicular to the in-plane bending stress in the girder web and be a much more significant problem. Cracks have not yet been discovered in the girder webs at floortruss-girder connections as were found at the floorbeam-girder connections discussed in Volume I.

Cracking was discovered at a total of five floortruss-girder connections. Unlike the floorbeam-girder details, all cracks were located at floortruss-girder connections not at piers. Three of the five connections with cracking were chosen for investigation in this project. In addition, three uncracked connections that were nearby the cracked connections were chosen for investigation. A total of five individual cracks in the connection plate to web weld (see Figure 3) were identified at the three cracked connections investigated during this phase of the project. Specific crack lengths for these five cracks are presented in Chapter Four. Since all cracks found were in the negative moment region of the girders in the web gap near the tension flange, the connections at one and two floortrusses away from piers have the potential for cracking in these bridges. Therefore, approximately 144 connections along the north and southbound lanes have the potential for similar cracking in the future.

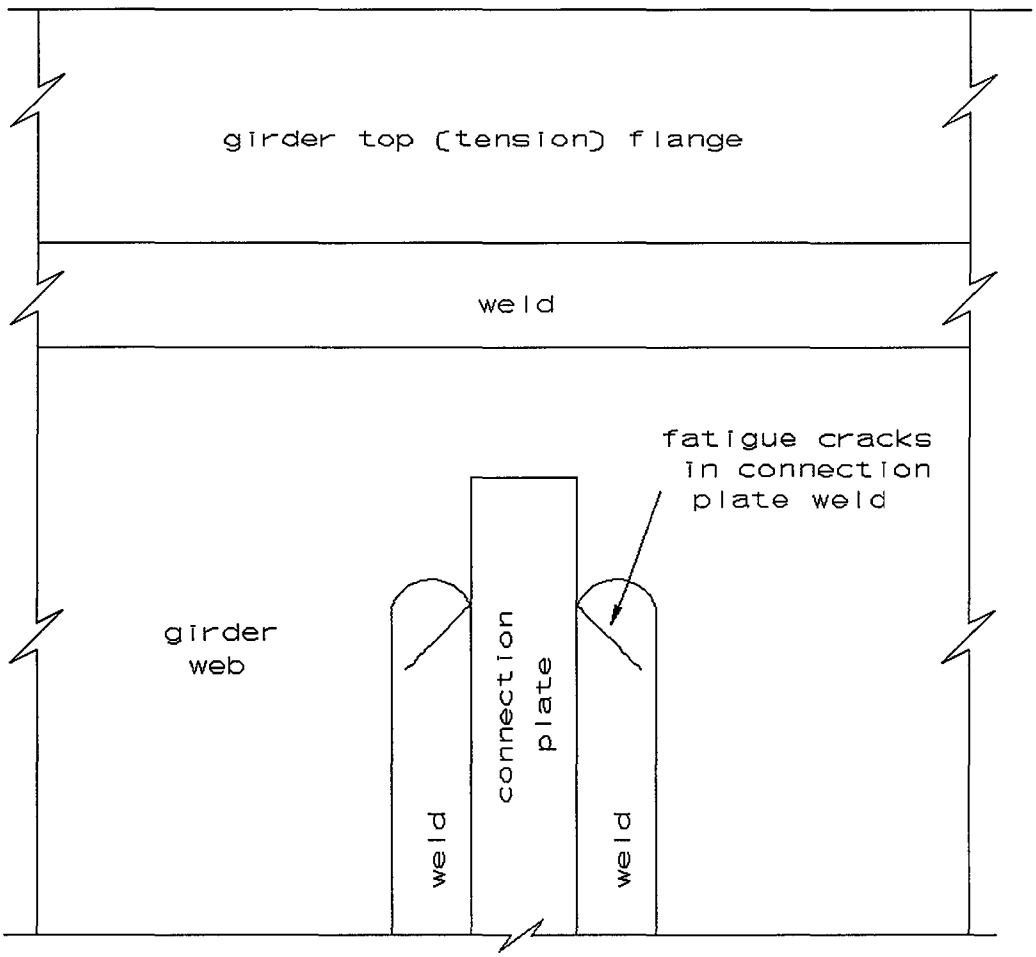

Figure 3. Typical Fatigue Cracks Found at Floortruss-Girder Connections

PROJECT OBJECTIVES

The two main questions originally posed by the AHD for this portion of AHD Research Project ST 2019-16 were:

1) Is it likely that distortion induced web cracking will occur in the girder webs at the floortruss-girder connections?

2) What is the best method of repairing the weld cracks at the floortruss-girder connections?

These questions along with other related questions were answered. Because the answer to the first question was found to be yes, the project objectives were modified somewhat as the project progressed. An added objective was to investigate the performance of a repair method that would potentially prevent distortion-induced cracking in the girder web.

The effectiveness of a rigid attachment retrofit designed by the AHD was proven in Volume I of this report to be a long-term solution to the cracking problem at the floorbeam-girder connections at piers. It appears reasonable that the rigid attachment retrofit will also prevent cracking and/or stop fatigue crack propagation at the floortruss-girder connections. However, the expense of this retrofit method, and its high cost relative to other known retrofit procedures, prompted the AHD to consider other possible retrofit procedures. After reviewing preliminary results from the field research obtained in July 1992, the AHD, together with Auburn University, developed two trial retrofit details to be implemented at two locations that were being tested in the field research. A separate variation of the chosen retrofit detail was performed at each of the test locations. This report includes discussion of the results after the retrofit was performed.

METHODOLOGY AND SCOPE OF REPORT

The project objectives were met through field tests performed during the summer of 1992. Field measurements were made to determine the magnitudes of the out-of-plane displacements and distortion-induced stresses at typical floortruss-girder connections. Measurements were made at floortruss-girder connections away from the girder supports at connections where weld cracks had been identified and at nearby connections. Measurements were made with loading from trucks of known weight and with loading from normal truck traffic crossing the bridges. These measurements were compared to the results of laboratory tests performed by other researchers to assess the potential for future cracking at similar connections along the bridge. Measurements were taken before and after the retrofit details were implemented to evaluate the performance of the particular retrofits employed.

A review of the field and laboratory investigations by others related to out-of-plane distortion-induced cracking was presented in Volume I. That literature review information also applies here. A review of previously identified retrofit procedures and a statistical literature review are presented in Chapter Two of this report. Chapter Three discusses the selection of the retrofit detail investigated in this portion of the project. Descriptions of the test locations, instrumentation, and data acquisition and reduction methods used for the I-65 bridges studied in this portion of the project are described in Chapters Four, Five, and Six. The test results and analyses of the test results are given in Chapters Seven and Eight. Conclusions and Recommendations are presented in Chapter Nine.

CHAPTER TWO

LITERATURE REVIEW

One goal of this project was to identify the best method for repairing the weld fatigue cracks that have been discovered at the floortruss connections. Early results of the project indicated that the most significant long-term problem at the connections would be distortion-induced cracking in the girder web. Hence, an overview of methods for repair of distortion-induced cracking is presented here. Background information on distortion-induced fatigue cracking and the previous laboratory investigations of the topic were discussed in Volume I of this report (Stallings et al. 1993) and will not be repeated here. General discussions contained in Volume I of typical instrumentation schemes, fatigue cycle counting methods, and effective stress range determination also apply here.

ASSESSMENT OF RETROFIT TYPES

Floortruss-girder connections of the type studied here have not been the subject of previous research. Studies of connections of solid-web floorbeams provide the nearest reasonable comparisons. Numerous retrofit schemes have been proposed for retrofitting fatigue cracks at floorbeam-girder connections. Koob et al. (1985) presented an extensive discussion of various retrofit procedures that were considered for retrofitting a system of bridges with floorbeam-girder connections in Illinois. These retrofit procedures were of

three main types: friction, rigid attachment, and loosening retrofits. An evaluation of retrofit types was made considering the ability to maintain quality workmanship, impact due to traffic disruption, installation difficulty, and the cost-effectiveness of the method. Much of the work of Koob et al. (1985) is referenced below because of the extensive nature of their discussions. However, many of the repair ideas are not unique to that report.

Friction Retrofits

Two friction type retrofits involve the use of wedges and compressed plates and appear in Figure 4. All retrofit figures show a section view of the connection looking in the longitudinal direction of the main girder. The purpose of these retrofits is to eliminate the out-of-plane displacement. The wedge type retrofit would involve machining inclined surfaces into the tops of the inside and outside stiffener plates. Steel wedges would be forced into these inclined surfaces and a jacking force would be maintained until the wedges could be welded to the stiffeners. The adjacent surfaces would require precise finishing. The compressed plate retrofit would involve loosely bolting thick slotted steel plates to the sides of the inside and outside stiffener plates. These loosely bolted plates would be jacked up against the top flange and the bolts would be tightened and the plates welded to the stiffeners while maintaining the jacking force. This procedure would require somewhat less preparation, machining, and finishing than the wedged retrofit.

Friction retrofits could reduce the out-of-plane displacements at cracked connections by locking, or tightening, up the connection. However, connections with these retrofits would likely loosen over time; the installation procedures for these two retrofits would be

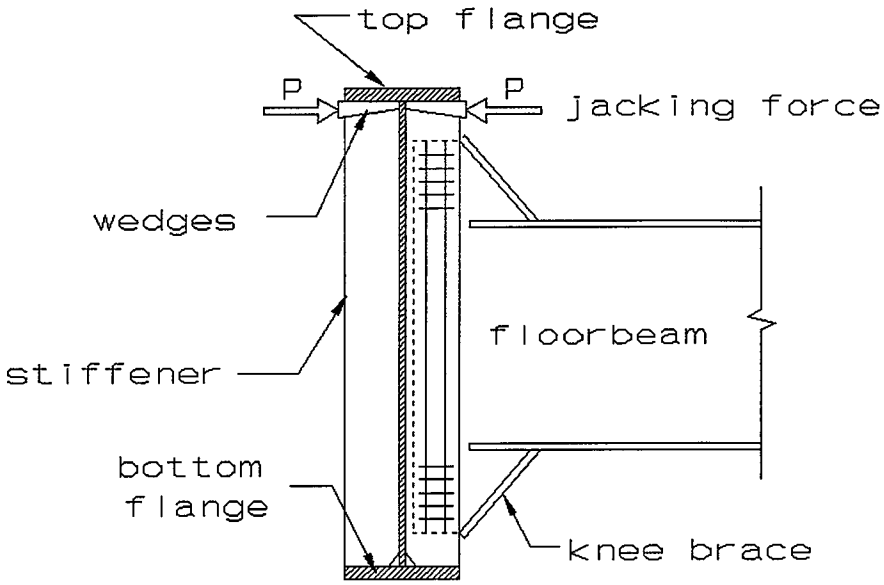

(a)

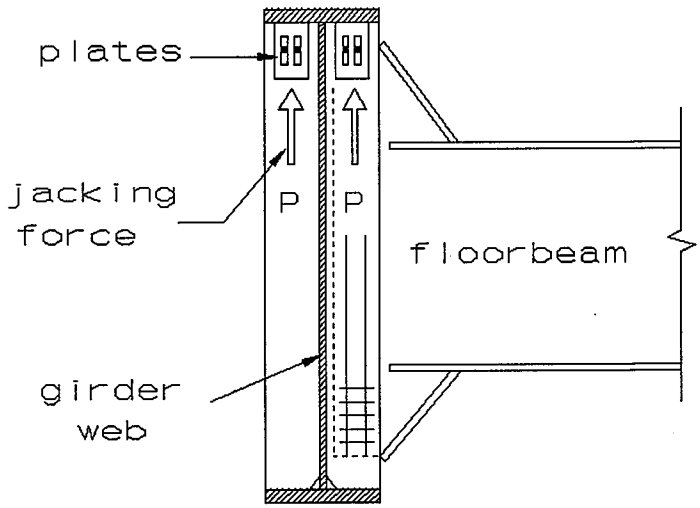

(b)

Figure 4. Examples of Friction Type Retrofits: (a) Wedges; (b) Compressed Plates

difficult for quality assurance; and the jacking force, if improperly applied, could subject the web gap to tensile stresses which could cause rapid crack extension. The field machining for the wedged retrofit would be prohibitively difficult.

Rigid Attachment Retrofits

The four rigid attachment procedures identified by Koob et al. (1985), which appear in Figures 5 and 6, included welded, through bolted, studded, and bracketed through a hole in the web. Again, the purpose of these repairs is to eliminate (or significantly reduce) the out-of-plane displacement in the web gap. The stiffener plate is fillet welded to the girder top flange in the welded repair. The through bolted repair involves removing the concrete deck to expose the top flange of the girder. An 8"X8"X1" steel angle is bolted to both sides of the interior stiffener and through bolted to the top flange through cored bolt holes. This is essentially the same as the positive attachment retrofit designed by the AHD and tested at floorbeam-girder connections at piers in Volume I of this report. The through bolted attachment is also the same basic design as studied by Fisher et al. (1990) in laboratory tests. The studded retrofit is similar to the through bolted retrofit, except that no concrete is removed. Instead, holes are drilled and tapped into the girder top flange to accept threaded studs for angle attachment.

The bracketed connection involves core-drilling and grinding out enough web material to accommodate two angles that are passed through the opening and positioned firmly against the inside and outside stiffener plates. Two smaller angles are attached transversely to the

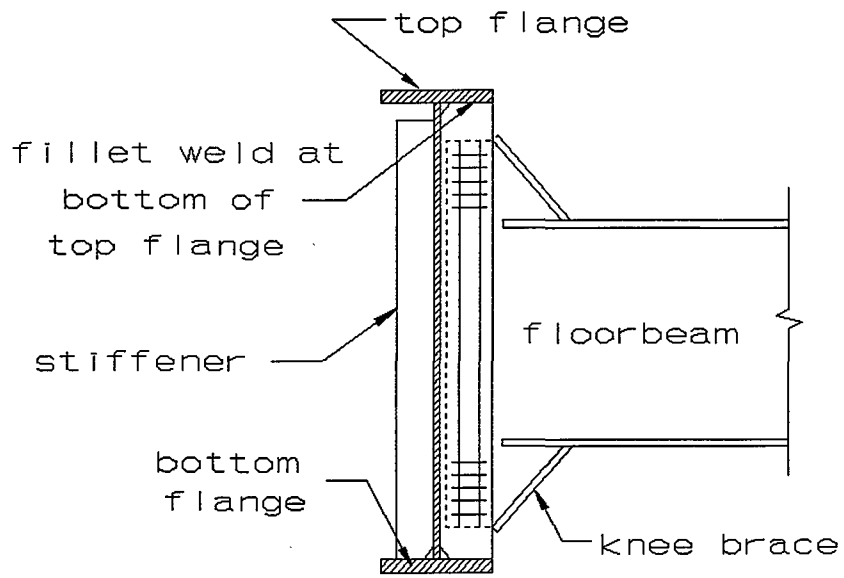

(a)

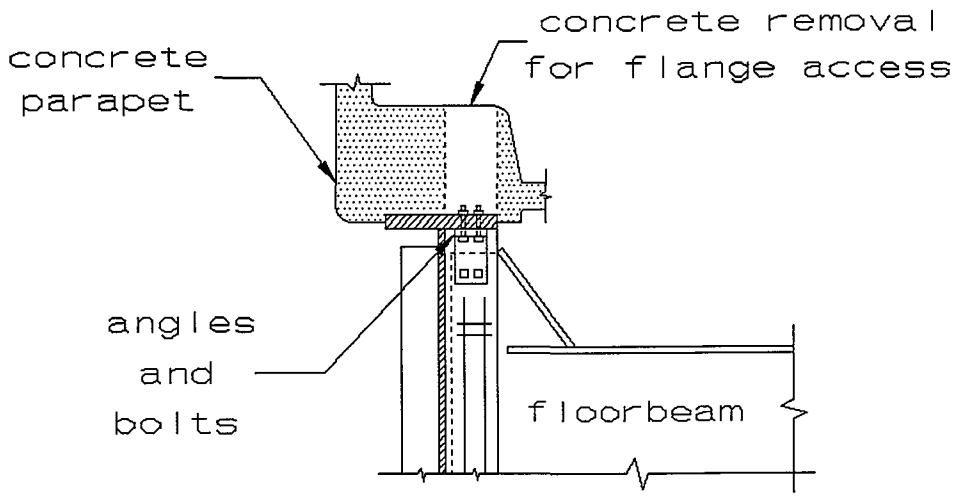

(b)

Figure 5. Examples of Rigid Attachment Type Retrofits: (a) Welded; (b) Through Bolted

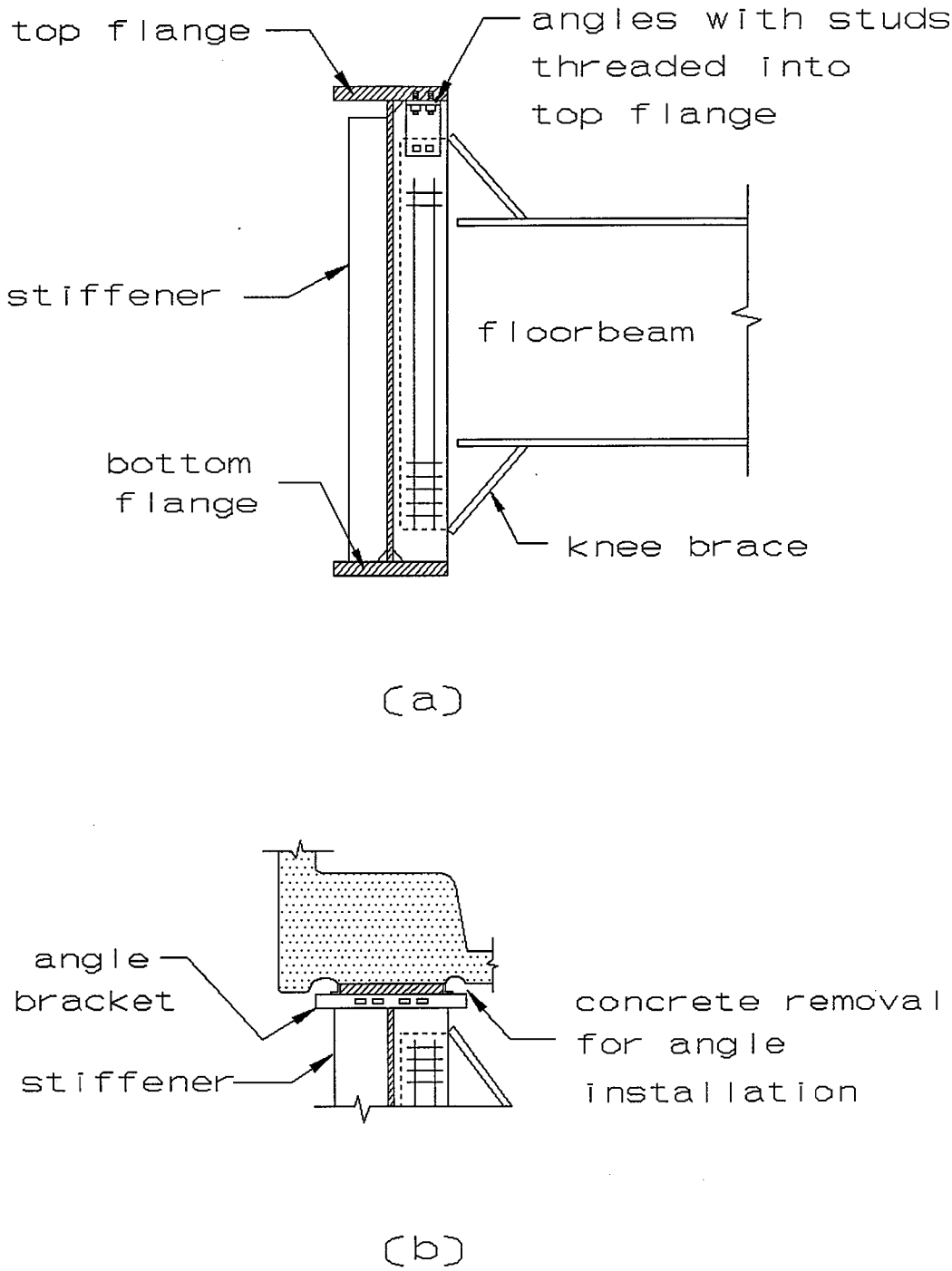

Figure 6. Examples of Rigid Attachment Type Retrofits: (a) Studded; (b) Bracketed Through a Hole in the Girder Web

two angles passed through the web. Concrete is removed around the sides of the main girder flange to the small angles to bear against the edges of the flange. One of the smaller angles would be attached to the larger angles before they are passed through the web, and the other angle would be attached after the two larger angles have been positioned through the web and jacking has been performed to tighten up the connection.

All of the rigid attachment repairs, except the through bolted retrofit could be installed from under the bridge without traffic disruption. The studded connection has some very distinct advantages in the ease of installation and the minimization of impact on traffic. One major concern is whether or not it is possible to achieve a slip resistant connection and maintain the slip resistance over a long period of time. Another concern is the potential for formation of fatigue cracks in the tension flange of the girder at the threaded bolt hole. However, the low stress levels commonly occurring in the tension flange in negative moment regions of the main girders make fatigue cracking less of a concern. The rigid attachment repairs are required at bearing stiffeners to transfer lateral loads into the support. Rigid attachments are very effective at minimizing out-of-plane distortions of the web gap as illustrated by the tests reported in Volume I of this report. The bracketed connection is not very desirable because of the difficulty of fitting-up the brackets, and it requires a good deal of concrete removal which might reduce the durability of the deck. The potential for obtaining a poor quality field weld is the primary concern with the welded attachment. The likelihood for achieving a good quality weld would be increased by stopping traffic on the bridge during the welding process.

Loosening Retrofits

Two loosening retrofits considered by Koob et al. (1985) were the slotted web and the lengthened web gap retrofits which appear in Figure 7. The slotted web retrofit involves cutting a slot into the web plate in the web gap. The slot would arrest crack extension from existing cracks as well as provide extra flexibility in the web plate in this region. The extra flexibility would reduce the stress ranges that result in fatigue cracking. The lengthened web gap retrofit consists of coring a 4 in. diameter hole through both the inside and the outside stiffener and then removing the top portion of each stiffener after the edges have been flame cut. After the portion of the stiffener and connected knee brace have been removed, then all edges are ground smooth to remove burs and weld and plate materials. These loosening retrofits cannot be used at bearing stiffener locations and little data is available on the extended performance of these retrofits. However, all of the work can be performed from under the bridge and these retrofits remove most existing web gap defects and provide a good inspection surface.

Summary of Retrofit Procedures

From the eight previously mentioned retrofit types, Koob et al. (1985) chose three types for investigation: the welded, the studded, and the web gap lengthening retrofits. The basic retrofit details for these three retrofit types are shown in Figures 8 through 10. The specific retrofit procedures developed for use in that project are given by Koob. A total of 2 welded, 2 studded, and 6 web gap lengthening retrofits were performed during that project.

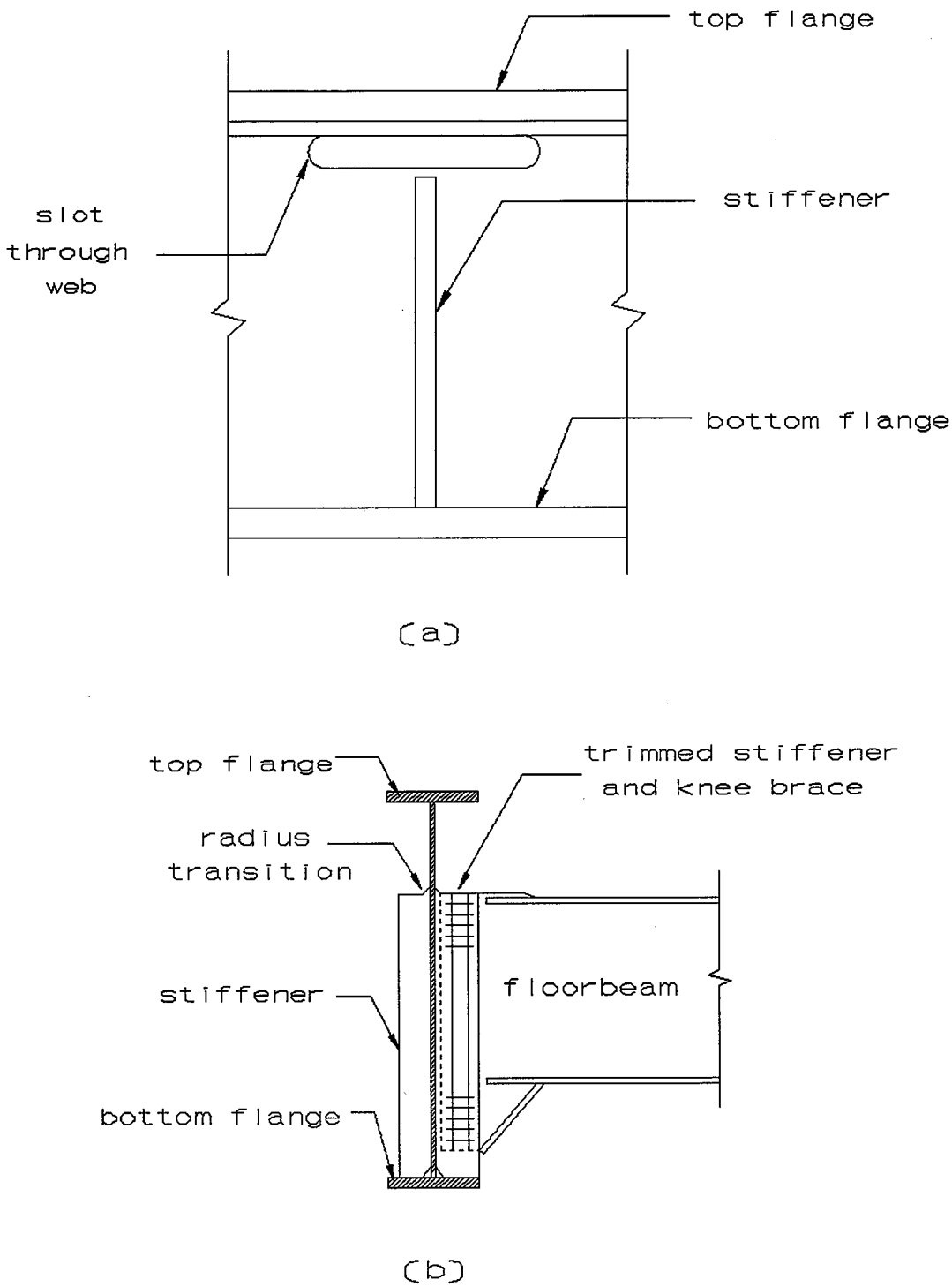

Figure 7. Examples of Loosening Type Retrofits: (a) Slotted Web; (b) Lengthened Web Gap

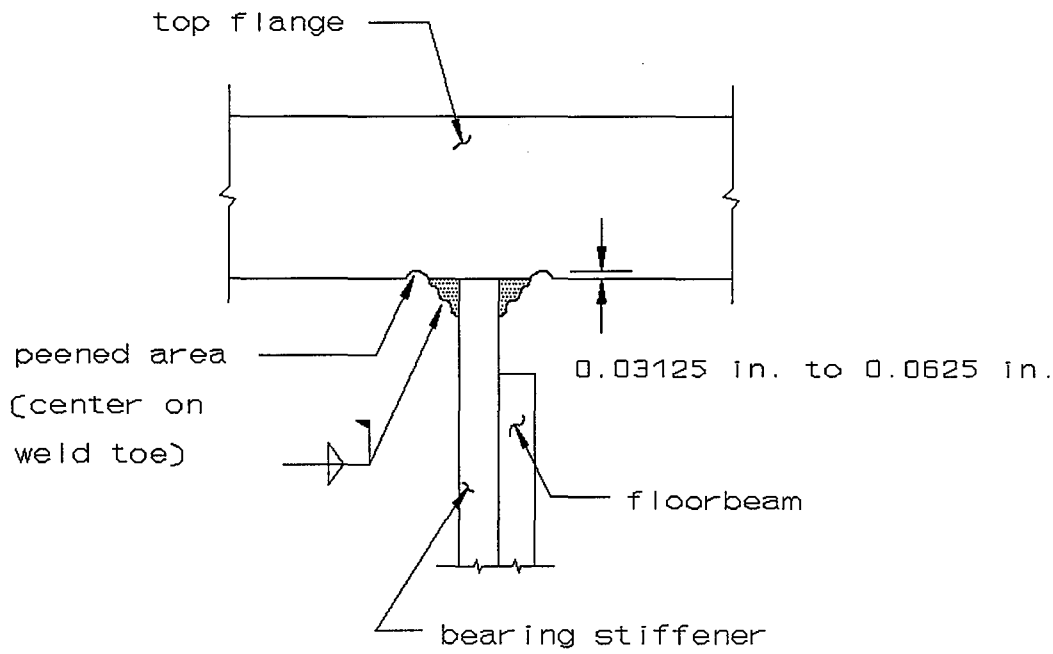

Figure 8. Basic Welded Retrofit Detail Chosen for Investigation by Koob et al. (1985)

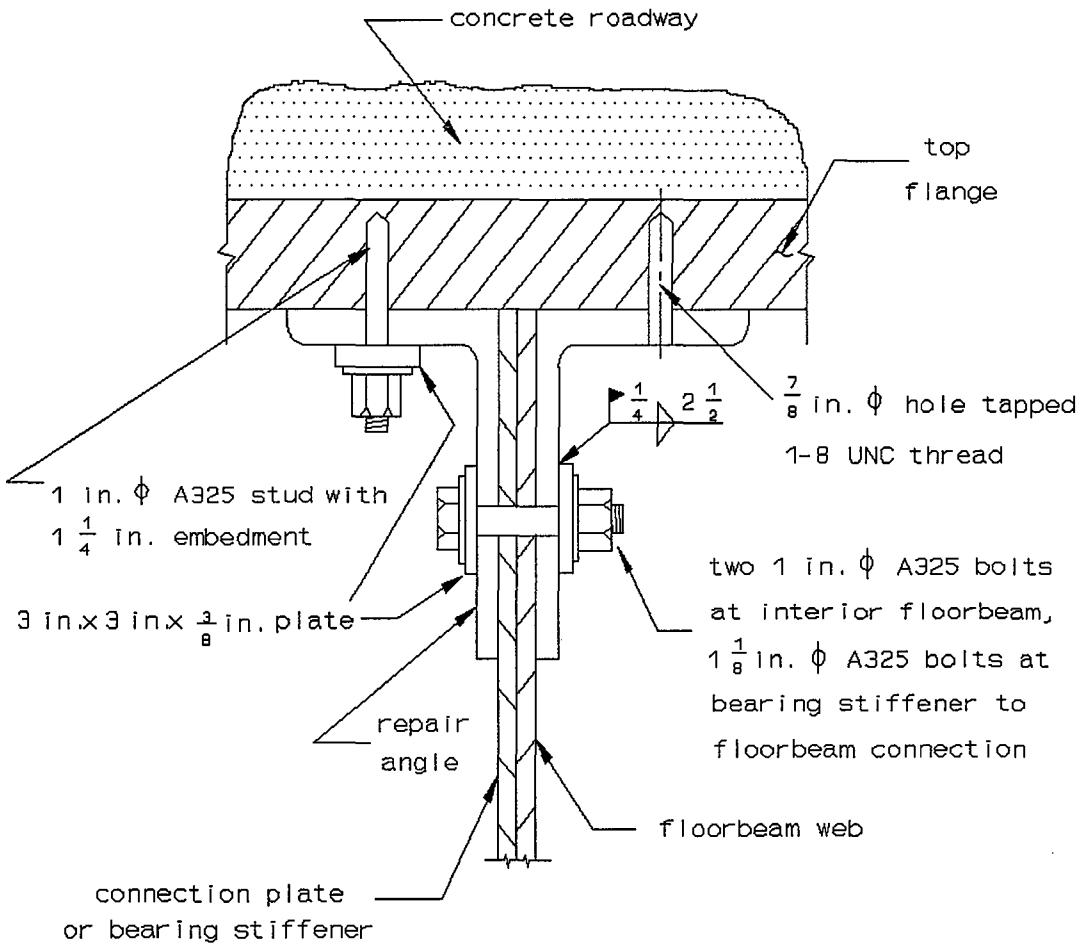

Figure 9. Basic Studded Retrofit Detail Chosen for Investigation by Koob et al. (1985)

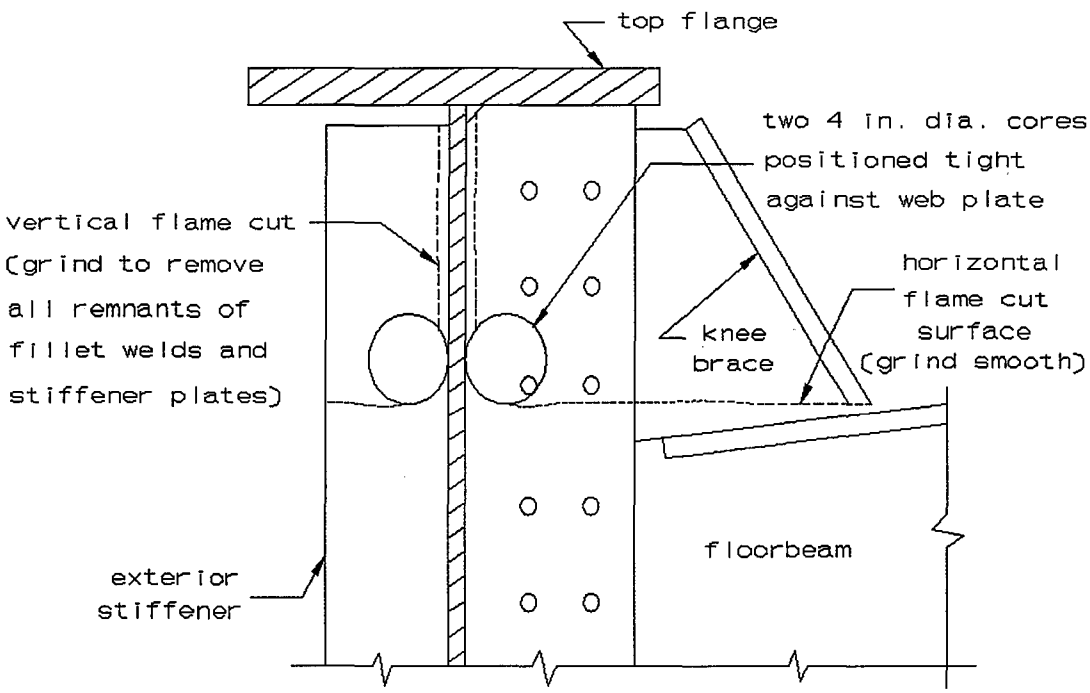

Figure 10. Basic Lengthened Web Gap Retrofit Detail Chosen for Investigation by Koob et al. (1985)

All three of the retrofit types tested were reported to have performed satisfactorily. However, the long-term performance of the connection has not yet been evaluated.

STATISTICAL REVIEW

Due to the vast amount of data collected during this project, the need arose for developing descriptions of the data and grouping the data into manageable and insightful forms. Some basic concepts of statistical analysis are discussed below. Further discussion of basic and advanced concepts are presented by Kachigan (1982) and others.

A fundamental part of statistical analysis is the frequency distribution. The frequency distribution is a representation of how frequently (or at what rate) an event occurs among a set of measured events. The most common methods for graphical representation of frequency distributions are the histogram and the frequency polygon. In fatigue literature, the histogram is most commonly used to represent stress ranges (Fisher et al. 1990, Keating et al. 1987, Galambos and Heins 1971). Figure 11 presents idealized histograms illustrating five common shapes of frequency distributions.

The rectangular or uniform distribution is one in which each possible value of the variable occurs equally often. This type of distribution is not common in physical systems since there is typically one or a small number of values that tend to occur most frequently. The U-shaped distribution is very polarized, with a very high or very low event being the most commonly occurring with few intermediate values. The J-shaped distribution could be regular or reverse J-shaped. The probability for occurrence in a regular J-shaped distribution increases as the independent variable increases and decreases for the reverse J-shaped

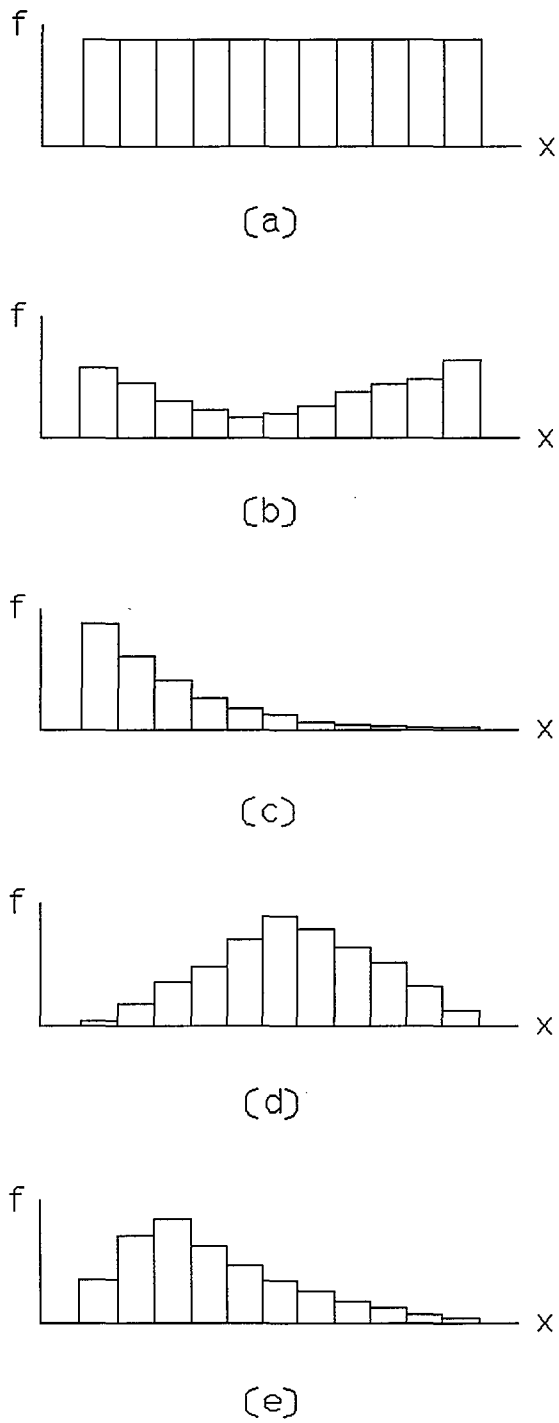

Figure 11. Idealized Histograms Illustrating Common Shapes of Frequency Distributions: (a) Uniform; (b) U-Shaped; (c) Reverse J-Shaped; (d) Bell-Shaped; (e) Skewed Right

distribution. The bell-shaped distribution is the most common distribution and displays increasing frequency at intermediate values of the independent variable. Skewed distributions are either skewed to the right or left. The direction of skew typically matches the direction of the distribution's tail. The skewed distributions exhibit shapes that fall somewhere between the bell-shaped and either the regular, or reverse, J-shaped distributions.

While the shape of the distribution is an important description, it is also important to give a more concise representation of the distribution. A single value which would serve as a typical or representative event for the distribution is called the central tendency, or location of the distribution. Common measures of central tendency include the mode, median, and mean. The mode is the value that occurs most frequently and is the peak value of the frequency distribution. Distributions that have two modes are considered bimodal. Bimodal and multimodal distributions usually indicate that two or multiple distinct groups of events, or values of the independent variable, are most commonly occurring. For example, if the stress measured at a certain point in a bridge is determined to be highly dependent on the traffic lane that a truck occupies as it crosses the span, then the distribution of stress ranges measured at that point could be expected to be bimodal for two traffic lanes. The median is the middle value of a distribution. Fifty percent of the values will fall above and below the median value. The mean is most commonly estimated by determining an arithmetic average. The fact that the mean considers all values, whether they be unusually high or low, tends to hamper the mean's ability to accurately reflect the central tendency. An unusually high value in a skewed distribution, for instance, will shift the mean to a position that is probably higher than the true central tendency.

When the mode, median, and mean are nearly equal (Figure 12 (a)), the distribution is essentially symmetrical in form. The mean tends to be shifted towards the tail of a skewed distribution. By definition, when the mean is greater than the median, then the distribution is skewed right (Figure 12 (b)), and when the mean is less than the median, then the distribution is skewed left (Figure 12 (c)). A simple comparison of the relative locations of the average and median values provides a simple indication of whether a distribution is skewed right or left. This approach is used in Chapters Seven and Eight.

The Rayleigh distribution is a frequency distribution that is commonly used to model random vehicle events for laboratory structural studies (Keating et al. 1987, Fisher et al. 1983, Schilling et al. 1978). This distribution is skewed right and is derived from Mohr's circle for joint probability as noted by Clough and Penzien (1975). An illustration of the shape and characteristics of the Rayleigh distribution is given in Figure 13 taken from Schilling et al. (1978).

When dealing with data that is measured on two variables the association or relationship between the variables is often of interest. This association is usually of two basic types, experimental and correlational. One variable is usually controlled while the other is measured in experimental association. However, correlational association involves two seemingly random variables, such as stresses and out-of-plane displacements due to random truck loadings. The extent of the relationship between the two variables is called the product moment correlation coefficient, or just the correlation coefficient. The coefficient is a single number that describes the relationship between the two variables just as the mean is a single measure of the central tendency. The correlation coefficient ranges from -1.0,

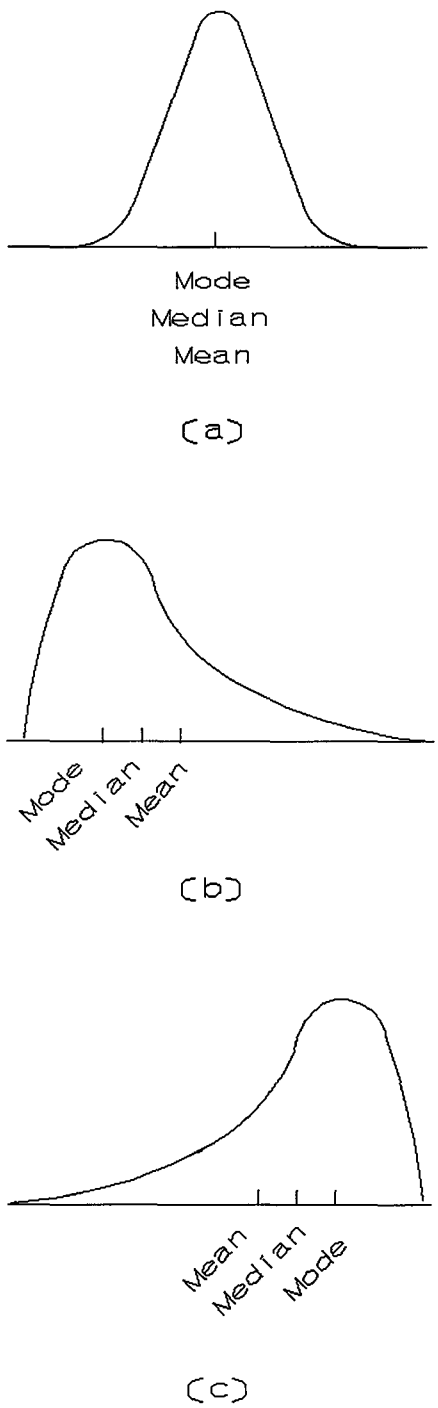

Figure 12. Relative Values of Mode, Median, and Mean for Differing Shapes of Frequency Distributions: (a) Symmetrical; (b) Skewed Right; (c) Skewed Left

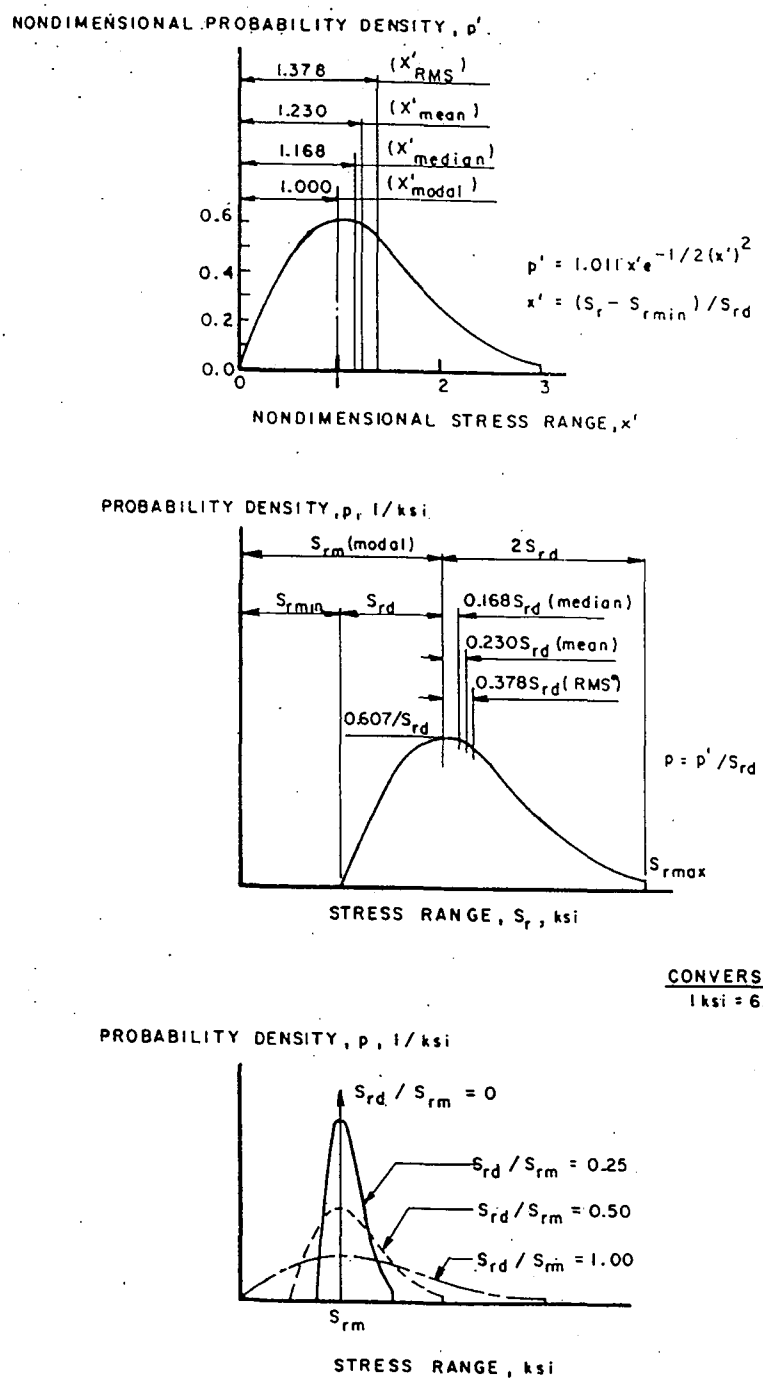

Figure 13. Shape and Characteristics of Rayleigh Probability Density Curves

perfect negative correlation, to +1.0, perfect positive correlation, with 0 indicating no correlation. Examples of varying degrees of correlation appear in Figure 14 (a) through (d). If the degree of positive correlation between stresses and out-of-plane displacements measured experimentally at these connection details is very nearly +1.0, then such stresses would be truly considered secondary stresses in nature. That means that the out-of-plane displacement caused by the distortion of the transverse bridge elements would be the clear source of the resulting stresses experienced in these regions.

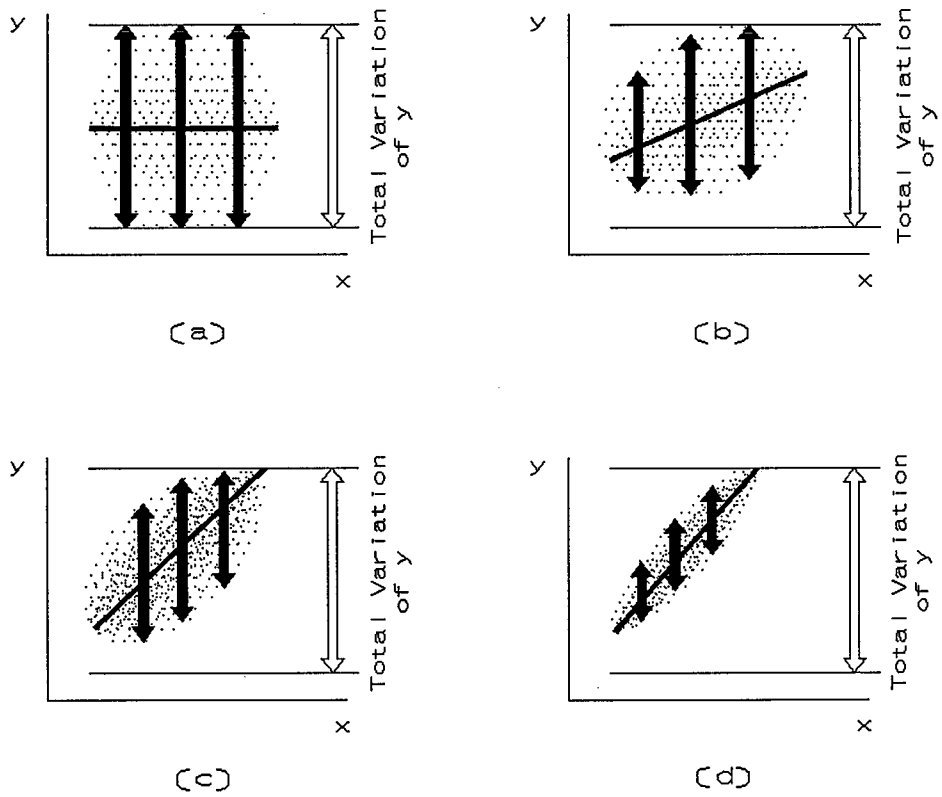

Figure 14. Varying Degrees of Correlation (a) Zero Correlation; (b) Low Correlation; (c) Moderate Correlation; (d) High Correlation

CHAPTER THREE

SELECTION OF RETROFIT PROCEDURE

The fatigue problem initially identified by AHD bridge inspectors was cracking through the throat of the floortruss to girder connection plate welds near the top of the welds as shown in Figure 3 of Chapter One. These cracks could easily be eliminated by grinding out the ends of the welds. However, data taken early on during the field tests revealed that stress ranges in the girder web plates at these floortruss connections far exceeded the fatigue limits defined for distortion-induced cracking of the web. If the weld cracks extended into the web, the distortion-induced stresses in the girder webs were found to be high enough that drilling holes at the crack tips would not provide a permanent repair of web cracks that are expected to occur. Hence, grinding out the cracks at the ends of the welds would solve the immediate fatigue problem, but would not address the long-term problem of cracking in the girder webs.

A positive attachment retrofit was the preferred retrofit at floorbeam connections tested in Volume I. The retrofit was found to be effective in reducing the distortion-induced stress conditions to acceptable levels. However, this retrofit was relatively expensive. A loosening retrofit was seen to have potential for providing great cost savings, but very little data was available on such a retrofit's long-term performance. Despite this, a loosening type retrofit was developed and implemented to attempt a reliable, low cost repair method.

Total removal of a connection plate section as illustrated in Figure 7 (b) of Chapter Two would provide a condition that would be difficult to repair if the loosening retrofit was unsuccessful. Rather than removing the entire width of the plate, the web gap would be lengthened by creating a slot in the connection plate as illustrated in Figure 15. Enough plate was left so that a positive attachment retrofit, which was known to be successful, could still be performed using the remaining portion of the connection plate if the slotted retrofit proved unsuccessful (whether through the findings of this research, or after implementation at a large number of connections).

Fisher et al. (1990) noted that removal of part of a transverse connection plate to soften the web gap region reduces the cyclic distortion-induced stresses and can significantly reduce crack growth rate. He concluded that the available data was insufficient to recommend a loosening retrofit procedure and stated that care should be taken to prevent web gap distortion from increasing substantially when this method is used. Fisher also suggested that the increased web gap length should be at least 20 times the web thickness, and not less than 12 in., to be fully effective at floorbeam-girder details. These guidelines appear to be based primarily on past experience.

For the I-65 bridges two connections were chosen for trial implementation of the connection plate slot retrofit. Slot lengths of 10 in. and 6 in. were chosen for investigation as shown in Figures 16 and 17. The exact locations of the retrofitted connections are discussed in Chapter Four.

The 10 in. slot length is 23 times the web thickness (0.4375 in.) and represents a compromise between the recommended minimum of 20 times the web thickness and 12 in.

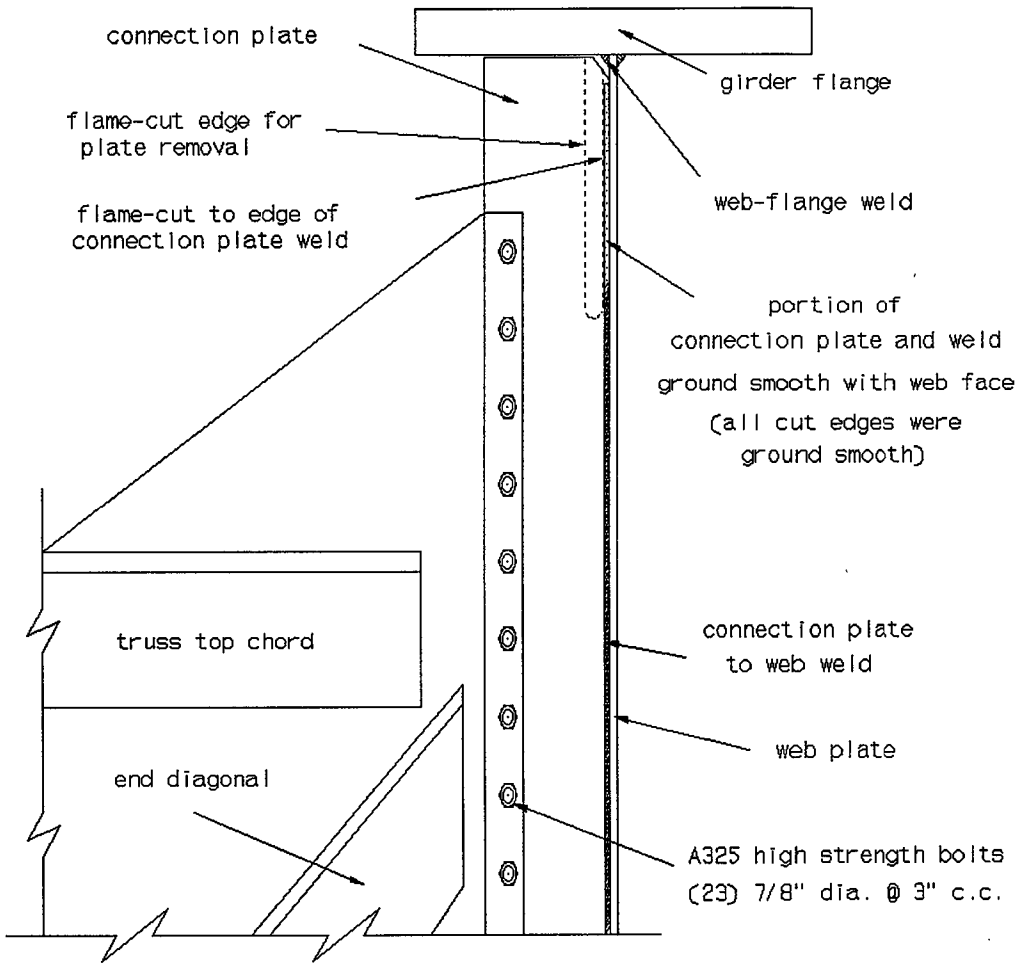

Figure 15. Typical Retrofit Procedure for Connection Plate Slot Retrofit

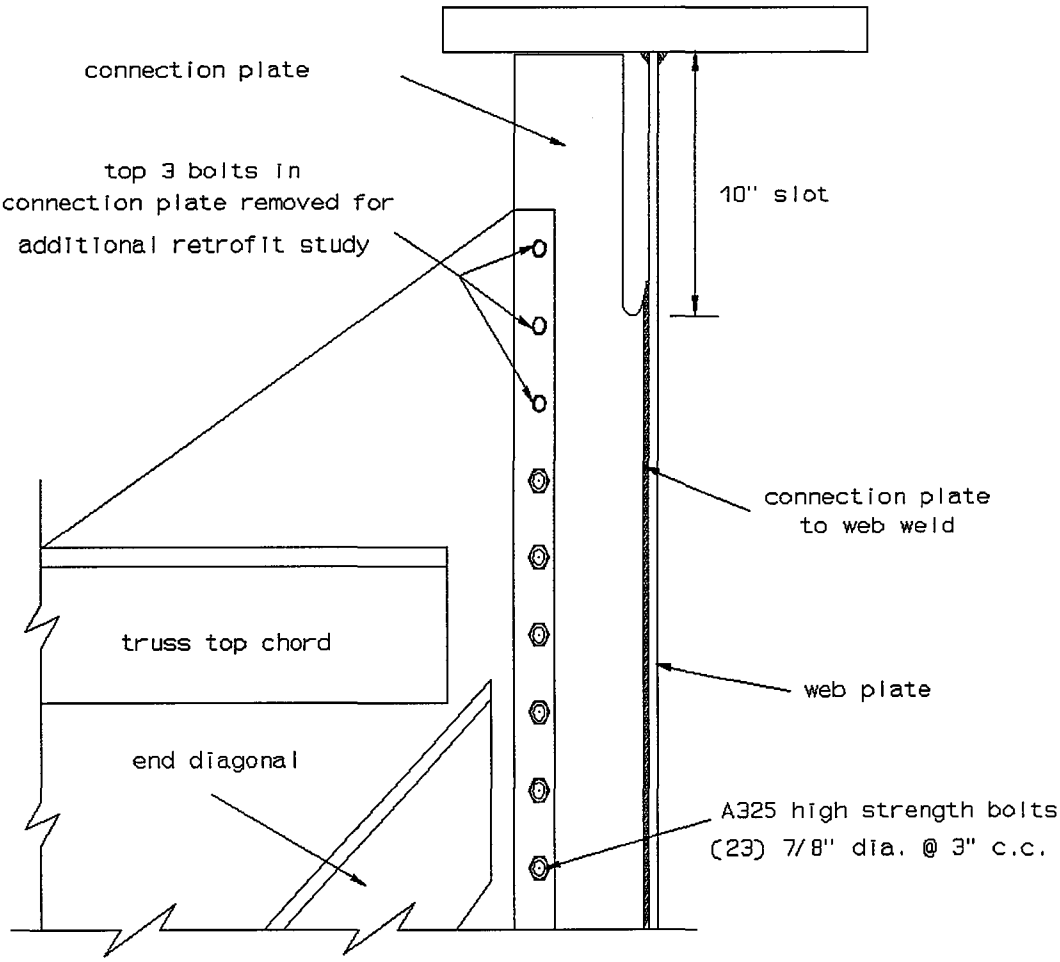

Figure 16. Ten Inch Slot in the Connection Plate and Position of the Three Bolts Removed for the Second Trial Retrofit

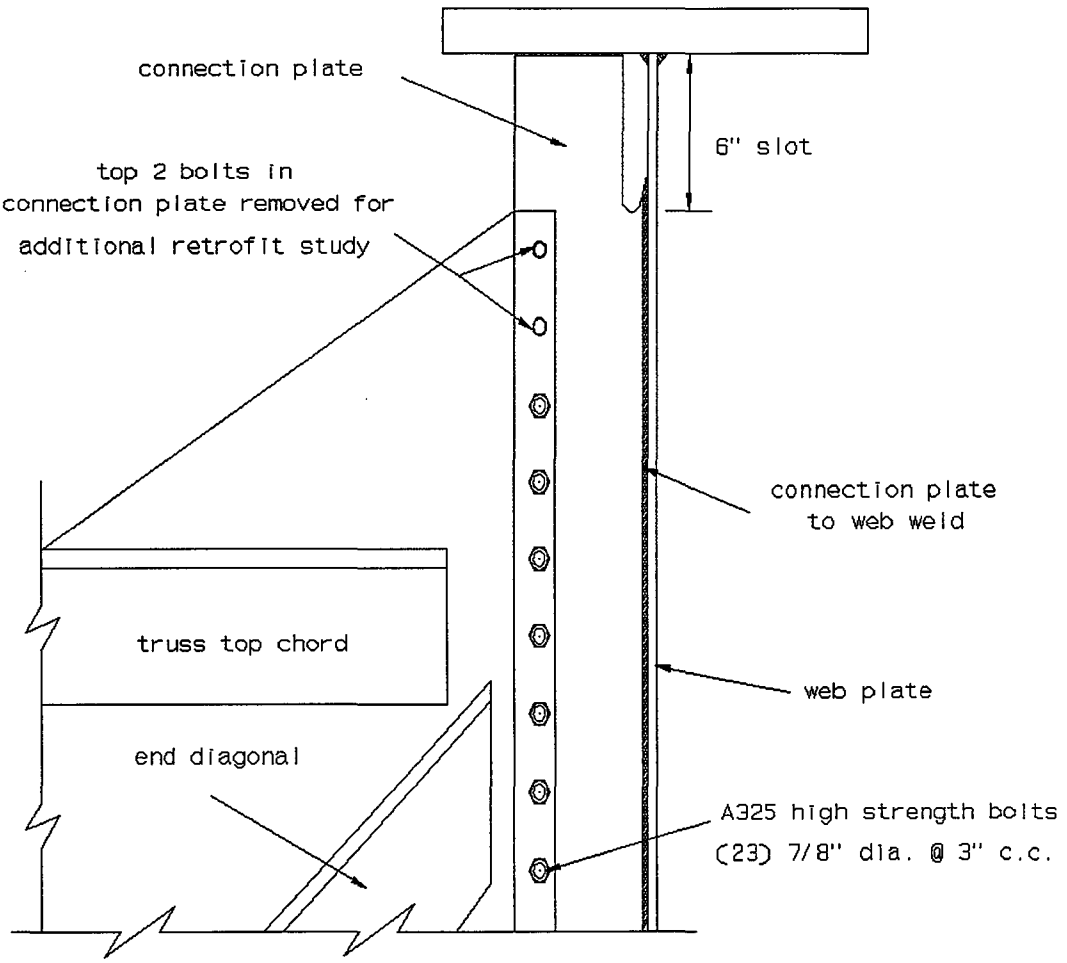

Figure 17. Six Inch Slot in the Connection Plate and Position of the Two Bolts Removed for the Second Trial Retrofit

Another retrofit configuration evaluated at this connection involved removing the top three bolts from the connection in addition to cutting the 10 in. slot as shown in Figure 16. The 6 in. slot provided a web gap length of 12 times the web thickness (0.5 in.) at this connection. The 6 in. slot was chosen to minimize the possibility of causing a substantial increase in web gap distortion. As shown in Figure 17, the 6 in. slot avoids drastic disruption of the connection since the top of the slot aligns with the top of the trapezoidal gusset plate. A second retrofit configuration evaluated at this connection consisted of removing the top two connection plate bolts in addition to the 6 in. slotted retrofit.

Figure 15 presents the typical retrofit procedure. A drill could not be placed near enough to the girder web to allow a pilot hole to be drilled at the bottom of the slot. So instead, the entire slot was flame-cut. The flame was applied to the connection plate at the side of the fillet weld and was not used to remove any part of the weld. This precaution was taken to ensure that the temperature of the web plate remained at an acceptable level. After the flame-cut slot was removed, all flame cut surfaces were smoothed with a hand-held pencil grinder. All remnants of the stiffener-connection plate and fillet weld in the flame-cut area were removed. Special attention was taken to ensure a very smooth radius and transition from the fillet weld to the web plate. The amount of web material removed during grinding was minimal. Figure 16 shows the 10 in. slotted retrofit and the positions of the three bolts that were removed in the second trial retrofit at that connection. Figure 17 shows the 6 in. slotted retrofit and corresponding locations of the two bolts removed during the second trial retrofit at that connection.

CHAPTER FOUR

TEST LOCATIONS

Two separate locations along the bridge spans with floortrusses were selected for testing. The pier location nearest to the instrumented details, as designated on the design drawings, identified these locations. The two locations were south of pier S3-11 and north of pier S3-4. The "S" designates southbound approach bridge piers. The pier S3-11 connections were at a girder depth of 106 in. and the pier S3-4 connections were at a girder depth of 126 in. These two locations were selected because all five locations with fatigue cracking identified by the AHD occurred at these two girder depths. The locations of these two sites along the six mile elevated sections of the bridge are shown in Figure 18. An enlarged view displays the location of these test sites relative to the tied arch main span. Pier S3-11 corresponds to Bent 38 on AHD maintenance drawings, while pier S3-4 corresponds to Bent 31. The AHD Maintenance Bureau referred to the pier location by the bent number. Floortruss numbering indicated how many floortrusses away from the pier, or bent, a certain tested location was.

The plate girders with transverse floortrusses at both locations tested were elements of three span continuous bridge sections. The positions of the two test locations along their respective three span sections appear in Figure 19. Floortruss-girder connections are present

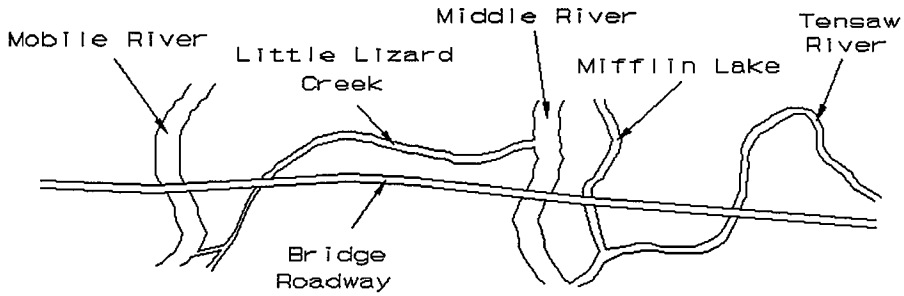

Plan View

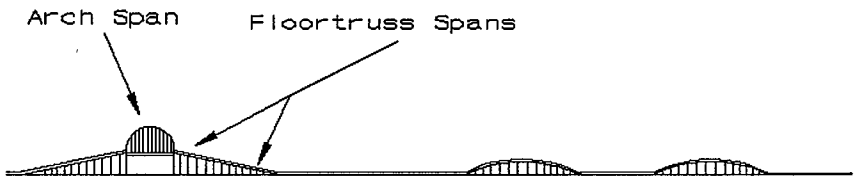

Elevation View

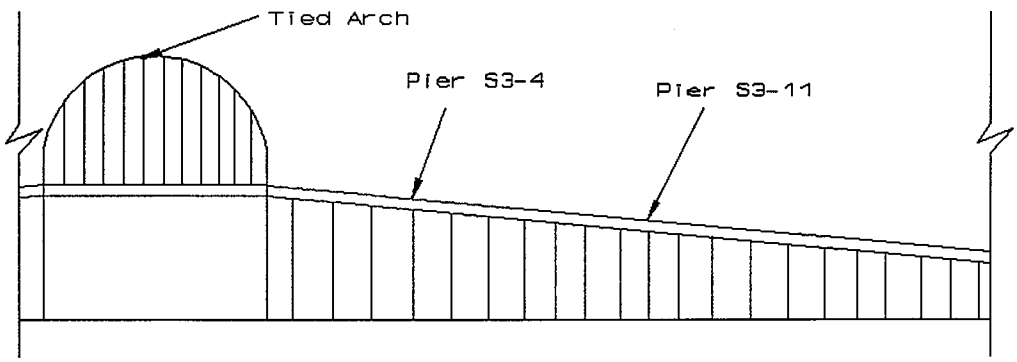

Enlarged View

Figure 18. Floortruss-Girder Test Locations on Mobile Delta Crossing Bridges

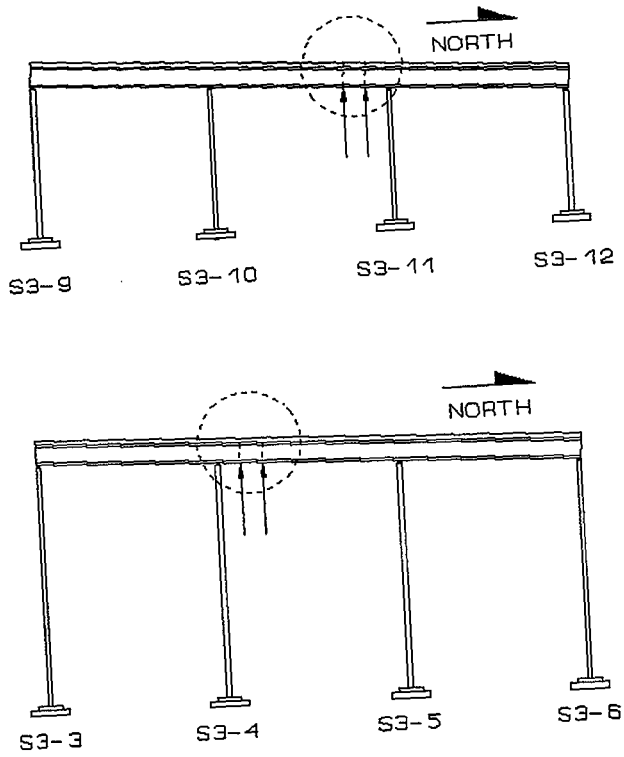

Figure 19. Position of Test Piers Along the Respective Continuous Spans

at three different girder depths along these bridges. Connections at the two shallowest depths, 106 in. and 126 in., were tested in this project.

A total of six different connections, three near each of the two test locations, were included in the testing. One connection at each of the two test locations was tested after a slotted connection plate retrofit was implemented. Figure 20 shows the locations of the six connections tested before retrofit and the two connections tested after retrofit along the respective single spans. In Figure 20, the west main girder was denoted girder 1 (G1) while the east girder was referred to as girder 2 (G2). Girder 1 was the outside girder (outside traffic lane) and girder 2 was the inside girder (inside traffic lane). The single span between pier S3-10 and pier S3-11 had six intermediate floortrusses spaced at 25 ft while the single span between pier S3-4 and pier S3-5 had seven intermediate floortrusses spaced at 25 ft. The transverse member at each pier location was a trussed frame. Connections at both ends of one floortruss at each of the two test locations were tested before retrofit. The tensile zone for the respective girder top flanges extended to 56.25 ft south of pier S3-11 and 59.375 ft north of pier S3-4. Therefore, the top flange was in tension at each connection tested.

The pier S3-11 connection chosen for retrofit, the outside girder connection of the first floortruss south of pier S3-11, had fatigue cracks in both the north and south side connection plate to web welds. The pier S3-4 connection chosen for retrofit, the outside girder connection of the second floortruss north of pier S3-4, did not have fatigue cracks. So retrofits were performed at a cracked and an uncracked connection which were at two different girder depths.

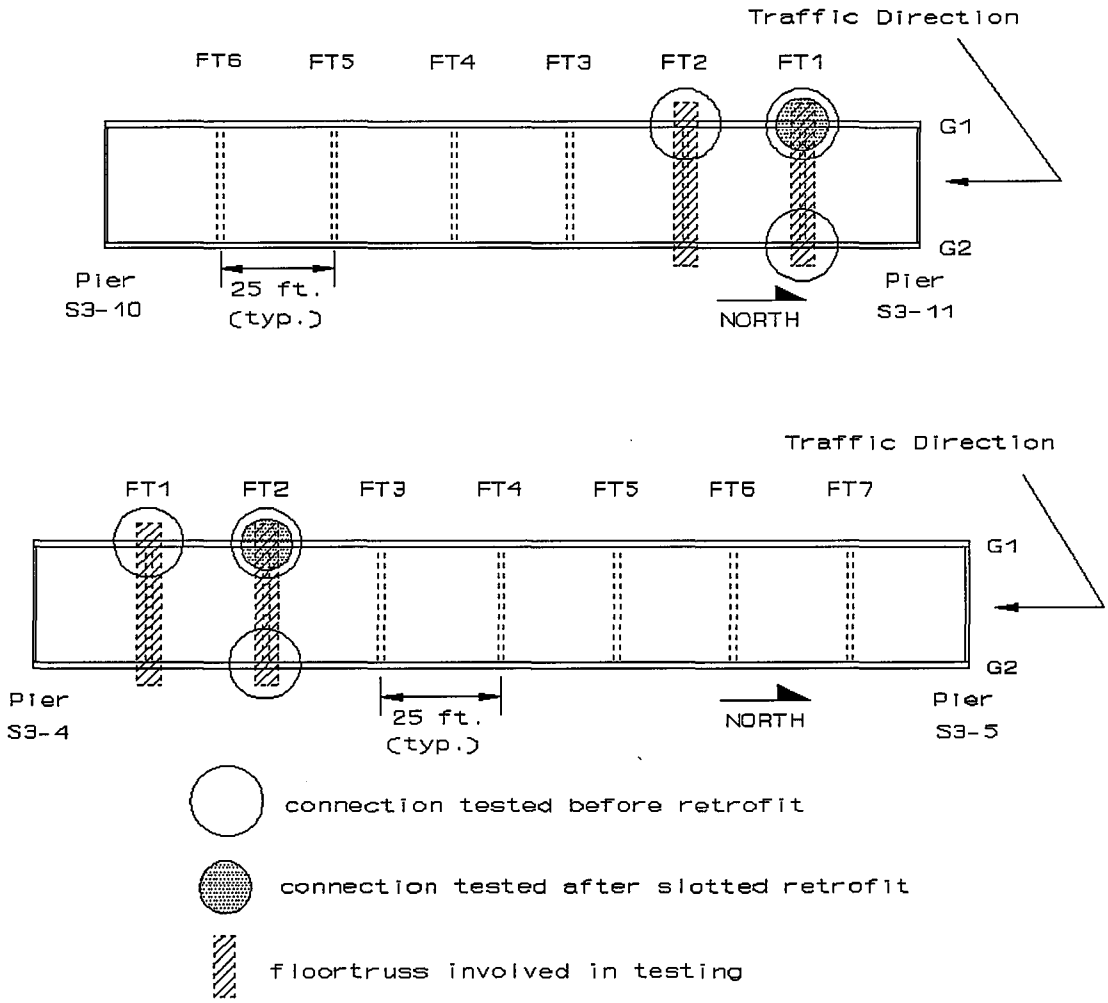

Figure 20. Plan View Showing Connections Tested Before and After Retrofit Along The Respective Single Spans of Each Continuous Span

Figure 21 displays the cross-section of the roadway at the floortruss-girder connections away from piers tested in this project. The locations of the web gap regions, connection plates, and truss members are shown in the figure. Stresses and displacements were measured in the web gap regions. Stresses were also measured on the connection plates and on the top and bottom chords and end diagonal chords.

The dimensions of the web gap regions at the six connections tested during this project varied due to the construction process. Most notably, the distance that the connection plate to web weld was left short of the tension flange was highly variable. A drawing depicting the web gap region dimensions appears in Figure 22. The "A" and "F" dimensions are always noted to be on the north side of the particular connection, and "B" and "G" are always the south side dimensions of the connection. The "C" dimension is commonly referred to as the stiffener clip. The web gap is commonly referred to as the distance from the bottom surface of the top flange to the toe of the connection plate to web weld, although very little out-of-plane distortion is expected to occur in the web-flange weld, as will be discussed in Chapter Seven. The web gap dimensions defined in Figure 22 and the five fatigue crack lengths that were identified in the welds at these six connections were field measured and appear in Table 2. The weld sizes (widths) measured sometimes varied roughly 20 percent from the north to the south side. These variations, although they may appear to be minor, had a significant impact on weld stress calculations which will be discussed in Chapters Seven and Eight.

The stringer size for the three stringers shown in Figure 21 was W24X61 at all connections tested. The connection plates were 1/2 in. thick and 7 in. wide.

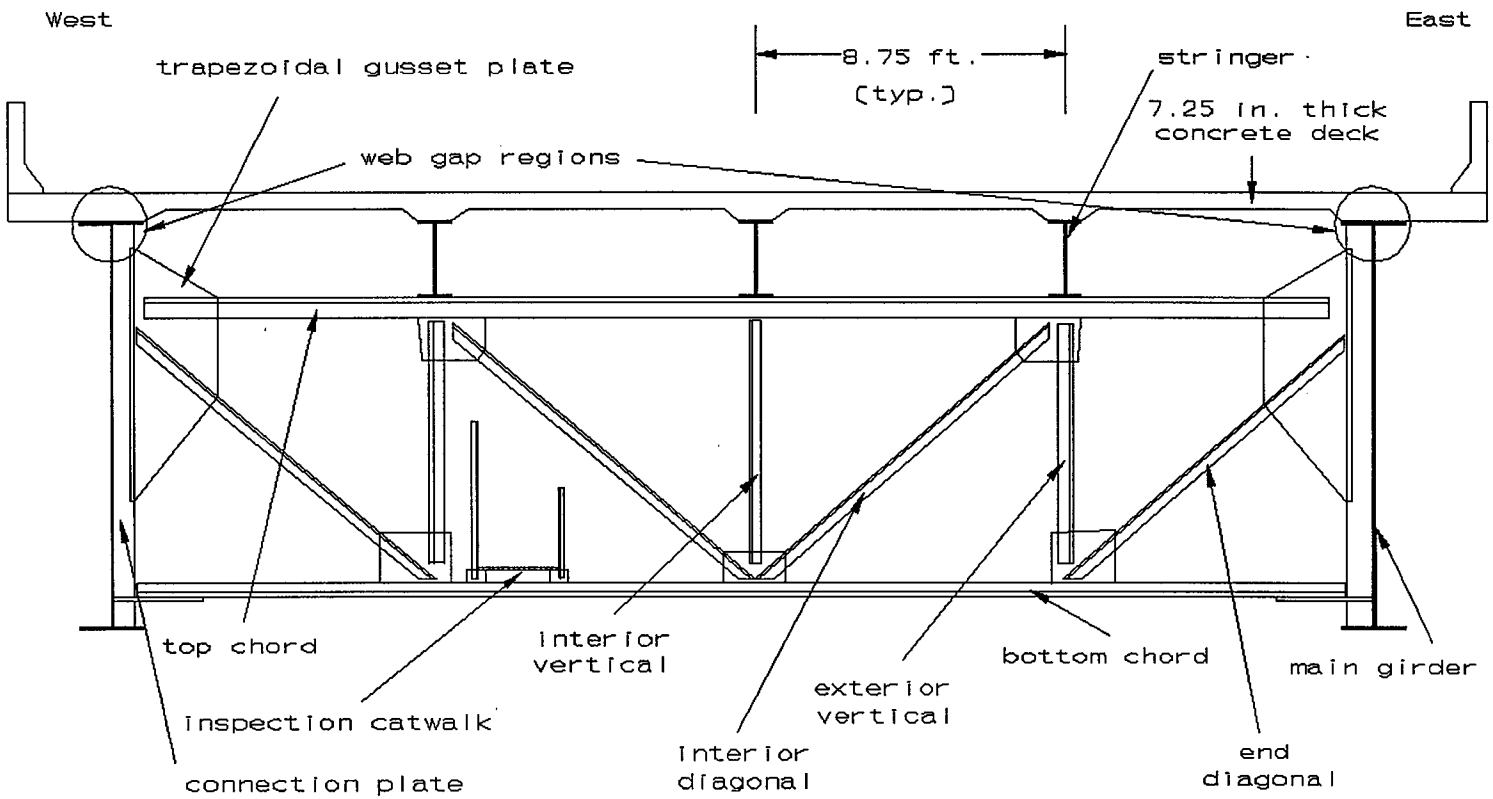

Figure 21. Cross-Section of Bridges at Floortruss-Girder Connections Away From Piers (Looking North)

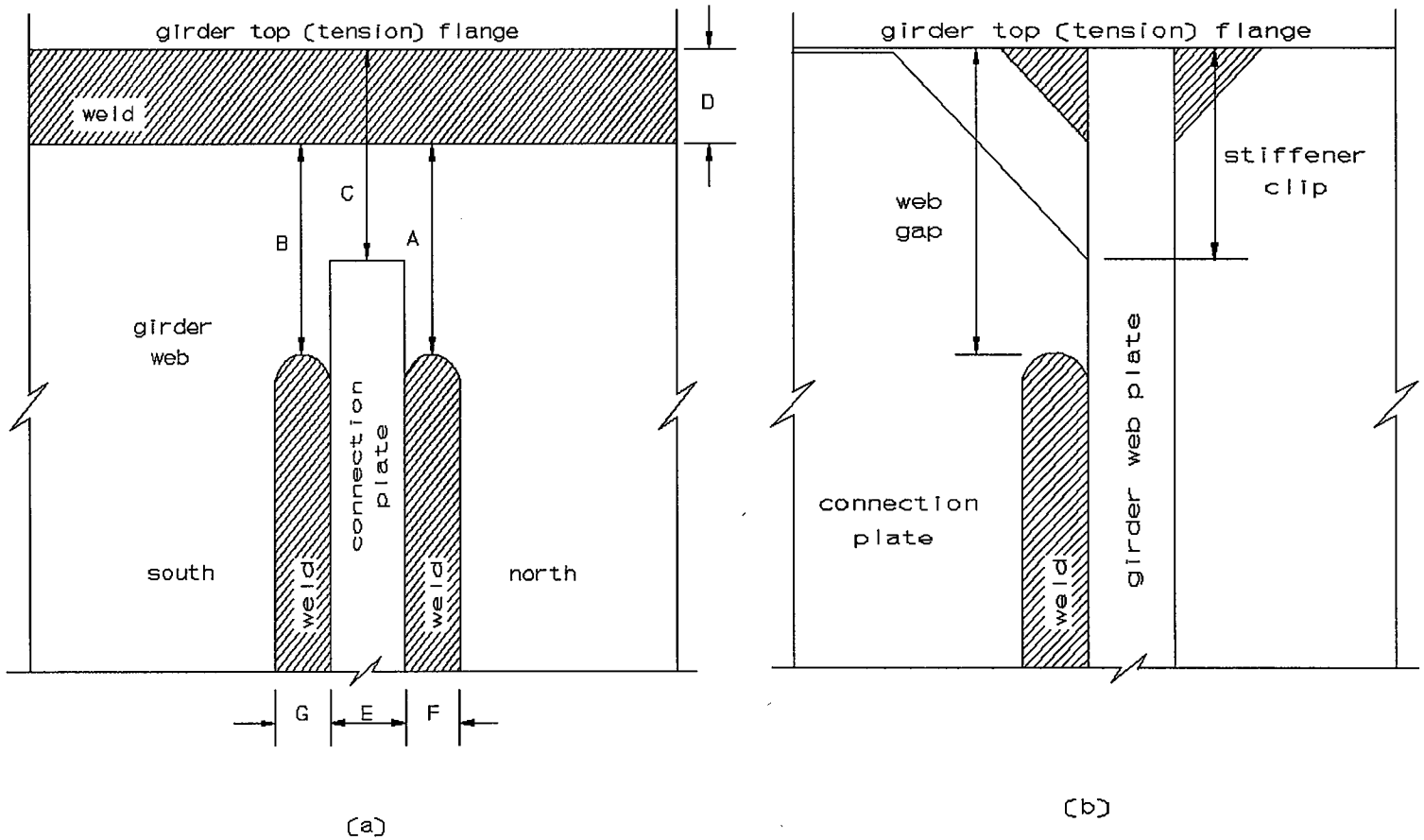

Figure 22. Typical Web Gap Region at Floortruss-Girder Connections Away From Piers: (a) Elevation of Inside Face of Girder; (b) Section View Looking in the Longitudinal Direction of the Bridge

Table 2. Web Gap Geometries and Crack Lengths

Variable Dimensions Defined in Figure 22 (in.)						
A	B	C	D	E	F	G
Pier S3-11: First Floortruss South, Outside Girder (106" Web)						
1.125* [0.375]	1.25* [0.375]	0.938	0.5	0.5	0.313	0.375
Pier S3-11: First Floortruss South, Inside Girder (106" Web)						
1.438* [0.25]	1.625* [0.25]	0.875	0.438	0.5	0.313	0.313
Pier S3-11: Second Floortruss South, Outside Girder (106" Web)						
0.938	0.938	0.938	0.469	0.5	0.375	0.375
Pier S3-4: First Floortruss North, Outside Girder (126" Web)						
1.0	1.125	0.938	0.438	0.5	0.313	0.375
Pier S3-4: Second Floortruss North, Outside Girder (126" Web)						
1.313	1.375	0.938	0.375	0.5	0.375	0.375
Pier S3-4: Second Floortruss North, Inside Girder (126" Web)						
1.25	0.875* [0.375]	1.0	0.375	0.5	0.313	0.375

* Weld crack present at this detail.
[ ] Length of weld crack during Summer 1992.

The dimensions of main plate girders at the connections tested appear in Table 3. "FT1" and "FT2" denote the first and second floortrusses away from the pier location as shown in Figure 20. The floortrusses are south of pier S3-11 and north of pier S3-4. The dimensions for the truss members appear in Table 4. All double angles in the top chord and diagonals were long legs back-to-back and oriented with the outstanding legs above the back-to-back legs. The bottom chords were double angles with short legs back-to-back and the outstanding legs beneath the short legs. Neutral axis dimensions in Table 4 were only included for members which were instrumented during the project.

Table 3. Plate Girder Dimensions

Floortruss	Top Flange Plate	Bottom Flange Plate	Web Plate
Pier S3-11 Locations			
Pier	3" X 22"	3" X 22"	7/16" X 106"
FT1	1 3/4" X 22"[a]	1 3/4" X 22"[a]	7/16" X 106"
FT2	1 3/4" X 22"	1 3/4" X 22"	7/16" X 106"
Pier S3-4 Locations			
Pier	2 3/4" X 24"	2 3/4" X 24"	1/2" X 126"
FT1	2 3/4" X 24"[b]	2 3/4" X 24"[b]	1/2" X 126"
FT2	1 3/8" X 24"	1 3/8" X 24"	1/2" X 126"

[a] Flange plates transition from 3" thick to 1 3/4" just inches north of FT1 and is 1 3/4" at FT1.

[b] Flange plates are 2 3/4" thick at FT1 and transition from 2 3/4" to 1 3/8" between FT1 and the next intermediate stiffener north of FT1 and remains 1 3/8" thick to the field splice north of FT2.

Table 4. Floortruss Member Double-Angle Dimensions

Description	Top[a] Chord	Bottom[a] Chord	End[a] Diagonals	Interior[a] Diagonals	Exterior[a] Verticals	Interior[a] Verticals
Pier S3-11: First Two Floortrusses South of Pier (106" Web)						
Size	6x4x3/4	6x4x3/4	8x4x3/4	7x4x1/2	5x7/2x3/8	7/2x3x3/8
Orientation[b]	LLBB	SLBB	LLBB	LLBB	LLBB	LLBB
Neutral Axis[c]	2.08 in.	1.08 in.	2.95 in.	----	----	----
Pier S3-4: First Two Floortrusses North of Pier (126" Web)						
Size	6x4x1/2	6x4x3/4	7x4x3/4	6x4x1/2	5x3x1/2	4x3x3/8
Orientation[b]	LLBB	SLBB	LLBB	LLBB	LLBB	LLBB
Neutral Axis[c]	1.99 in.	1.08 in.	2.51 in.	----	----	----

[a] Locations shown in Figure 21.
[b] Angle orientation is denoted by LLBB for long legs back-to-back and SLBB for short legs back-to-back.
[c] Distance to neutral axis from extreme fibers of outstanding legs. (See Figure 34)

CHAPTER FIVE

INSTRUMENTATION AND DATA ACQUISITION

Working Environment

The underside of the bridge at floortruss-girder connections was accessible by an inspection catwalk that was included by the bridge designers to facilitate maintenance and inspection. The catwalk was supported on the bottom truss chord members and was situated about six and a half feet west (toward the outside girder) of the bridge centerline and ran parallel to the main girders. A number of platforms located west of the outside lane curb wall provided access from the roadway to encaged ladders which descended to intermediate platforms and ascended to the inspection catwalk. The majority of equipment and materials used during field testing was transported along the catwalk.

In addition to the inspection catwalk, the AHD installed a network of reusable platforms and scaffolds that was accessible from the catwalk. This network was installed prior to the beginning of field work and further expedited the field testing. The location of the work platforms and scaffolds used at the pier S3-11 and pier S3-4 test locations appear in Figures 23 and 24, respectively. The reusable platforms consisted of aluminum planks supported by structural steel members.

The platforms were of two types: pier and connection. The pier platforms were bolted around the pier cap and served as the overall staging area for the test locations. All

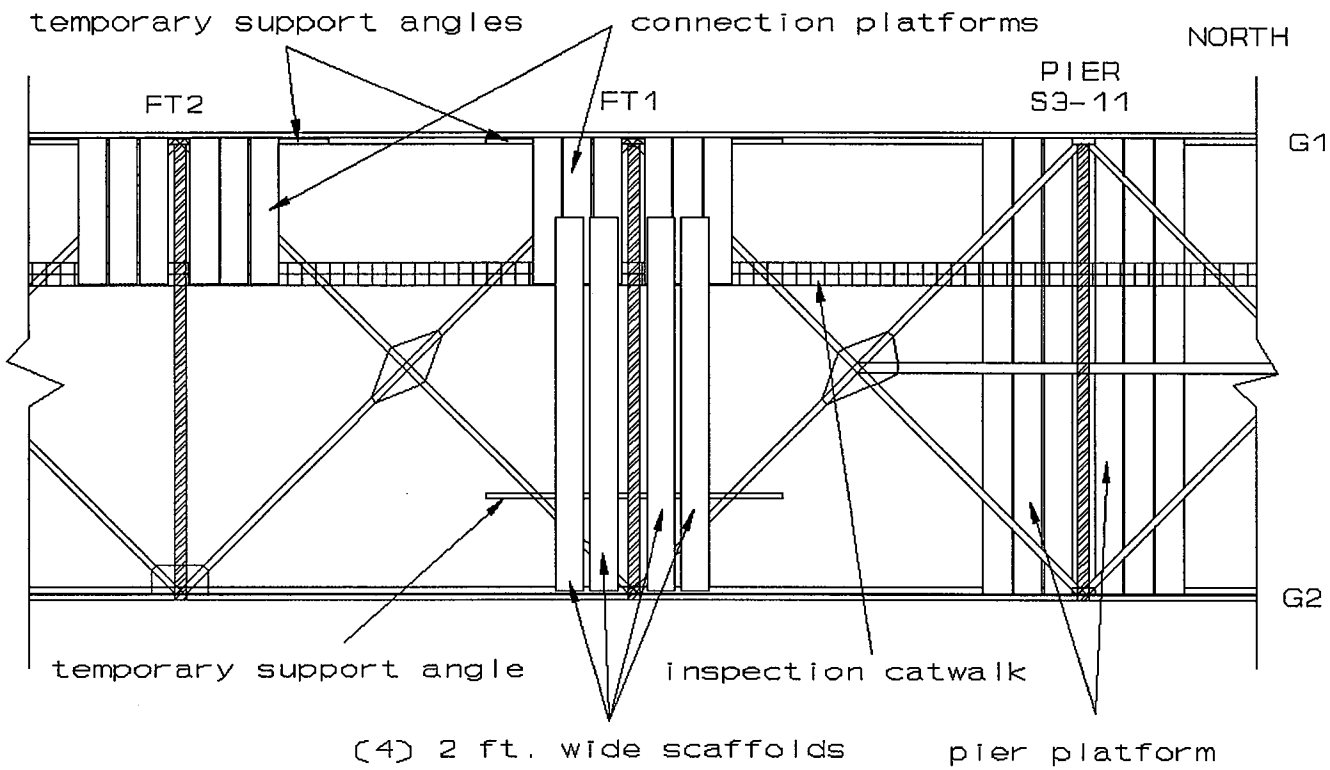

Figure 23. Plan View (with Concrete Deck Removed) of Work Platforms and Scaffolds Used at Pier S3-11 Test Locations

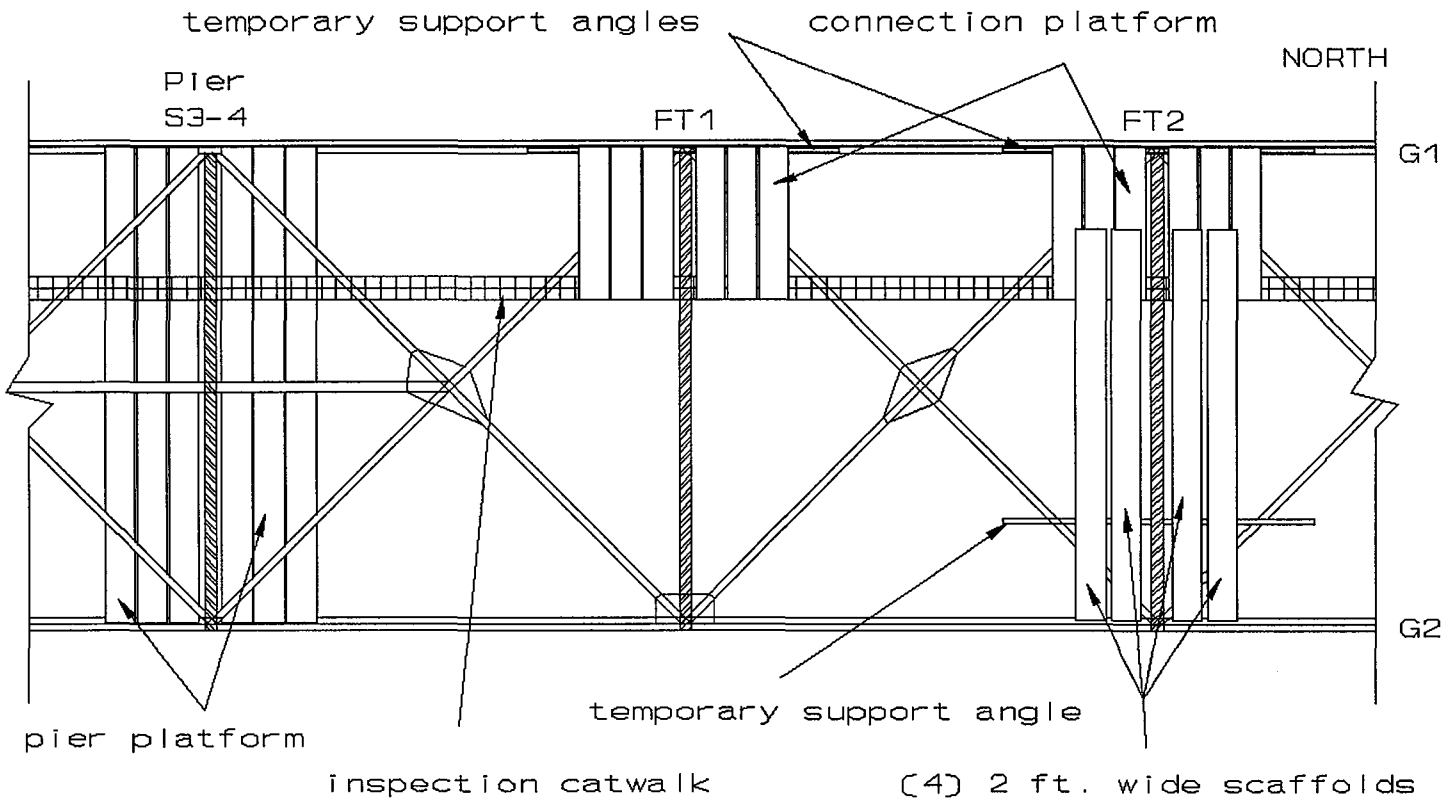

Figure 24. Plan View (with Concrete Deck Removed) of Work Platforms and Scaffolds Used at Pier S3-4 Test Locations

computer and data acquisition hardware was located on the pier platform, because the equipment would be subjected to less vibration with the platform bolted around the pier cap than it would if supported by the superstructure. Connection platforms were installed around the connections to be instrumented on the outside girder of the bridge. These connection platforms were placed lengthwise from the girder web face to the catwalk and supported by the catwalk and temporary support angles. The platforms were slightly sloped downward toward the girder web face. The connection platforms provided a small staging area and work platform for the instrumentation work.

A total of four scaffold planks (2 ft wide X 27 ft long), two on each side of the floortruss, were run transversely to access the inside girder connection at both locations. One end of the scaffolds was placed on the connection platform, and the other end was butted against the inside girder web face and supported by a temporary support angle that was clamped to the lateral cross bracing that ran between floortruss connections.

Use of the bucket and boom truck (Reach-All) during instrumentation of the bridges was minimal as compared to the previous summer's field testing due to greater access provided by the scaffolding. The Reach-All was used to relocate the portable generators and other sensitive and heavy equipment. It was also used to prepare and instrument gage locations on the outside faces of the main girders and other positions that could not be accessed by the network of platforms and scaffolds. Both test locations had the platform and scaffold networks installed at the same time allowing instrumentation work to proceed at one location while testing was being conducted at the other. This eliminated down time for preparation of the work site.

Instrumentation

The instrumentation used included electrical resistance strain gages for measuring surface strains on the girders and truss chords and linear variable differential transformers (LVDTs) for measuring the out-of-plane displacement of the connection plate. The strain gages were self-temperature compensating foil gages with polyamide encapsulation and preattached leads. The preattached leads allowed rapid soldering of the gages to light-gage stranded wires. All gages used before retrofit were manufactured by BLH Electronics, Inc. When gage supplies ran out, all 0.125 in. gage length gages used after retrofit were ordered from another gage maker, Measurements Group, Inc., and used for instrumentation. All gages used at these locations had a nominal resistance of 120 ohms and had a gage factor ranging from roughly 2.0 to 2.1.

Before gage installation, the weathered steel surface had to be prepared for the highly sensitive strain gages. The steel surface was initially ground with a hand held pencil bit electric grinder. Then a hand held 4-1/2 in. diameter electric disk grinder with 60 and 120 grit disks was used to further smooth the surface. Occasionally, a narrow belt grinder was used to grind surfaces that could not be reached by the disk grinder, like the web plate surface in the upper corners of the tight fit connection. The grinding removed all major surface imperfections of the steel and produced a shiny, mirror-like luster in the steel.

After completion of the grinding, local imperfections were removed in the positions the gages were to be applied by hand sanding with 200 and 400 grit sandpaper. The hand sanding removed the grit channels that were created in the steel from the grinding to create an extremely flat, smooth surface for bonding the gages. After hand sanding, the steel

surface appeared graphite-like, with a gun-metal gray color and dull luster. The gage had to be applied relatively soon after the 400 grit sandpaper was used, because the extremely humid air at these locations would readily form a rust film on this weathering steel. Once the surface was smooth, ball point pens were used to mark the center of the gage position with crosshairs. The ball point pen created visible crosshairs without sharply marring the surface and thereby prevented a sharp surface feature from cutting the gage foil or gage wires when the gage was attached to the surface. The surface was then cleaned with methyl-ethyl-ketone (MEK) and gauze pads.

An aluminum plate and precision tweezers were cleaned with MEK and gauze pads in preparation for gage mounting. The gages were held with the tweezers while being cleaned with MEK and placed on the aluminum plate. Cellophane tape was pressed firmly on the outside surface of the gage and then the gage was removed from the plate and positioned on the center of the crosshairs at the gage location. A Permabond 910 Adhesive Kit manufactured by BLH Electronics, Inc. was used to bond the gages to the metal surface. The adhesive was fast-curing (1 to 5 minutes full cure), acrylic-based adhesive with excellent electrical properties and good humidity resistance and required only 30 to 45 seconds of contact pressure to set the gage.

After the gage was set, it was checked to ensure no air bubbles were under the gage, and that the gage was still centered on the crosshairs. Then the cellophane tape was removed and any loose tape particles were removed with MEK and a gauze pad. A freon purge was then used to remove moisture and oil from the outside gage surface and adjacent surfaces, and the gage was immediately covered with drafting, or masking, tape. Electrical tape was

placed at the base of each gage under the lead wires to prevent grounding the wires to the metal surface and to prepare the gage for soldering.

A piece of light-gage stranded wire was soldered to each gage lead wire with a small diameter resin core solder. Each gage lead wire was then covered with electrical tape to ensure that neither wire would come into contact with the other lead wire or the steel bridge member. The masking tape was also covered with electrical tape to improve moisture resistance. The light-gage stranded wire was cut to extend over a short distance to a screw-type block, or cinch, connector. Five-minute epoxy was used to attach the cinch connectors to the surfaces of the bridge near the gage. All surfaces covered with electrical tape including the gages and wire connections were waterproofed by covering them with an adhesive backed neoprene pad. Three-wire grounded shielded cable, which reduced electrical noise effects, was used to connect the gages wired into the cinch connectors with the data acquisition system.

The cinch connectors allowed a rapid connection and disconnection process. Without the cinch connectors, the shielded cable would have to be directly wired to the gage and would subject the fragile gage leads to high tension from the shielded cable weight. The cinch connectors also enabled reuse of the shielded cable without severing a direct connection to the gage. Two of the three wires in the shielded cable were connected to one side of the strain gage, and the remaining wire was connected to the other side of the gage. The ground wire was unattached at the cinch connector end of the shielded cable. The end of the shielded cable that was connected to the data acquisition system was wired into screw terminal blocks (STBs) in a quarter bridge three-wire completion configuration. Each STB

had an eight channel, or gage, capacity. All ground wires from the shielded cables connecting to a single STB were wired to a common cinch connector and grounded to the ground terminal located on each STB.

All out-of-plane displacements were measured with GCD-121-250 Linear Variable Differential Transformers manufactured by Lucas Schaevitz, Inc. The devices were roughly 7.5 in. in length and had a dynamic measurement range of approximately +/- 0.25 in. and had a resolution of 0.0001 in. The LVDTs were attached to aluminum angles and bolted through the edge of the stay-in-place forms adjacent to the inside edge of the girder top flange. Attachment to the stay-in-place forms was thought to provide a fixed point for attachment since the forms were locked into place with the tension flange which was relatively immovable with the concrete deck poured right on top of it. The displacements of the web were relative to this nearly fixed top flange surface. The LVDTs measured the displacement of the connection plates at approximately half an inch below the bottom of the tension flange. This provided an indirect measurement of the out-of-plane displacement of the girder web plate in the web gap region plus a minor displacement due to the connection plate bending toward the bridge centerline. The typical LVDT arrangement is pictured in Figure 25.

The displacements after the slotted retrofits were measured at the same position as before retrofit and were expected to yield greater connection plate bending with the lengthened web gap. However, this connection plate bending effect was still believed to be minor.

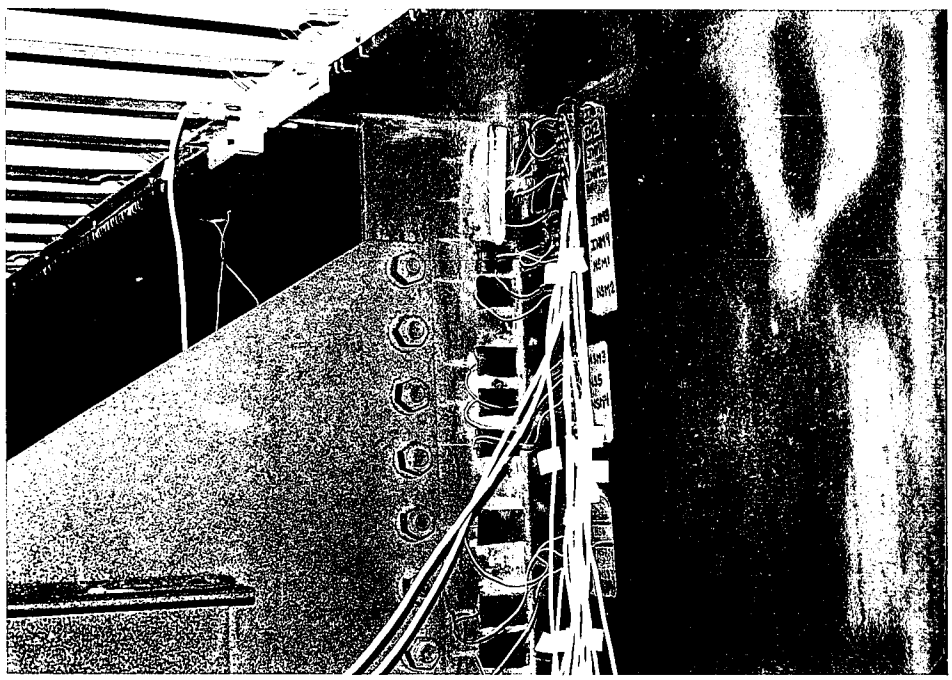

Figure 25. Typical LVDT Arrangement at Floortruss-Girder Connection

Before retrofit, the entire instrumentation process for all three connections and associated floortruss members at each connection for a test location took two to two and a half weeks. After retrofit since only one connection was instrumented for each major test location, full instrumentation was completed in two to four days.

Transducer Positions

Before retrofit over 110 transducers, both strain gages and LVDTs, were used at the pier S3-11 locations. After reviewing data at these locations, that number was trimmed to 90 transducers used at the pier S3-4 locations before retrofit. Roughly 30 transducers were used after retrofit at each connection of the two connections tested. Four areas at these test locations were instrumented with strain gages: the web gaps, the connection plates, the floortruss members, and the girder flanges. Normally, gages with 1/8 in. gage length were installed in the web gaps, on the connection plates, and on the bottom truss chord members. Gages with 1/4 in. gage lengths were used for top and diagonal floortruss members, while 3/8 in. gage lengths were used for girder flanges. Some deviations from these normal gage selections resulted from gage shortages experienced during the field tests.

Figure 26 shows the typical gage locations and the numbering scheme for gages installed in the web gap region. The numbering scheme used for the testing at floorbeam-girder connections in the summer of 1991 was adopted for identification of gages placed in relatively the same positions during the summer of 1992. An "I" in the gage name represented a gage positioned on the inside of the web plate, while an "O" signified a gage positioned on the outside of the web plate. An "N" in the gage name denoted a gage

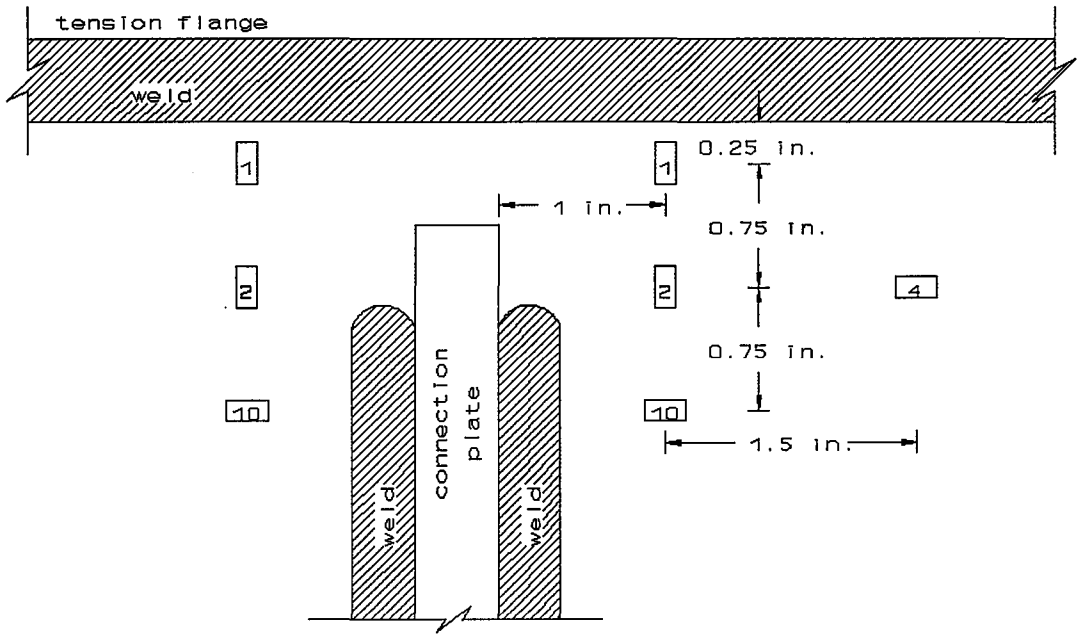

Figure 26. Numbering and Locations of Strain Gages on Girder Web Before Retrofit

position on the north side of the connection plate, while an "S" denoted a gage position on the south side of the connection plate. This notation applies to all figures. The number 1 and 2 gages measured strains in the vertical direction, while the number 4 and 10 gages measured strains in the horizontal direction. Some individual gages were omitted during the project after test data was examined from previous tests. The girder number, as defined in Chapter Four, was also used to define a single gage in the overall test configuration. For example, the number 1 web plate gage on the north side of the connection plate at the outside girder connection was denoted as gage ON1G1.

Figure 27 and 28 show the gage locations installed in the web gap region after retrofit at the pier S3-11 and pier S3-4 location, respectively. The number 1 and 2 gage positions were the same as before retrofit. The four gage locations near the retrofitted top of the connection plate weld were modified from previous tests and were only used on the north side of the connection plate on the inside face of the girder web plate. Therefore, these gages were referred to as INM1 through INM4 for inside, north side, modified gage position number 1 through 4. Gages 1 and 2 were oriented to measure strains vertically and to perform an extrapolation to the top of the connection plate weld, while the number 3 and 4 gages were oriented to measure strains horizontally to extrapolate to the side of the connection plate weld.

The numbering and locations of strain gages on the connection plate before retrofit appear in Figure 29. The gages were oriented to measure strains horizontally from the edge of the connection plate to web weld and were aligned one inch away from the web face. The trapezoidal connection plate that was bolted to the connection plate was omitted from Figure

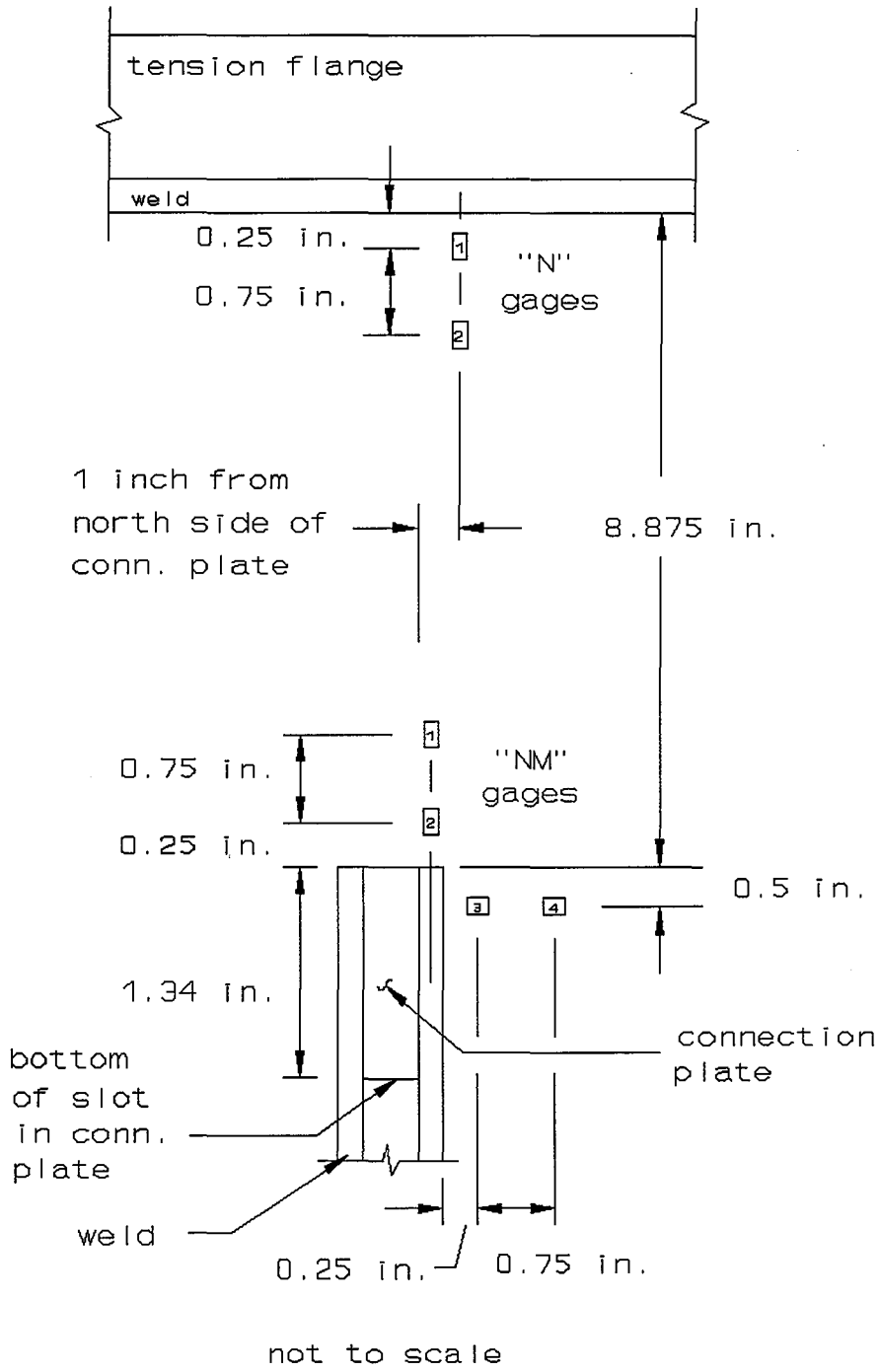

Figure 27. Numbering and Locations of Strain Gages on the Girder Web After Retrofit at the Outside Girder Connection of the First Floortruss South of Pier S3-11

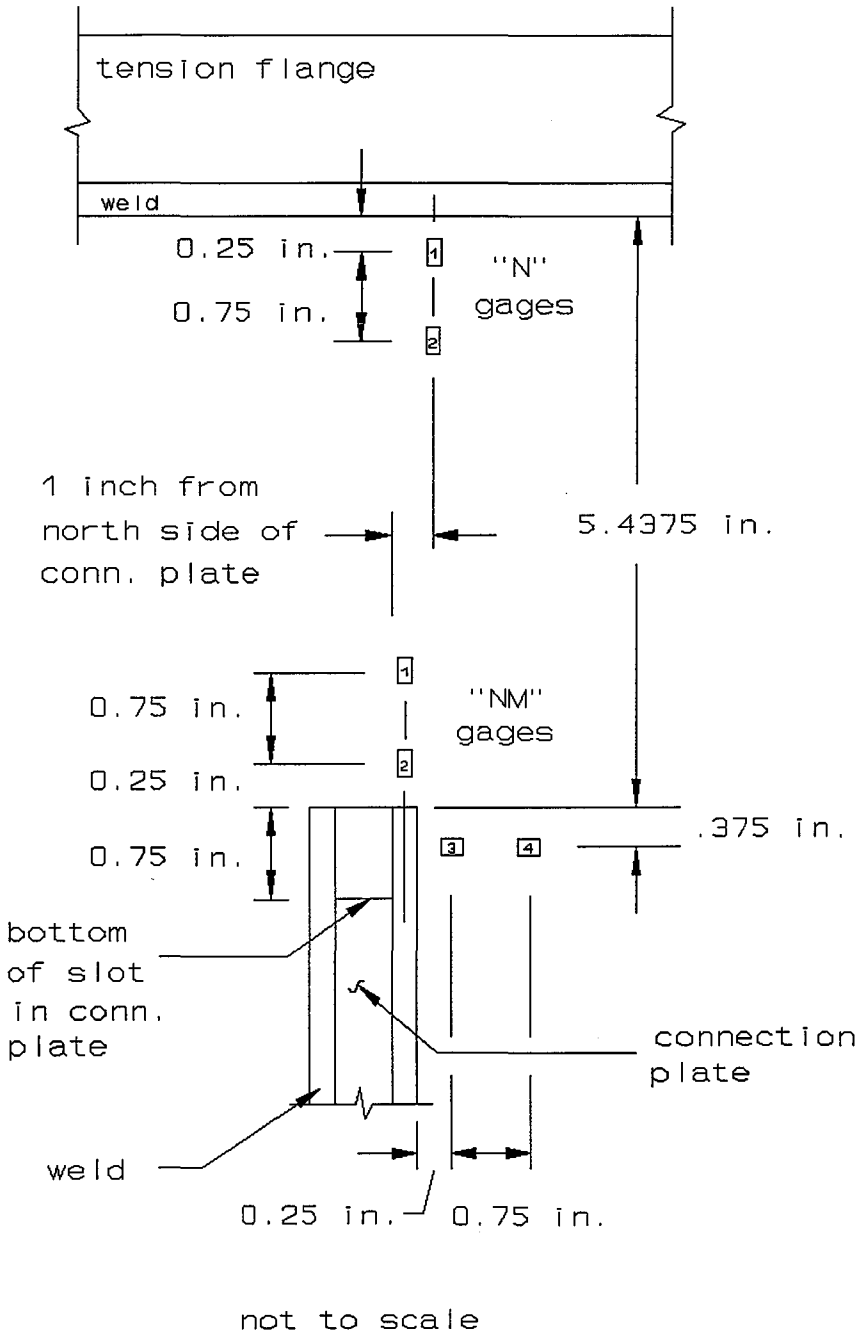

Figure 28. Numbering and Locations of Strain Gages on the Girder Web After Retrofit at the Outside Girder Connection of the Second Floortruss North of Pier S3-4

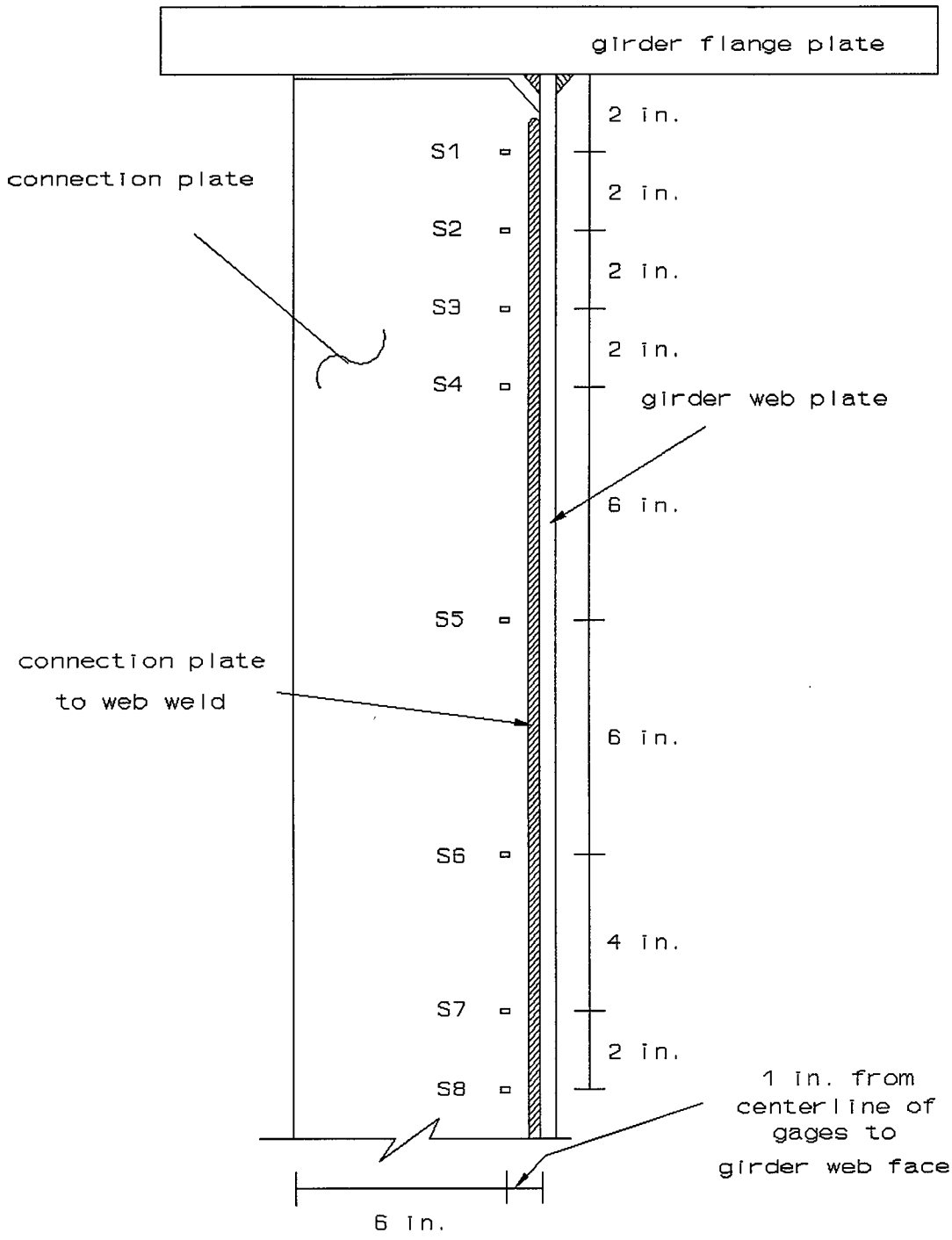

Figure 29. Numbering and Locations of Strain Gages on the Connection Plate Before Retrofit

29 for simplification. A stiffener (connection plate) gage was denoted by using an "S". Additionally, an "N" or an "S" was again used to specify the north or south side of the plate. NS1 denoted gage 1 on the north side of the plate, while SS1 denoted gage 1 on the south side of the plate.

The numbering and locations of strain gages on the connection plate after retrofit at the pier S3-11 and S3-4 location appear in Figure 30 and 31. Gage numbering was modified from the before retrofit status at both connections tested after retrofit. The number 6 gage location was found to be in a zone on the plate that experienced nearly pure bending behavior, as will be described in Chapter Seven, and was chosen after data analysis as a low point for gage location on the connection plate. For both connections tested after retrofit the number 5 and 6 gage positions were retained and not modified from the before retrofit gage locations. The gage names for these gages were, as before, NS5, SS5, NS6, SS6.

Four additional positions were chosen at both connections for modified gage locations. The modified gage positions were chosen relative to the number 5 and 6 gages and the bottom of the retrofit radius edge. The modified number 1 gage position was located 3/8 in. below the bottom of the retrofit radius edge which was centered at 7/8 in. from the girder web face. This location was used at both retrofitted connections. A 1 in. distance was used for positioning all gages away from the girder web face, except the modified number 1 gage. The slot width for both connections retrofitted was approximately 1.375 in. "SM" was used to denote the four stiffener gages in modified positions. NSM2, for instance, would denote the north side connection plate gage in the modified position number 2. The four modified

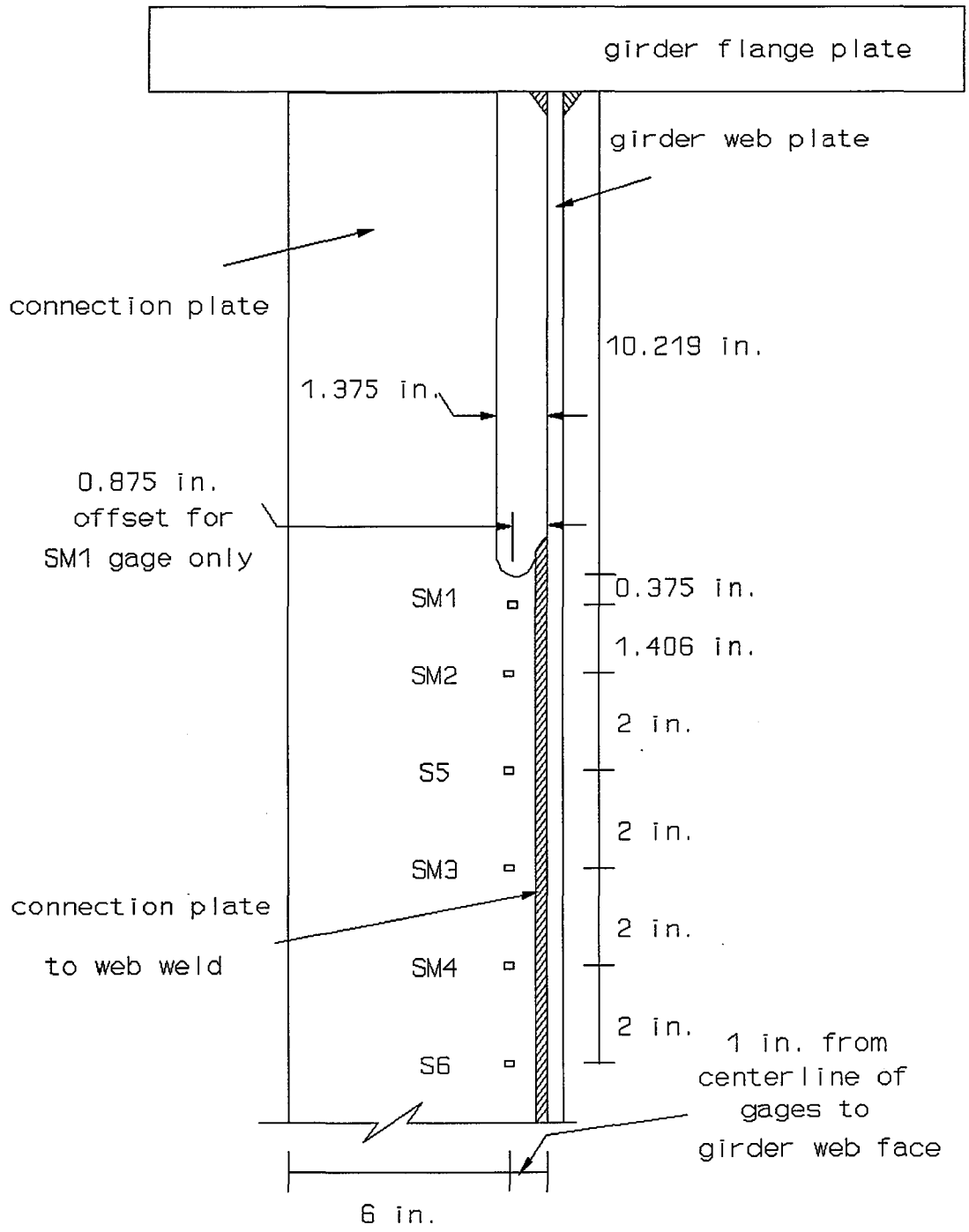

Figure 30. Numbering and Locations of Strain Gages on the Connection Plate at the Outside Girder Connection of the First Floortruss South of Pier S3-11 After Retrofit

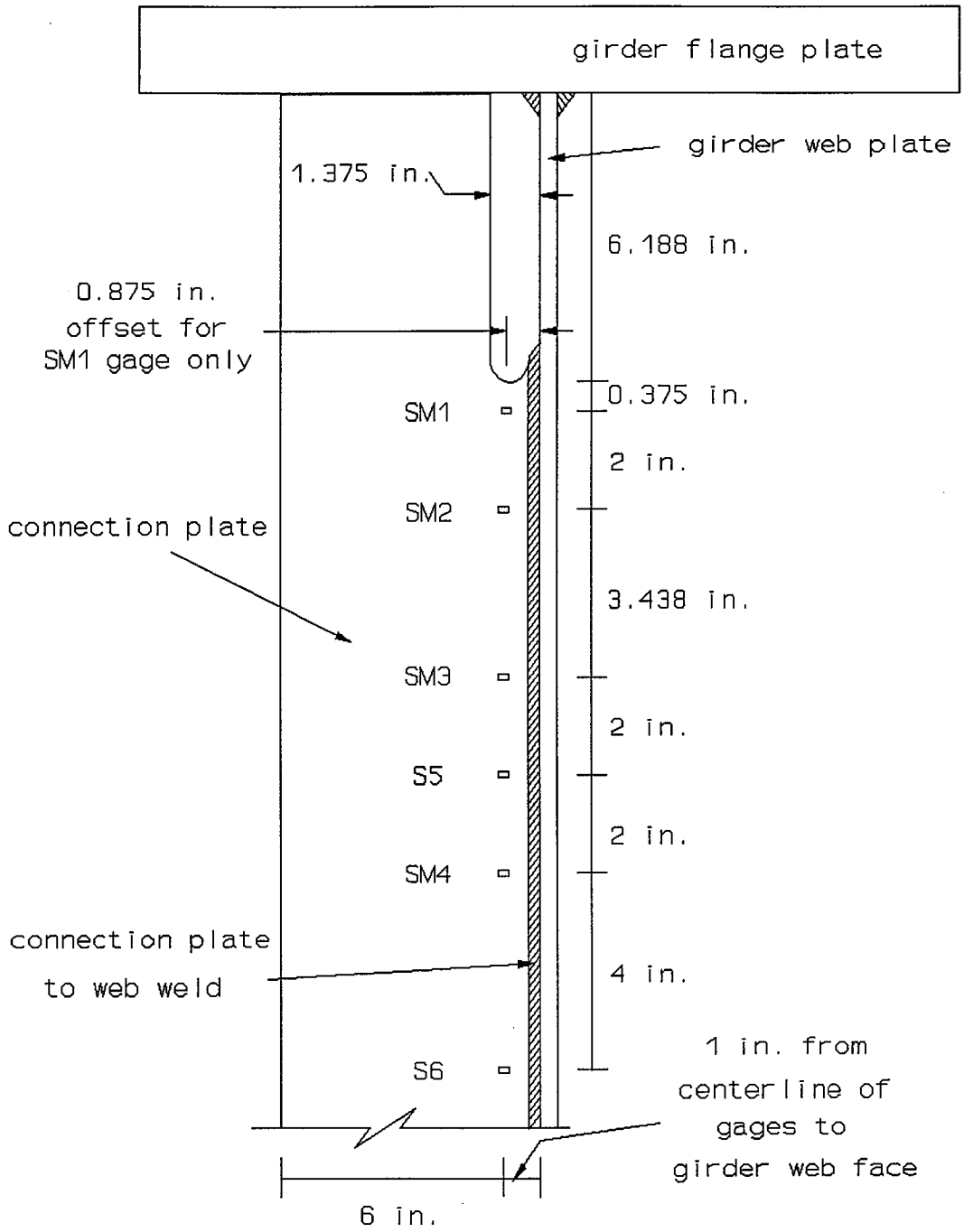

Figure 31. Numbering and Locations of Strain Gages on the Connection Plate at the Outside Girder Connection of the Second Floortruss North of Pier S3-4 After Retrofit

gage positions differed between the two connections tested after retrofit due to the difference in slot lengths.

For the majority of the truss instrumentation, only the centroidal axes of the double angles of the outer truss members nearest to the connections tested were chosen for gage locations. The truss members were shown in Figure 21 and the truss double angle dimensions were shown in Table 4. The neutral axis dimension for each floortruss type that was gaged was also included in the table. The top chord, bottom chord, and end diagonals near the connection tested were chosen for gage locations. Figure 32 shows the typical locations of the gages and fill plates, commonly called spacer plates, on the outer truss members of the transverse floortrusses at the pier S3-11 locations. Measurements for gages located on top and diagonal members were made relative to the inside edge of the trapezoidal gusset plate, and the dimensions appear above the truss members in the figure. The bottom chord gages were located relative to the inside edge of the fill plate that was bolted between the bottom truss chord double angles. The fill plate was butt welded to the web gusset plate. The top and bottom chord and end diagonal gage positions were referred to as "TC", "BC", and "DC"; respectively. NTC denoted the north side top truss gage, while STC denoted the south side top truss gage. The dimensions shown in Figure 32 below the top and diagonal members are the distances from the inside edge of the trapezoidal gusset plate to the centerline of the spacer plates. The dimensions shown below the bottom truss chord member are the distances from the inside edge of the web gusset fill plate to the centerline of the spacer plates.

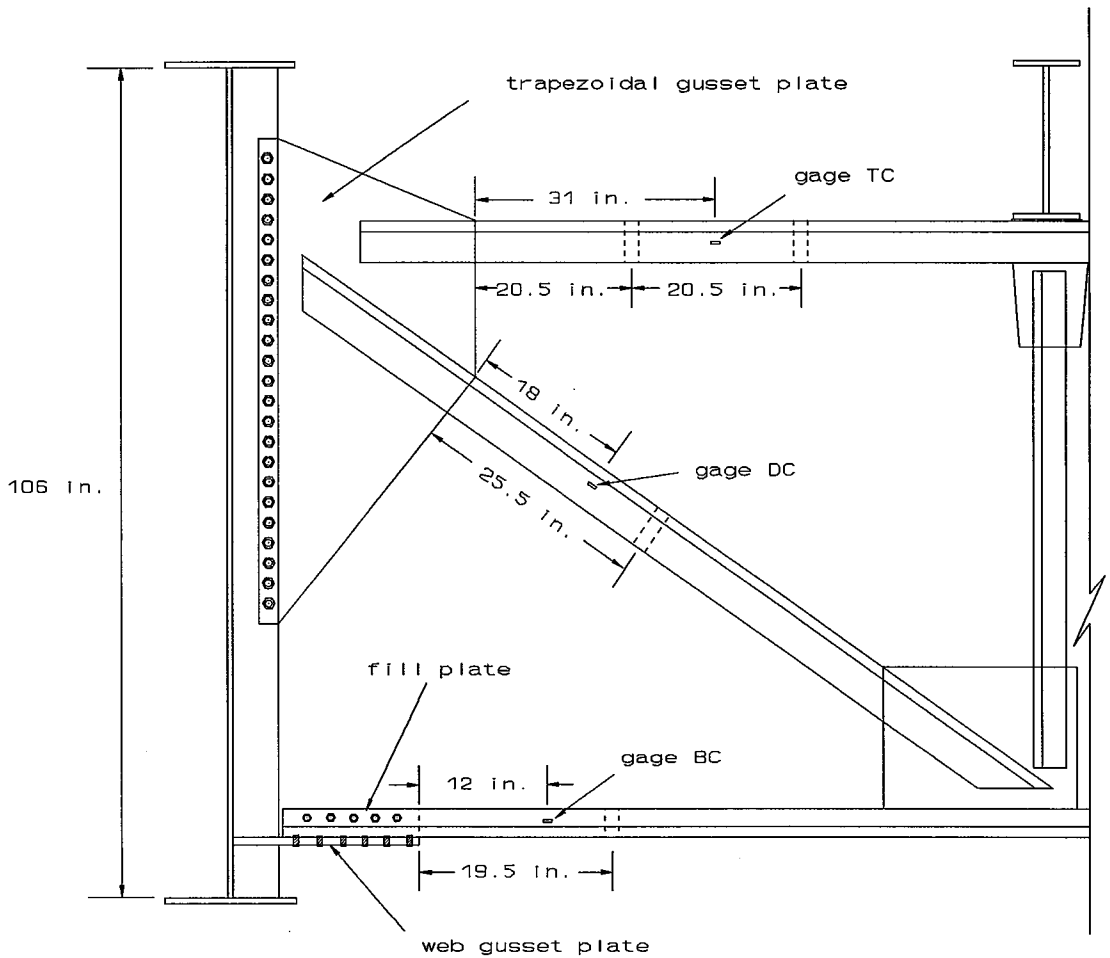

Figure 32. Typical Gage and Fill Plate Locations on Floortruss Members at Pier S3-11 Locations (Looking North)

The dimensions shown in Figure 32 apply to all three connections tested at the pier S3-11 locations, except for the inside girder connection at the first floortruss south of pier S3-11. At that location the single spacer on the diagonal is centered at 22 in., instead of 25.5 in., from the inside edge of the trapezoidal gusset plate. The gage location on the diagonal truss at that particular connection was chosen to be centered at 15 in., instead of 18 in., away from the inside edge of the plate. The typical locations of the gages and fill plates on the outer truss members of the transverse floortrusses at pier S3-4 locations appear in Figure 33. The dimensions in this figure apply to all three connections tested at the pier S3-4 locations. Figure 34 shows side and cross-section views of how the gages were positioned on the double angles of the three truss chord members nearby all tested connections. The overall double angle dimensions and distances to the neutral axes varied for pier locations and were noted in Table 4. Each gage was centered on the neutral axis and was oriented to measure strains longitudinally along the floortruss member. All dimensions and configurations in Figures 32 through 34 apply to the after retrofit tests, since no modifications were made to the truss members during the retrofit.

Figure 35 shows the locations of girder flange gages near the connections that were tested. The numbering scheme was the same as was used for the floorbeam-girder connections tested during the summer of 1991. The top (tension) flange gage, number 8, and the bottom (compression) flange gage, number 9, were oriented longitudinally along the main girder flange to measure in-plane bending of these plate surfaces. These flange gages were originally mounted, at pier S3-11 connections, one-half the distance from the girder web face to the girder flange edge and 12 in. from the face of the connection plate. The web gusset

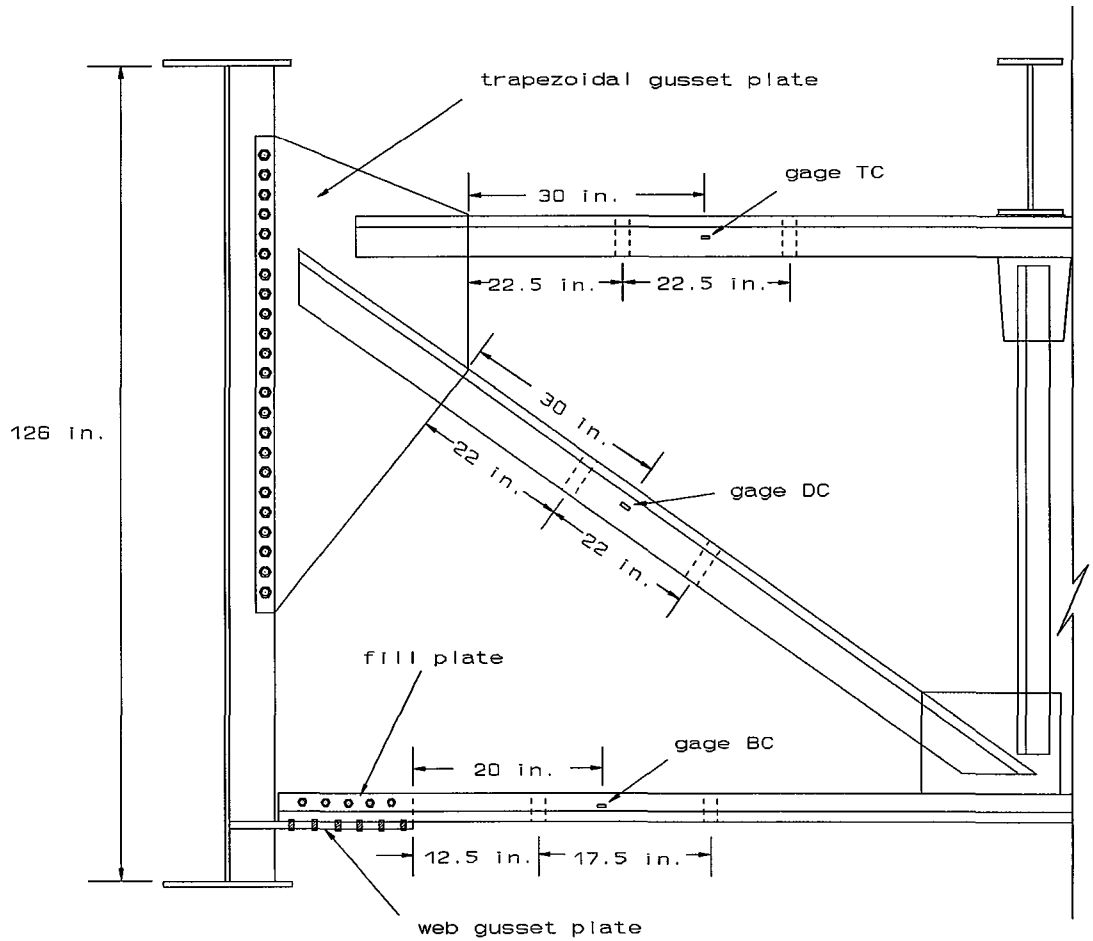

Figure 33. Typical Gage and Fill Plate Locations on Floortruss Members at Pier S3-4 Locations (Looking North)

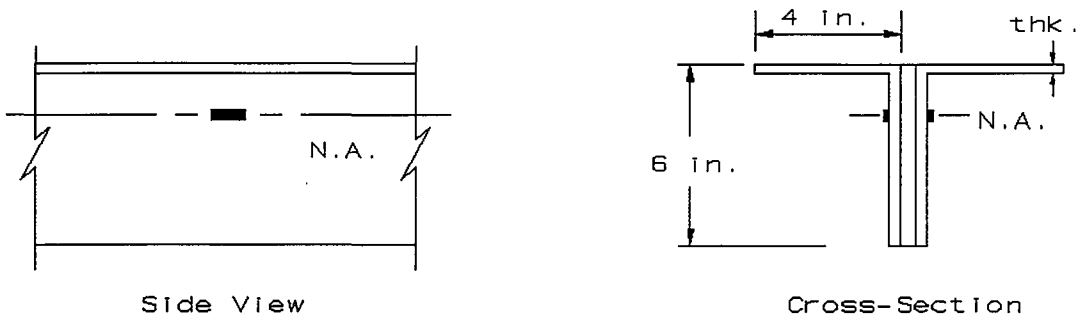

(a)

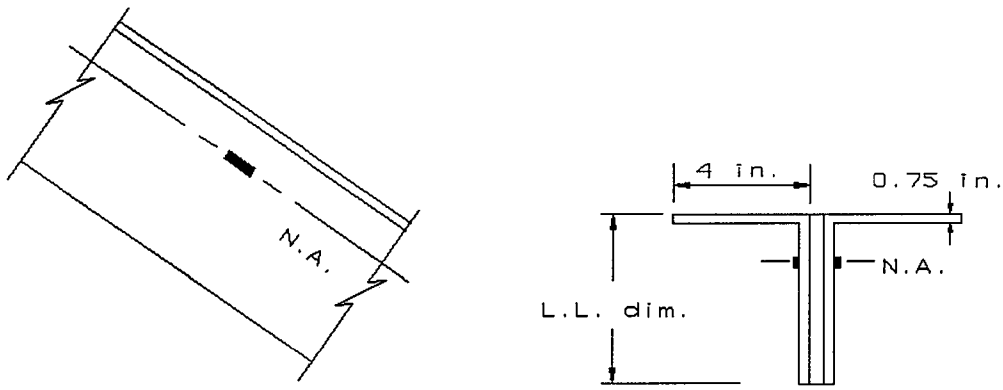

(b)

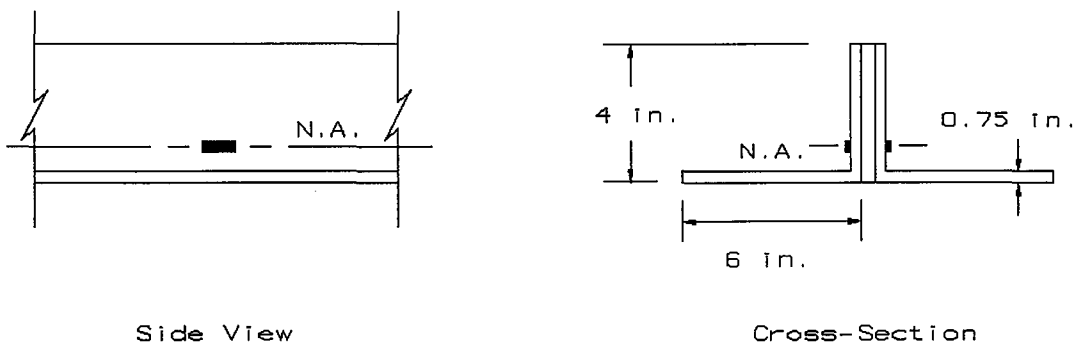

(c)

Figure 34. Gage Locations on the Neutral Axes of the Truss Members: (a) Top Chord; (b) End Diagonal; (c) Bottom Chord

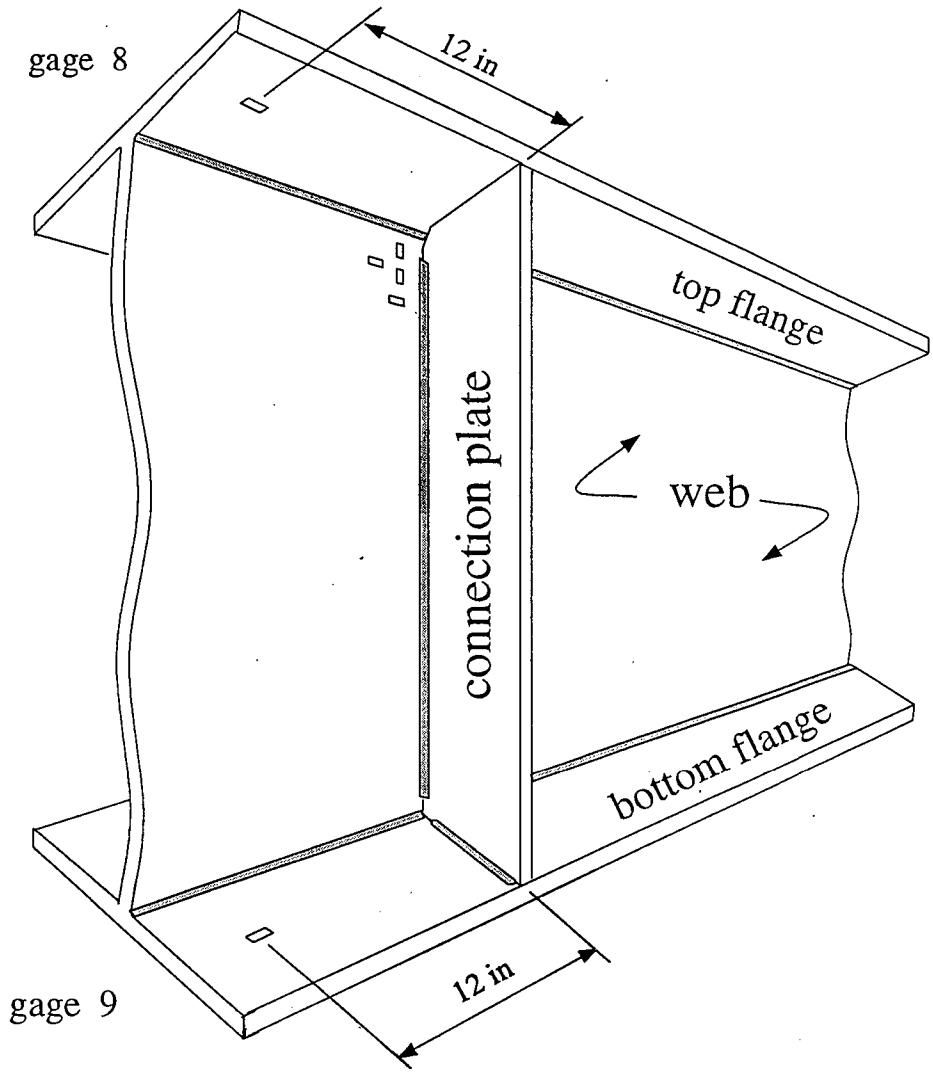

Figure 35. Numbering and Locations of In-Plane Bending Gages on Girder Flanges

plate that was welded to the girder web face at approximately 6 in. above the top of the bottom flange surface hampered instrumentation of the bottom flange gages. Therefore, the gage positions for the top and bottom girder flanges were moved to 24 in. from the connection plate face for the pier S3-4 locations. All flange gages were located south of the respective connection plate at each connection for all connections tested, except at the outside girder connection of the second floortruss south of pier S3-11. There the gages were mounted north of the connection plate, since there was a girder field splice just south of the connection.

Tables 5 and 6 list the types of gages installed at each of the six connections tested before retrofit. The beginning "I" or "O" designates either inside or outside details, which only varied for web plate and girder flange gages. The trailing "N" or "S" designates any type gage on either the north or south side of the connection plate. The "I" or "O" designations shown in the gage tables only apply to the web plate and girder flange gages. The connection plate and truss gages were considered as inside details for these gage tables. The trailing "N" or "S" was the only designation in the gage location column needed to identify to connection plate and truss gages. However, in the gage location column, these locations were referred to as "IN" or "IS" to be consistent with the web plate and girder flange gage designations. The gage sizes were denoted "S" for the smallest gage size used during the project (0.125 in. gage length), "M" for the middle-sized gage used (0.25 in. gage length), and "L" for the largest gage used (0.375 in. gage length). Tables 7 and 8 present the types of gages installed at each of the two connections tested after the slotted retrofits. All gages on the web plate and connection plate that were installed at modified locations

Table 5. Gages Installed at Pier S3-11 Locations Before Retrofit

Location[a]	Web Plate[b]				Connection Plate[b]								Truss[b]			Flange[b]	
	1	2	4	10	1	2	3	4	5	6	7	8	TC	DC	BC	8	9
(a) Gages on Outside Girder at the First Floortruss South																	
IS	S	S		S	S				S			S	M	M	S	L	L
OS	S																
IN	S	S	S	S	S	S	S	S	S	S	S	S	M	M	S		
ON	S	S															
(b) Gages on Inside Girder at the First Floortruss South																	
IS	S	S		S	S				S			S	M	M	S	L	L
OS	S																
IN	S	S	S	S	S	S	S	S	S	S	S	S	M	M	S		
ON	S	S															
(c) Gages on Outside Girder at the Second Floortruss South																	
IS	S	S		S	S				S			S	M	M	S		
OS	S																
IN	S	S	S	S	S	S	S	S	S	S	S	S	M	M	S	L	L
ON	S	S															

[a] Gage location and numbering defined in Figures 26 through 35; IS= Inside, South; OS= Outside, South; IN= Inside, North; ON= Outside, North.

[b] Gage types are: S= FAE-12-12-S6EL, 1/8 in. gage length (BLH Electronics, Inc.),
M= FAE-25-12-S6EL, 1/4 in. gage length (BLH Electronics, Inc.),
L= FAE-37-12-S6EL, 3/8 in. gage length (BLH Electronics, Inc.).

Table 6. Gages Installed at Pier S3-4 Locations Before Retrofit

Location[a]	Web Plate[b]				Connection Plate[b]								Truss[b]			Flange[b]	
	1	2	4	10	1	2	3	4	5	6	7	8	TC	DC	BC	8	9
(a) Gages on Outside Girder at the First Floortruss North																	
IS	S	S		S	S				S			S	M	M		L	L
OS																	
IN	S	S	S	S	S	S	S	S	S	S	S	S	M	M	S		
ON	S	S															
(b) Gages on Outside Girder at the Second Floortruss North																	
IS	S	S		S	S							S	M	M		L	L
OS																	
IN	S	S		S	S	S	S	S	S	S	S	S	M	M	S		
ON	S	S															
(c) Gages on Inside Girder at the Second Floortruss North																	
IS	S	S		S	S							S	M	M		L	L
OS																	
IN	S	S		S	S	S	S	S	S	S	S	S	M	M	S		
ON	S	S															

[a] Gage location and numbering defined in Figures 26 through 35; IS= Inside, South; OS= Outside, South; IN=Inside, North; ON= Outside, North.

[b] Gage types are: S= FAE-12-12-S6EL, 1/8 in. gage length (BLH Electronics, Inc.),
M= FAE-25-12-S6EL, 1/4 in. gage length (BLH Electronics, Inc.),
L= FAE-37-12-S6EL, 3/8 in. gage length (BLH Electronics, Inc.).

Table 7. Gages Installed at the Outside Girder Connection of the First Floortruss South of Pier S3-11 After Retrofit

	Web Plate[b]						Connection Plate[b]						Truss[b]			Flange[b]	
Location[a]	1	2	M1	M2	M3	M4	M1	M2	5	M3	M4	6	TC	DC	BC	8	9
IS							S	S	S	S	S	S	M	M	S	L	L
OS																	
IN	S	S	S	S	S	S	S	S	S	S	S	S	M	M	S		
ON	S	S															

[a] Gage location and numbering defined in Figures 26 through 35; IS= Inside, South; OS= Outside, South; IN= Inside, North; ON= Outside, North.

[b] Gage types are: S= EA-06-125BT-120, 1/8 in. gage length (Measurements Group, Inc.),
M= FAE-25-12-S6EL, 1/4 in. gage length (BLH Electronics, Inc.),
L= FAE-37-12-S6EL, 3/8 in. gage length (BLH Electronics, Inc.).

Table 8. Gages Installed at the Outside Girder Connection of the Second Floortruss North of Pier S3-4 After Retrofit

	Web Plate[b]						Connection Plate[b]						Truss[b]			Flange[b]	
Location[a]	1	2	M1	M2	M3	M4	M1	M2	M3	5	M4	6	TC	DC	BC	8	9
IS							S	S	S	S	S	S	M	M	S	L	L
OS																	
IN	S	S	S	S	S	S	S	S	S	S	S	S	M	M	S		
ON	S	S															

[a] Gage location and numbering defined in Figures 26 through 35; IS= Inside, South; OS= Outside, South; IN=Inside, North; ON= Outside, North.

[b] Gage types are: S= EA-06-125BT-120, 1/8 in. gage length (Measurements Group, Inc.),
M= FAE-25-12-S6EL, 1/4 in. gage length (BLH Electronics, Inc.),
L= FAE-37-12-S6EL, 3/8 in. gage length (BLH Electronics, Inc.).

were denoted by an M. For example, "M1" denotes a number 1 gage at a modified location. All other gage locations were denoted similar to Tables 5 and 6.

Data Acquisition

All field test data during the summer of 1992 was collected with a MEGADAC 3008AC dynamic data acquisition system (Technical Manual 1991). The unit was manufactured by OPTIM Electronics Corporation and was capable of recording data from multiple channels at an overall rate of 25,000 samples per second. A maximum of thirty-two channels could be utilized with this unit, but typically, only twenty-seven were used. For a typical test 24 channels were used for strain gages, and 3 channels were used for LVDTs. The three LVDTs that were used at each test site were wired into a single connector that was plugged into one eight channel card. Therefore, only three of these eight channels could be used during testing. The number of gages that could be connected during any test, 24, was considerably less than the 40 gage capacity of the MEGADAC 2200C used during the summer of 1991. The data download time was much shorter with the newer MEGADAC and the capabilities of transforming the raw data as it was being sampled by the system were much greater than with the MEGADAC 2200C.

All data was recorded directly to the MEGADAC and automatically transferred to the hard drive of the computer. A 486 - 33 Megahertz personal computer equipped with a compatible software package TCS3000 (Technical Manual 1991) was used to drive the MEGADAC. Communication between the computer and MEGADAC was provided by an

IEEE-488 interface. At the end of each test day, the test data was copied to 3M DC2120 mini data cartridge tapes, each with a 120 Megabyte capacity.

Field testing experience with the previous MEGADAC data acquisition system indicated problems were likely when recording data under hot, humid conditions. Therefore, it was important that an environmental chamber be built to protect the computer and data acquisition system from the heat and humidity common in the Mobile Delta. The resulting chamber, shown in Figure 36, provided protection for the equipment and could be broken down into two sections for easier transport under the bridge. The lower section housed a 4500 BTU air conditioner, an LVDT power supply, a 486 - 33 Mhz computer, a 3-mode full protection 6-outlet spike/surge suppressor, and computer tapes, diskettes, and software manuals. The upper section was fully open to air movement from the lower section and housed the MEGADAC and the computer VGA monitor. The keyboard was connected through the two sections and placed on an external tray mounted waist-high in front of the head-high mounted monitor. The chamber was well cooled, but access doors on the chamber had to be kept open on many test days to prevent condensation from building up in the two sections. The new MEGADAC 3008AC was found to be notably more sensitive to the temperature and humidity in the chamber than the previous MEGADAC 2200C, used during the summer of 1991.

All electrical equipment housed in the environmental chamber was powered by one of two available portable AC generators. Each generator was transported under the bridge and was positioned on the catwalk at least one pier location away from the test site. The generators were located past the pier connections at least one pier away to reduce the noise

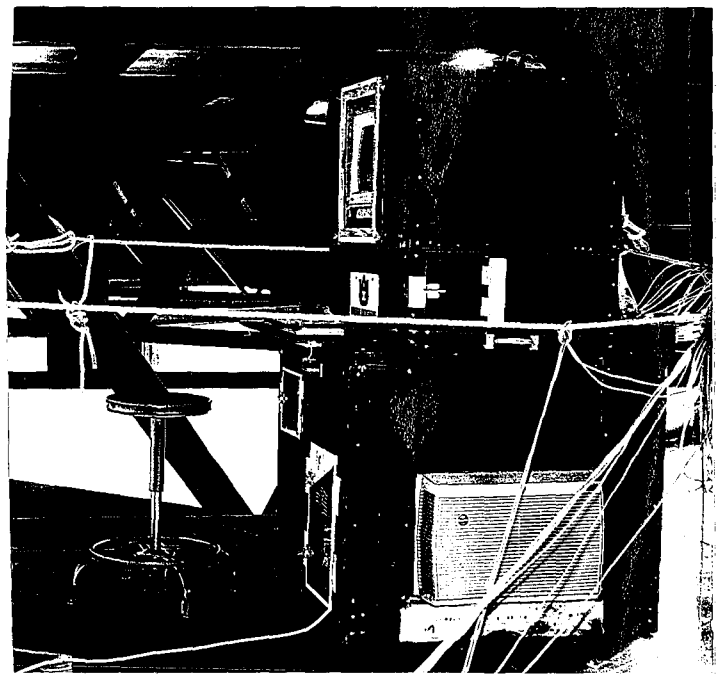

Figure 36. Environmental Chamber

level at the test site. Heavy duty extension cords were used to transfer the proper current and voltage over roughly two hundred feet to the environmental chamber without a significant loss in power.

CHAPTER SIX

DATA COLLECTION AND REDUCTION

All site preparation, instrumentation, and field testing for the six connections tested before retrofit was performed in a two month period from the third week of June 1992 through the second week of August 1992. The work and testing at the two floortruss connections tested after retrofit was performed simultaneously with the instrumentation and testing of the two tied arch floortrusses that were reported in Volume II of this report. All field activities were completed during the second week of September 1992. The preparation and testing at these locations was performed between the hours of 7:00 a.m. and 8:00 p.m. Monday through Friday.

After completely instrumenting a test site, the environmental chamber housing the computer and data acquisition system was assembled on the pier platforms installed by the AHD, as described in Chapter Five. The transducer cables extended from this instrumentation to the STBs at the data acquisition system. Then sample test runs were performed to identify defective gages and short circuits which required repair and to ensure that the transducer signals were within the balance interval required for data recording with the MEGADAC 3008AC. Such problems were easily identified if the transducer would not balance. After all gages and LVDTs were balanced, plots of strain and displacement versus time were viewed to determine whether the transducer appeared to experience either erratic

or unresponsive behavior that was not expected for the transducer location. Usually gage problems were corrected by restoring the integrity of the gage wiring and cable connections. If problems still existed the strain gage was replaced.

The sample run involved recording one or multiple truck crossings selected at random from the traffic and observing the measured results of all transducers. Individual gage magnitudes were noted to identify reasonable magnitudes for self triggering the data acquisition system to capture primarily the heavy trucks crossing the bridge. These magnitudes were also used for periodic future checks for identifying gage malfunctions and to illustrate the general structural behavior of the web gap, connection plate, girder flanges, and floortruss elements.

After the network of transducers were performing properly and all sample testing was completed, data collection began for trucks in controlled and uncontrolled test configurations. The controlled tests involved trucks of known weights and lane positions and were referred to as calibration tests. The uncontrolled tests involved random traffic conditions for trucks of unknown weights traveling in the normal traffic stream and were referred to as random truck tests.

CALIBRATION TESTS

The calibration tests were performed to investigate the structural behavior under known traffic loading and to determine the relationship between the stress range magnitudes and truck weights for select locations. The relationships between truck weight, position, and the out-of-plane displacement resulting from truck loading were also investigated. These

particular relationships were analyzed using the vertical force component measured in the diagonal truss chord. Due to the fact that the number of gages chosen for analysis exceeded the limited number of gage channels available through the data acquisition system, two sets of calibration tests had to be performed at both the test locations tested before retrofit. The first calibration test at each location was completed within three and one-half hours. Then the data was transferred from the computer hard drive to data tapes and new transducer cables were connected to 24 gage channels at the STBs and at the cinch connectors on the gage ends of the transducer cables. This took approximately one hour. The second calibration test at each major location was saved to new experiment files and was completed within three and one-half hours. A similar procedure was used for after retrofit calibration tests. At each of the two connections tested after retrofit a complete calibration test was performed with the slotted retrofit alone and then another complete calibration test was performed after AHD maintenance crews had removed the top two, or three (depending on the connection), connection plate bolts. Each calibration test after retrofit was completed in approximately three hours because a fewer number of truck positions was chosen for after retrofit analysis.

Two different test trucks, one 3-axle truck (dump truck) and one 5-axle truck (lowboy), were used for all floortruss-girder connections tested before and after retrofit. The 3-axle truck was typically loaded with sand or stone aggregate while the 5-axle truck was loaded with temporary concrete barrier walls. All test trucks and drivers were supplied by the AHD. Axle dimensions for each test truck and variables that were used to identify the specific axle of each truck appear in Figure 37. Tables 9 and 10 present the axle weights of

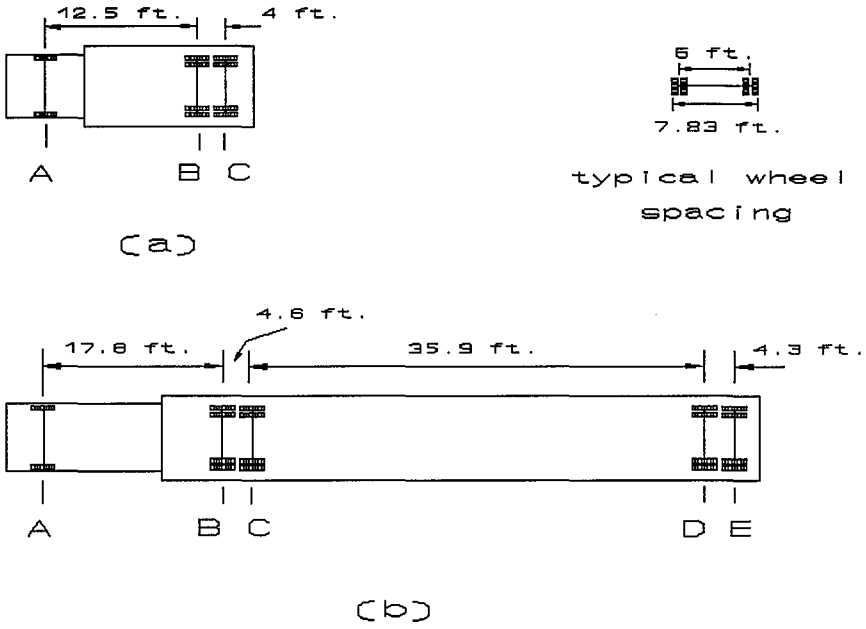

Figure 37. Trucks Used for Calibration Tests: (a) 3-Axle Truck (Dump Truck); (b) 5-Axle Truck (Lowboy)

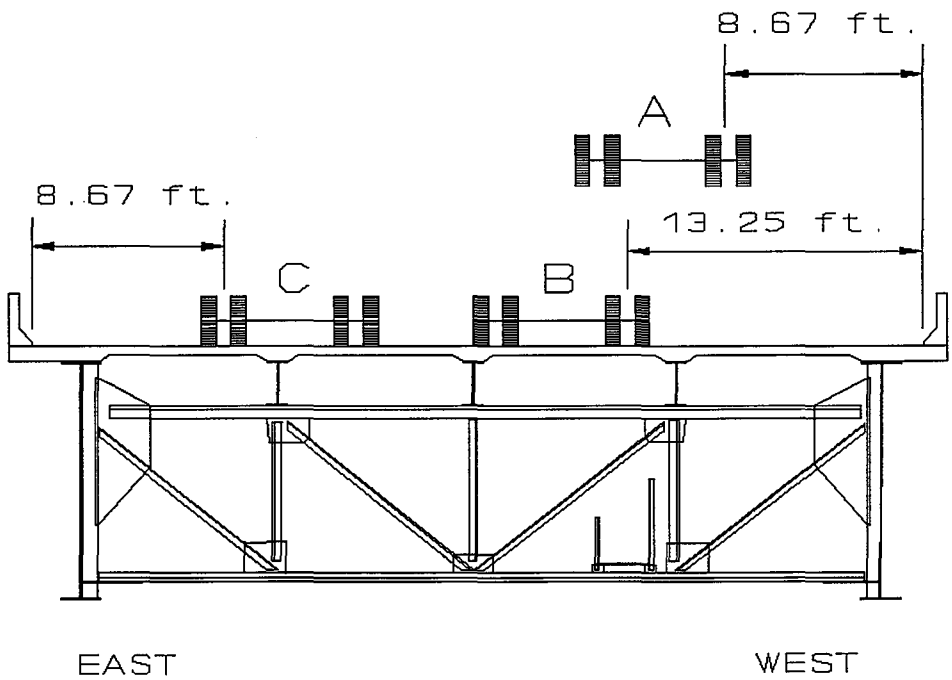

Figure 38. Test Lanes A, B, and C Used for Calibration Tests (Looking South at Southbound Lanes)

Table 9. Calibration Truck Weights for S3-11 Before Retrofit

Truck	Side[a]	Axle A (lbs)	Axle B (lbs)	Axle C (lbs)	Axle D (lbs)	Axle E (lbs)	Total (lbs)	Legal (lbs)
3-Axle	L	5,700	11,500	11,500	----	----		
	R	5,600	10,800	10,600	----	----	55,700	60,000
5-Axle	L	5,300	8,400	8,600	10,900	10,000		
	R	5,000	8,200	7,700	10,700	9,500	84,300	80,000

[a] L = Left (driver's) side; R = Right side.

Table 10. Calibration Truck Weights for S3-4 Before Retrofit

Truck	Side[a]	Axle A (lbs)	Axle B (lbs)	Axle C (lbs)	Axle D (lbs)	Axle E (lbs)	Total (lbs)	Legal (lbs)
3-Axle	L	5,600	10,100	10,000	----	----		
	R	5,700	10,500	10,000	----	----	51,900	60,000
5-Axle	L	5,100	8,400	8,400	8,900	10,100		
	R	5,000	8,100	8,200	8,100	9,600	79,900	80,000

[a] L = Left (driver's) side; R = Right side.

the test trucks at both major test locations tested before retrofit while Tables 11 and 12 list axle weights for the trucks used at the two connections tested after retrofit.

For strains and displacements measured at girder one to be compared to those at girder two, symmetrical loading conditions were necessary. However, the existing lanes on the bridges (two 11.5 ft traffic lanes and one 10.5 ft emergency lane) were not symmetrical with respect to the centerline of the bridge structure. An additional fictitious lane that was symmetrical about the centerline of the structure with the fast traffic lane was used for some calibration tests to produce a loading symmetric about the centerline of the structure with loading in the fast lane. Figure 38 illustrates the three different lane positions utilized for testing. The fictitious lane was called lane A, the slow lane (outside lane) was referred to as lane B, and the remaining fast lane (inside lane) was considered as lane C. Dashed spray paint lines were run the length of the span to identify the three lanes on the concrete deck and to locate truck wheels longitudinally and horizontally for specific test positions.

During the calibration tests, traffic control was provided by the AHD. At least one of the two regular traffic lanes was open to traffic at all times. A typical event sequence for calibration tests appears in Table 13. The calibration operations were directed from the roadway. Instructions were relayed by hand held radios to the test truck drivers and personnel who manned the computer and data acquisition system.

Four basic operations were performed during calibration tests: balance tests, static tests, crawl runs, and fast runs. The balance tests consisted of measurements recorded over a short time duration (2 seconds) with no vehicular activity on the continuous span and with little vibrational effects from vehicles that were approaching or had passed the continuous

Table 11. Calibration Truck Weights for S3-11 After Retrofit

Truck	Side[a]	Axle A (lbs)	Axle B (lbs)	Axle C (lbs)	Axle D (lbs)	Axle E (lbs)	Total (lbs)	Legal (lbs)
3-Axle	L	5,400	10,600	10,400	----	----		
	R	5,700	11,100	11,300	----	----	54,500	60,000
5-Axle	L	5,200	8,900	8,600	10,500	9,800		
	R	4,800	8,500	8,100	9,700	8,900	83,000	80,000

[b] L = Left (driver's) side; R = Right side.

Table 12. Calibration Truck Weights for S3-4 After Retrofit

Truck	Side[a]	Axle A (lbs)	Axle B (lbs)	Axle C (lbs)	Axle D (lbs)	Axle E (lbs)	Total (lbs)	Legal (lbs)
3-Axle	L	5,500	12,500	11,900	----	----		
	R	5,800	11,500	11,700	----	----	58,900	60,000
5-Axle	L	4,800	8,600	8,800	8,800	9,000		
	R	4,400	8,500	8,700	8,600	9,000	79,200	80,000

[b] L = Left (driver's) side; R = Right side.

Table 13. Typical Event Sequence for Calibration Tests

Event	Truck	Lane	Traffic Control
Balance	------	-	Lane C Open
Crawl	3-Axle	A	Lane C Open
Static	3-Axle	A	Lane C Open
Crawl	3-Axle	B	Lane C Open
Static	3-Axle	B	Lane C Open
Balance	------	-	Lane C Open
Crawl	5-Axle	A	Lane C Open
Static	5-Axle	A	Lane C Open
Crawl	5-Axle	B	Lane C Open
Static	5-Axle	B	Lane C Open
Balance	------	-	Lane C Open
Balance	------	-	Lane B Open
Crawl	3-Axle	C	Lane B Open
Static	3-Axle	C	Lane B Open
Balance	------	-	Lane B Open
Crawl	5-Axle	C	Lane B Open
Static	5-Axle	C	Lane B Open
Balance	------	-	Lane B Open
Fast Run	3-Axle	B	No Traffic Control
Fast Run	5-Axle	B	No Traffic Control
Fast Run	3-Axle	B	No Traffic Control
Fast Run	5-Axle	B	No Traffic Control
Fast Run	3-Axle	C	No Traffic Control
Fast Run	5-Axle	C	No Traffic Control
Fast Run	3-Axle	C	No Traffic Control
Fast Run	5-Axle	C	No Traffic Control

span being tested. The scanning rate for balance data was either 100 or 400 scans per second depending on the type of test file that the balance data was recorded in. The purpose of the balance was to establish a zero live load state.

The second type of calibration operation was the static test, which consisted of parking the test truck in a number of positions along the test span in each of the three test lanes and recording data for approximately 2 seconds with no traffic on the continuous span being tested. Seven span positions, denoted 1 through 7, were chosen for before retrofit testing at the pier S3-11 locations and appear in Figure 39. The positions were closely spaced near the instrumented floortrusses and one position was included on each of the two single spans that flank the single test span. Data for loading at the position on the adjacent span would indicate if measurable responses were present with trucks on adjacent spans of the continuous structure. Positions 1 and 7 were dropped from the after retrofit calibration test sequence at the outside girder connection of the first floortruss south of pier S3-11.

Six span positions, denoted 1 through 6, were chosen for testing before retrofit at the pier S3-4 locations and appear in Figure 40. One position was included on the south side single span adjacent to the test span of this three span continuous bridge. Positions 1 and 6 were dropped from the after retrofit calibration test sequence at the outside girder connection of the second floortruss north of pier S3-4.

The 5-axle truck was positioned during the static tests by aligning the rear axle of the front tandem over the test position as shown in Figure 41. The front axle of the rear tandem of the 3-axle truck was aligned over the test position as also shown in Figure 41. Therefore, the middle axle of each respective test truck was positioned over a test position.

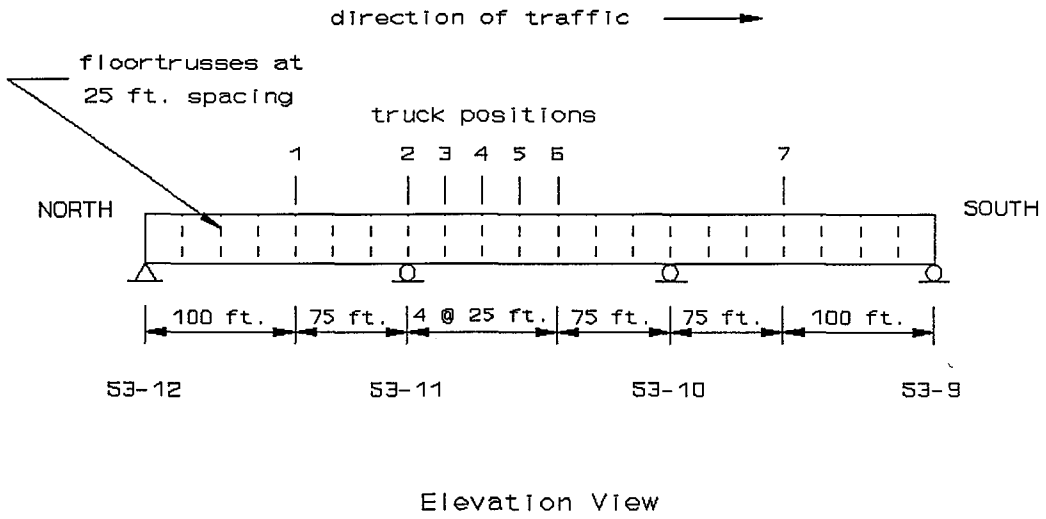

Figure 39. Span Positions Used for Static Calibration Tests at Pier S3-11 Locations

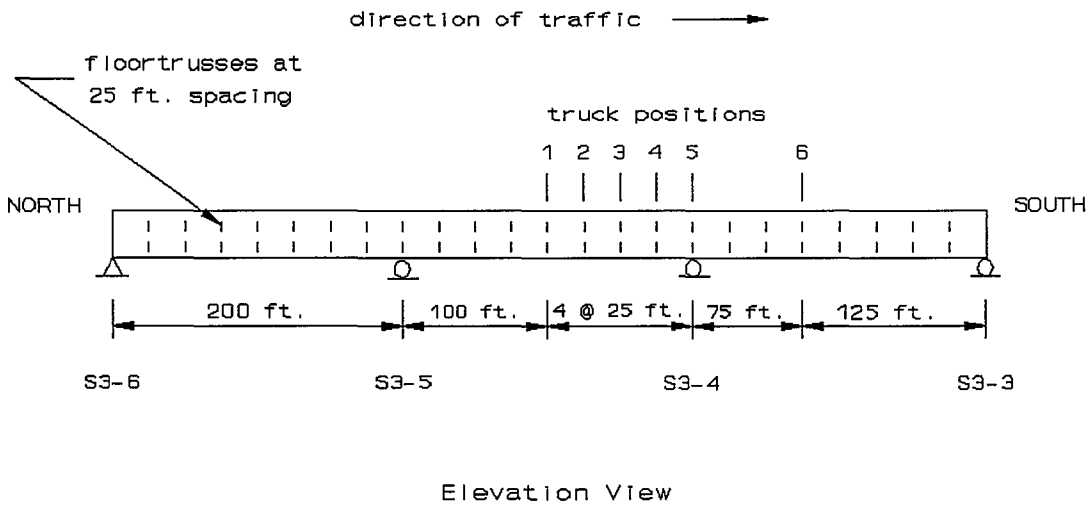

Figure 40. Span Positions Used For Static Calibration Tests at Pier S3-4 Locations

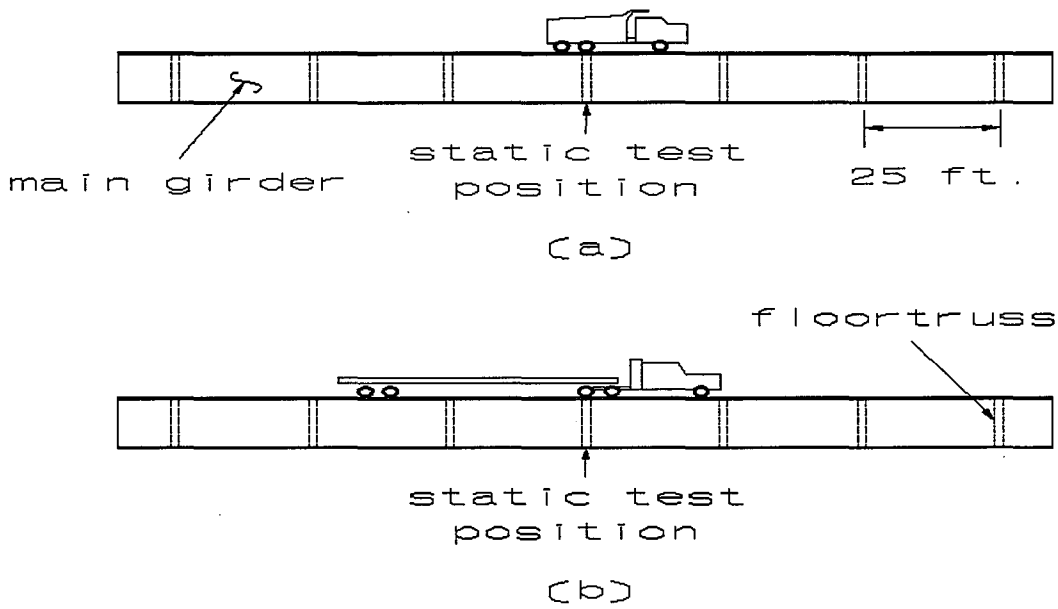

Figure 41. Truck Axle Positioning for Static Calibration Tests: (a) 3-Axle Truck (Dump Truck); (b) 5-Axle Truck (Lowboy)

The data during static tests was scanned at 100 scans per second. The primary data transformation for this type of test involved averaging the minor strain fluctuations experienced by the strain gages during the 100 scans per second that were scanned for two seconds. Since the static strains were constant, averaging removed the random stationary noise from the data.

The purpose of the crawl runs was to provide comparisons to the static tests with minimal dynamic effects. The purpose of the fast runs was to determine the response at the test locations under the dynamic loading conditions of normal traffic. Crawl and fast runs were made in lanes B and C, but not in lane A due to safety considerations. During crawl runs, test trucks maintained a 15 mph speed over the full length of the continuous span. Slower speeds were desirable but not possible because of the relatively long period of time required for the calibration truck to cross the span. It was not possible to find long time periods when other vehicles would not cross the span with the test truck since one lane was open to traffic at all times. For fast runs, the trucks were driven at normal traffic speeds, usually between 55 and 70 mph. Both lanes were open to normal traffic during the fast runs. The truck drivers blended into traffic so that no other heavy vehicles were on the three span segments of interest as the test truck crossed. This was called a clear run. Each truck made at least one clear run in lanes B and C which sometimes took two or three tries.

Fast run data was recorded at 400 scans per second. Fewer scans per second were recorded for static tests than for dynamic tests because the static strains were theoretically constant (independent of time) and only a small number of readings was necessary for accurate results. For the dynamic tests, a greater number of scans per second is required to

obtain an accurate measure of the peaks in the dynamic strain records. The primary data transformation for fast runs involved determining the overall maximum and minimum strains per record and calculating their difference (strain range). A comparison of the maximum strains from the crawl and fast run calibration tests would give a good estimate of the impact effect on strains measured at particular locations from vehicles passing at high speed. Ideally, if the crawl speed could have been kept to a minimum, the strain response for a particular gage would have matched the response for a series of static tests at all positions along the span. The peak strain for this ideal crawl run would have been exactly equal to the static strain recorded for the corresponding static test position because there would have been no impact effect from an ideal crawl run. During field testing at these locations a sufficiently slow crawl speed could not be established such that the entire test run could be recorded by the data acquisition system. Therefore, an analysis of crawl runs for this portion of the project could not be performed.

RANDOM TRUCK TESTS

While the calibration tests were important for establishing behavior for trucks of known weights and positions, the random tests provided the behavior for normal traffic loading. At each location susceptible to fatigue damage, the stress ranges for all random truck records were used to calculate an equivalent constant amplitude stress range, or effective stress range. Effective stress ranges are explained in detail later in this chapter. An analysis of data from the floorbeam-girder connections tested in the first portion of this

project indicated that recording 250 random trucks to use for effective stress range calculations would produce reasonably accurate values.

During the random tests there was no traffic control on the roadway and all testing equipment, including portable generators, was located under the roadway. These steps were taken to ensure that the speeds and lane positions followed normal traffic patterns. An equipment van was parked in the emergency lane during the random tests, but was parked over two continuous span lengths south of the south end of the particular continuous span being tested. This preserved the truly random nature of the truck traffic as it crossed the test span. At least one graduate assistant monitored the equipment under the bridge at all times during testing.

A self triggering mechanism within the data acquisition system was used to activate the data recording process for random truck testing. The system continuously scanned a selected gage for strains that exceeded a prescribed limit which was set to capture heavy truck loadings. The limit was determined after analyzing sample test runs. For experiment files consisting of primarily web gap gages, the trigger was chosen as the IN1 gage with the trigger magnitude set at +66 microstrain (1.91 ksi). For experiment files which consisted of primarily of connection plate gages, gage NS1 was chosen for triggering at +66 microstrain. When any data value for a trigger gage exceeded the trigger magnitude, data was also recorded for pre-trigger and post-trigger time intervals. The data acquisition system recorded all data scans for 3 seconds before and 1.5 seconds after a trigger limit was exceeded. The pre- and post-trigger time lengths were chosen to allow the gages which experienced the slowest relative response time, the girder flange gages, to complete their

response cycle for a single truck crossing. The response cycle time varied for all gages, but the sample runs were used to define the pre- and post-trigger time lengths for only girder flange gages. Approximately seven to eight hours was required to collect 250 heavy truck crossings for each test setup.

DATA REDUCTION

As discussed in Chapter Five, the data collected during all random and calibration tests was processed by the data acquisition system, transferred to the computer hard disk, and then transferred to mini data cartridge tapes after testing was complete. The test files were then deleted from the hard drive to provide room for new test data. Complete random tests and calibration tests at one test setup could be stored on two mini data cartridge tapes.

The data reduction process began after completion of all field tests performed during the summer of 1992 when the test equipment was returned to Auburn University. When data from a specific test was to be reviewed, that specific test data stored on the mini cartridge tapes was copied onto the hard disks of several 386 and 486 personal computers, each equipped with the TCS3000 software.

Random truck and fast run calibration data records were reviewed to determine strain ranges using the peak-to-peak method, as discussed in Volume I. An illustration of the peak-to-peak method appears in Figure 42. A strain range determined by the peak-to-peak method is the absolute difference between the maximum and minimum strain values. Each truck crossing was considered to create one strain range. Relatively short C language transform equations were coded into the TCS3000 test files to calculate the maximum, minimum, and

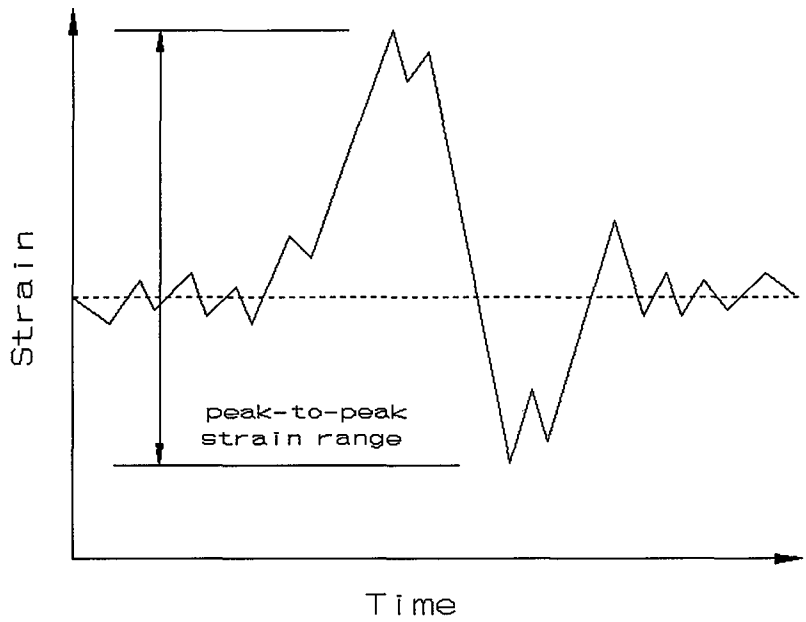

Figure 42. Illustration of Peak-to-Peak Method

difference, or strain range, values for each truck crossing. The strain versus time plots were viewed for each gage to ensure the integrity of the data, determine the relative time response of each gage, identify the behavior at gage positions, and reveal whether the structural element experienced primarily tensile or compressive strains due to truck traffic. The strain ranges were taken directly from the digital monitors portion of TCS3000. The stress ranges were then obtained by multiplying the modulus of elasticity for steel of 29,000 ksi by the recorded strain range.

An additional type of data analysis was performed to determine the effect of fast truck passes on connection plate behavior. The view graphics portion of TCS3000, was used to determine the time of peak strain experienced by the top north side gage, either NS1 or NSM1, and the strains experienced by all other connection plate (stiffener) gages at that time instant were noted.

Transform equations were developed to average the strain readings of the balance tests and static tests. The static strains were averaged from each scan of the 100 scans recorded per second for approximately 2 seconds for each test. Only balance tests taken in sequence with the static tests were averaged for comparison with the static values. The balance test scan rate was dependent on the test in which the balance was performed (i.e., 100 scans per second during the static tests, and 400 scans per second for random and fast calibration tests). Therefore, the balance tests used for the static tests were also averaged for each scan of the 100 scans recorded per second for approximately 2 seconds for each test. Since the balance and static measurements should result in a constant value, the accuracy of the measurements was enhanced by the averaging process, which eliminated random

stationary electronic noise. The true static strain value for a particular gage under static loading was determined by finding the difference between the average strain recorded during the static test and the average strain recorded during the balance test. As before, stress values were determined by multiplying the strain by the modulus of elasticity for steel.

EFFECTIVE STRESS RANGE

A primary goal of reducing the variable amplitude data gathered in the field tests reported here was to determine effective stress ranges at critical locations. The effective stress range can be calculated from variable amplitude stress range data by numerous methods which were mentioned in Volume I. The two most common methods are the root-mean-square (RMS) and Miner's effective stress range, also called the root-mean-cubed method (RMC). Both methods can be represented by the following equation:

$$S_r = \left[\sum_{i=1}^{k} \frac{(n_i S_{ri}^{\,b})}{N} \right]^{\frac{1}{b}} \qquad [1]$$

where k is the total number of stress ranges; i is the current stress range; n_i is the number of stress cycles at the ith stress range, S_{ri}; and N is the total number of cycles. The choice of the variable b determines which effective stress range method is used. The root-mean-square method uses a value of 2 for b, while the Miner's effective stress range uses a value of 3 for b. For the Miner's effective stress range, b is related to the slope of a log-log plot for constant amplitude fatigue life data and is usually given a value of 3 (Keating et al. 1987).

Of special importance to the effective stress range calculation was the number of stress cycles to be considered. Depending on the number of scans recorded per second and the overall gage response time length, the potential number of cycles to be considered could number in the thousands. During the data analysis of the floorbeam-girder results at the first location tested during the summer of 1991, strain ranges were recorded for a primary, secondary, and tertiary cycles for each of the 788 truck records collected there. Effective stress ranges were calculated for various groupings of data. For instance, the effective stress ranges were calculated for a number of gages from strain ranges recorded for primary cycles only, primary and secondary cycles only, and primary, secondary, and tertiary cycles. The cycle groupings were analyzed in data set groupings, such as, the first 100 trucks, the second 100 trucks, the first 150 trucks, the first 200 trucks, etc. These investigations produced two important results. Consideration of only the primary cycle of a data record produced relatively the same effective stress range values as consideration of the primary and secondary, and the primary, secondary, and tertiary cycles. Secondly, any grouping of 200 truck data records produced essentially the same calculated effective stress ranges as were produced by every other grouping of 200 truck data records. The data set number of 200 was the lowest number of events in a grouping of all test groups which produced these results. In view of these findings, only a primary strain range, or cycle, was recorded for each truck record for the remainder of the data analysis for that portion of the project and for the two portions of the project for which field tests were performed during the summer of 1992. Also, after consideration of time limits and data group sizes, a sample group of 250

trucks was chosen for all effective stress range calculations. This size would provide somewhat more accuracy than a group of 200 trucks.

Both the RMS method and Miner's method have shown good correlation with experimental data (Fisher 1978, Yamada and Albrecht 1976, Fisher et al. 1989). Miner's effective stress range tends to give a larger result than the RMS method (Fisher et al. 1989). Miner's effective stress range is also more theoretically based (Yamada and Albrecht 1976). However, the RMS method has been reported to show slightly better correlation to test data but results in a less conservative value (Fisher et al. 1989). Both methods have been widely used but since the Miner's effective stress range produces a more conservative estimate than the RMS method, it is more commonly used for bridge fatigue life estimates. All effective stress ranges calculated during this project were Miner's effective stress ranges.

CHAPTER SEVEN

RESULTS AT CONNECTIONS BEFORE RETROFIT

BEHAVIOR AT TEST LOCATIONS

There were three different girder web depths for the plate girder spans that employed floortrusses for the transverse support system. The original project proposal called for the study of connections with the deepest and the shallowest depth of the three girder depths. However, because all five cracks identified by AHD bridge inspectors were at the locations with the two shallowest girder depths, these two girder depth locations were chosen instead for instrumentation and testing.

Tests were performed at three floortruss-girder connections at both the 106 in. and the 126 in. girder web depth locations. The area of primary interest was the area where the floortruss end diagonal and top chord connect to the plate girder web near the top flange. All connections tested were in a negative moment region for the plate girder, so the top flange was the tension flange. The 106 in. girders were tested at floortruss-girder connections 25 and 50 ft south of pier S3-11. The 126 in. girders were tested at connections 25 and 50 ft north of pier S3-4. At one connection for each of the two girder depths, testing was conducted before and after the softening retrofit. These test locations were described in Chapter Four (see Figure 20). The same general behavior was exhibited by all connections tested.

The in-plane and out-of-plane behavior was similar to that observed in tests of floorbeam-girder connections reported in an earlier phase of this project (Volume I, Stallings et al. 1993). The records from gages on the plate girder flanges measuring in-plane strain indicated a measurable response for trucks traveling from end to end of a continuous plate girder segment. The out-of-plane strain gages recorded short structural response durations that peaked when the middle axle of the truck was located above the test location. The out-of-plane response oscillations damped out far more rapidly than the in-plane response. The out-of-plane displacements measured by the LVDTs at all test locations demonstrated that the stiffener-connection plate assemblies moved inward (toward the bridge span centerline) as a truck crossed the floortruss.

In-Plane Stresses at Web Gap

The in-plane stresses measured on the girders' compression (bottom) flanges (No. 9 gage in Figure 35 of Chapter Five) generally ranged from 0.5 to 2.0 ksi in magnitude. The tension flange in-plane stresses were found to be about one-sixth to one-third the magnitude recorded at the compression flange. The maximum stress range measured on the tension flange at floortruss-girder connections (No. 8 gage in Figure 35) was 0.4 ksi, while the stress ranges were commonly 0.2 ksi. The low in-plane stress ranges in the top flange recorded for these connections were attributed to the closeness of the web gap to the neutral axis of the composite girder (plate girder, stay-in-place forms, concrete deck, and concrete curb wall). The in-plane strains were also measured on the web adjacent to web gaps (No. 4 gage) at the three connections at both test locations. The differences between strains measured on the

webs and tension flanges indicated that the out-of-plane distortion of the web slightly increased the in-plane stresses in the web gap region.

Later in this report out-of-plane bending stresses will be compared to fatigue limits determined by Fisher et al. (1990) from laboratory tests. The in-plane bending stresses used in those laboratory tests were 6 to 12 ksi. Fisher's laboratory work revealed that, generally, fatigue cracking occurred at a lower number of fatigue cycles for higher in-plane stresses in the web gap. This suggests that the floortruss-girder connections tested in this portion of the project should perform somewhat better than the specimens tested by Fisher due to the lower in-plane bending stresses.

Truss Member Behavior and Force Resultants

The truss members (comprised of a double angle pair) framing into each connection tested were gaged at the neutral axes of the top and bottom chords and the end diagonal as noted in Chapter Five. A detailed floortruss analysis was beyond the scope of this portion of the project. However, the truss members were gaged to determine the nature and magnitude of the axial forces transferred through these members to the connection plate. The north and south side angles of the three double angle pairs were gaged at the connections at pier S3-11. The difference between the strains measured in the north angle and the south angle for all three double angle pairs was very small, ranging from 0 to 3 microstrain (0 to 0.1 ksi) for typical truck crossings. Because of the small difference, the instrumentation was simplified, and only the north side gages were used at the remaining test locations.

The strain record for the bottom chord gages was very similar in shape to the in-plane strain record for the main girder compression flange gage. A bottom chord gage typically experienced a maximum compressive stress between one second and one-half second before the truck was directly above the floortruss. The response changed from compressive to tensile as the truck passed directly above and then reversed to compressive again after the truck had passed.

The bottom truss chord members experienced very small strains relative to the top chords and end diagonals. The strain records commonly revealed peak-to-peak strains of 15 $\mu\epsilon$ (0.4 ksi stress). The strains in the top chord, end diagonal, and bottom chord were used to calculate the horizontal forces in these three members. The horizontal force in the bottom chord was less than required to balance the sum of the horizontal forces in the top chord and end diagonal. This indicated that the unbalanced force was resisted by the connection plate and its attachment to the girder web and to the bottom flange. The resultant horizontal reaction produced by the unbalanced force caused out-of-plane distortion of the web gap.

The strain record for the top chord and end diagonal resembled the response of the out-of-plane bending gages on the girder web, with very little response at times when the trucks were not directly over the test position. As a truck passes over a floortruss, a tensile force is developed in the end diagonal of the truss. The vertical component of the tensile force transfers the vertical truck loading into the gusset and connection plates and into the girder web. The horizontal component of the tensile force in the diagonal is resisted primarily by a compressive force developed in the top chord, and to a much lesser degree by a horizontal reaction (shown as V in Figure 44 (b) discussed in the next section) in the web

gap resulting from the out-of-plane distortion of the girder web in the web gap. Strain gages on the end diagonals measured stresses commonly ranging from +0.9 to +2.5 ksi. The maximum recorded stress was +3.0 ksi. The top chord stresses commonly ranged from -0.4 to -1.8 ksi, with a maximum recorded stress of -2.1 ksi.

Connection Plate Stresses and Web Interaction

The stress behavior of the connection plates was investigated by installing strain gages along the surface of the plates at locations on the north and south sides of the plates as illustrated in Figures 29 through 31. The purpose of investigating the stresses in the connection plate was to determine how the horizontal forces which cause out-of-plane distortion in the web gap are transferred from the truss into the girder web. Hence, the strain gages on the plates were oriented to measure strains in the horizontal direction on the connection plate. A typical stress record for the connection plate gages is shown in Figure 43. All the stresses plotted in Figure 43 occurred at the same instant in time as a heavy truck crossed the floortruss.

As heavy trucks crossed the bridge, secondary forces in the structure tended to cause the connection plate to bend and rotate slightly about a vertical axis. This bending of the connection plate accounts for the differences in recorded stresses from the north to the south side of the plate as illustrated in Figure 43. For example, in Figure 43 at a distance 14 in. from the girder flange, the stresses on the north and south sides of the connection plate were practically equal in magnitude, yet opposite in sign. These stresses indicate a condition of pure bending at that location about the connection plate's minor axis (vertical axis at mid-

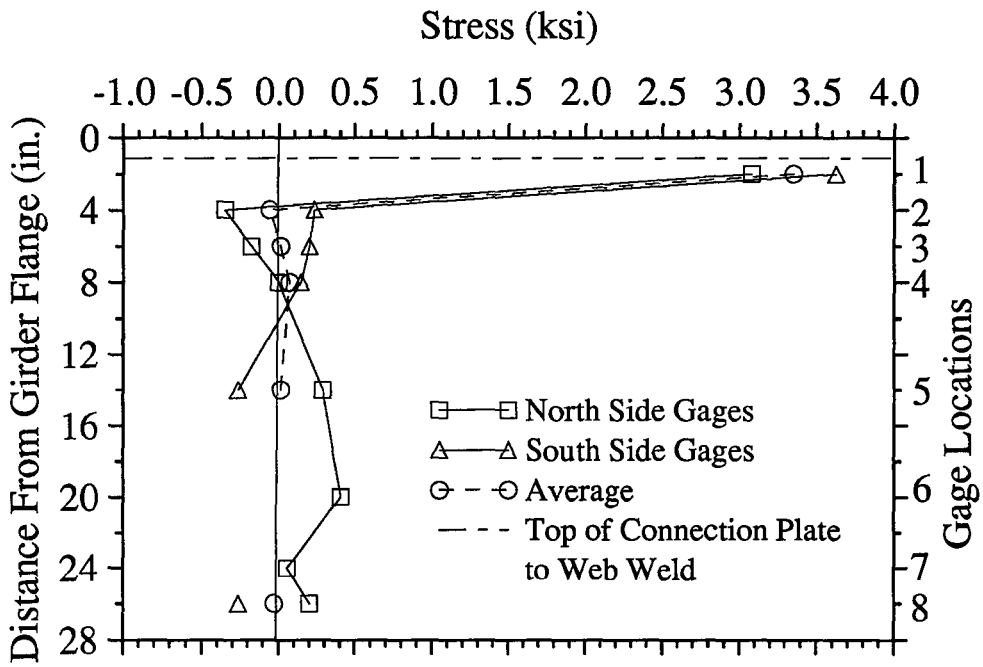

Figure 43. Typical Distribution of Horizontal Stress in the Connection Plate (at the Outside Girder of the First Floortruss South of Pier S3-11 Before Retrofit)

thickness of the plate). Inspection of a large number of stress plots similar to Figure 43, some with different gage patterns, indicates that pure bending of the connection plate typically began between 14 and 20 in. down the plate below the top flange.

Much different stress conditions existed toward the top of the connection plates. Near the top of the connection plate, the average of the stresses on the north and south sides was not zero. Since the average stress (dashed line in Figure 43) is the axial stress, Figure 43 indicates that there was significant axial stress in the connection plate at the top near the web gap. Inspection of a number of stress records indicated that the zone of axial tensile stress at the top of the connection plate typically extended 6 to 8 in. below the top of the connection plate to web weld. The zone of compressive axial stress typically covered the next 2 to 4 in. below the tensile zone. The axial stress at the top of the connection plate results from the horizontal force required to produce out-of-plane distortion of the girder web gap. Figure 44 shows an idealized distribution of axial stress along a plane cut through the connection plate that will be used to illustrate this point.

The plane cut through the connection plate in Figure 44 (a) is 1 in. from the face of the web which corresponds to the location of strain gages placed on the connection plate. The tensile and compressive forces shown result from integrating the tensile and compressive stresses over the area of the plate. In Figure 44 (b), a cross section through the web gap is shown with idealized fixed boundaries and the shears and moments required to produce double curvature distortion of the web gap. The shear (or horizontal force) required to produce the out-of-plane displacement in the web gap is provided by the resultant (unbalance) of the forces T_1, T_2, and C. The bending moment at the bottom of the web gap required to

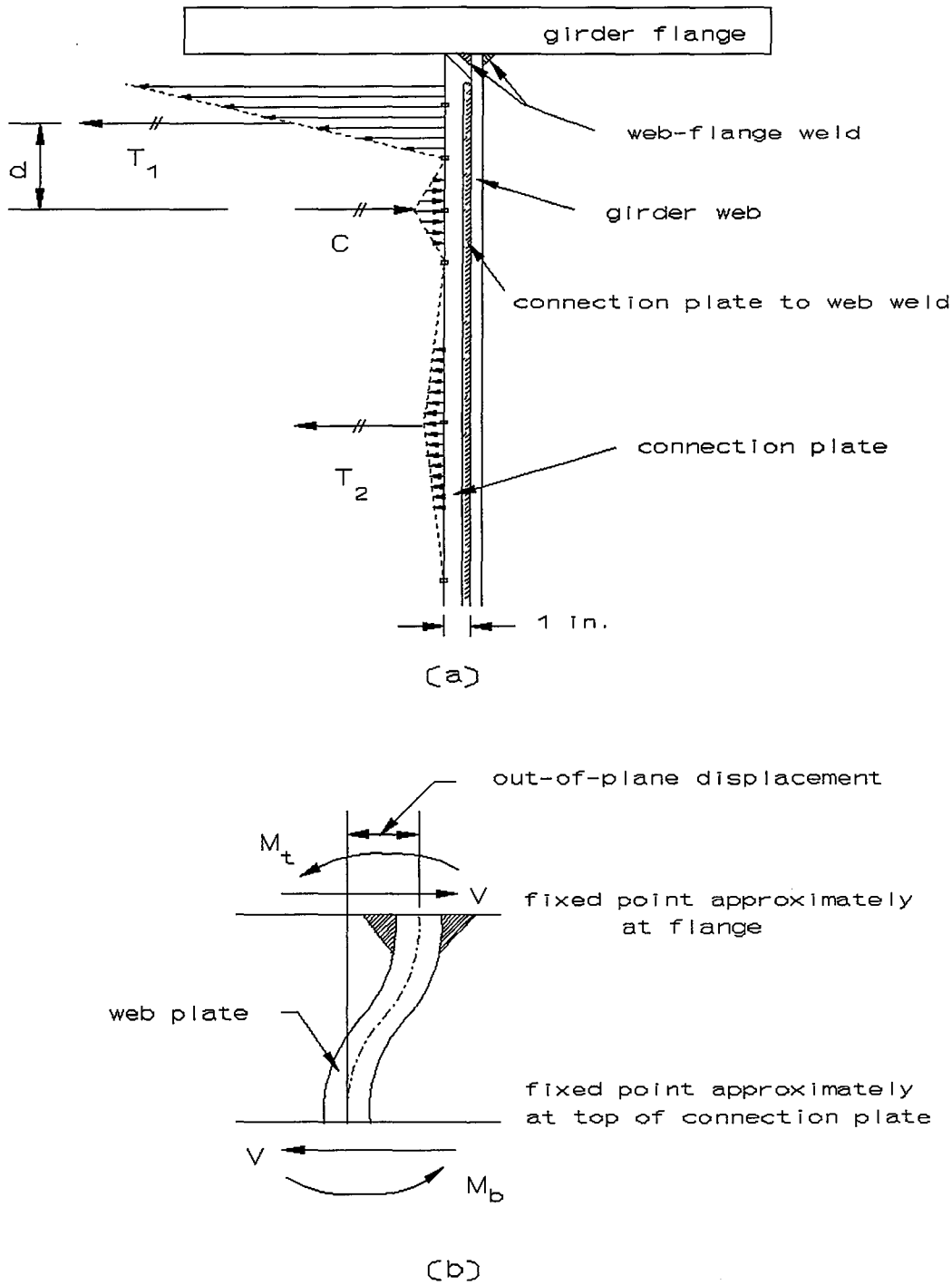

Figure 44. Interaction of Connection Plate and Girder Web Plate: (a) Idealized Distribution of Horizontal Stress in Connection Plate; (b) Distortion in Web Gap Region

produce double curvature results primarily from the separation of T_1 and C by the moment arm, d.

STRESSES FROM STATIC TESTS

One objective of performing static tests at each test location was to determine the test truck, truck position, and truck lane that produced the highest web gap stresses. The 3-axle truck in the slow traffic lane (lane B) in position 3 (above the floortruss being tested) produced the worst case loading for all six connections tested. Distortion-induced stress distributions in the web gap region for the 3-axle test truck loading at all six connections appear in Figures 45 through 50. The 3-axle test truck produced the maximum stresses measured for either test truck.

A linear extrapolation technique was used to estimate the stresses at critical locations in the web gap region. The linear extrapolation technique involved extrapolation of stresses measured at two gage positions to an additional (critical) position which could not physically be gaged. In Figures 45 through 50 the critical positions on the girder web plate used for extrapolations were the web-flange weld toe (inside and outside) and the top of the connection plate to web weld. The stress extrapolations are represented by the dashed and dot-dashed lines in Figures 45 through 50. Extrapolation of stresses will be discussed in further detail in a later section.

Another objective of performing static tests was to investigate symmetry in the test results. In earlier tests at floorbeam-girder connections (Volume I, Stallings et al. 1993), stresses and displacements measured near web gaps for static tests indicated a lack of

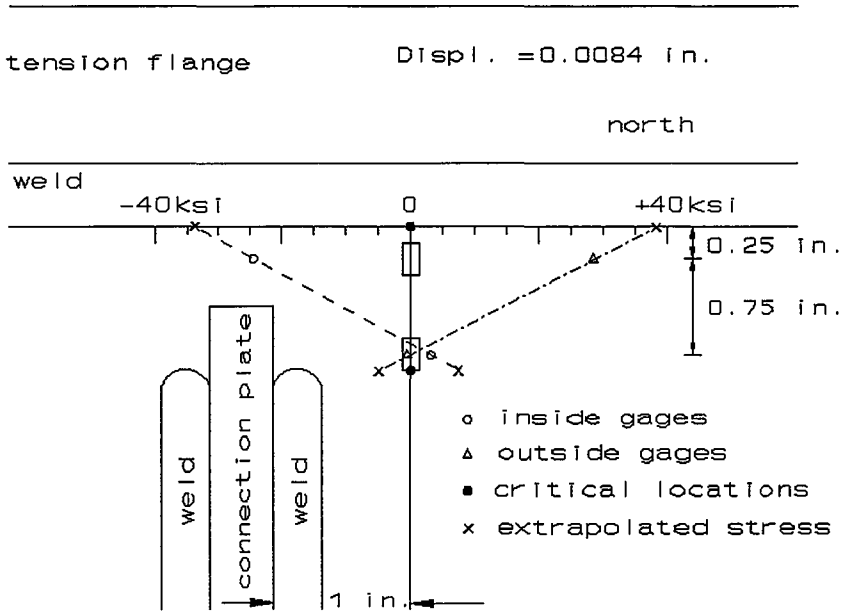

Figure 45. Static Stress Distribution on Outside Girder at the First Floortruss South of Pier S3-11 (106 in. Girder) Before Retrofit with 3-Axle Truck in Outside Lane

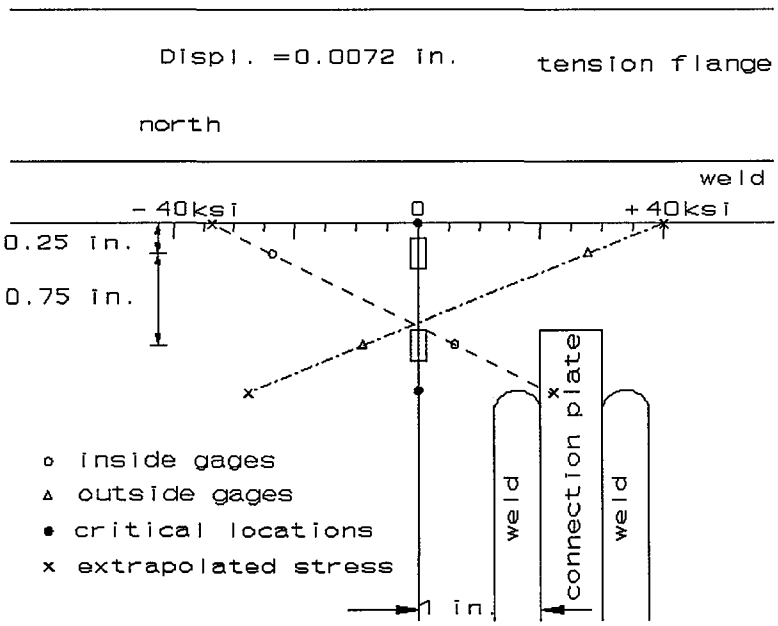

Figure 46. Static Stress Distribution on Inside Girder at the First Floortruss South of Pier S3-11 (106 in. Girder) Before Retrofit with 3-Axle Truck in Outside Lane

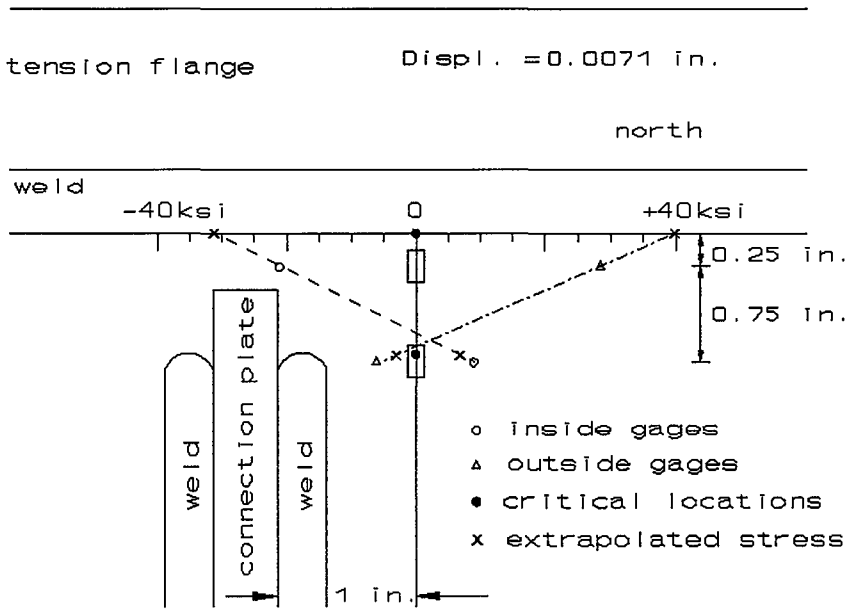

Figure 47. Static Stress Distribution on Outside Girder at the Second Floortruss South of Pier S3-11 (106 in. Girder) Before Retrofit with 3-Axle Truck in Outside Lane

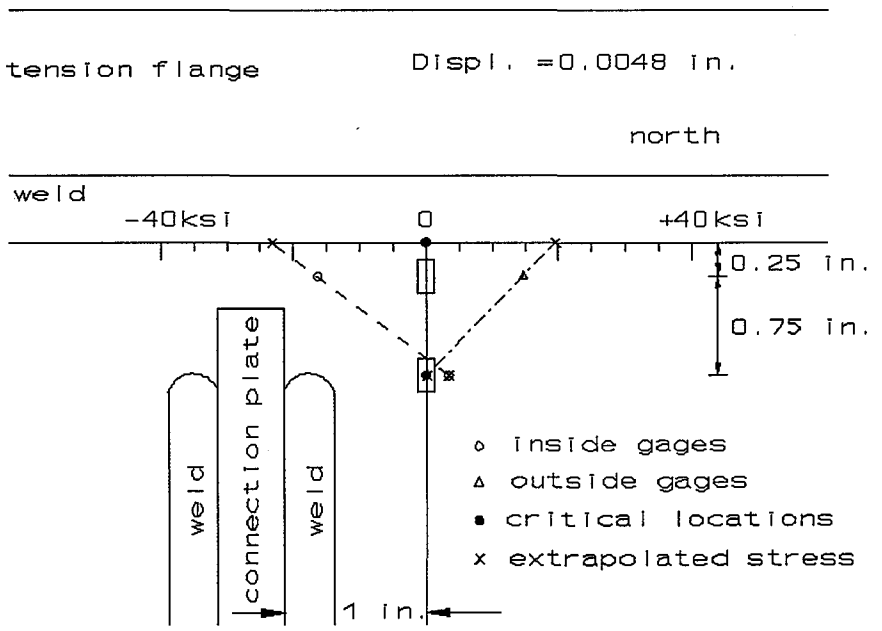

Figure 48. Static Stress Distribution on Outside Girder at the First Floortruss North of Pier S3-4 (126 in. Girder) Before Retrofit with 3-Axle Truck in Outside Lane

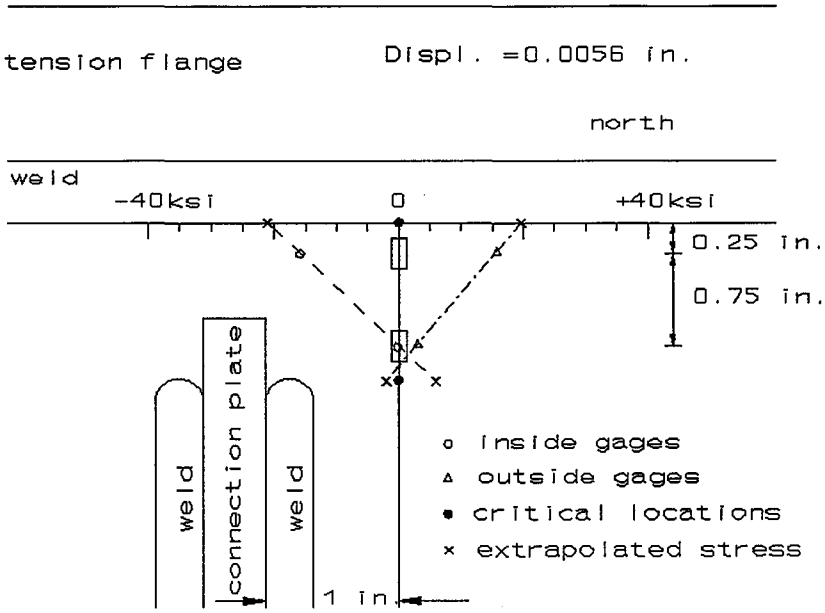

Figure 49. Static Stress Distribution on Outside Girder at the Second Floortruss North of Pier S3-4 (126 in. Girder) Before Retrofit with 3-Axle Truck in Outside Lane

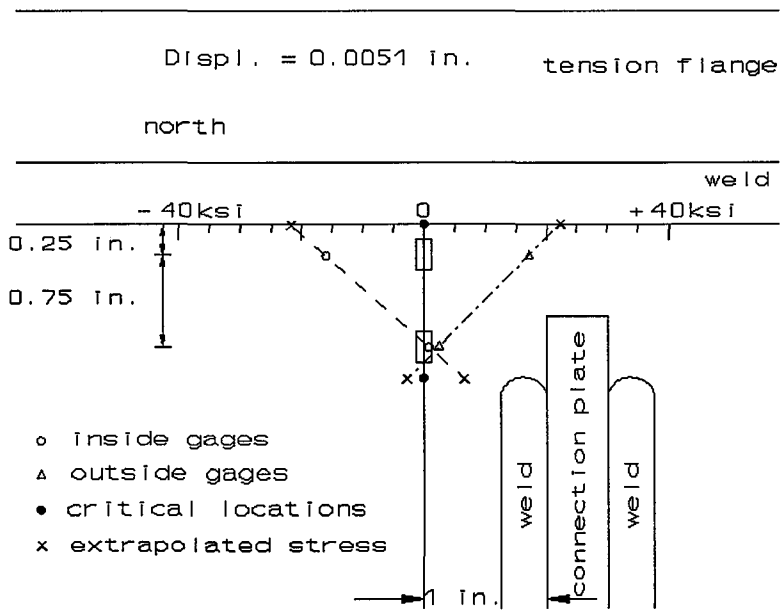

Figure 50. Static Stress Distribution on Inside Girder at the Second Floortruss North of Pier S3-4 (126 in. Girder) Before Retrofit with 3-Axle Truck in Outside Lane

symmetry in measurements. The lack of symmetry was attributed to variations in geometry at the connections. Symmetrical loading applied to a symmetrical structure would be expected to produce the same response at the outside girder (on slow lane side) from a truck in lane A (see Figure 38) as at the inside girder (on fast lane side) from the same truck in lane C. Likewise, the same response would be expected at the outside girder from a truck in lane C as at the inside girder from the same truck in lane A. Even the relative vertical displacement between the main girders at locations away from piers for a truck in either lane A or C would be symmetric for a symmetric structure.

The question of whether there was symmetry in the responses at the six connections tested in this project was investigated separately for global response and the local response structural details. Investigation of the global static response was conducted through examining the axial stresses in the end diagonals of the floortrusses tested at pier S3-11 (first floortruss south) and pier S3-4 (second floortruss north). Local static stress response was investigated at the outside web-flange welds and at the top of connection plate welds at the girder connections of these two floortrusses. The global and local responses to the worst truck load (3-axle truck) are compared in Figures 51 through 56. The notation in each figure legend denotes the test lane loaded (referred to as LN A, for lane A, or LN C, for lane C) and the girder at which the stresses in the figure were measured (referred to as OUT. G., for outside girder, or IN. G., for inside girder). The origin of the horizontal axis in the figures was chosen as the floortruss location being tested.

The stresses measured in the end diagonals of the trusses at both test locations are shown in Figure 51 and 52 to be nearly symmetric. The small variations in the results are

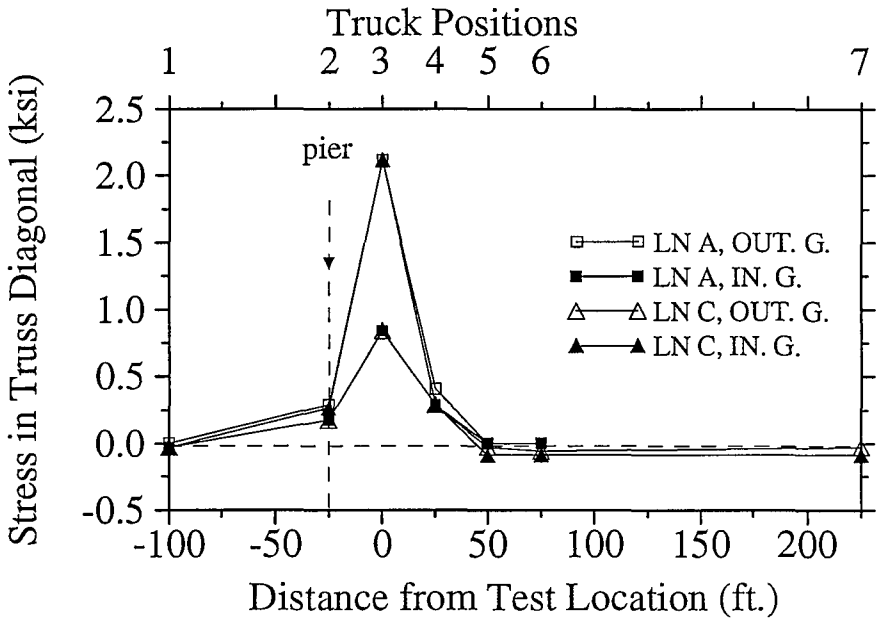

Figure 51. Static Axial Stress in End Diagonals of the First Floortruss South of Pier S3-11 Before Retrofit with 3-Axle Truck in Lane A or C

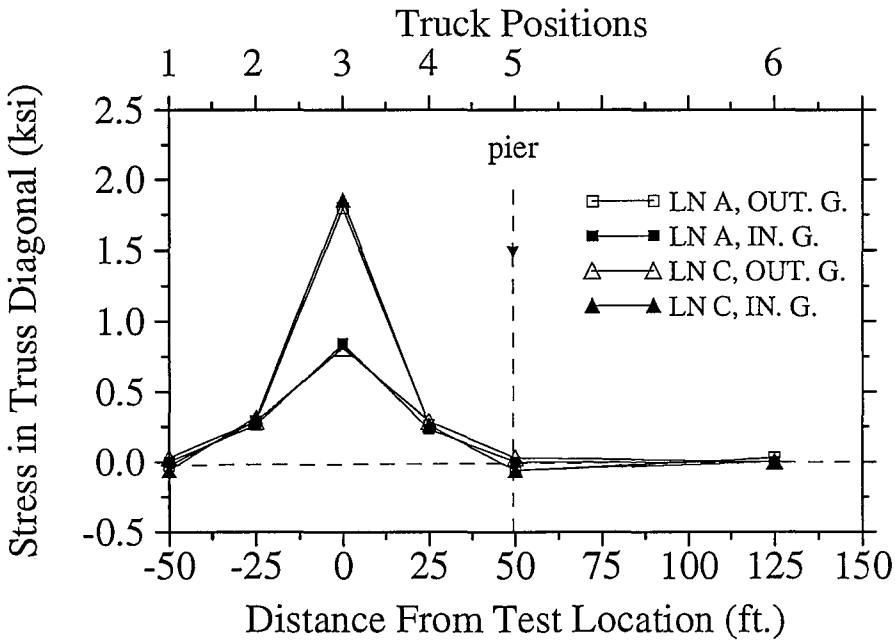

Figure 52. Static Axle Stress in End Diagonals of the Second Floortruss North of Pier S3-4 Before Retrofit with 3-Axle Truck in Lane A or C

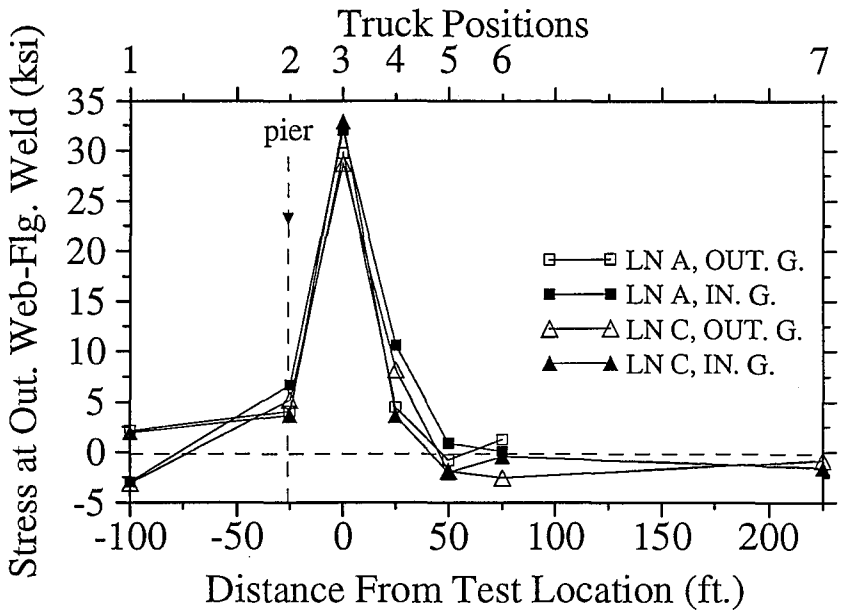

Figure 53. Static Stress at the Outside Web-Flange Weld at the First Floortruss South of Pier S3-11 Before Retrofit with 3-Axle Truck in Lane A or C

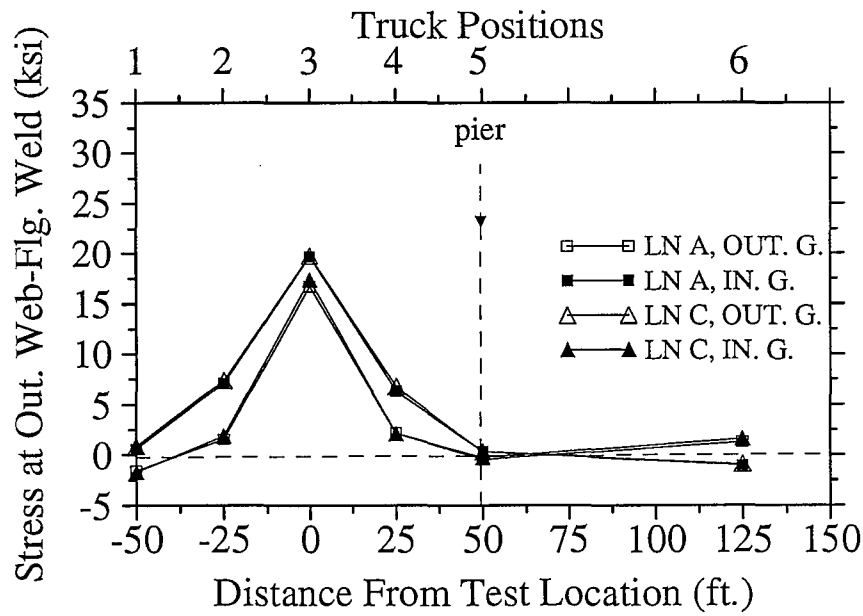

Figure 54. Static Stress at the Outside Web-Flange Weld at the Second Floortruss North of Pier S3-4 Before Retrofit with 3-Axle Truck in Lane A or C

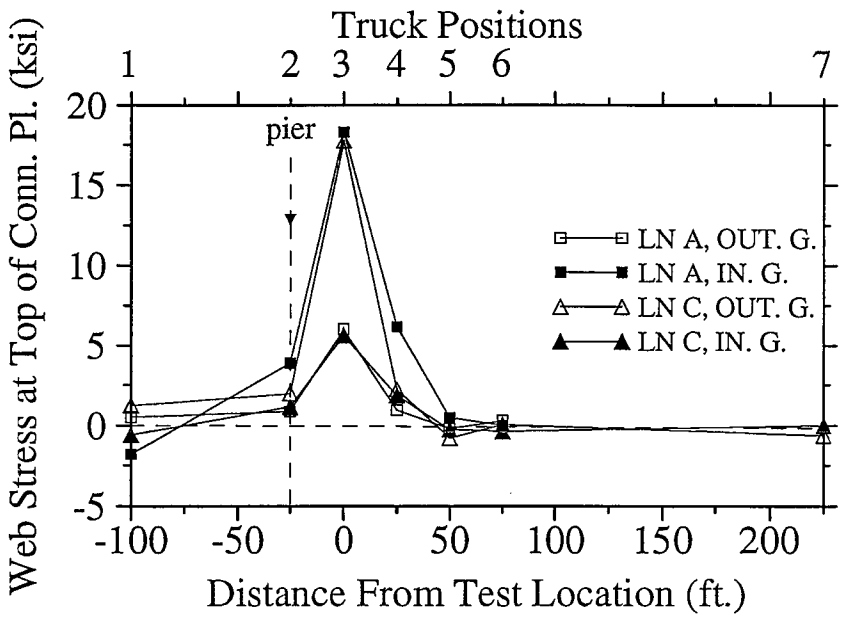

Figure 55. Static Stress at the Top of the Connection Plate Weld at the First Floortruss South of Pier S3-11 Before Retrofit with 3-Axle Truck in Lane A or C

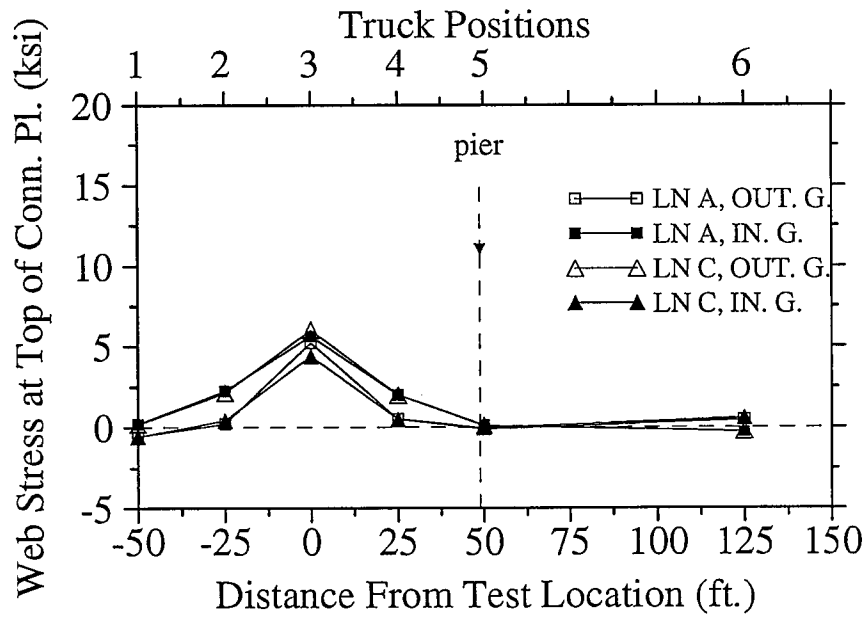

Figure 56. Static Stress at the Top of the Connection Plate Weld at the Second Floortruss North of Pier S3-4 Before Retrofit with 3-Axle Truck in Lane A or C

generally smaller than the expected level of precision in the static measurements of +/- 0.15 ksi. It should also be noted that the bridge geometry was not exactly symmetric. For example, the roadway section sloped slightly down from east to west. Still, the results in Figures 51 and 52 indicate that overall the structure behaved as if it were symmetric.

The stress responses at the outside web-flange welds at the connections at each end of the first floortruss south of pier S3-11 (Figure 53) are not as symmetric as those for the outside web-flange welds at each end of the second floortruss north of pier S3-4 (Figure 54). The plots of Figure 54 show excellent agreement. The plots for symmetric conditions in Figure 53 differ by up to 3 ksi. However, this difference of 3 ksi still represents only 10 percent of the maximum stresses recorded.

The plots of stresses at the top of the connection plate weld on the inside face of the girder web in Figures 55 and 56 also show some deviations from symmetry. The largest deviations were 3 to 5 ksi for truck positions away from the floortruss where the measurements were taken.

The stresses plotted in Figures 51 through 56 show some deviation from symmetry. The global responses appear to be very symmetrical. The local response symmetry was shown to be far more dependent on local geometry. However, the results are much more symmetric than the results reported earlier from tests of floorbeam-girder connections (Stallings et al. 1993). The reason for this is not clear. However, there are two primary differences between the floortruss-girder connections and the floorbeam-girder connections. First, the floortruss-girder connections are far more flexible than the floorbeam-girder connections. The boundary conditions at these connections were far less severe than at the

floorbeam-girder connections because the bottom flange of the girder is not restrained laterally by a pier support. The connection plates are much thinner, and the girder web height to thickness ratio is greater at the floortruss connections. The slenderness ratio at the second floortruss north of pier S3-4 is even greater than that at the first floortruss south of pier S3-11. The floorbeam-girder connections tested also had vertical stiffener plates welded to the outside of the girder webs, while the floortruss locations did not. Secondly, the measured stresses at the floortruss connections were much larger than those measured at floorbeam-girder connections. Hence, measurements at the floortruss-girder connections would tend to be less affected by normal measurement errors.

CRITICAL LOCATIONS AND CALCULATION OF WEB GAP STRESSES

Crack initiation in web gaps at the end of a transverse connection plate of the type used at the floortruss-girder connections results from cyclic stresses created by the out-of-plane distortion of the web gap. The two locations in the girder web most susceptible to fatigue cracking are at the toe of the web-flange weld and at the top of the connection plate to web fillet weld. The potential for fatigue cracking at these locations is a complex function of the connection geometry, level of distortion-induced stresses, and the residual shrinkage stresses created in the web gap due to the welding together of the web, flange, and connection plate.

Crack initiation at the web-flange welds would generally be assumed to occur on the outside (tensile) face of the girder web where the highest distortion-induced tensile stresses occur. However, fatigue cracks could initiate on the inside (compression) face of the girder

web as a result of residual stresses at the top of the web-flange weld. The presence of residual tensile stresses changes part or all of the stress range in a compression region into a tensile stress range. Therefore, the stress ranges on the inside (compression) face of the girder are important for comparison to other stress conditions. The stresses and stress ranges at the web-flange weld and at the top of the connection plate weld were determined through linear extrapolation of the actual strain gage readings on the face of the web as illustrated in Figures 45 through 50 for static tests.

Obviously the linear extrapolation technique provides an estimate of the stresses and the stress ranges at critical locations. The actual stress profiles in similar connections have been found to be somewhat nonlinear. Some additional inaccuracy in this technique involves the extrapolation of stress ranges instead of calculation of stress ranges from continuous extrapolation of stresses. A continuous extrapolation technique would involve extrapolation of the gage stresses at each scan of the recorded data set. A stress range would then be determined from this continuous set of extrapolated stresses. This continuous extrapolation technique was not programmed into the data acquisition software used during the majority of this project. Instead, the stress range for one gage was extrapolated with the stress range for a second gage to estimate the stress range at a critical location. Extrapolation of stress ranges is theoretically correct if the maximum and minimum stresses at both gages occur at exactly the same times.

To check the accuracy of the extrapolation of stress ranges, the data acquisition system was programmed in a limited number of test files to display stresses at some critical locations from continuous extrapolation of the gage readings. Stress ranges determined from

these continuous extrapolation plots were compared to stress ranges calculated by extrapolation of stress ranges at the gage location. These comparisons indicated that stress ranges determined by extrapolation of stress ranges were larger than the stress ranges determined from the continuous extrapolation plots, typically by 10 to 20 percent for the highest magnitude stress ranges recorded in this project. Hence, determining stress ranges by extrapolation of stress ranges is considered to be conservative. For smaller magnitude stress ranges the conservative difference was found to be approximately equivalent to the mechanical and electronic noise recorded by the gage displaying the greatest magnitude for the particular extrapolation. This noise was generally 0.15 to 0.30 ksi.

Despite the overestimate produced by performing the extrapolations with stress ranges, it is important to note that this overestimate represents a conservative estimate of the stresses and stress ranges at critical locations. This type of extrapolation was used in previous studies by Fisher et al. (1978, 1979, 1980, 1987, 1989, 1990).

Cracks also tend to form in the throats of the connection plate to web welds in the web gap region where there is a high stress concentration. Test results reported by Fisher et al. (1990) indicate that this type crack will tend to propagate into the web and through the web thickness. All five locations presently identified by AHD bridge inspectors with cracks in floortruss connections in the I-65 bridges occurred at the top end of the inside connection plate to web weld. Hence, the stresses in the throat of the connection plate to web weld were considered of particular interest.

The connection plate strain gages were used to calculate horizontal stresses in the connection plate which were used to calculate stresses in the connection plate to web weld.

This was accomplished by first extrapolating the stresses in the connection plate at the gage locations to estimate the stress in the plate at the top of the connection plate weld. The actual stress in the connection plate consisted of axial and bending stresses as previously discussed. Since the connection plate stresses near the top of the connection plate weld were predominantly axial, the relatively small bending stresses were neglected to simplify the analysis. The stress in the connection plate at the top of the connection plate weld was assumed to act on a unit strip of the connection plate at the top of the connection plate weld. The stress in the weld on each side of the plate was then found by equating the force on the unit length of weld to half the force on the unit strip of connection plate. In equation form, the weld stress is:

$$\sigma_{weld} = \sigma_{plate} \left(\frac{t}{2}\right) \left(\frac{1}{(0.707)\ (s)}\right) \qquad [2]$$

where t= plate thickness; and s= the fillet weld size. The area of each weld was taken as the unit length times the throat dimension, which was the fillet weld size times the cosine of 45 degrees (0.707). The fillet weld size for each location is given in Table 2 of Chapter Four. The fillet weld size at all connections varied somewhat in approximately the uppermost nine inches. The variability for the fillet weld size was as much as +/- 1/8 in. for some locations. The top end of the weld was enlarged in a number of locations due to the termination of the weld.

The maximum weld stress calculated from either side of the connection plate always occurred at the north side of the connection plate. For typical stress records as shown in

Figure 43, the difference in stresses between the top two gage locations was always somewhat greater for the north side. This produced a calculated stress range in the north side top of the connection plate weld that was slightly higher than or equal to that at the south side. In the remainder of this chapter, only the stresses or stress ranges in the weld on the north side are reported.

EFFECTIVE STRESS RANGES FROM TRUCK TRAFFIC

The severity of the fatigue loading and potential for cracking at the floortruss-girder connections can be evaluated from the effective stress ranges at critical locations resulting from random truck traffic. The effective stress range is an equivalent constant amplitude stress range for a sample group of test events of varying amplitude. All effective stress ranges reported here are Miner's effective stress ranges calculated using equation 1 presented in Chapter Six.

The stress ranges for random trucks at the critical locations were determined through linear extrapolation of the actual gage readings as described in the previous section. The extrapolated stress ranges were then used to calculate Miner's effective stress ranges, Sre's, for the critical locations. The results of the effective stress range calculations are presented in Table 14 with the maximum single stress range, Sr, recorded at each test connection. The signs on the stress ranges are shown as positive for locations where the stress was primarily tensile and negative where the stress was primarily compressive. Due to limits on time and on the number of data channels that could be recorded simultaneously, only a small number of truck crossings were available for calculating effective stress ranges in the connection

Table 14. Effective Stress Ranges at Critical Locations for Random Truck Data Before Retrofit

Web Plate Stress[a] Top of Conn. Plate Weld Sre (ksi)	Weld Stress Top of Conn. Plate Weld Sre (ksi)	Outside Web-[a] Flange Weld Sre (ksi)	Inside Web-[a] Flange Weld Sre (ksi)
Pier S3-11: First Floortruss South, Outside Girder (106" Web)			
+5.2 (+8.6*)	+8.7 (+14*)[b]	+22 (+38*)	-19 (-33*)
Pier S3-11: First Floortruss South, Inside Girder (106" Web)			
+17 (+27*)	+7.8 (+15*)[c]	+30 (+58*)	-25 (-41*)
Pier S3-11: Second Floortruss South, Outside Girder (106" Web)			
+5.0 (+9.2*)	+7.5 (+10*)[d]	+28 (+46*)	-22 (-36*)
Pier S3-4: First Floortruss North, Outside Girder (126" Web)			
+2.7 (+4.1*)	+10 (+16*)[b]	+15 (+24*)	-17 (-27*)
Pier S3-4: Second Floortruss North, Outside Girder (126" Web)			
+4.4 (+7.6*)	+5.3 (+9.1*)[b]	+13 (+22*)	-13 (-22*)
Pier S3-4: Second Floortruss North, Inside Girder (126" Web)			
+5.0 (+8.3*)	+7.4 (+12*)[b]	+18 (+30*)	-17 (-29*)

(*) Maximum recorded single stress range, Sr, for a random data file.
[a] Stress ranges calculated from 250 sampled trucks.
[b] Stress ranges calculated from 50 sampled trucks.
[c] Stress ranges calculated from 44 sampled trucks.
[d] Stress ranges calculated from 39 sampled trucks.

plate weld. Hence, those values in Table 14 are not as accurate as the other values in the table, but they are an indicator of the stress levels in the welds.

The largest magnitude effective stress ranges and maximum stress ranges were experienced at the outside web-flange weld for all pier S3-11 (106" web) locations. The largest magnitudes at pier S3-4 (126" web) locations occurred at the inside web-flange weld at the first floortruss north of the pier. The second floortruss connections at pier S3-4 showed the highest magnitudes for both the inside web-flange weld (outside girder) and the outside web-flange weld (inside girder). The inside girder connection at the first floortruss south of pier S3-11 experienced the largest stresses for all six connections tested.

Discussion of Overall Maximum Stress

The overall maximum extrapolated stress range, Sr, measured at any of the test locations was +58 ksi as shown in Table 14. This stress range occurred at the outside web-flange weld at the inside girder connection of the first floortruss south of pier S3-11. The gages used for the extrapolation to the outside web-flange weld were ON1 and ON2. As illustrated in Figure 26 of Chapter Five the ON1 gage was 0.25 in. below the toe of the web-flange weld and the ON2 gage was 0.75 in. below the ON1 gage. The strain records for these gages for the truck crossing that resulted in the 58 ksi stress range appear in Figures 57 and 58. The strain records in Figure 57 and 58 indicate that the truck created both tension and compression at the gage locations and at the outside web-flange weld. By adjusting the recorded strains for the small initial offsets from zero, the minimum strain at ON2 was -345 $\mu\epsilon$ and the maximum strain at ON1 was +1307 $\mu\epsilon$. Extrapolation of gage ON1 and ON2

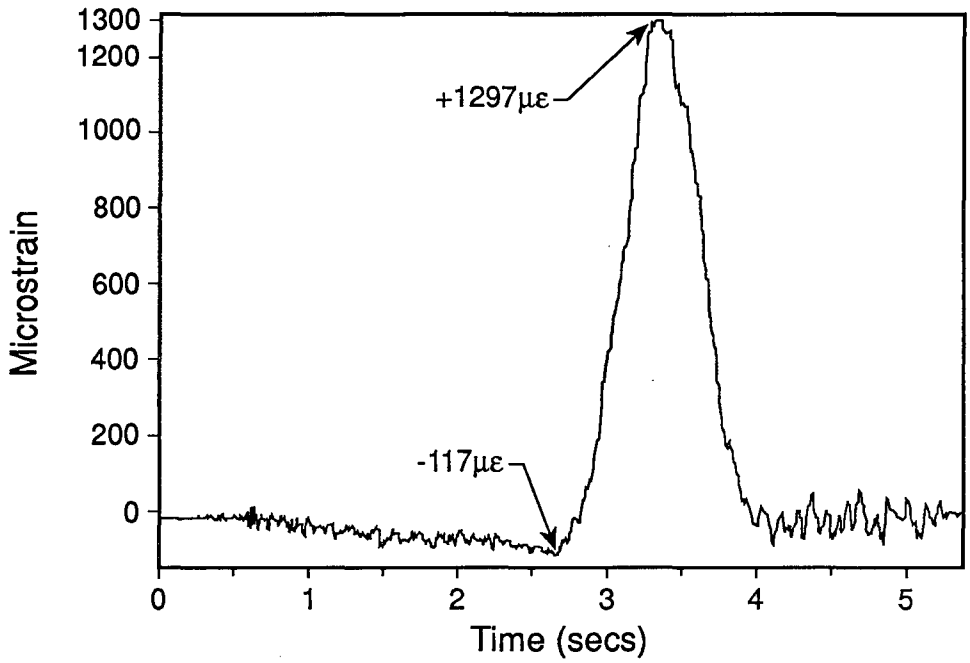

Figure 57. Gage ON1 Strain Record that Contributed to the Maximum Extrapolated Stress Range Measured for Random Trucks

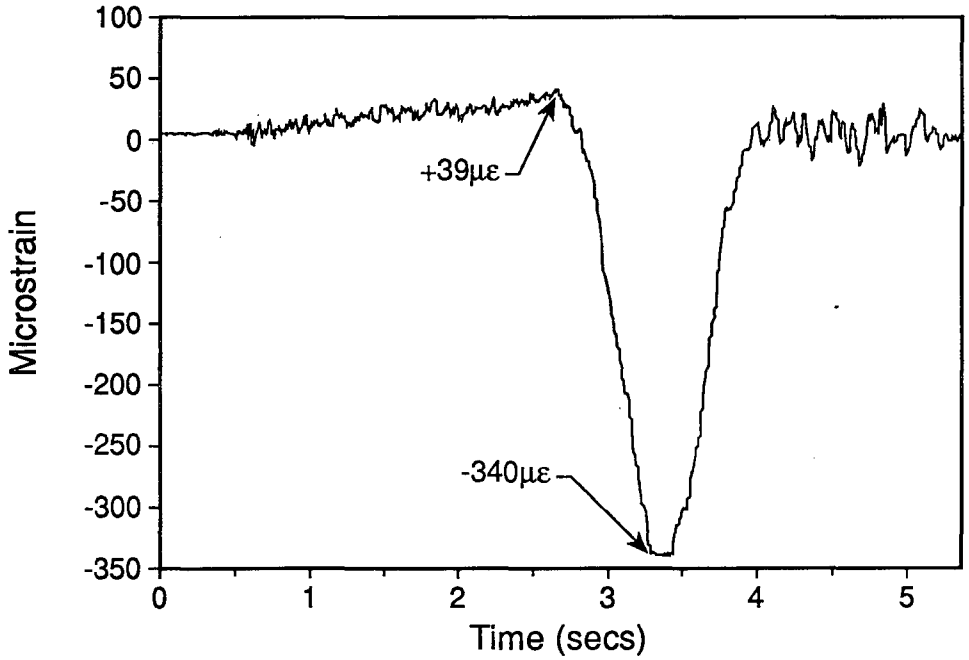

Figure 58. Gage ON2 Strain Record that Contributed to the Maximum Extrapolated Stress Range Measured for Random Trucks

strains to the web-flange weld toe results in a maximum tensile strain of +1858 $\mu\epsilon$. This extrapolated maximum tensile strain exceeds the nominal yield strain of 1720 $\mu\epsilon$ for A588 Grade 50 weathering steel by 8 percent. This indicates that the steel at the edge of the web-flange weld yielded during the truck crossing.

The prospect of recording an event which would cause yielding of the web in the web gap was initially very surprising. There are a few factors which could have introduced error into the data collection and reduction process so that the actual stress at the web-flange weld could have been less than the yield stress. The most significant is the use of linear extrapolation from the gage locations to the toe of the weld. Past finite element studies (Fisher et al. 1990) have indicated that the use of linear extrapolation is a reasonable method for using strain gage results of the type presented here, but it is only an approximate approach. However, regardless of the potential for error in the extrapolated stress, the maximum recorded stress at the ON1 gage location was 38 ksi which is close to the yield strength. The possibility of having yielding in the web gap is also confirmed by recent cases in Alabama where considerable plastic deformation was found by bridge inspectors in web gaps at two different plate girder bridges.

The maximum stress range event is reported here as 58 ksi based on multiplying the extrapolated strain range by the modulus of elasticity. The positive peak of the strain range did exceed the yield strain, so the actual peak positive stress was limited to the material yield stress. This means that the actual "stress" range was less than 58 ksi. However, the event is reported as 58 ksi to provide an accurate indicator of the extrapolated "strain" range.

Stress Range Histograms

Stress ranges for the bottom edge of the outside web-flange fillet weld and the web plate at the top of the connection plate to web fillet welds appear in histogram format in Figures 59 through 70. These stress range histograms provide a convenient record of the measured stress conditions. Overall, the histograms indicate that the measured stress ranges were very high, especially at the web-flange welds. The stress ranges were generally higher than those measured at floorbeam-girder connections in an earlier phase of this project (Volume I, Stallings et al. 1993). The largest effective stress range reported then was 12.0 ksi at floorbeam-girder connections away from piers. The maximum stress range recorded at any location is shown in Figure 62 at 58 ksi.

For laboratory tests Keating et al. (1987), Schilling et al. (1978), Fisher et al. (1983), and others have assumed a Rayleigh type distribution of stress ranges for modeling random vehicle loadings. The Rayleigh distribution is a skewed right distribution with a single peak in the frequency distribution. An illustration of the shape and characteristics of the Rayleigh distribution was shown in Figure 13 of Chapter Two.

Approximately two-thirds of the histograms shown for pier S3-11 connections and all shown for pier S3-4 connections were, generally, skewed right distributions. This skewed right tendency was mainly the result of a few relatively high stress ranges that shifted the mean to the right. Although the majority of distributions were skewed right, the histograms did not represent a clear Rayleigh distribution. Some of the histograms have two pronounced peaks (bimodal) which matches the shape commonly found for truck weight distributions from weight-in-motion studies as discussed by Moses et al. (1987). Still, use of the Rayleigh

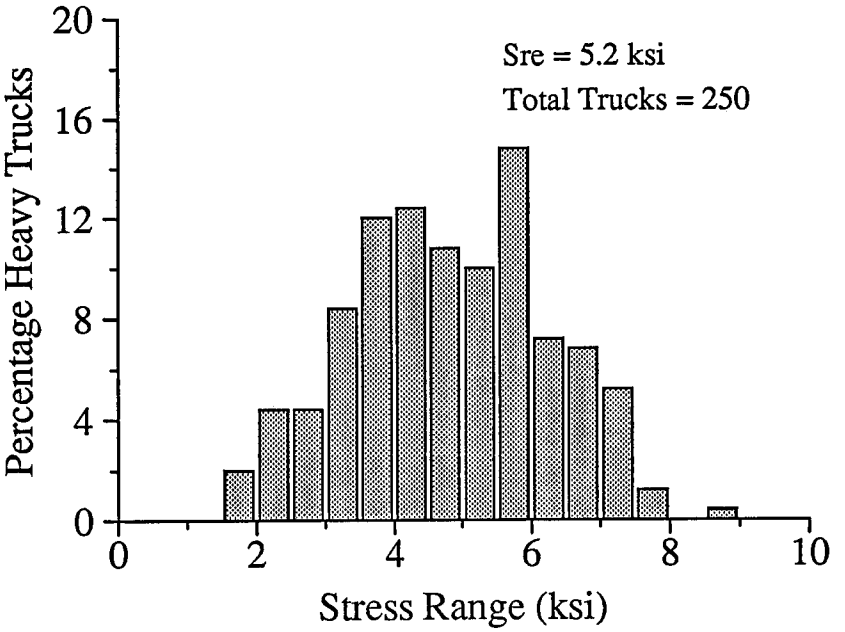

Figure 59. Web Plate Stress Ranges at the Top of the Connection Plate Weld on the Outside Girder at the First Floortruss South of Pier S3-11 Before Retrofit

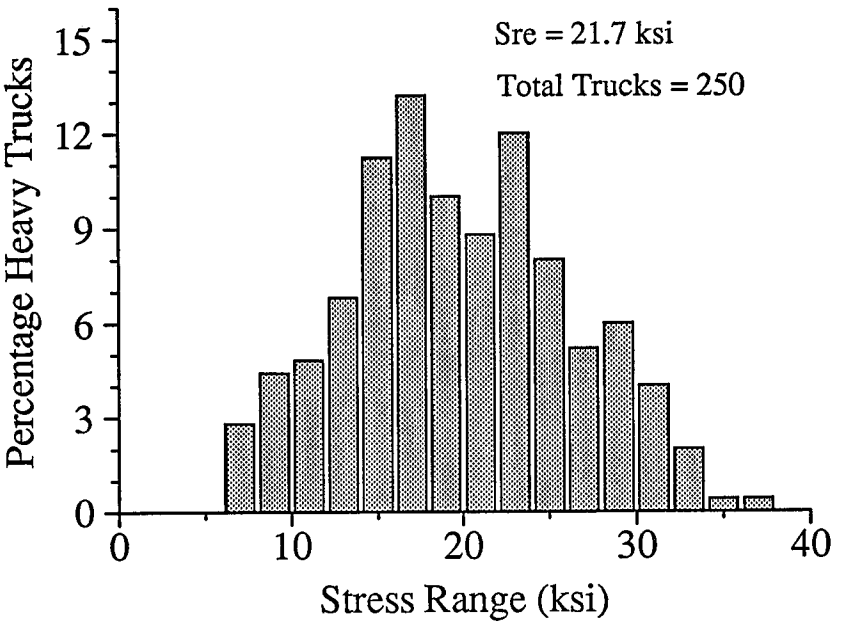

Figure 60. Web Plate Stress Ranges at the Outside Web-Flange Weld Toe on the Outside Girder at the First Floortruss South of Pier S3-11 Before Retrofit

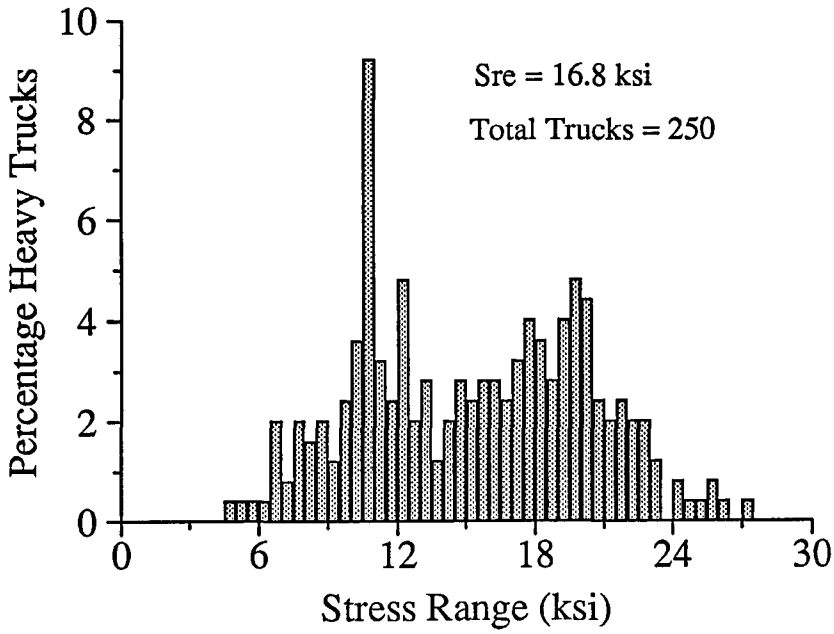

Figure 61. Web Plate Stress Ranges at the Top of the Connection Plate Weld on the Inside Girder at the First Floortruss South of Pier S3-11 Before Retrofit

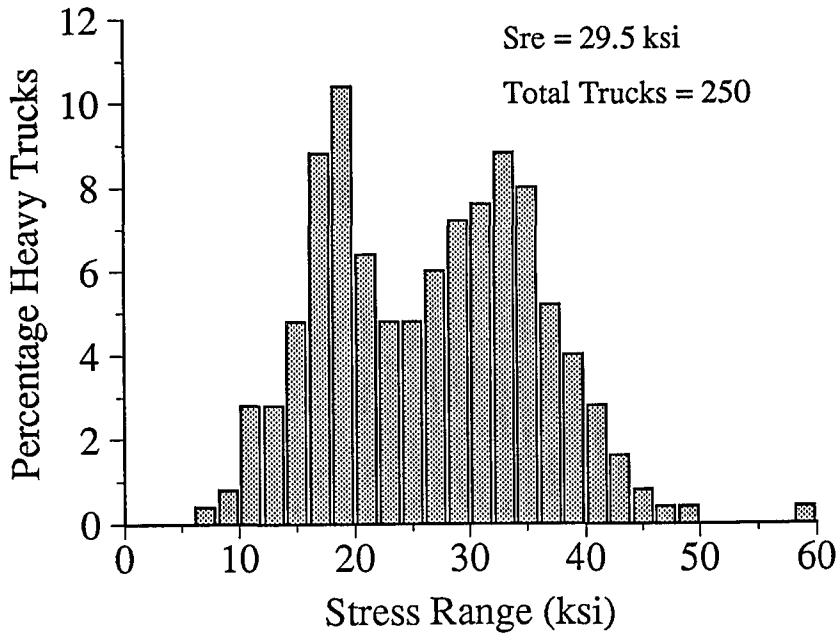

Figure 62. Web Plate Stress Ranges at the Outside Web-Flange Weld Toe on the Inside Girder at the First Floortruss South of Pier S3-11 Before Retrofit

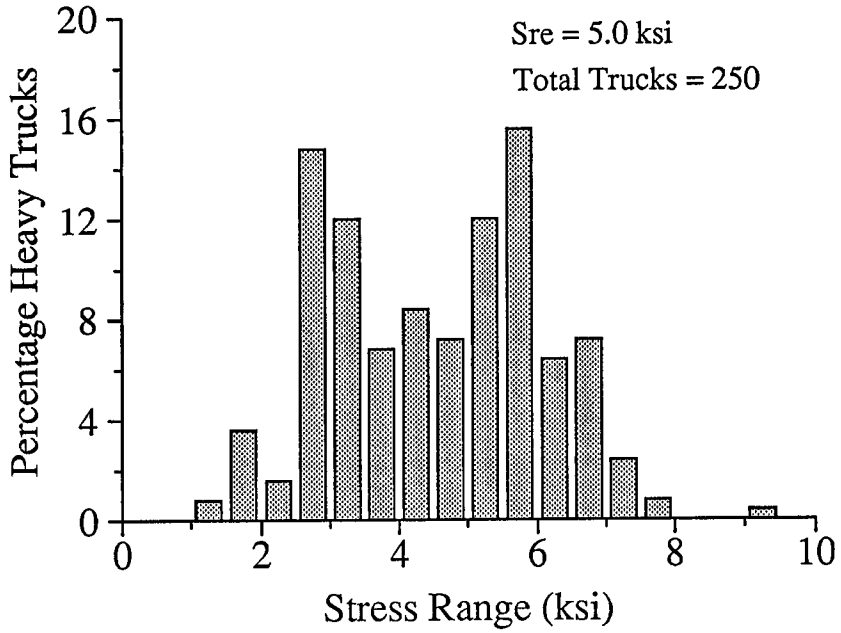

Figure 63. Web Plate Stress Ranges at the Top of the Connection Plate Weld on the Outside Girder at the Second Floortruss South of Pier S3-11 Before Retrofit

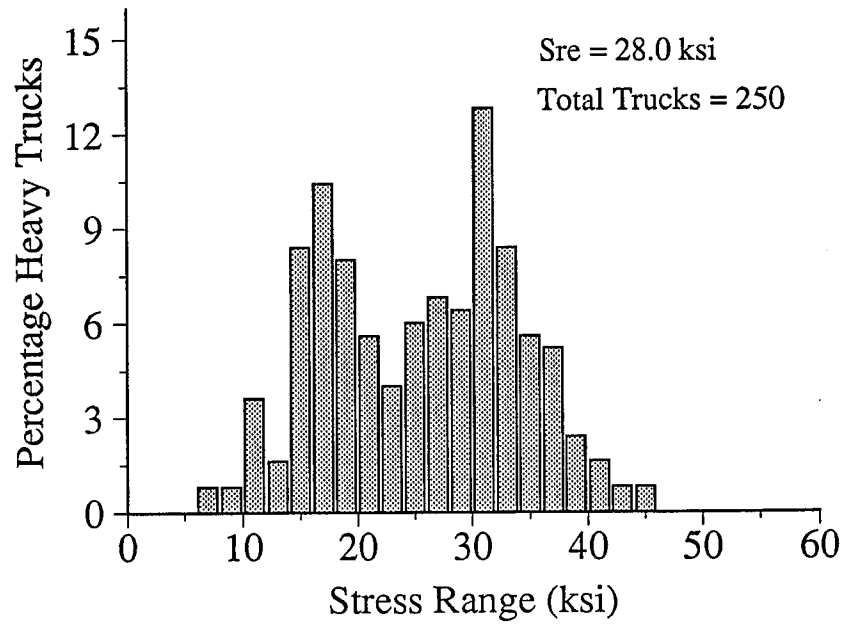

Figure 64. Web Plate Stress Ranges at the Outside Web-Flange Weld Toe on the Outside Girder at the Second Floortruss South of Pier S3-11 Before Retrofit

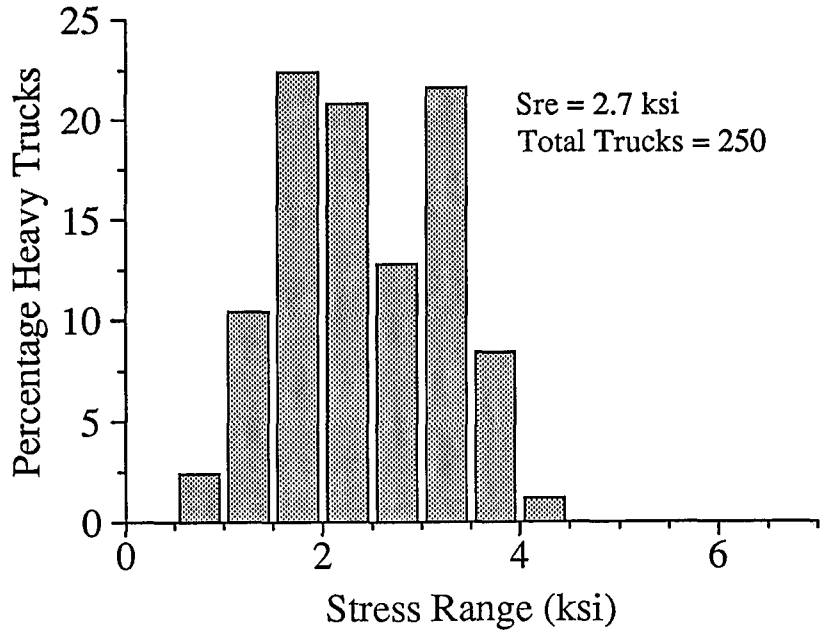

Figure 65. Web Plate Stress Ranges at the Top of the Connection Plate Weld on the Outside Girder at the First Floortruss North of Pier S3-4 Before Retrofit

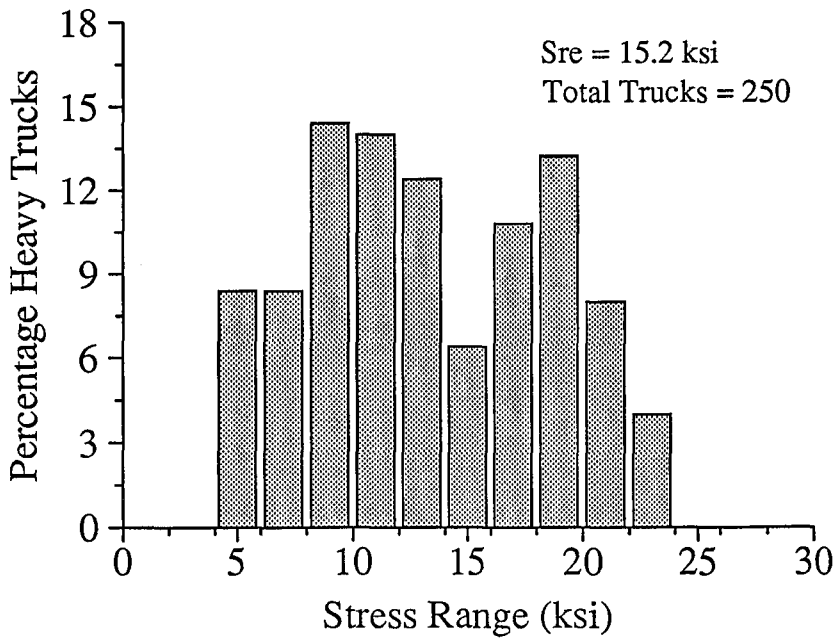

Figure 66. Web Plate Stress Ranges at the Outside Web-Flange Weld Toe on the Outside Girder at the First Floortruss North of Pier S3-4 Before Retrofit

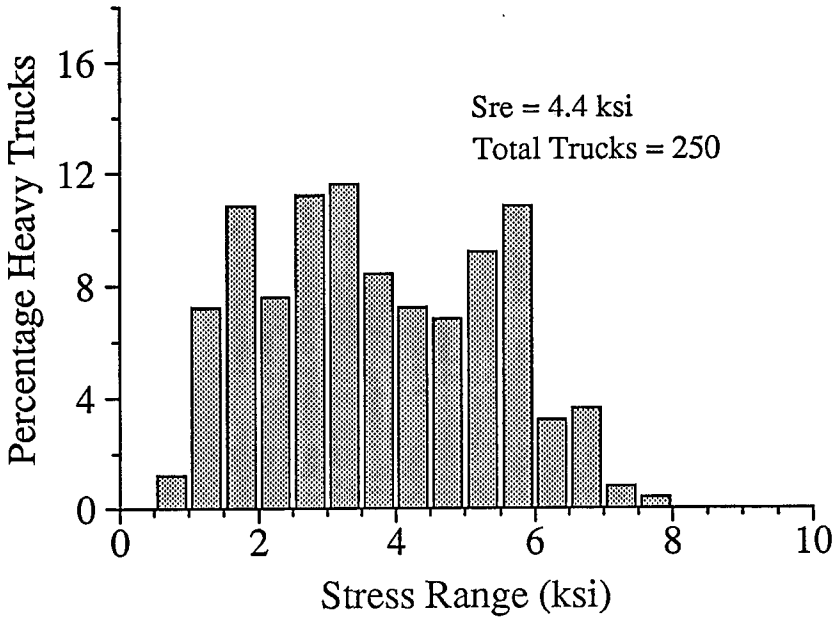

Figure 67. Web Plate Stress Ranges at the Top of the Connection Plate Weld on the Outside Girder at the Second Floortruss North of Pier S3-4 Before Retrofit

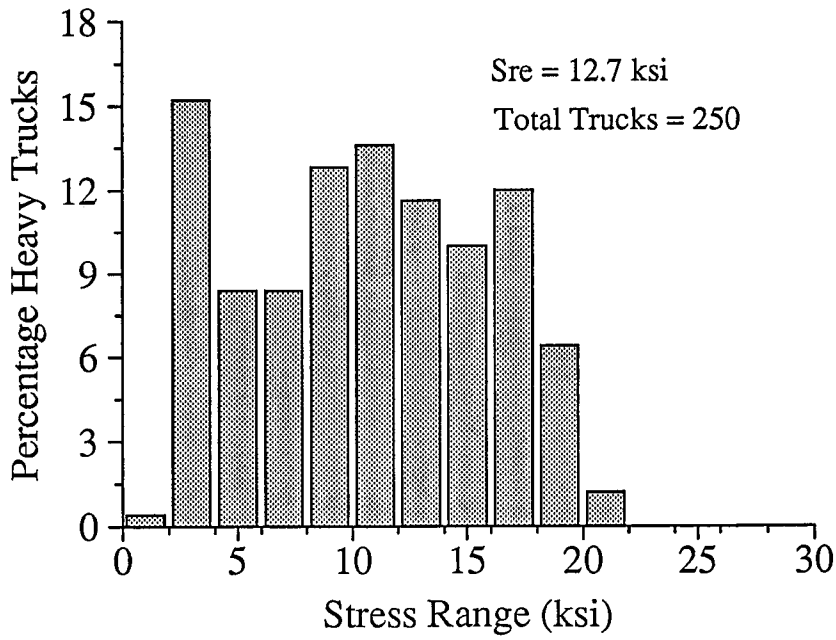

Figure 68. Web Plate Stress Ranges at the Outside Web-Flange Weld Toe on the Outside Girder at the Second Floortruss North of Pier S3-4 Before Retrofit

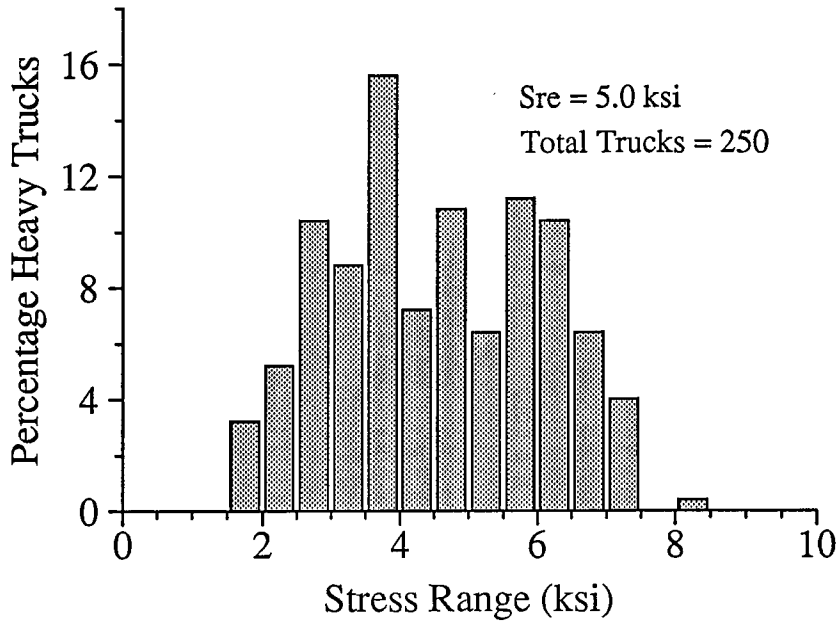

Figure 69. Web Plate Stress Ranges at the Top of the Connection Plate Weld on the Inside Girder at the Second Floortruss North of Pier S3-4 Before Retrofit

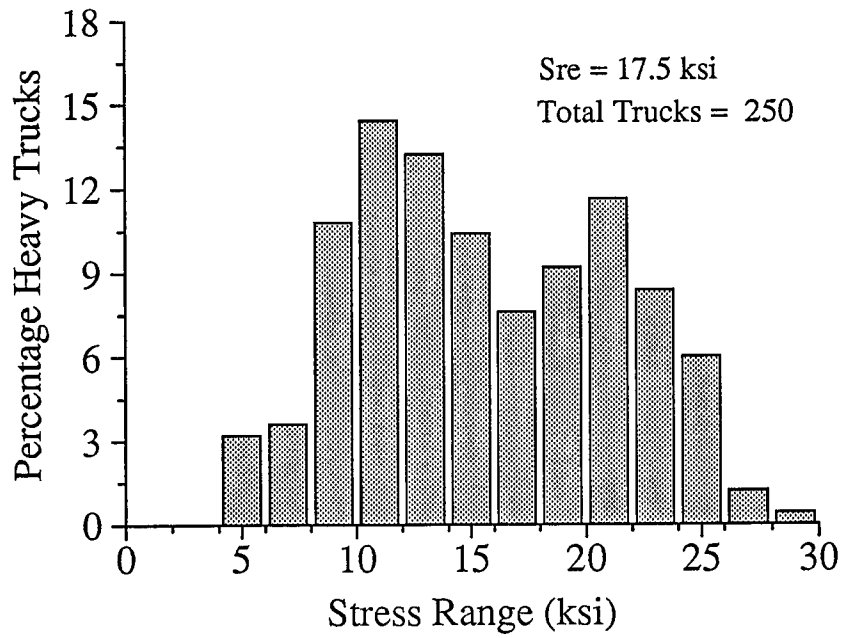

Figure 70. Web Plate Stress Ranges at the Outside Web-Flange Weld Toe on the Inside Girder at the Second Floortruss North of Pier S3-4 Before Retrofit

distribution for simulated random structural load histories in laboratory tests appears to be very reasonable. No distribution could be expected to model random loading histories with better accuracy than the Rayleigh distribution.

In spite of the fact that the histograms displayed several bimodal and multi-modal central tendencies the histograms did not provide sufficient proof for suggesting a frequency distribution that would be more appropriate for simulating random load histories than the Rayleigh distribution. Some parameters that affected the histogram shapes included the number of truck crossings recorded, the choice of cell widths for plots, the choice of the trigger level for recording a truck crossing, the sample population, and the specific structural response of the particular connection tested. The first three parameters mentioned were entirely the preference of the researchers and were based on the specific project objectives and time limitations. The sample population was made up of combinations of truck weight and axle spacings that may not have been common to other locations. The relatively unique connection response of these particular connections was already mentioned and will be further discussed in later sections.

Exceedance Rates at Critical Locations

Researchers in previous fatigue tests have studied the relationship between fatigue crack propagation and the rate that the applied stress ranges exceeded the constant-amplitude fatigue limit. Keating et al. (1987) and Fisher et al. (1983) noted that previous research revealed fatigue crack initiation and propagation could occur for exceedance rates as low as

0.1 percent even when the effective stress range (equivalent constant-amplitude stress range) was less than the constant-amplitude fatigue limit.

Based on fatigue tests of plate girders with transverse connection plates subjected to out-of-plane bending, Fisher et al. (1990) estimated constant-amplitude fatigue limits for the web plate surface at the top of the connection plate weld and the girder web-flange weld to be 10 ksi and 15 ksi, respectively. The fillet welds connecting the connection plates to the girder webs are transversely loaded and the fatigue limit for these welds is defined in AASHTO (1993) Table 10.3.1B. The allowable fatigue stress range on the throat of transversely loaded fillet welds is a function of the weld size and transverse connection plate thickness as shown in the following equation:

$$S_r = S_r^C \left(\frac{0.06 + 0.79\ H/t}{1.1\ t^{\frac{1}{6}}} \right) \qquad [3]$$

where S_r^C= allowable stress range for Category C (10 ksi); H= the weld size; and t= transverse connection plate thickness. For the weld and connection plate sizes at the connections tested, the fatigue limits calculated from this equation range from 5.7 to 6.7 ksi. For simplicity a fatigue limit of 6 ksi for the fillet welds will be used at all connections. Table 15 presents the exceedance rates at the critical locations for all six connections tested in this project. These exceedance rates represent the percentage of measured stress ranges that exceed the applicable fatigue limit. Note that although the stresses at the inside web-flange weld were primarily compressive, exceedance rates are shown since compressive stress ranges can cause fatigue crack initiation near a weld.

Table 15. Fatigue Limit Exceedance Rates at Critical Locations for Random Truck Data Before Retrofit

Web Plate Stress[a] Top of Conn. Plate Weld	Weld Stress Top of Conn. Plate Weld	Outside Web-[a] Flange Weld	Inside Web-[a] Flange Weld
% Exceeding 10 ksi	% Exceeding 6 ksi	% Exceeding 15 ksi	% Exceeding 15 ksi
Pier S3-11: First Floortruss South, Outside Girder (106" Web)			
0.0	74[b]	77	60
Pier S3-11: First Floortruss South, Inside Girder (106" Web)			
86	45[c]	90	83
Pier S3-11: Second Floortruss South, Outside Girder (106" Web)			
0.0	54[d]	91	70
Pier S3-4: First Floortruss North, Outside Girder (126" Web)			
0.0	76[b]	39	47
Pier S3-4: Second Floortruss North, Outside Girder (126" Web)			
0.0	26[b]	24	24
Pier S3-4: Second Floortruss North, Inside Girder (126" Web)			
0.0	34[b]	52	47

[a] Exceedance rates calculated from 250 sampled trucks.
[b] Exceedance rates calculated from 50 sampled trucks.
[c] Exceedance rates calculated from 44 sampled trucks.
[d] Exceedance rates calculated from 39 sampled trucks.

Inspection of Table 15 indicates that a large percentage of the stress ranges measured at the web-flange weld exceed the fatigue limit of 15 ksi. In fact, the histograms of the previous section indicate that at four of the six connections tested, a significant percentage of stress ranges exceeded the AASHTO Category B fatigue limit of 16 ksi for the weathering steel base metal. These high exceedance rates indicate that fatigue cracking can be expected in the future at the web-flange welds of the floortruss-girder connections. The results in Table 15 indicate that cracking of the connection plate fillet welds can also be expected. It is interesting that only one of the six connections experienced stress ranges above 10 ksi on the web plate at the top of the connection plate to web weld. However, at this one location the exceedance rate was very high. Hence, cracking in the web at the top of the connection plate to web welds can be expected at some locations in the future.

Fast Run Test Truck Results at Critical Locations

In Volume I of this report (Stallings et al. 1993), test truck stress ranges for fast run calibrations were reported for each traffic lane. Addition of the stress ranges and the displacement ranges recorded for each lane was assumed to be reasonable for estimating the responses that would result from side-by-side truck crossings. The stress and displacement ranges resulting from adding the slow and fast lane results for the 5-axle test truck provides a reasonable limit on the magnitude of the stress ranges that will occur a significant number of times from normal legal traffic. While side-by-side crossings of heavy 3-axle trucks are quite possible, those are not as likely as for the 5-axle trucks. Sums of the slow and fast lane test results (lane B+C) at the floortruss-girder connections tested during this phase of

the project appear in Table 16 for the 5-axle test truck and Table 17 for the 3-axle test truck. The stress ranges at these floortruss-girder connections were significantly larger than the stress ranges at the floorbeam-girder connections in Volume I of this project report (Stallings, et al. 1993).

It is interesting to note from Table 16 that the inside girder connection of the first floortruss south of pier S3-11 experienced the maximum overall stress range, but did not have the greatest overall out-of-plane displacement range for the calibration test data. Note that data for estimation of the stress range in the connection plate weld for test trucks was only available at the two connections chosen for retrofit analysis. Data presented in the next section indicates that there was a unique relationship between stress ranges and out-of-plane displacement ranges for each of the six connections tested.

As previously noted, the lane B+C stress ranges were used to estimate the stress ranges expected at the test locations for side-by-side heavy truck crossings. The estimated stress ranges for side-by-side 5-axle truck loadings at the web-flange weld at the pier S3-11 connections exceeded the yield stress of 50 ksi (Table 16). Numerous critical locations at all six connections tested before retrofit were reported with stress ranges exceeding the yield stress under side-by-side 3-axle test truck loading (Table 17). These results initially seemed unreasonable. Therefore, an analysis was performed of data recorded during static calibrations in which a simulated side-by-side truck crossing was recorded. These records were not a part of the original calibration scheme, but were recorded as a potential indicator of maximum load cases. The tests consisted of the 5-axle test truck parked in lane B as a random 5-axle truck crossed the span in lane C. An analysis of the data from these

Table 16. Stress and Displacement Ranges at Critical Locations for 5-Axle Test Truck Fast Runs (Typical Loading) Before Retrofit

Test	Web Pl. Str. Top Conn. Pl. Weld Sr (ksi)	Weld Str. Top Conn. Pl. Weld Sr (ksi)	Out. Web-Flg. Weld Sr (ksi)	In. Web-Flg. Weld Sr (ksi)	Displ. Top of Conn. Pl. (in.)
Pier S3-11: First Floortruss South Outside Girder (106" Web)					
Max Random	+8.6	+14	+38	-33	+0.0093
Test Lane B	+7.0	+11	+36	-32	+0.0083
Test Lane C	+5.7	+9.0	+29	-26	+0.0067
Lane B+C	+13	+20	+65	-58	+0.0150
Pier S3-11: First Floortruss South, Inside Girder (106" Web)					
Max Random	+27	-----	+58	-41	+0.0107
Test Lane B	+23	-----	+41	-36	+0.0076
Test Lane C	+16	-----	+30	-26	+0.0054
Lane B+C	+39	-----	+71	-62	+0.0130
Pier S3-11: Second Floortruss South, Outside Girder (106" Web)					
Max Random	+9.2	-----	+46	-36	+0.0084
Test Lane B	+6.2	-----	+36	-28	+0.0065
Test Lane C	+5.9	-----	+35	-28	+0.0066
Lane B+C	+12	-----	+71	-56	+0.0131
Pier S3-4: First Floortruss North, Outside Girder (126" Web)					
Max Random	+4.1	-----	+24	-27	+0.0056
Test Lane B	+3.0	-----	+19	-22	+0.0045
Test Lane C	+3.0	-----	+18	-21	+0.0043
Lane B+C	+6.0	-----	+37	-43	+0.0088
Pier S3-4: Second Floortruss North, Outside Girder (126" Web)					
Max Random	+7.6	+9.1	+22	-29	+0.0058
Test Lane B	+4.8	+6.3	+17	-18	+0.0048
Test Lane C	+5.4	+6.3	+19	-20	+0.0054
Lane B+C	+10	+13	+36	-38	+0.0102
Pier S3-4: Second Floortruss North, Inside Girder (126" Web)					
Max Random	+8.3	-----	+30	-29	+0.0068
Test Lane B	+6.1	-----	+22	-22	+0.0052
Test Lane C	+3.9	-----	+15	-14	+0.0031
Lane B+C	+10	-----	+37	-36	+0.0083

Table 17. Stress and Displacement Ranges at Critical Locations for 3-Axle Test Truck Fast Runs Before Retrofit

Test	Web Pl. Str. Top Conn. Pl. Weld Sr (ksi)	Weld Str. Top Conn. Pl. Weld Sr (ksi)	Out. Web-Flg. Weld Sr (ksi)	In. Web-Flg. Weld Sr (ksi)	Displ. Top of Conn. Pl. (in.)
Pier S3-11: First Floortruss South Outside Girder (106" Web)					
Max Random	+8.6	+14	+38	-33	+0.0093
Test Lane B	+8.0	+12	+42	-37	+0.0096
Test Lane C	+6.6	+11	+34	-30	+0.0079
Lane B+C	+15	+23	+76	-67	+0.0175
Pier S3-11: First Floortruss South, Inside Girder (106" Web)					
Max Random	+27	-----	+58	-41	+0.0107
Test Lane B	+25	-----	+46	-39	+0.0085
Test Lane C	+20	-----	+37	-31	+0.0065
Lane B+C	+45	-----	+83	-70	+0.0150
Pier S3-11: Second Floortruss South, Outside Girder (106" Web)					
Max Random	+9.2	-----	+46	-36	+0.0084
Test Lane B	+8.8	-----	+51	-40	+0.0093
Test Lane C	+7.0	-----	+41	-33	+0.0077
Lane B+C	+16	-----	+92	-73	+0.0170
Pier S3-4: First Floortruss North, Outside Girder (126" Web)					
Max Random	+4.1	-----	+24	-27	+0.0056
Test Lane B	+3.9	-----	+25	-28	+0.0059
Test Lane C	+3.6	-----	+22	-26	+0.0053
Lane B+C	+7.5	-----	+47	-54	+0.0112
Pier S3-4: Second Floortruss North, Outside Girder (126" Web)					
Max Random	+7.6	+9.1	+22	-29	+0.0058
Test Lane B	+7.0	+8.6	+24	-25	+0.0068
Test Lane C	+6.8	+9.2	+23	-25	+0.0067
Lane B+C	+14	+18	+47	-50	+0.0135
Pier S3-4: Second Floortruss North, Inside Girder (126" Web)					
Max Random	+8.3	-----	+30	-29	+0.0068
Test Lane B	+8.1	-----	+29	-29	+0.0070
Test Lane C	+6.2	-----	+23	-22	+0.0051
Lane B+C	+14	-----	+52	-51	+0.0121

simulated side-by-side trucks showed stresses that were 10 to 25 percent less than the lane B+C stresses from 5-axle test truck calibration tests at those positions.

This suggests that the extremely high stress ranges estimated by adding lane B and lane C stress ranges for test truck crossings are reasonable to use as a load case. The fact that the test trucks produced stress ranges that were among the highest recorded for all trucks does mean that the majority of side-by-side truck crossings occurring on the test spans in normal traffic would not produce stress ranges as severe as estimated by adding lane B and lane C. It also indicates that extremely heavy trucks traveling the bridge spans were never recorded in side-by-side crossings. Still, it is reasonable to expect that the bridge has and will, over the remaining life, undergo side-by-side truck crossings with truck weights and axle spacings comparable to those noted in Chapter Six for the 5-axle test truck. Even more importantly, the overall maximum load case for the side-by-side 3-axle test trucks could be a potential loading case in the bridge history, even though this type of truck was not as common in the general traffic stream. Such load combinations would certainly subject these connections to yielding (most severely at the web-flange weld) as previously discussed in the section "Discussion of Overall Maximum Stress". Symptoms of yielding in the web gap region found in recent cases in Alabama by bridge inspectors at two different plate girder bridges may be an indication of similar conditions in the bridges tested during this phase of the project.

OUT-OF-PLANE DISPLACEMENTS

The stresses in the web gap, connection plate, and connection plate to web weld result from out-of-plane distortion of the web in the web gap as previously discussed. Hence, the magnitudes of the displacements in the web gaps are of interest, although at the present time there is no method for evaluating the potential for fatigue cracking in the web gap from out-of-plane displacement measurements alone. Plots and regression analyses in the following sections of stresses at critical locations versus web gap displacement provide background that could be used in future projects to develop such a method.

Statistics from the out-of-plane displacement range measurements for the six connections tested before the retrofit under random truck loading are shown in Table 18. These displacement ranges were measured with LVDTs mounted on the edge of the connection plate at 0.5 in. below the top flange as illustrated in Figure 25 of Chapter Five. Displacement ranges are considered important here as opposed to the maximum displacements because the ranges are directly related to the fatigue stress ranges in the web gap. The displacement ranges were primarily the result of inward movement (positive) at the top of the connection plate when a truck was directly above the test location. Small outward (negative) displacements were measured as a truck approached or moved away from the test location. The maximum inward displacement was typically 80 to 90 percent of the full displacement range.

The results shown in Table 18 indicate that the pier S3-11 connections experienced greater displacements than the pier S3-4 connections. The average displacement range varied only 0.0006 in. overall between the three pier S3-11 connections and 0.0008 in. overall

Table 18. Displacement Range Statistics at Test Locations for Random Truck Data Before Retrofit

Average (in.)	Std. Dev. (in.)	Maximum (in.)
Pier S3-11: First Floortruss South, Outside Girder		
+0.0041	+0.0015	+0.0093
Pier S3-11: First Floortruss South, Inside Girder		
+0.0047	+0.0017	+0.0107
Pier S3-11: Second Floortruss South, Outside Girder		
+0.0046	+0.0015	+0.0084
Pier S3-4: First Floortruss North, Outside Girder		
+0.0031	+0.0013	+0.0056
Pier S3-4: Second Floortruss North, Outside Girder		
+0.0027	+0.0016	+0.0058
Pier S3-4: Second Floortruss North, Inside Girder		
+0.0035	+0.0014	+0.0068

between the three pier S3-4 connections. The standard deviation, which is a measure of the sample population dispersion, was nearly equivalent for all tested connections. As was the case for the stress range measurements, the overall maximum displacement range for all connections tested before retrofit under random truck loading, 0.0107 in., occurred at the inside girder connection of the first floortruss south of pier S3-11. This maximum displacement range was recorded during the same truck crossing that created the maximum stress ranges.

Histograms of displacement ranges for the six connections tested before retrofit appear in Figures 71 through 76. The displacement histograms were noted to have basically the same shapes as the stress range histograms at critical locations for the corresponding connections. The recorded displacements at all three connections at pier S3-4, and similarly at pier S3-11, were generated by the same trucks. Yet, as illustrated by Figure 75, a large number of small displacement ranges were recorded at the outside girder connection of the second floortruss north of pier S3-4, as compared to those measured at the other two connections of pier S3-4 shown in Figures 74 and 76. This illustrates the uniqueness of the structural behavior at this connection which is discussed further in the next section.

Critical Web Gap Location Stresses Versus Displacements

Plots of stress range versus displacement range for the web plate stress at the outside web-flange weld and at the top of the connection plate weld for all test locations are shown in Figures 77 through 88. These plots show 250 data points from trucks (and/or vehicles) of a wide variety of weights, axle spacings, and lane spacings. The data from fast runs of the

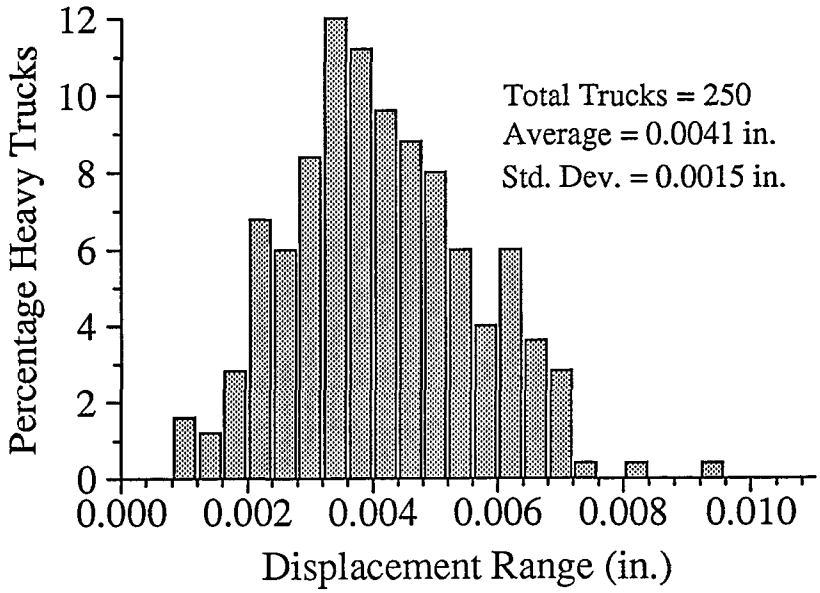

Figure 71. Out-of-Plane Displacement Ranges at the Outside Girder at the First Floortruss South of Pier S3-11 Before Retrofit

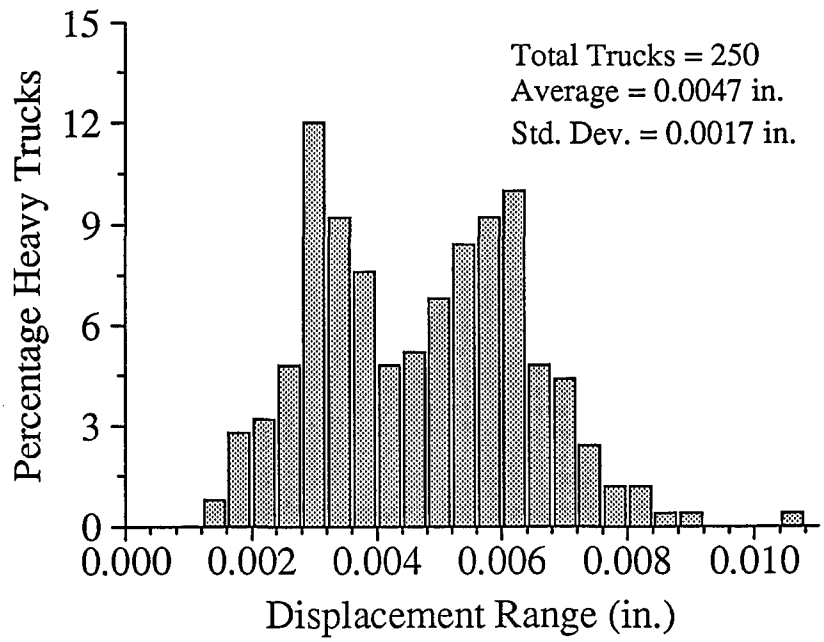

Figure 72. Out-of-Plane Displacement Ranges at the Inside Girder at the First Floortruss South of Pier S3-11 Before Retrofit

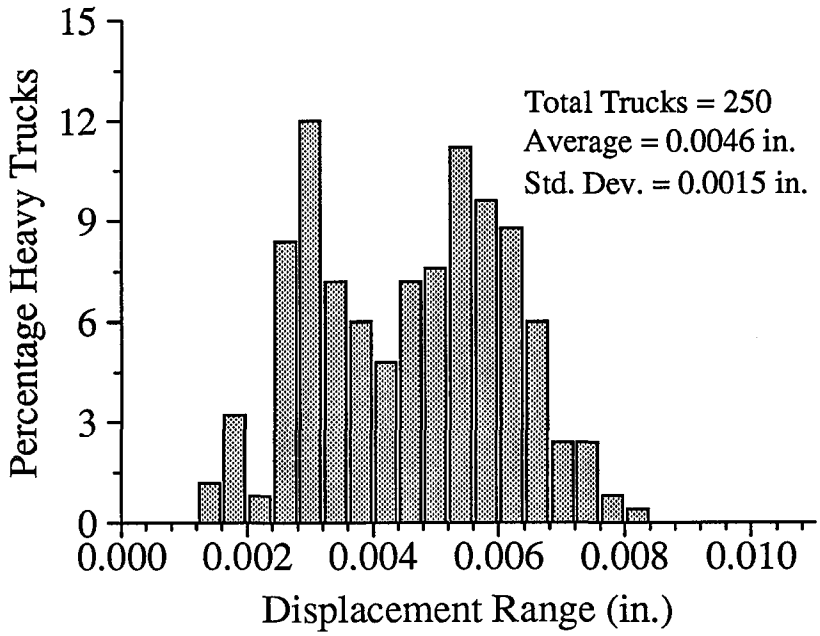

Figure 73. Out-of-Plane Displacement Ranges at the Outside Girder at the Second Floortruss South of Pier S3-11 Before Retrofit

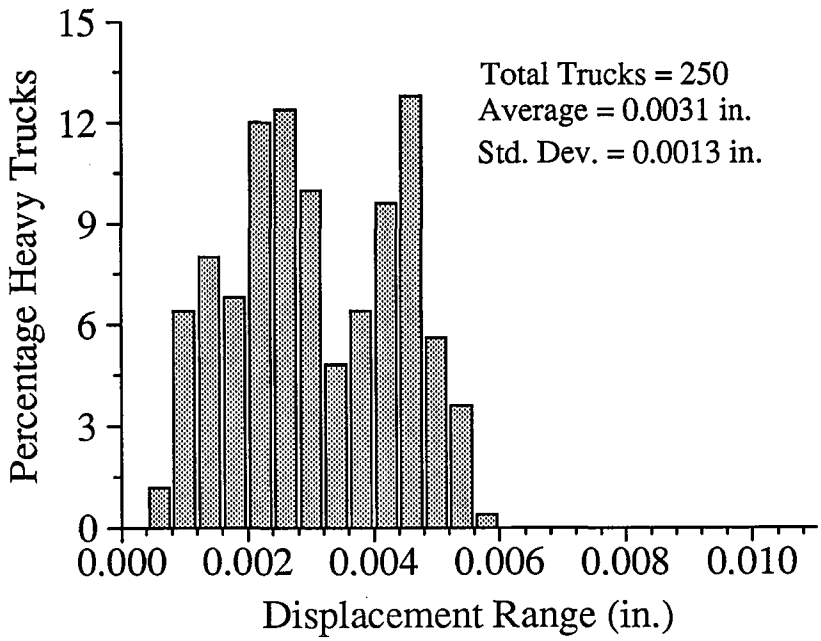

Figure 74. Out-of-Plane Displacement Ranges at the Outside Girder at the First Floortruss North of Pier S3-4 Before Retrofit

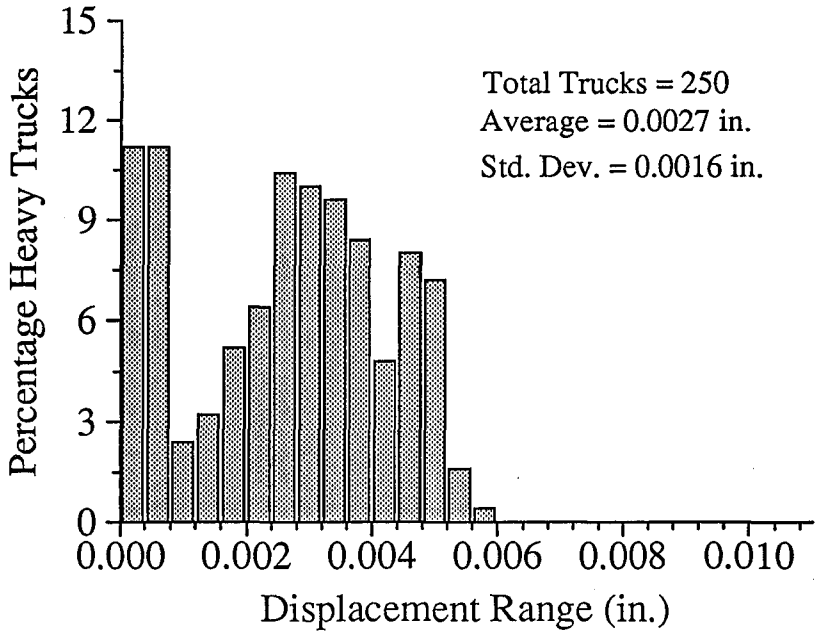

Figure 75. Out-of-Plane Displacement Ranges at the Outside Girder at the Second Floortruss North of Pier S3-4 Before Retrofit

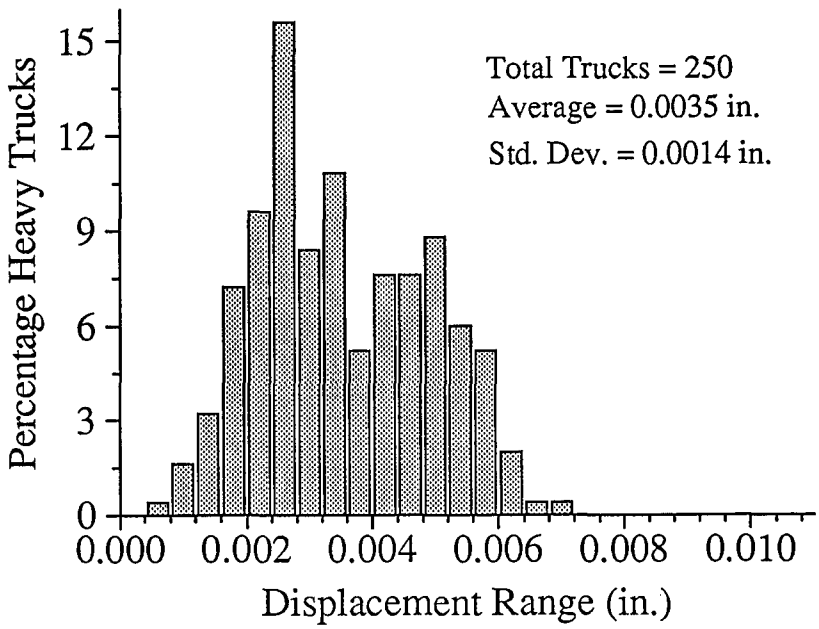

Figure 76. Out-of-Plane Displacement Ranges at the Inside Girder at the Second Floortruss North of Pier S3-4 Before Retrofit

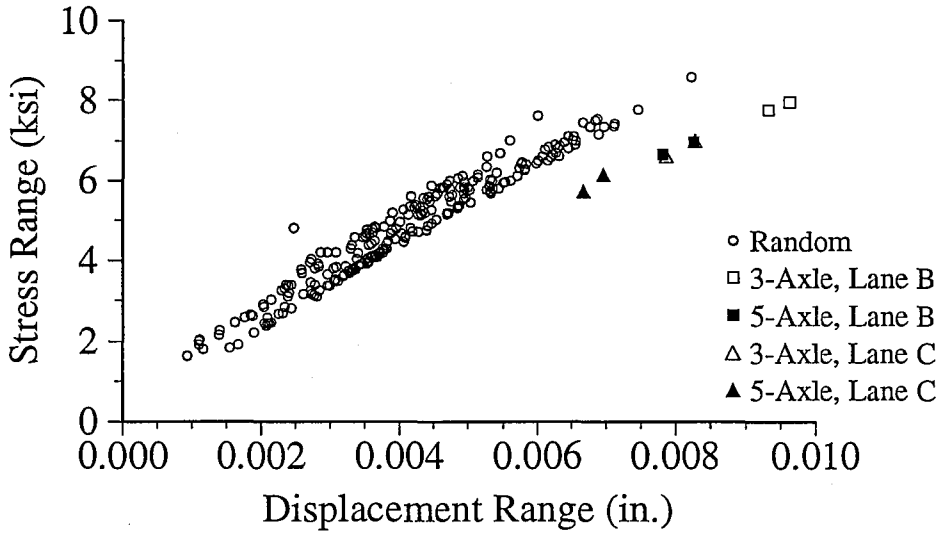

Figure 77. Web Plate Stress Range at the Top of the Connection Plate Weld Versus Out-of-Plane Displacement Range at the Outside Girder of the First Floortruss South of Pier S3-11 Before Retrofit

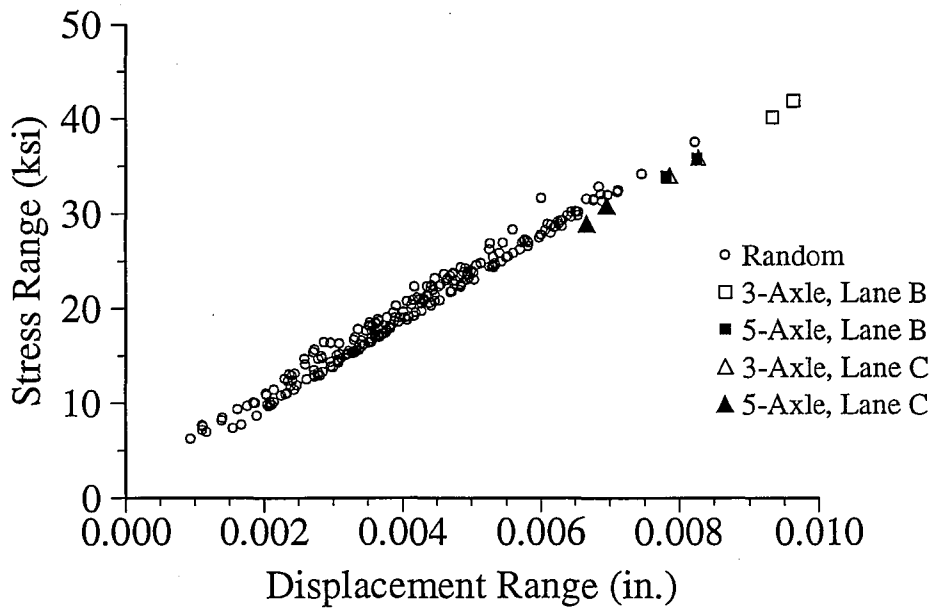

Figure 78. Web Plate Stress Range at the Outside Web-Flange Weld Toe Versus Out-of-Plane Displacement Range at the Outside Girder of the First Floortruss South of Pier S3-11 Before Retrofit

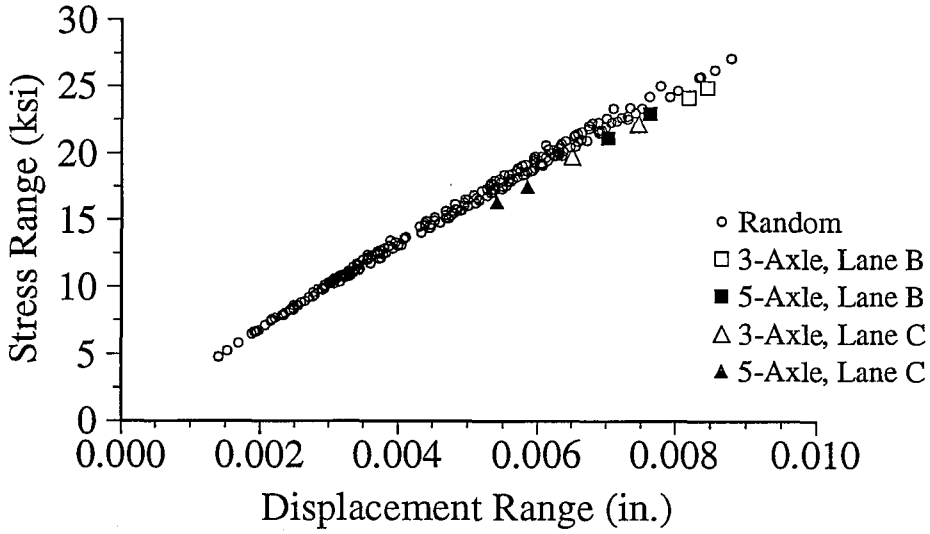

Figure 79. Web Plate Stress Range at the Top of the Connection Plate Weld Versus Out-of-Plane Displacement Range at the Inside Girder of the First Floortruss South of Pier S3-11 Before Retrofit

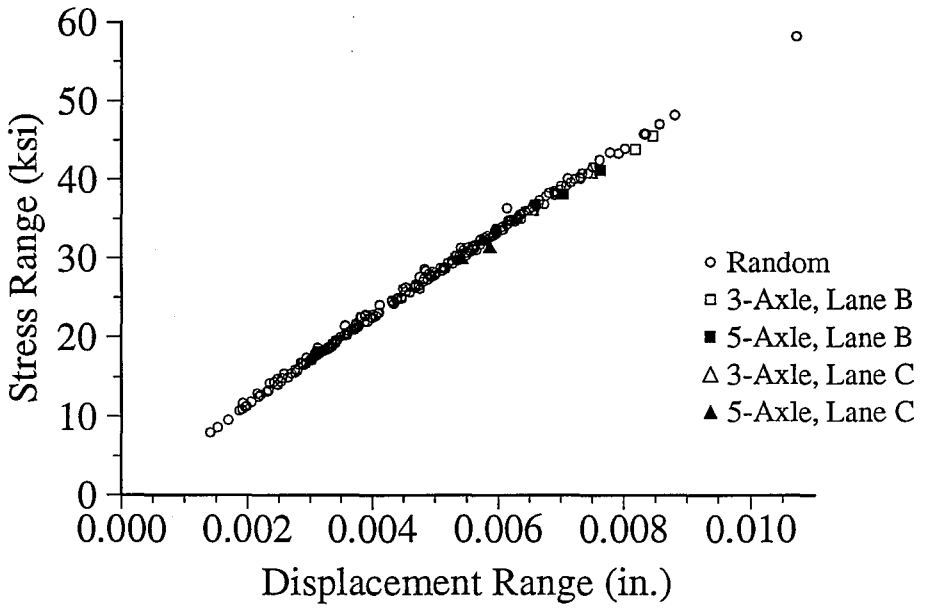

Figure 80. Web Plate Stress Range at the Outside Web-Flange Weld Toe Versus Out-of-Plane Displacement Range at the Inside Girder of the First Floortruss South of Pier S3-11 Before Retrofit

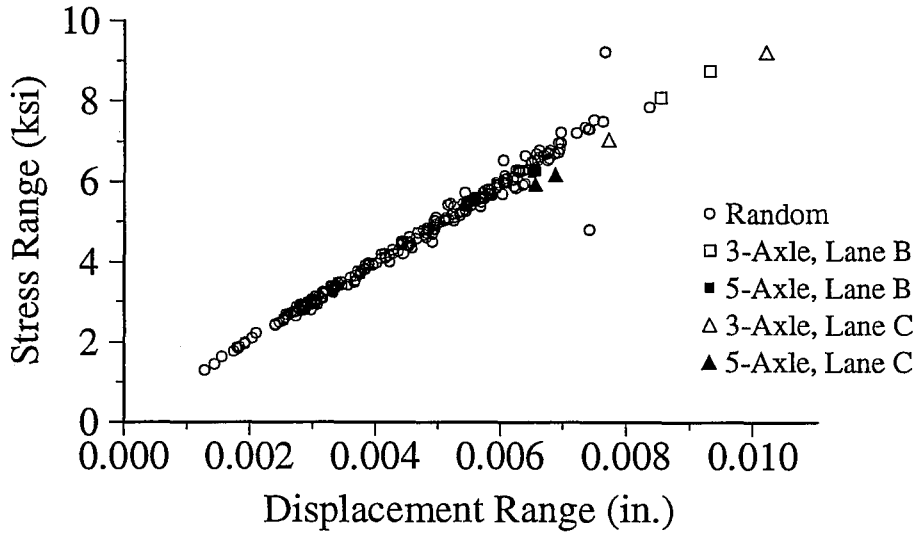

Figure 81. Web Plate Stress Range at the Top of the Connection Plate Weld Versus Out-of-Plane Displacement Range at the Outside Girder of the Second Floortruss South of Pier S3-11 Before Retrofit

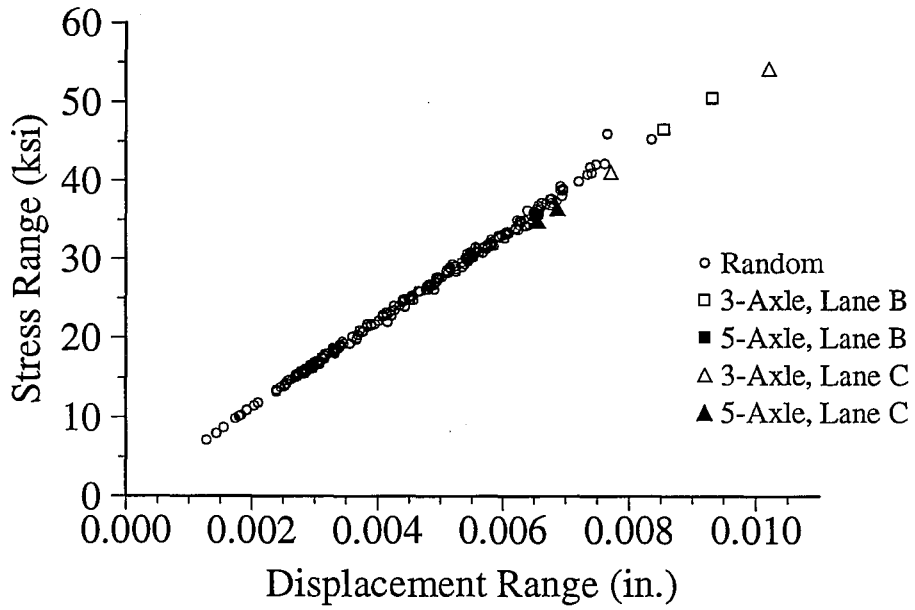

Figure 82. Web Plate Stress Range at the Outside Web-Flange Weld Toe Versus Out-of-Plane Displacement Range at the Outside Girder of the Second Floortruss South of Pier S3-11 Before Retrofit

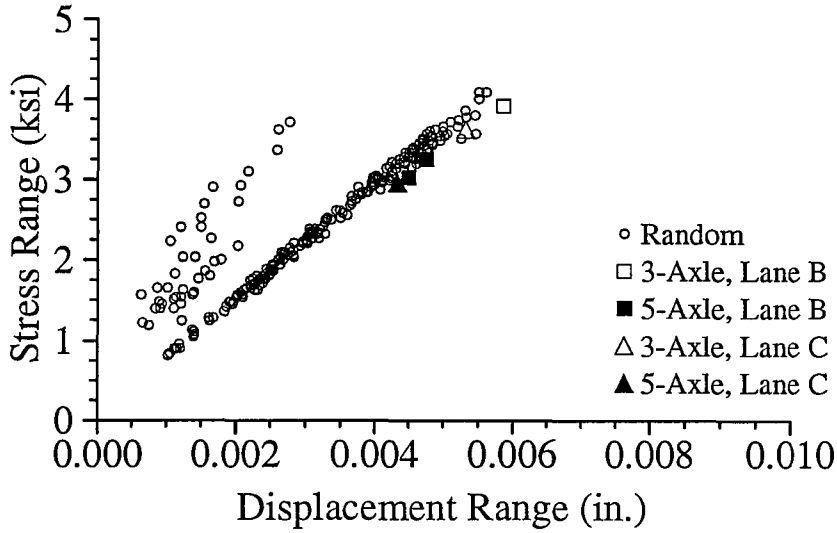

Figure 83. Web Plate Stress Range at the Top of the Connection Plate Weld Versus Out-of-Plane Displacement Range at the Outside Girder of the First Floortruss North of Pier S3-4 Before Retrofit

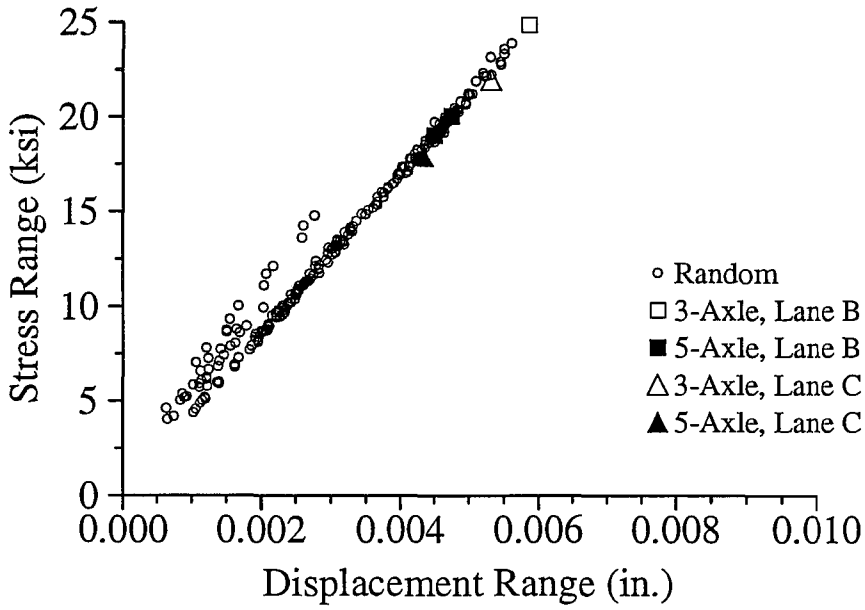

Figure 84. Web Plate Stress Range at the Outside Web-Flange Weld Toe Versus Out-of-Plane Displacement Range at the Outside Girder of the First Floortruss North of Pier S3-4 Before Retrofit

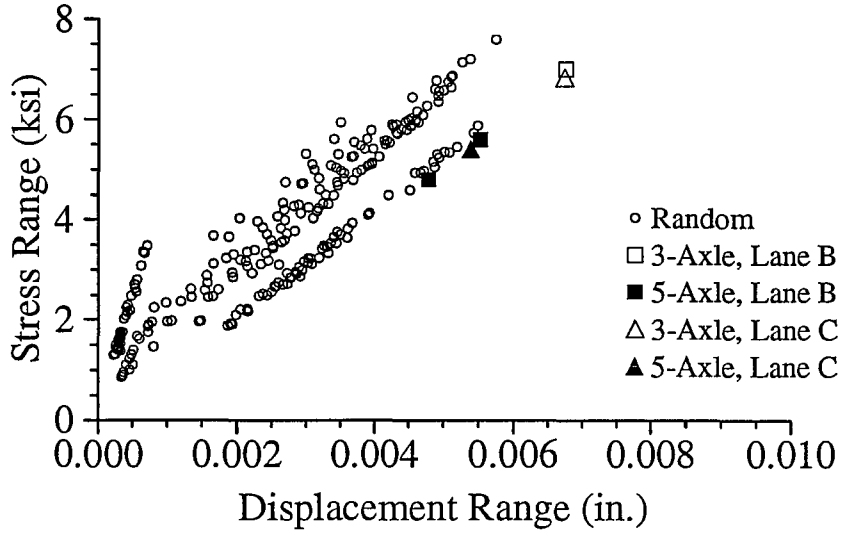

Figure 85. Web Plate Stress Range at the Top of the Connection Plate Weld Versus Out-of-Plane Displacement Range at the Outside Girder of the Second Floortruss North of Pier S3-4 Before Retrofit

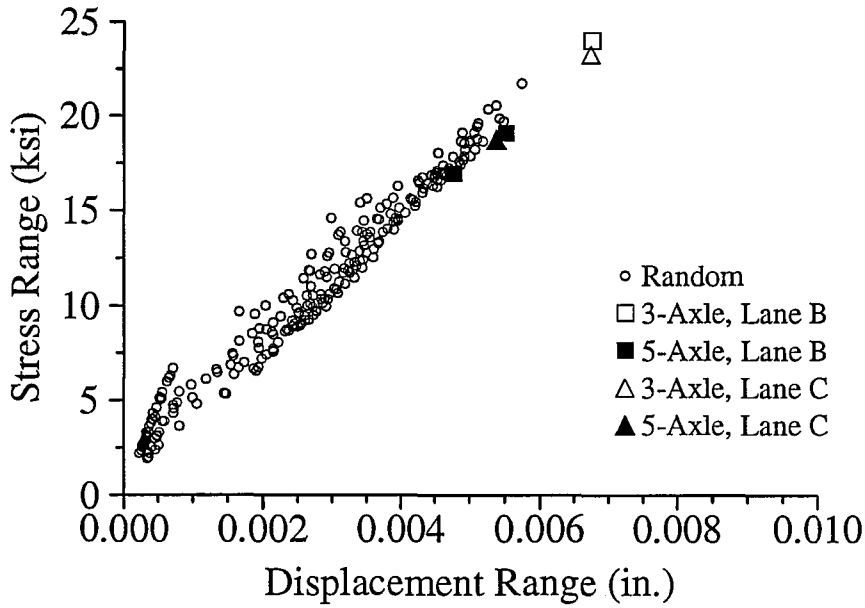

Figure 86. Web Plate Stress Range at the Outside Web-Flange Weld Toe Versus Out-of-Plane Displacement Range at the Outside Girder of the Second Floortruss North of Pier S3-4 Before Retrofit

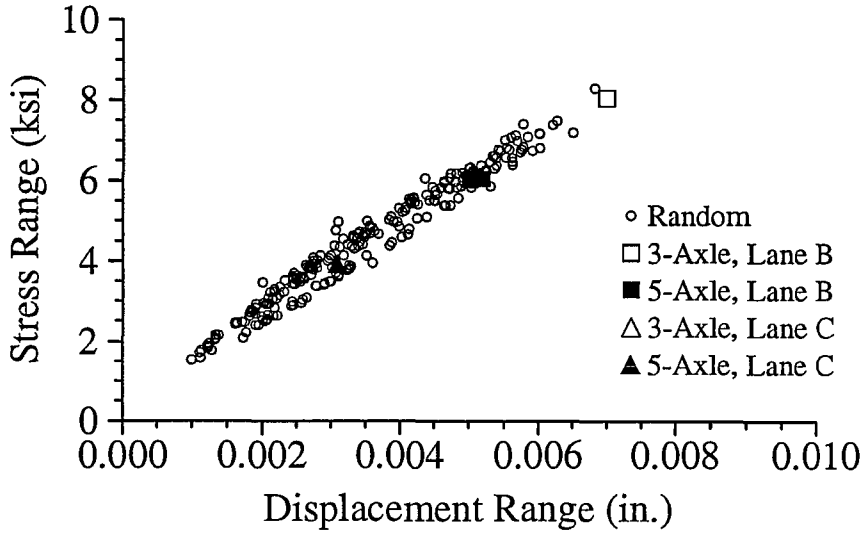

Figure 87. Web Plate Stress Range at the Top of the Connection Plate Weld Versus Out-of-Plane Displacement Range at the Inside Girder of the Second Floortruss North of Pier S3-4 Before Retrofit

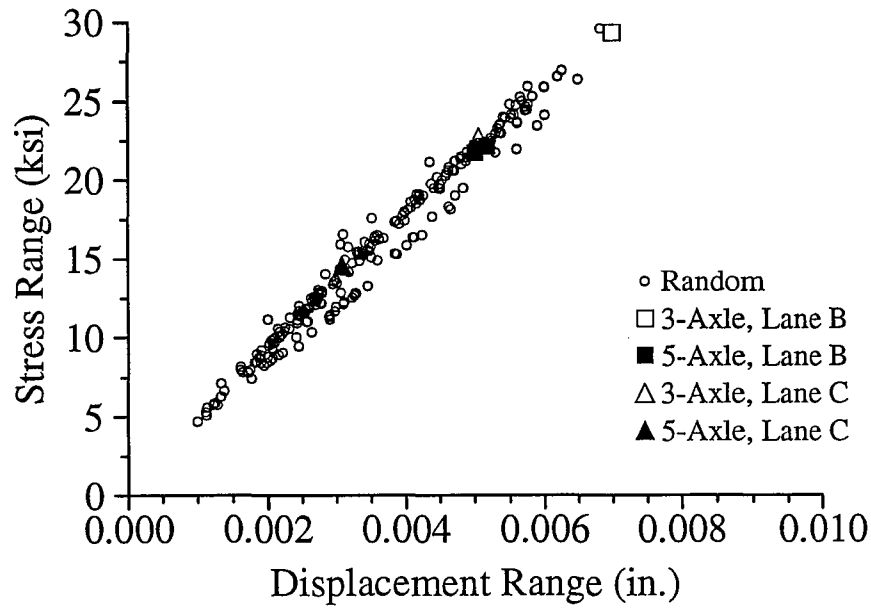

Figure 88. Web Plate Stress Range at the Outside Web-Flange Weld Toe Versus Out-of-Plane Displacement Range at the Inside Girder of the Second Floortruss North of Pier S3-4 Before Retrofit

test trucks in lanes B and C also appear in the plots. The nearly linear grouping of the data for all locations indicated that the stresses and displacements were well matched. Therefore, for a given displacement at a connection, a reasonable estimate of the stress could be made, and vice-versa. The test trucks were in the upper range of all recorded stress and displacement ranges for all locations and connections tested. The 3-axle test truck produced the greatest stress and displacement ranges for all locations tested.

The stress ranges recorded in the web gap are a combination of all vertical stresses produced by bending of the web plate and by axial forces in the vertical direction on the web gap. If the web gap stresses are assumed to result entirely from bending, the relationships between web gap stresses and out-of-plane displacement would be linear with zero stress at zero displacement. The slopes of these linear relationships should be a function of the connection geometry and the deformed shape of the web gap. Variations in the basic deformed shape of the web gap, which could result from various lane positions and truck configurations, would produce variations in slope. Data taken from the normal traffic stream would include a wide range of truck configurations as well as truck combinations in various lanes. This could produce a large amount of scatter in data of the type shown in Figures 77 through 88. Axial tensile or compressive stress in the vertical direction in the web plate would be independent of out-of-plane displacement.

As mentioned above, the data in Figures 77 through 88 show some clear linear patterns. Most of the data points fall along straight lines which suggests that the majority of the truck crossings produced a similar deformed shape of the web gap and the entire structure. Very clear linear relationships are seen in Figures 80 and 82. However, some

plots such as Figures 83 and 85 show some scatter in the data.

Linear regression analyses were performed on all the random data collected at each connection. The results of the analyses are shown in Table 19. The small values shown in Table 19 for the regression constants indicate that the response in the web gaps was reasonably consistent for all the trucks. Also, the correlation coefficients shown in Table 19 are noted to be very close to one. A correlation coefficient of one, as discussed in Chapter Two, would indicate that the relationship between the stress and displacement data is perfectly described by the linear relationship found through the regression analysis. Hence, the correlation coefficients indicate that the regression results provide a very good fit to the data.

A relatively high degree of scatter was noted for the inside connection plate weld stress range versus displacement range plots at the pier S3-4 connections. The data appeared in a more banded pattern. The plots of stress ranges versus displacement ranges for the web plate at both the inside connection plate weld (Figure 85) and the outside web-flange weld (Figure 85) at the outside girder connection of the second floortruss north of pier S3-4 show a large group of data points along a steep line at very low displacement ranges.

These findings suggested three possibilities: the out-of-plane displacement ranges measured at the connection were unusually low; the extrapolated stress ranges calculated at the critical locations of the connection were unusually high; or a combination of the two. Therefore, the histograms for displacement ranges and stress ranges were reviewed to determine if any of these quantities were linked to this behavior. Low displacement ranges were previously noted at this same connection in the histogram shown in Figure 75 and,

Table 19. Regression Analyses of Critical Location Stress Ranges Versus Displacement Ranges for Random Truck Data Before Retrofit

Outside Web-Flange Weld			Web Plate at Top of Conn. Plate Weld		
Correlation Coefficient	Regression Coefficient (ksi/in.)	Regression Constant (ksi)	Correlation Coefficient	Regression Coefficient (ksi/in.)	Regression Constant (ksi)
Pier S3-11: First Floortruss South, Outside Girder (106" Web)					
0.992	4430	1.6	0.975	975	0.8
Pier S3-11: First Floortruss South, Inside Girder (106" Web)					
0.999	5450	0.9	0.965	2850	1.8
Pier S3-11: Second Floortruss South, Outside Girder (106" Web)					
0.999	5530	0.1	0.989	974	0.1
Pier S3-4: First Floortruss North, Outside Girder (126" Web)					
0.993	3970	1.2	0.913	564	0.7
Pier S3-4: Second Floortruss North, Outside Girder (126" Web)					
0.986	3280	1.9	0.921	970	1.2
Pier S3-4: Second Floortruss North, Inside Girder (126" Web)					
0.990	4130	1.0	0.984	1100	0.7

All regression statistics were obtained from Figures 77 through 88.

therefore, a large number of the displacements appear to be relatively low. The stress histograms for the critical positions on the girder web plate (in Figures 67 and 68) did not show large groups of either relatively high or relatively low stress ranges. Therefore, the unusual behavior does not appear to be linked to the girder web plate stresses. In addition to the behavior being linked to the stresses in the web plate and the out-of-plane distortion of the web plate, the connection behavior could have been impacted by the connection plate (since the LVDT was mounted on the connection plate). To study this impact, the stress at the NS1 gage position on the connection plate was chosen because it is a good indicator of the magnitude of the horizontal force imposed on the web gap by the connection plate.

The stress range histogram for the NS1 gage position on the connection plate near the top of the connection plate to web weld (see Figure 29) was then investigated at the outside girder connection of the second floortruss north of pier S3-4. The histogram of stress ranges for the NS1 gage appears in Figure 89. This histogram shows a significant percentage of small stress ranges for this gage location at this connection, which is similar to the histogram of displacement ranges in Figure 75. The stress range histograms for the NS1 gage at the other two pier S3-4 connections tested did not exhibit this behavior. Those two histograms resembled the majority of histograms already presented in Figures 59 through 76. The observation of a relatively large number of small displacement ranges at that connection and small stress ranges at the NS1 gage location, coupled with the initial steep line of data points in Figures 85 and 86 suggests, that the stresses in the web were being created with relatively little out-of-plane displacement. No clear proof is available for why this occurred, but it possibly resulted from binding of the top of the connection plate on the top flange. Binding

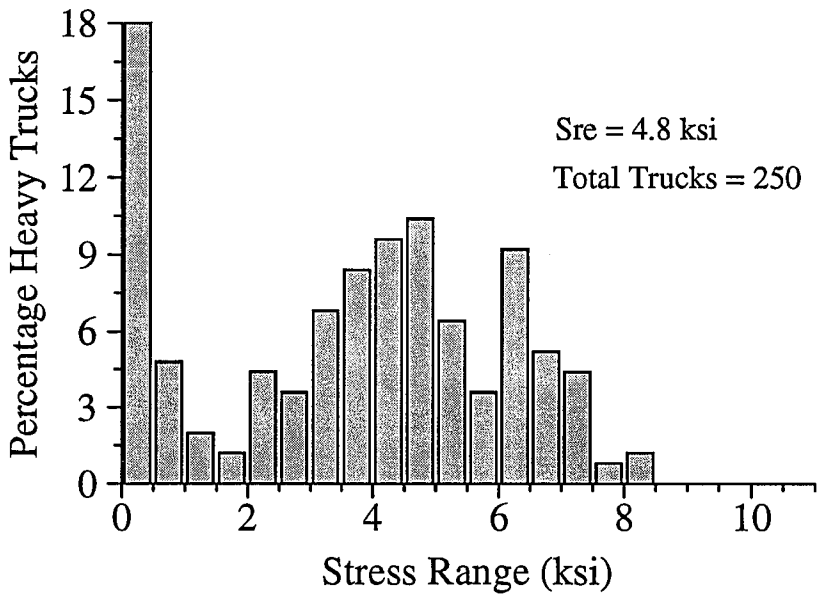

Figure 89. Stress Ranges at the NS1 Gage on the Connection Plate at the Outside Girder of the Second Floortruss North of Pier S3-4 Before Retrofit

of the connection plate could cause a wedging or prying action so that axial tension was created in the web gap. This axial tension, as previously mentioned, would be independent of the level of out-of-plane displacement. Therefore, the data points in the steep line at low displacements could result from a large axial stress relative to the bending stress, which was created by the out-of-plane displacement. Also, if connection plate binding were occurring, the connection plate would be likely to hinder the out-of-plane distortion of the girder web plate, thereby producing lower measured displacement ranges.

Truss Force Components Versus Displacements

Plots of vertical force component range versus displacement range for the end diagonal truss members at all test locations are shown in Figures 90 through 95. The statistics of the linear regression analyses performed for these relationships appear in Table 20. The same random truck records and calibration data that were used for all the previous discussions and illustrations of this chapter were used in these plots. However, the plots appear more dispersed than the stress versus displacement plots already presented. The plots were initially developed to determine whether the out-of-plane displacement at each connection was well matched to the vertical force applied to the connection by a truck loading. The data in Figures 90 through 95 and in Table 20 indicate that the quantities are not well matched. The correlation coefficients in Table 20 are relatively low. The regression constants indicate that the response in the end diagonals was not nearly as consistent as the response noted in the web gaps (Table 19). However, some interesting observations can be made from the figures.

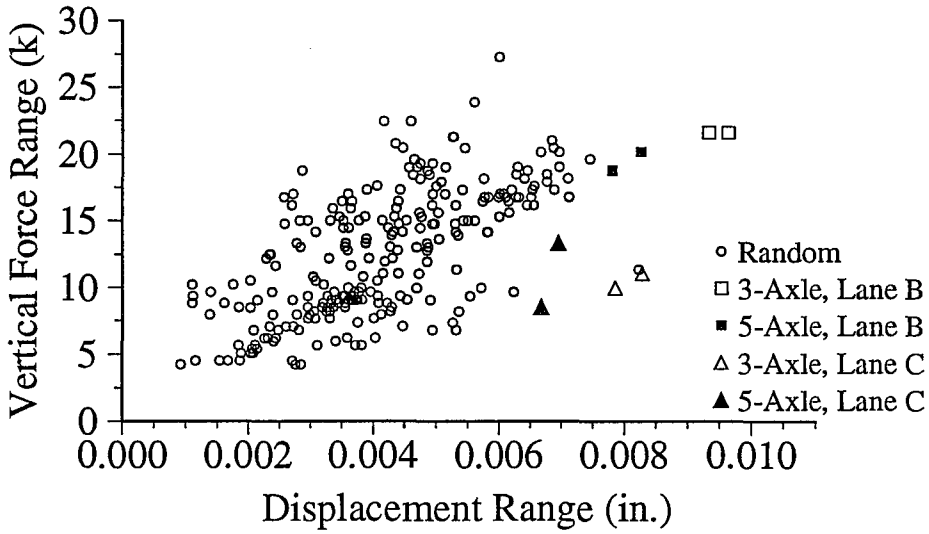

Figure 90. Vertical Force Component Range in the End Diagonal Versus Out-of-Plane Displacement Range at the Outside Girder of the First Floortruss South of Pier S3-11 Before Retrofit

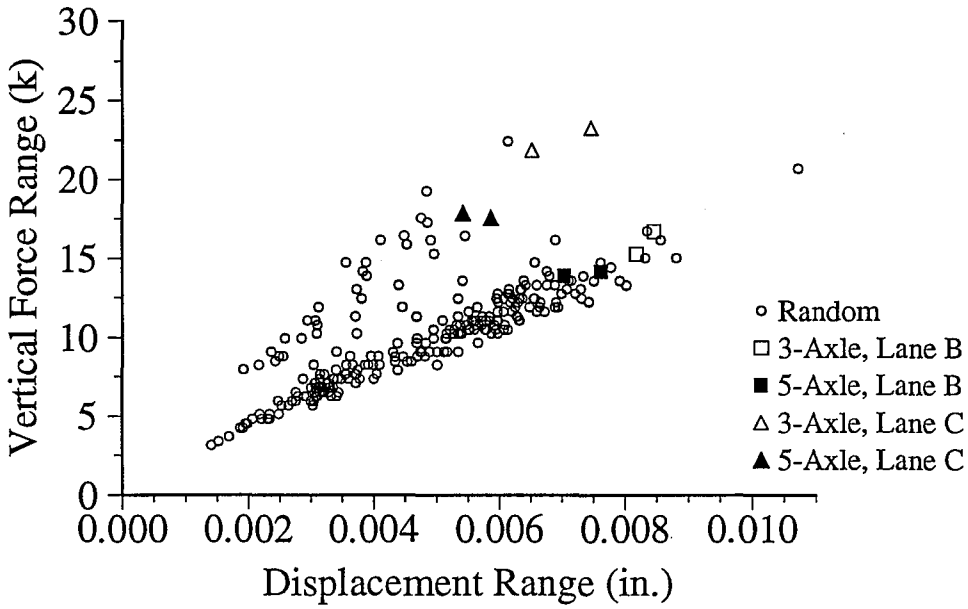

Figure 91. Vertical Force Component Range in the End Diagonal Versus Out-of-Plane Displacement Range at the Inside Girder of the First Floortruss South of Pier S3-11 Before Retrofit

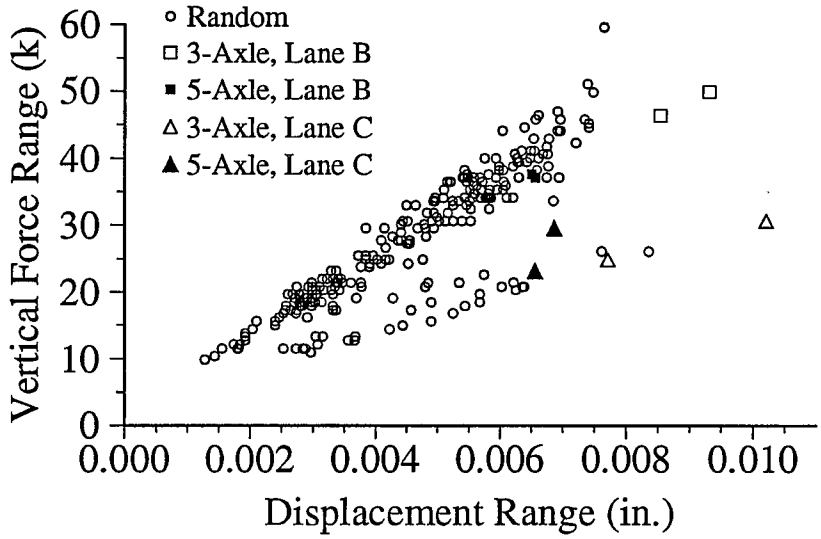

Figure 92. Vertical Force Component Range in the End Diagonal Versus Out-of-Plane Displacement Range at the Outside Girder of the Second Floortruss South of Pier S3-11 Before Retrofit

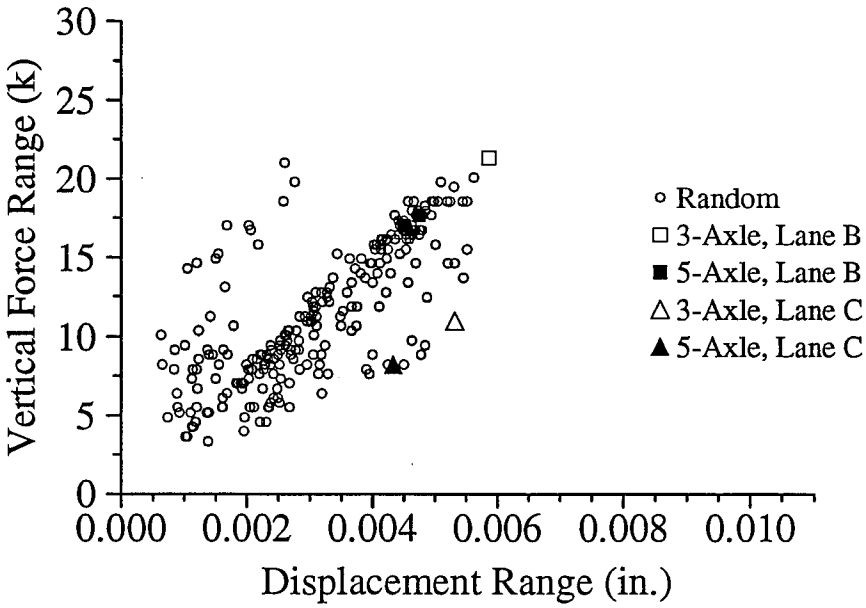

Figure 93. Vertical Force Component Range in the End Diagonal Versus Out-of-Plane Displacement Range at the Outside Girder of the First Floortruss North of Pier S3-4 Before Retrofit

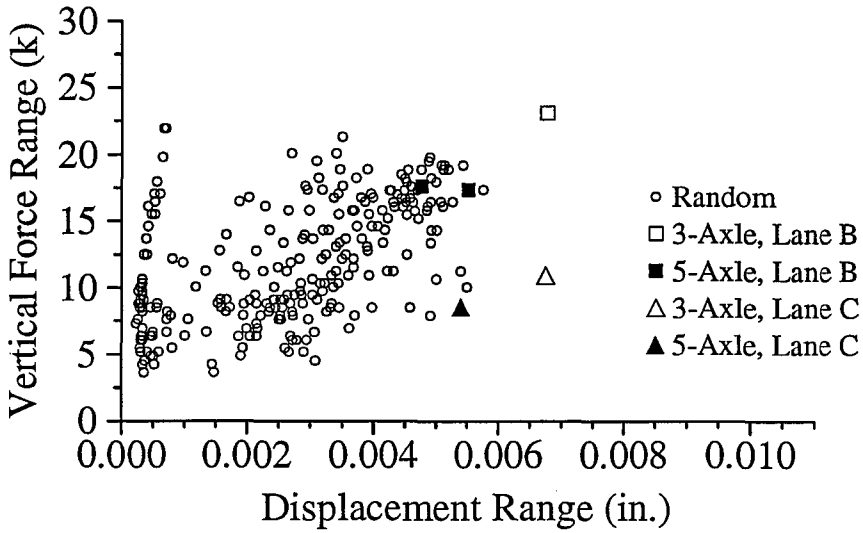

Figure 94. Vertical Force Component Range in the End Diagonal Versus Out-of-Plane Displacement Range at the Outside Girder of the Second Floortruss North of Pier S3-4 Before Retrofit

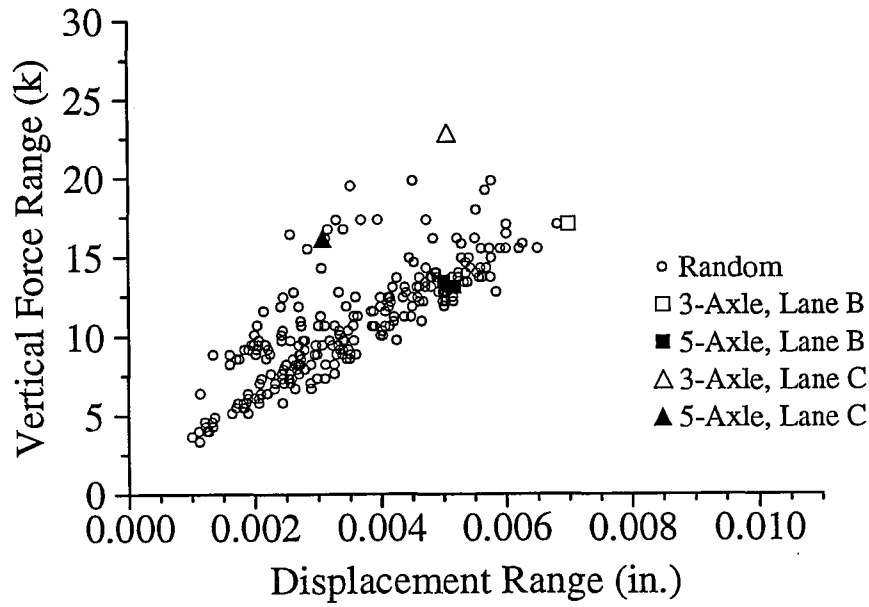

Figure 95. Vertical Force Component Range in the End Diagonal Versus Out-of-Plane Displacement Range at the Inside Girder of the Second Floortruss North of Pier S3-4 Before Retrofit

Table 20. Regression Analyses of Vertical Force Ranges in End Diagonals Versus Displacement Ranges for Random Truck Data Before Retrofit

Vertical Force Ranges in End Diagonals		
Correlation Coefficient	Regression Coefficient (ksi/in.)	Regression Constant (ksi)
Pier S3-11: First Floortruss South, Outside Girder		
0.660	2150	3.7
Pier S3-11: First Floortruss South, Inside Girder		
0.774	1510	3.0
Pier S3-11: Second Floortruss South, Outside Girder		
0.860	2740	0.9
Pier S3-4: First Floortruss North, Outside Girder		
0.762	2600	3.4
Pier S3-4: Second Floortruss North, Outside Girder		
0.542	1570	7.7
Pier S3-4: Second Floortruss North, Inside Girder		
0.810	2070	3.5
All regression statistics were obtained from Figures 90 through 95.		

The test truck data shows the vertical force transferred to the connection was dependent on the lane the truck was in as it crossed the span. This relationship was expected based on statics, since a greater portion of the total truck weight (plus impact effect) should be supported by the connection nearest to the truck. All outside girder connections tested were noted to have the greatest vertical force component for test trucks located in the outside lane, lane B. Likewise, the two inside girder connections tested exhibited the greatest vertical component for test trucks located in the inside lane, lane C. This lane dependence produced somewhat banded plots. The largest number of vehicles was always contained in the band associated with lane B. This was expected for a two lane (one-way roadway) segment of interstate on an uphill grade. Although it is impossible to be certain, it is likely that some of the scatter in Figures 85 through 95, as well as in Figures 77 through 84, resulted from combinations of vehicles in both traffic lanes staggered along the spans.

It is also important to note from the figures that the displacement range at all connections for a given test truck was greatest for that truck crossing in lane B. A truck in this lane, positioned closest to the roadway centerline, maximized the out-of-plane displacements at both ends of the floortrusses. Similar results were noted for stresses in static tests discussed in the section "STRESSES FROM STATIC TESTS". The lane C displacements for test trucks for some of the connections were very near the values for lane B. Figure 94 for the outside girder connection of the second floortruss north of pier S3-4 displays a large number of small magnitude displacements that were previously discussed.

POTENTIAL FOR CRACKING

Constant-amplitude fatigue limits of 6, 10, and 15 ksi were used to evaluate the potential for fatigue cracking in the top of the connection plate to web fillet weld, in the web plate at the top of the connection plate to web weld, and at the toe of the web-flange weld; respectively. The fatigue limit of 6 ksi in the fillet weld is based on the AASHTO (1993) Table 10.3.1B. Calculation of the fatigue limit based on the AASHTO provisions resulted in values ranging from 5.7 to 6.7 ksi for the various weld thicknesses at the six floortruss-girder connections. The fatigue limit of 6 ksi is used for all connections for simplicity. The fatigue limits for cracking in the web are based on laboratory tests performed by Fisher et al. (1990). The laboratory specimens and in-plane stress conditions used by Fisher were somewhat different from the geometry and stress conditions at the floortruss-girder connections of interest here, but the lab test results are used in the absence of more appropriate research on welded connections of this type. A primary difference in the stress conditions is that the in-plane stress ranges measured at the web gaps at the floortruss-girder connections were significantly less than the 6 and 12 ksi stress ranges used by Fisher in the laboratory tests. The lower in-plane stress ranges would tend to improve the fatigue strength of the I-65 floortruss-girder connections over that of the laboratory test specimens.

The fatigue limits of 10 ksi and 15 ksi in the web plate at the top of the connection plate to web weld and at the toe of the web-flange weld, respectively, were suggested by Fisher et al. (1990). However, cracking did occur in some test specimens with constant-amplitude stress ranges at the end of the connection plate weld between 7.5 and 10 ksi as illustrated by the data in Figure 96. Stresses measured in the lab test specimen web gaps and

extrapolated to the critical locations indicated that higher stress ranges generally occurred at the web-flange weld, although the end of the connection plate weld was more susceptible to fatigue cracking. Stress ranges in excess of 15 ksi were required at the web-flange weld to cause fatigue cracking.

In general, only a part of the applied stress ranges must exceed the constant-amplitude fatigue limit for fatigue cracking to develop from variable-amplitude loading. Therefore, the maximum stress ranges from the field tests were used for comparison with the fatigue limits to determine whether stress conditions were severe enough to cause fatigue cracking. These maximum stress ranges, which were measured over short time periods, could be expected to occur a significant number of times during the service life of the bridge. Estimates of maximum load cases were also made by adding the fast run calibration test truck results obtained for the 5-axle truck in the slow and fast traffic lanes. These maximum load cases are shown in Tables 16 and 17.

Finite element analyses were performed for the floorbeam-girder connections discussed in Volume I of this report (Stallings et al. 1993). Those analyses verified that the maximum web gap stresses would actually occur near the centerline of the connection plate. Multiplication factors were developed from the analyses to adjust the maximum stress ranges recorded at each connection for the offset between the line of strain gages and the centerline of the connection plate. The geometry differences between the floortruss-girder connections and the floorbeam-girder connections prohibited the application of those factors to the stress ranges here. The greater flexibility and slenderness of the web and the connection plate at the floortruss connections, as well as, the fact that vertical stiffeners were not used on the

outside of the web suggest that there is less of a stress concentration at the floortruss connection plates than at the floorbeam connection plates. Although some stress concentration would be expected, the measured stress ranges were alone used to evaluate the potential for fatigue cracking.

As shown in Table 16, the maximum weld stress at the top of the connection plate weld determined from random tests and from adding the stresses from the 5-axle test truck crossings in lane B and C for all six connections exceeded the constant-amplitude fatigue limit of 6 ksi for the fillet weld. Therefore, fatigue cracks can be expected to develop in the welds at all six connections tested. This conclusion is substantiated by the fact that cracked welds have been found at five different floortruss-girder connections along the bridge spans. Based on the high stress ranges at all connections tested, cracking at the welds can be expected at a large percentage of the similar connections along the plate girder spans.

The stress ranges in the web at the top of the connection plate weld at only one test location were clearly large enough to cause fatigue cracking. These stress ranges were measured at the inside girder connection of the first floortruss south of pier S3-11. The maximum stress range (Table 16) at that location measured from the normal traffic stream was 27 ksi, which is well in excess of the 10 ksi fatigue limit. The maximum stress ranges measured for random truck traffic at four of the remaining five connections were 8 to 9 ksi. By combining the stress ranges measured for the 5-axle test trucks in the slow and fast traffic lanes, estimates of the maximum stress range were 10 to 13 ksi at those connections. These results indicate that fatigue cracking is very likely to occur in the web at five of the six connections tested. The potential for web cracking is estimated to be even greater by

considering the likelihood that cracks initiating in the connection plate to web welds will propagate into the web.

The maximum stress ranges at the girder web-flange weld at all test locations were significantly larger than the maximum stress ranges at the top of the connection plate weld. At all six connections the maximum random stress range recorded exceeded the 15 ksi fatigue limit by a wide margin. It should also be pointed out that the maximum stress ranges at all six test locations exceeded the AASHTO fatigue limit of 16 ksi for plain weathering steel without welds. Hence, fatigue cracking can be expected at the web-flange welds at all test locations. This conclusion also suggests that cracking at the web-flange weld is likely at a large percentage of the similar connections along the spans. The stress ranges for the maximum possible load cases estimated in Table 16 by adding the lane B and C results for the 5-axle truck are extremely large. These large stress ranges indicate that yielding of the web in the web gap is very likely when side-by-side heavy trucks cross the spans.

The discussion above indicates that fatigue cracking of the connection plate to web welds and the girder webs is likely at a large number of the similar connections along the bridges. Given that weld cracks have already been found at 5 connections, it is reasonable to expect that additional cracks will periodically be found in future bridge inspections. A method of repairing the weld cracks and improving the fatigue resistance of the web to distortion-induced stresses is investigated in the next chapter. Because of the high distortion-induced stresses at the 106 in. girder connections, the repair method will be recommended as a preventative measure for extending the fatigue life of those connections. To provide the AHD Maintenance Bureau with sufficient information to evaluate the relative importance of

such a preventative maintenance program, it is important to make some estimates, or predictions, of how many years will pass before fatigue cracking in the girder webs occurs at a significant number of floortruss-girder connections. Due to the empirical nature of the information available, it is not possible to make precise estimates of the remaining lives of the connections. Hence, the numbers of years discussed below should be considered only as reasonable engineering estimates.

Fatigue data from laboratory tests performed by Fisher et al. (1990) on transverse connection plate details exposed to various levels of distortion-induced stress ranges are in Figure 96. The data points indicate the number of cycles at the time cracking was first observed. Also, the data points with arrows indicate the number of cycles at which a test was stopped, and no fatigue cracking occurred. Also shown are effective stress ranges results obtained from the field tests of the I-65 floortruss-girder connections. Effective stress ranges are shown because they are the best indicators of the applied stress ranges for use in estimating fatigue life. Blocks are used for the field test results to indicate the range of stress range values measured in the field tests and the estimated number of cycles that have been applied to date (October, 1993). Solid and dashed lines representing the AASHTO fatigue categories A, B, and C are also shown.

The plots in Figure 96 indicate that the most severe stress conditions in the web plate were found at the outside web-flange weld. Also at one connection (of a 106 in. girder) the effective stress range at the top of the connection plate was very high. For most of the connections, the effective stress ranges at the top of the connection plate welds are low enough that a very long time will be required for cracking to occur there. The effective

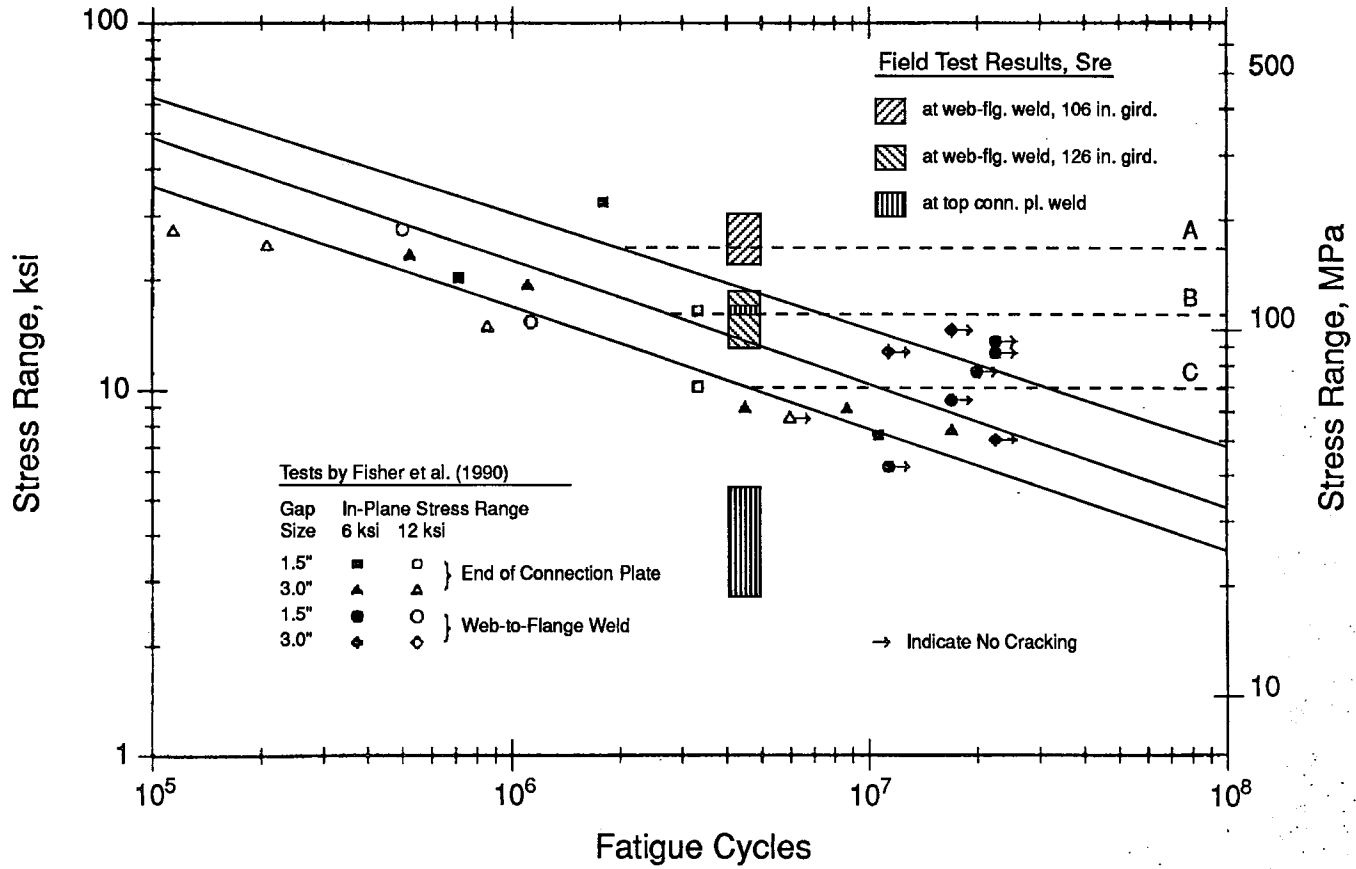

Figure 96. Effective Stress Ranges at Floortruss-Girder Connections Transposed on Laboratory Results From Fatigue Tests of Transverse Connections by Fisher et al. (1990)

stress ranges at the web-flange welds were relatively high and appear in a peculiar location in Figure 96. Since no fatigue cracks have occurred at floortruss-girder connections in the I-65 bridges at the web-flange welds, these connections have survived more cycles than did the small number of lab test specimens (Fisher et al. 1990) that cracked at similar stress ranges. However, the floortruss-girder connections have not been exposed to the 10 to 20 million cycles at which most fatigue tests are stopped if no cracking occurs. Comparison to data presented in NCHRP Report 286 (Keating and Fisher 1986) that was used to establish the AASHTO fatigue categories A and B result in a similar conclusion. Hence, there is no truly comparable data that can be used to estimate the remaining life of the connections. Based on the high effective stress ranges measured at the 106 in. girders and general trends from fatigue data, a dividing line of 15 million cycles will be estimated for making fatigue life predictions. Based on the past and current traffic volume, the I-65 bridges will reach a total fatigue life of 15 million cycles in approximately 18 years. With some allowance for increased traffic volume, this estimated total fatigue life of 15 million cycles will be reached in approximately 15 years from now. For planning purposes, it is estimated that distortion-induced web cracking will occur at a significant number of floortruss-girder connections along the 106 in. girders within the next 15 years. It is also estimated that the majority of the connections at the 126 in. girders will survive the next 15 years without distortion-induced web cracking if cracks that occur in the connection plate to web welds are removed and not allowed to propagate into the web. Because the stresses measured at the 126 in. girders were lower than those measured at the 106 in. girders, the stresses occurring at the 146 in. girders are estimated to be even lower. Hence, the majority of the floortruss-girder

connections at the 146 in. girders should also survive the next 15 years without distortion-induced web cracking given that cracks in the connection plate to web welds are not allowed to propagate into the web.

CHAPTER EIGHT

RESULTS AT CONNECTIONS AFTER RETROFIT

The results presented in Chapter Seven showed a high potential for fatigue cracking at the floortruss-girder connections. The results indicated that weld cracks similar to those previously found by AHD bridge inspectors in the connection plate to web welds are likely to form. Also, distortion-induced fatigue cracking in the girder webs is very likely, especially at the girders with 106 in. deep webs. Therefore, a retrofit detail was developed for study at these connections. The selection of the retrofit detail was discussed in Chapter Three.

There were two connections chosen for implementation of a softening type retrofit. The specific retrofit type was a variation of the web gap lengthening retrofit discussed in Chapter Two. The web gap at the outside girder connection of the first floortruss south of pier S3-11 was lengthened to approximately 10 in. (see Figure 16 of Chapter Three), while the web gap at the outside girder connection of the second floortruss north of pier S3-4 was lengthened to approximately 6 in. (see Figure 17 of Chapter Three). As mentioned in Chapter Three, retrofits at each connection included a second retrofit study in which connection bolts were removed from the stiffener-connection plate assembly. The top three connection bolts were removed at the outside girder connection of the first floortruss south of pier S3-11 where the 10 in. slot was used, and the top two bolts were removed at the outside girder connection of the second floortruss north of pier S3-4 where the 6 in. slot was used.

In the remainder of this report, the specific retrofitted connections will be referenced as the 6 in. slot and the 10 in. slot locations or connections.

BEHAVIOR AT TEST LOCATIONS

The overall (global) structural behavior after retrofit was unchanged from before retrofit, as expected. In-plane and out-of-plane behavior still maintained the characteristic patterns that were identified before retrofit. The nature of the truss member behavior was also relatively unchanged after retrofit. For all calibration test truck crossings with all retrofits, the axial stress ranges in the top chord increased after retrofit. The amount of increase ranged from 13 to 142 percent more than the before retrofit data for a corresponding test at the 10 in. slot location. At the 6 in. slot location the amount of increase ranged from 20 to 188 percent more than the before retrofit magnitudes for a corresponding test. This increase is believed to result from the reduced horizontal resistance of the web gap and connection plate after the slotted retrofit. Although some of these percentage increases are large, the maximum stress range in the top chord members obtained by adding the stresses due to the 3-axle test truck in the fast and slow lanes was less than 3.6 ksi compression at both the 6 in. and 10 in. slots. The axial stress ranges in the end diagonals were reduced from before retrofit magnitudes by 3 to 20 percent for the 10 in. slot location and varied from a 7 percent reduction to a 16 percent increase for the 6 in. slot location. The axial stress ranges in the end diagonals obtained by adding the stress ranges due to the 3-axle test truck in the fast and slow lanes was also less than 3.6 ksi at both the 6 in. and 10 in. slots.

Connection Plate Stresses

Strain gages were installed on the connection plates at each of the two test connections after the retrofit was performed. The gages were placed at locations on the north and south sides of the connection plates in patterns similar to those used before the retrofit. The gage locations are described in Chapter Five and shown in Figures 30 and 31. The purpose of investigating the stresses in the connection plate was to determine how the horizontal forces which cause the out-of-plane distortion of the web gap are transferred after the trial retrofits were performed.

A typical stress record from normal truck traffic for the connection plate gages at the 10 in. slot location with a fully bolted connection plate appears in Figure 97. Figure 98 displays a typical stress record at the 10 in. slot location with the top three connection plate bolts removed. Figures 99 and 100 show typical stress records for the connection plate gages at the 6 in. slot location with a fully bolted connection plate and with the top two connection plate bolts removed, respectively.

Each of the four figures display stresses measured on the connection plate at a particular instant in time as a heavy truck crossed the floortruss. The vertical axes of Figures 97 through 100 display the distance down from the end (bottom) of the slot radius in the connection plate to the gage locations. The stresses in Figures 97 through 100 were measured for four different trucks, and therefore, the stress magnitudes are not directly comparable but are similar. However, the shapes of the horizontal stress distributions are comparable. Both Figures 97 and 99 show that the stresses on the north and south sides change from tension to compression between the SM1 and SM2 gage positions (see Figures

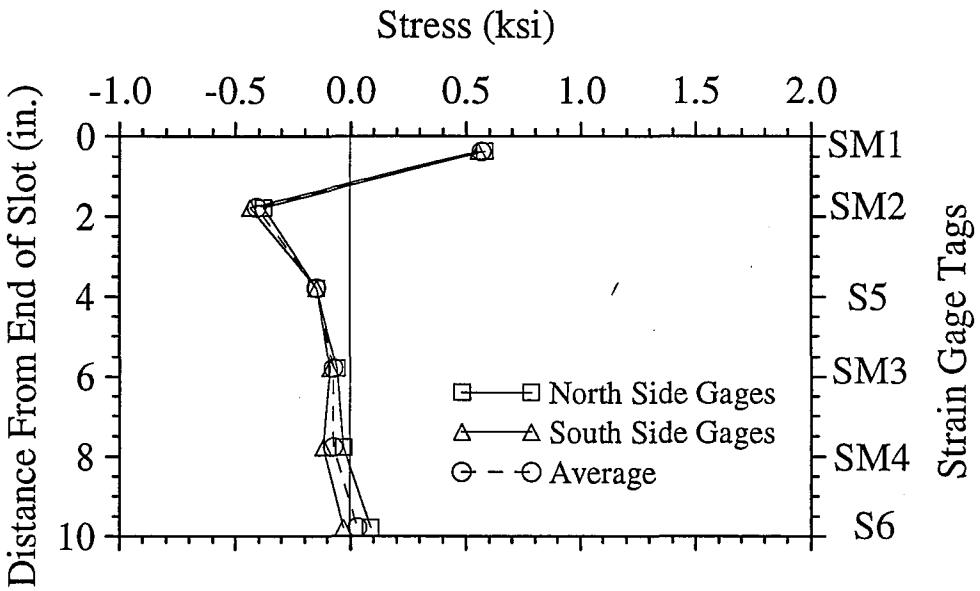

Figure 97. Typical Distribution of Horizontal Stress in the 10 Inch Slotted Connection Plate

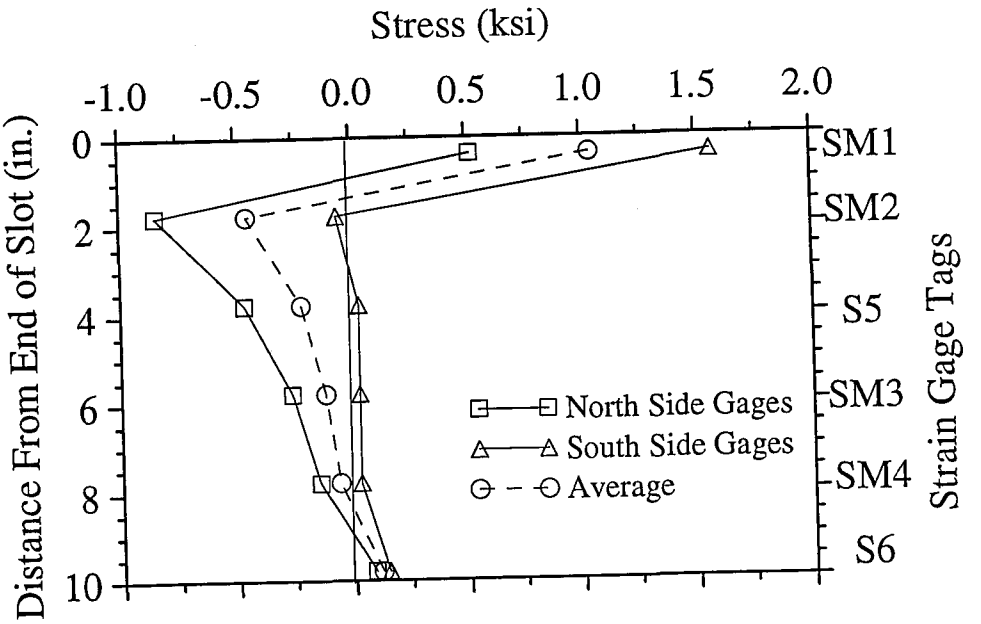

Figure 98. Typical Distribution of Horizontal Stress in the 10 Inch Slotted Connection Plate with the Top Three Bolts Removed

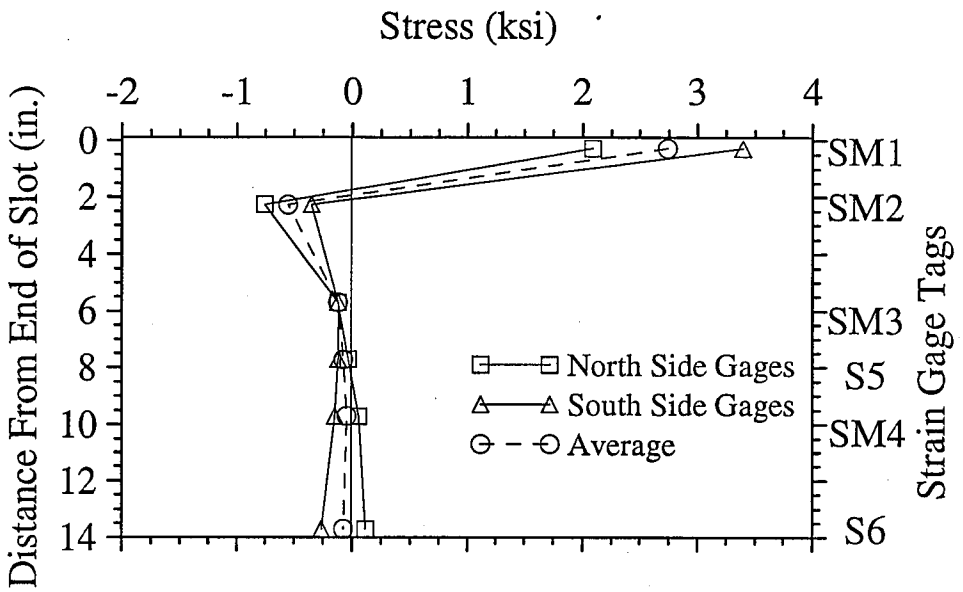

Figure 99. Typical Distribution of Horizontal Stress in the 6 Inch Slotted Connection Plate

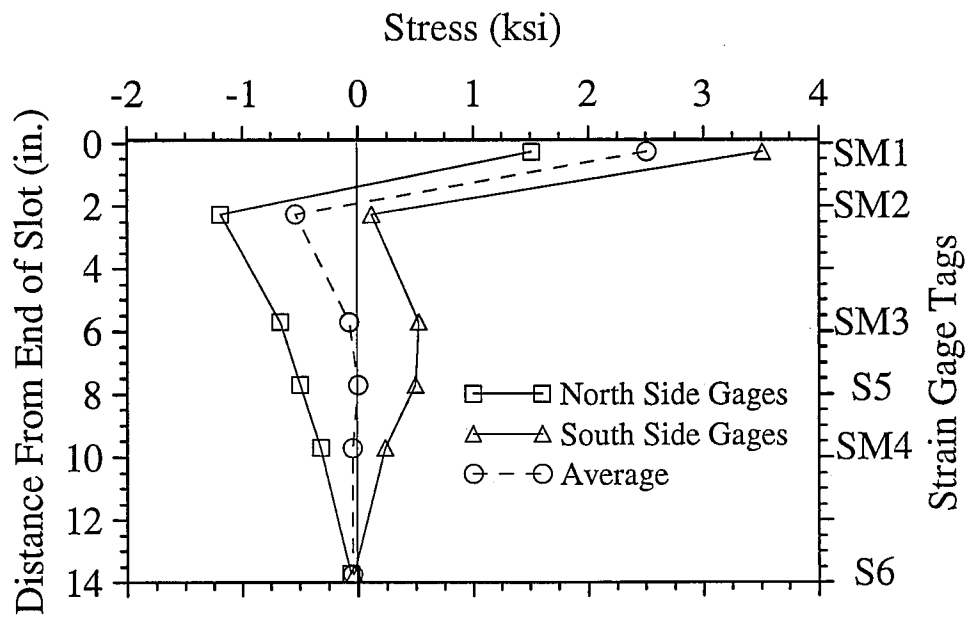

Figure 100. Typical Distribution of Horizontal Stress in the 6 Inch Slotted Connection Plate with the Top Two Bolts Removed

30 and 31) for the retrofitted connections with all bolts in the connection plate. Figures 98 and 100 with the top three and two connection plate bolts removed, respectively, show the web gap lengthening retrofit was further loosened by the removal of connection plate bolts. The further loosening allowed greater freedom for connection plate bending in this region. The bending was very pronounced in the region dominated by the axial force effects (upper plate region).

After connection plate bolt removal, the uppermost remaining connection plate bolt was centered approximately 6.375 in. below the end of the 10 in. slot, and approximately 7.5 in. below the end of the 6 in. slot in the connection plate. At these bolt locations at each connection with bolts removed, the axial stress, average of the north and south side stresses, was approximately zero.

Before retrofit, the stress in the north side connection plate to web weld was estimated to be slightly higher than the stresses in the south side weld for all six connections tested. After the two retrofit studies (slotted and slotted with bolts removed) were performed at each of the two connections tested after retrofit, the south side connection plate to web weld stresses for all tests were found to be greater than the north side. Therefore, for simplicity only north side weld stresses were evaluated before retrofit and only south side weld stresses were evaluated after retrofit. The difference in the weld stresses in some cases was considerable. The south side weld stresses and stress ranges were higher due to a greater stress difference between the south side SM1 and SM2 gage locations than for the north side. The greater difference in recorded stresses for the two uppermost south side connection plate gages (SSM1 and SSM2) produced greater extrapolated stresses and stress

ranges on the connection plate at the end of slot radius, which corresponded to a higher weld stress on the south side fillet weld. The stress difference also indicated the slotted connection plates were rotating from south to north in the uppermost plate region. The bending associated with this rotation caused a greater elongation of the extreme fibers on the south side of the slotted connection plate than on the north side, thereby producing greater measured stresses for the south side of the plate than for the north.

The end of the slot radius is a point of stress concentration for the connection plate and for that reason was chosen as the appropriate location for calculation of weld stresses. The weld stresses were determined from the connection plate stresses extrapolated to the end of the slot radius, in a manner similar to that described in Chapter Seven. It is impossible to predict whether or not higher stresses occur in the fillet weld at a location above the bottom of the slot radius (see Figure 16 for geometry). The stresses in the small region above the bottom of the slot are expected to be highly variable. At some point in this small region, the tapered edge of the connection plate is too small to sustain stresses and, in turn, cannot transfer stresses to the fillet welds. Hence,the connection plate stress at the bottom of the slot radius was chosen for weld stress determination although the maximum weld stress could be marginally higher at some location just above the bottom of the slot.

WEB GAP STRESSES FROM STATIC TESTS

Stresses and displacements for static test truck loadings in the two traffic lanes appear in Tables 21 and 22. The data in the tables is from static tests with the trucks directly above the floortruss before and after both the slotted retrofits. Stress distributions after the 10 in.

Table 21. Static Stresses and Displacements at the 10 Inch Slotted Connection, Before and After Retrofits with Truck Directly Above Floortruss

Truck	Lane	Retrofit Status[a]	Outside Web-Flange Weld (ksi)	Inside Web-Flange Weld (ksi)	Conn. Plate Weld B.R.[b] (ksi)	Conn. Plate Weld A.R.[c] (ksi)	Side of Conn. Plate Weld (ksi)	Weld Stress (ksi)	Displ. Near Top of Conn. Pl. (in.)
5-Axle	Slow	Before	+23	-21	+5.4	----	----	+7.8[n]	0.0051
5-Axle	Slow	Slot	+5.8	-5.5	-3.7	+8.6	+5.3	+2.7[s]	0.0167
5-Axle	Slow	Bolts	+5.8	-5.5	-3.8	+8.8	+5.5	+2.8[s]	0.0170
5-Axle	Fast	Before	+19	-17	+3.9	----	----	+6.5[n]	0.0045
5-Axle	Fast	Slot	+4.8	-4.7	-3.2	+7.0	+4.8	+1.7[s]	0.0155
5-Axle	Fast	Bolts	+4.8	-4.6	-3.2	+7.0	+4.8	+1.7[s]	0.0142
3-Axle	Slow	Before	+38	-33	+7.5	----	----	+12[n]	0.0084
3-Axle	Slow	Slot	+8.2	-7.9	-5.3	+12	+7.7	+3.6[s]	0.0239
3-Axle	Slow	Bolts	+8.3	-7.9	-5.4	+13	+8.0	+3.6[s]	0.0243
3-Axle	Fast	Before	+29	-26	+5.6	----	----	+9.3[n]	0.0068
3-Axle	Fast	Slot	+6.5	-6.4	-4.3	+9.5	+6.4	+2.2[s]	0.0194
3-Axle	Fast	Bolts	+6.5	-6.3	-4.3	+9.5	+6.4	+2.2[s]	0.0194

[a] Slot = with slot in connection plate; Bolts = after slotted retrofit and with the top three connection plate bolts removed.
[b] Location of critical web plate stress at the top of the connection plate weld before retrofit.
[c] Location of critical web plate stress at the top of the connection plate weld after retrofit.
[n] Weld stress on north side of the connection plate.
[s] Weld stress on south side of the connection plate.

Table 22. Static Stresses and Displacements at the 6 Inch Slotted Connection, Before and After Retrofits with Truck Directly Above Floortruss

Truck	Lane	Retrofit Status[a]	Outside Web-Flange Weld (ksi)	Inside Web-Flange Weld (ksi)	Conn. Plate Weld B.R.[b] (ksi)	Conn. Plate Weld A.R.[c] (ksi)	Side of Conn. Plate Weld (ksi)	Weld Stress (ksi)	Displ. Near Top of Conn. Pl. (in.)
5-Axle	Slow	Before	+15	-15	+4.9	----	----	+6.8[n]	0.0041
5-Axle	Slow	Slot	+11	-9.4	-5.0	+12	+6.9	+4.4[s]	0.0116
5-Axle	Slow	Bolts	+12	-11	-5.8	+13	+8.0	+5.8[s]	0.0136
5-Axle	Fast	Before	+17	-19	+5.1	----	----	+8.0[n]	0.0052
5-Axle	Fast	Slot	+13	-12	-6.6	+14	+9.1	+5.5[s]	0.0152
5-Axle	Fast	Bolts	+12	-12	-6.3	+14	+8.8	+5.1[s]	0.0145
3-Axle	Slow	Before	+20	-21	+6.7	----	----	+9.2[n]	0.0056
3-Axle	Slow	Slot	+18	-16	-8.7	+20	+12	+8.2[s]	0.0204
3-Axle	Slow	Bolts	+18	-17	-9.0	+20	+12	+9.0[s]	0.0209
3-Axle	Fast	Before	+20	-22	+6.0	----	----	+9.1[n]	0.0061
3-Axle	Fast	Slot	+17	-16	-8.6	+19	+12	+7.4[s]	0.0201
3-Axle	Fast	Bolts	+16	-15	-8.3	+18	+12	+6.8[s]	0.0192

[a] Slot = with slot in connection plate; Bolts = after slotted retrofit and with the top two connection plate bolts removed.
[b] Location of critical web plate stress at the top of the connection plate weld before retrofit.
[c] Location of critical web plate stress at the top of the connection plate weld after retrofit.
[n] Weld stress on north side of the connection plate.
[s] Weld stress on south side of the connection plate.

and 6 in. slotted retrofits with all bolts in place for the 3-axle test truck appear in Figures 101 and 102, respectively. These figures display the critical locations of the web plate used for stress analysis and are further discussed later in this section. All stresses and stress ranges mentioned in this chapter were measured on the north side of the stiffener-connection plate assembly, except the weld stresses and stress ranges extrapolated from connection plate gages. The stresses listed in the columns "Outside Web-Flange Weld" and "Inside Web-Flange Weld" were determined by extrapolation of measured stresses on the inside and outside faces of the web to the toe of the web-flange weld, as discussed in Chapter Seven. In each table, the column that is titled "Conn. Plate Weld B.R." lists before and after retrofit stresses in the web plate at the critical location that was referred to in Chapter Seven as the top of the connection plate weld. Measured stresses were extrapolated to this critical location in the before retrofit web gap geometry. In the after retrofit web gap geometry, this position no longer has critical stress significance. However, stresses were determined at this position after retrofit to illustrate that the stress conditions in this upper web plate region changed from tension to compression.

The next column in Table 21 and 22, denoted "Conn. Plate Weld A.R.", gives the web plate stresses extrapolated to the new, after retrofit, top of the connection plate to web weld, which is in a critical stress region. The extrapolation was performed using stresses measured by the gages numbered 1 and 2 (denoted NM1 and NM2 in Figures 27 and 28 of Chapter Five) above the top of the connection plate weld in Figures 101 and 102. The column labeled "Side of Conn. Plate Weld" lists horizontal web plate stresses extrapolated from horizontally mounted gages numbered 3 and 4 in Figures 101 and 102 (illustrated in

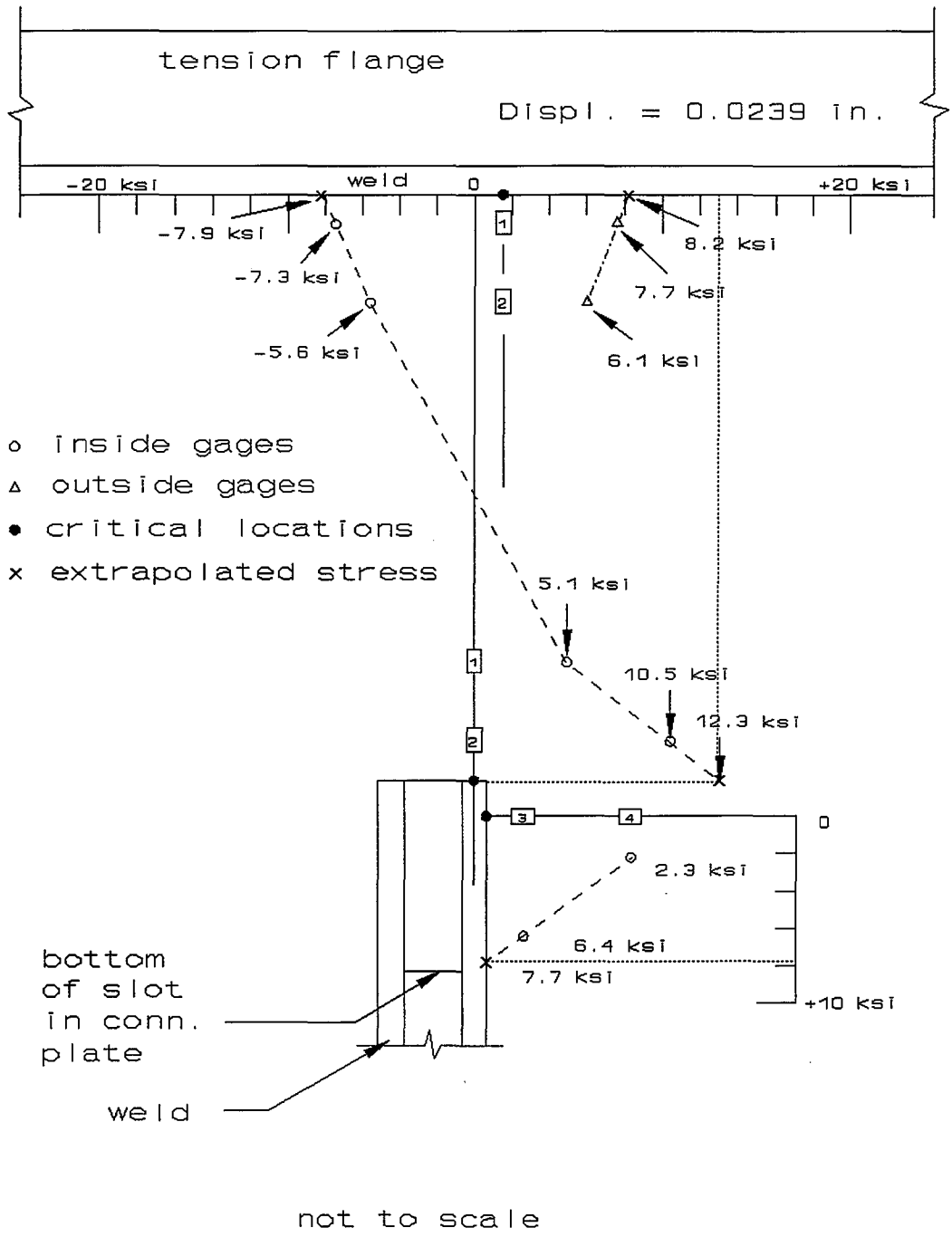

Figure 101. Static Stress Distribution at the 10 Inch Slotted Connection with 3-Axle Test Truck in Outside Lane

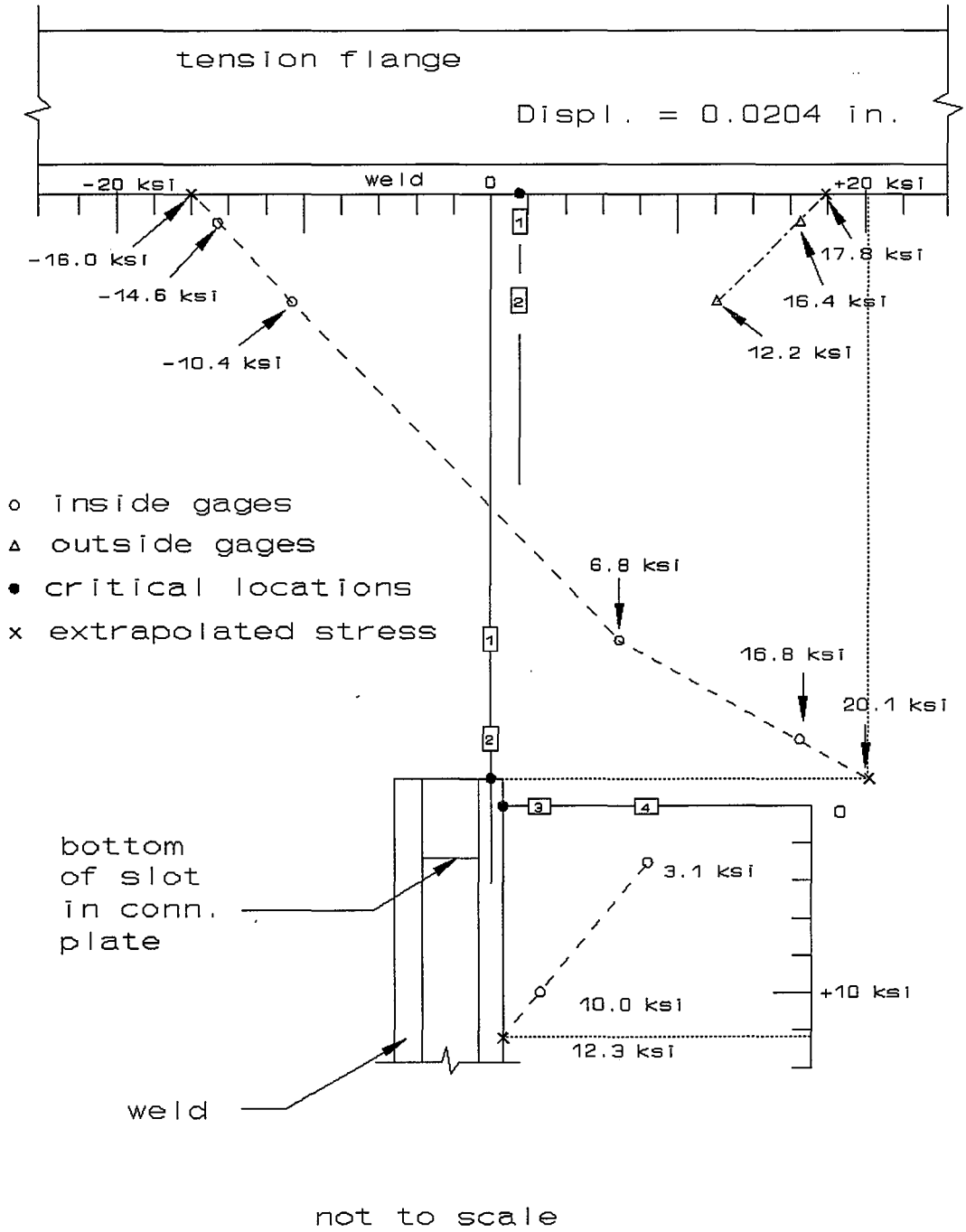

Figure 102. Static Stress Distribution at the 6 Inch Slotted Connection with 3-Axle Test Truck in Outside Lane

Chapter Five, Figures 27 and 28, gages NM3 and NM4) to the side of the fillet weld near the top of the weld. The two horizontally mounted gages were mounted a short distance below the point at the top of the fillet weld where the fillet weld size was not reduced by grinding. This point was also a short distance above the end of the slot radius in the connection plate. The column titled "Weld Stress" lists connection plate to web fillet weld stresses as determined from connection plate stresses through methods discussed in Chapter Seven for the before retrofit condition and in the previous section of this chapter for the after retrofit condition.

It is noted from Table 21 that the 10 in. slotted connection experienced the maximum stresses for each test truck while the truck was located in the slow lane (lane B). The out-of-plane displacements measured near the top of the connection plate also followed that pattern. The overall maximum stresses and displacements were created by the 3-axle test truck in the slow lane. From inspection of Table 22 it is noted that at the 6 in. slotted connection, the 5-axle test truck in the fast lane (lane C) produced greater stresses and displacements than the 5-axle test truck in the slow lane. This deviation from the pattern of slow lane loadings creating the largest stresses and displacements is believed to be the result of differential vertical displacement between the two main girders, as discussed below.

When the middle axle of the 5-axle test truck was positioned above the first floortruss south of pier S3-11, which was the loading position for the stresses in Table 21, the rear tandem of the test truck was on the opposite side of the pier from the test location. Hence, a large percentage of the total truck weight was transferred directly to the floortruss over the pier and then to the pier support. This loading would produce very little main girder

deflection, and the effects of differential girder displacements would be minimal. With the middle axle of the 5-axle truck positioned above the second floortruss north of pier S3-4, which was the case for the measurements in Table 22, the rear tandem of the five axle truck was near midspan for the main girders in the span being tested. This would produce significant main girder displacements with the truck in either traffic lane. With the test truck in the fast lane, the outside girder would deflect downward more than the inside girder. This differential displacement would tend to pull the connection plate at the outside girder inward. This inward displacement and associated stresses would be additive to the effects of the truck loading directly over the floortruss.

The response at the 6 in. slotted connection to the 3-axle truck static loadings was similar to that just discussed for the 5-axle truck, except the stress at the inside web-flange weld and displacement from the fast lane loading slightly exceeded those from the slow lane loading for the before retrofit status. Stresses and displacements at several other critical locations from fast lane 3-axle truck loading approached the stresses and displacements from the slow lane loading, but did not exceed them. In spite of these few exceptions, the 3-axle truck in the slow lane was still considered to be the overall worst case loading that the bridges were subjected to during the field tests. The fact that more stresses and displacements for the fast lane 3-axle truck static loading did not exceed the slow lane 3-axle truck static loading, like for the 5-axle test truck static loadings at this location, was due to the differences in truck lengths and axle spacings. Since the 3-axle truck was very short, it would create much less vertical deflection of the main girders when parked over the floortruss at the 6 in. slotted connection plate location than the 5-axle truck. Hence, the

effects of the differential vertical displacement between the main girders was not as significant for this static loading case.

Since the 3-axle truck in the slow lane above the floortruss for the connection being tested was determined to produce the overall maximum web gap stresses for test trucks, the web plate static stress distributions for this load case are presented. These distributions were presented in Figure 101 and 102 for the connections with the 10 in. slot and 6 in. slot, respectively, with all bolts in the connection plate. The dimensions of the lengthened web gaps with the 10 in. and 6 in. slot appear in Figures 27 and 28 of Chapter Five. In Figures 101 and 102, the dashed line drawn in the lengthened web gap from the top two vertically mounted inside gage positions (centered 1 in. north of the connection plate face) to the bottom two vertically mounted inside gage positions (centered along the north side connection plate weld centerline) is an estimate of the vertical stress distribution along the inside face of the web. This estimated distribution illustrates the out-of-plane bending in the lengthened web gap. The actual stress distribution would probably display slightly more curvature near the ends of these lines as the stress increases approaching points of stress concentration. Also shown in Figures 101 and 102 are stresses extrapolated to the web-flange weld on the outside face of the web, and horizontal stresses extrapolated to the edge of the connection plate to web weld. All the stress magnitudes and distributions for these connections after the top bolts were removed were almost exactly the same as with all bolts in the connection plate. Therefore, stress distributions for loading cases with the bolts removed were not included here.

The change in results at critical locations due to the retrofit was of major interest to the research. The percentage changes in stresses and displacements for the static tests appear in Tables 23 and 24. Looking at Table 23, a stress reduction exceeding 75 percent for the web plate at the outside web-flange weld, 73 percent for the web plate at the inside web-flange weld, and 64 percent for the weld stress was noted for the connection with the 10 in. slot. The web plate stress for the before retrofit top of the connection plate to web weld position changed from tension before retrofit to compression after retrofit and experienced an 18 to 32 percent reduction in magnitude. The loosening retrofit elevated the out-of-plane displacements to roughly 200 percent greater than the before retrofit static displacements for the 10 in. slotted connection.

The only stress that showed an apparent increase as a result of the retrofits was the stress at the top of the connection plate to web weld where increases of up to 79 percent are shown in Table 23. However, these increases resulted from calculating the percentage change between stresses at two different points since the web gap geometry changed. The positions of the strain gages used to determine the stresses at these critical points also changed, which contributed significantly to these apparent increases. Before the retrofit, the stresses at the top of the connection plate to web weld were determined by extrapolation using strain gage measurements taken along a line 1 in. from the north side of the connection plate (see Figures 27 and 28 of Chapter Five for geometry). This approach tends to underestimate the actual maximum stress of interest, possibly by as much as a factor of 2 or 3 (Fisher et al. 1990). After the retrofit, the stresses were determined by extrapolation of measurements taken along a line that matched the centerline of the weld. This method

Table 23. Percentage Change[a] of Static Stresses and Displacements at Critical Locations After Retrofit at the 10 Inch Slotted Connection with Trucks Directly Above Floortruss

Truck	Lane	Retrofit Status[b]	Outside Web-Flange Weld (%)	Inside Web-Flange Weld (%)	Conn. Plate Weld A.R.[c] (%)	Weld Stress (%)	Displ. Near Top of Conn. Pl. (%)
5-Axle	Slow	Slot	-75	-73	+59	-65	+228
5-Axle	Slow	Bolts	-75	-73	+63	-64	+233
5-Axle	Fast	Slot	-75	-73	+79	-74	+244
5-Axle	Fast	Bolts	-75	-73	+79	-74	+216
3-Axle	Slow	Slot	-78	-76	+60	-69	+185
3-Axle	Slow	Bolts	-78	-76	+73	-69	+189
3-Axle	Fast	Slot	-77	-75	+70	-76	+185
3-Axle	Fast	Bolts	-77	-76	+70	-76	+185

[a] Negative values indicate a decrease, positive values indicate an increase.
[b] Slot = comparison with slotted retrofit to before retrofit; Bolts = comparison with slotted retrofit and bolts removed to before retrofit.
[c] Comparison of critical web plate stress at the top of the connection plate weld after retrofit comparing to stress at critical location before retrofit.

Table 24. Percentage Change[a] of Static Stresses and Displacements at Critical Locations After Retrofit at the 6 Inch Slotted Connection with Trucks Directly Above Floortruss

Truck	Lane	Retrofit Status[b]	Outside Web-Flange Weld (%)	Inside Web-Flange Weld (%)	Conn. Plate Weld A.R.[c] (%)	Weld Stress (%)	Displ. Near Top of Conn. Pl. (%)
5-Axle	Slow	Slot	-27	-39	+153	-35	+183
5-Axle	Slow	Bolts	-21	-30	+163	-15	+232
5-Axle	Fast	Slot	-26	-73	+173	-31	+192
5-Axle	Fast	Bolts	-28	-73	+167	-36	+179
3-Axle	Slow	Slot	-10	-76	+200	-11	+264
3-Axle	Slow	Bolts	-10	-76	+196	-2	+273
3-Axle	Fast	Slot	-16	-75	+210	-19	+230
3-Axle	Fast	Bolts	-18	-76	+198	-25	+215

[a] Negative values indicate a decrease, positive values indicate an increase.

[b] Slot = comparison with slotted retrofit to before retrofit; Bolts = comparison with slotted retrofit and bolts removed to before retrofit.

[c] Comparison of critical web plate stress at the top of the connection plate weld after retrofit comparing to stress at critical location before retrofit.

provides a much better estimate of the actual maximum stress. Because of the difference between the gage locations used to determine the stresses at the end of the connection plate to web weld, it is possible that the maximum stress at the top of the connection plate before retrofit was underestimated and therefore, the percent change could have actually decreased. This is contrary to the percentages shown in Table 23.

In Table 24 for the 6 in. slot at the pier S3-4 connection, the stress reduction was 10 to 20 percent for the web plate at the outside web-flange weld, 21 to 39 percent for the web plate at the inside web-flange weld, and 2 to 36 percent for the weld stress. The web plate stress for the top of the connection plate to web weld position changed from tension before retrofit to compression after retrofit, but experienced stresses 2 to 43 percent higher than before retrofit. The out-of-plane displacements at this connection were roughly equal to those measured at the pier S3-11 connection, which was about 200 percent greater than the before retrofit displacements.

Based on the static test results, the 10 in. slot at the pier S3-11 connection outperformed the 6 in. slot at the pier S3-4 connection. The 10 in. slot produced much greater stress reductions than the 6 in. slot for relatively the same increase in out-of-plane displacements. The test results indicated that removing bolts from the connection did not have a significant effect on the stresses or displacements at either connection. Although the retrofits were performed at two different girder depths and floortruss positions, the comparisons of the changes in stresses at the two connections before and after retrofit appear reasonable. The pier S3-4 connection experienced lower static stress magnitudes than the pier S3-11 connection before retrofit, yet after retrofit, the initially higher magnitude stresses

at 10 in. slot location were reduced to magnitudes less than the stresses at the 6 in. slot location after retrofit. In view of this fact, the comparisons between these two slot lengths and locations were reasonable.

EFFECTIVE STRESS RANGES FROM TRUCK TRAFFIC

The severity of the fatigue loading and effectiveness of the retrofits at the floortruss-girder connections can be evaluated from the effective stress ranges at critical locations resulting from random truck traffic. The stress ranges for random trucks at the critical locations (in the connection plate to web weld and in the web plate as shown in Figures 101 and 102) were determined through linear extrapolation as described in Chapter Seven. The extrapolated stress ranges were then used to calculate Miner's effective stress ranges, Sre's, for the critical locations. The results of the effective stress range calculations are presented in Table 25 along with the maximum single stress range, Sr, recorded at each test connection. The signs on the stress ranges are shown as positive for locations where the stress was primarily tensile and negative where the stress was primarily compressive. Due to limits on time and on the number of data channels that could be recorded simultaneously, only a small number of truck crossings were available for calculating effective stress ranges in the connection plate weld. Hence, those values in Table 25 are not as accurate as other values in the table, but they are a reasonable indicator of the stress levels in the welds.

Table 26 lists the percentage changes in effective stress ranges resulting from the slotted retrofit trial configurations. The 10 in. slot location effective stress ranges were reduced by at least 71 percent at the outside web-flange weld, 66 percent at the inside web-

Table 25. Effective Stress Ranges at Critical Locations for Random Truck Data Before and After Retrofit

Retrofit Status[a]	Outside Web-[b] Flange Weld Sre (ksi)	Inside Web-[b] Flange Weld Sre (ksi)	Conn. Plate[b] Weld B.R.[d] Sre (ksi)	Conn. Plate[b] Weld A.R.[e] Sre (ksi)	Side of Conn.[b] Plate Weld Sre (ksi)	Weld Stress B.R.& A.R. Sre (ksi)
10 Inch Slot: Pier S3-11, First Floortruss South, Outside Girder (106" Web)						
Before	+22 (+38*)	-19 (-33*)	+5.2 (+8.6*)	---- (----*)	---- (----*)	+8.7[n] (+14*)[c]
Slot	+6.4 (+14*)	-6.5 (-13*)	-4.4 (-9.1*)	+9.4 (+20*)	+6.0 (+13*)	+3.0[s] (+6.1*)[b]
Bolts	+6.4 (+13*)	-6.0 (-12*)	-4.1 (-8.0*)	+9.5 (+19*)	+6.0 (+12*)	+2.8[s] (+5.4*)[b]
6 Inch Slot: Pier S3-4, Second Floortruss North, Outside Girder (126" Web)						
Before	+13 (+22*)	-13 (-22*)	+4.4 (+7.6*)	---- (----*)	---- (----*)	+5.3[n] (+9.1*)[c]
Slot	+11 (+20*)	-9.8 (-18*)	-5.3 (-10*)	+12 (+22*)	+7.5 (+14*)	+5.3[s] (+10*)[b]
Bolts	+12 (+28*)	-11 (-25*)	-6.1 (-13*)	+14 (+32*)	+8.6 (+20*)	+5.8[s] (+12*)[b]

(*) Maximum recorded single stress range, Sr, for a random data file.

[a] Slot = with slot in connection plate; Bolts = after slotted retrofit with the top connection plate bolts removed.

Stress ranges calculated from sampled trucks totalling: [b] 250, [c] 50.

[d] Location of critical web plate stress at the top of the connection plate weld before retrofit.

[e] Location of critical web plate stress at the top of the connection plate weld after retrofit.

[n] Weld stress on north side of the connection plate.

[s] Weld stress on south side of the connection plate.

Table 26. Percentage Change[a] of Effective Stress Ranges at Critical Locations After Retrofit for Random Truck Data at the 10 and 6 Inch Slot Locations

Retrofit Status[b]	Outside Web-Flange Weld (%)	Inside Web-Flange Weld (%)	Conn. Plate Weld A.R.[c] (%)	Weld Stress (%)
10 Inch Slot: Pier S3-11, First Floortruss South, Outside Girder (106" Web)				
Slot	-71	-66	+81	-66
Bolts	-71	-68	+83	-68
6 Inch Slot: Pier S3-4, Second Floortruss North, Outside Girder (126" Web)				
Slot	-15	-25	+173	0
Bolts	-8	-15	+218	+9

[a] Negative values indicate a decrease, positive values indicate an increase.
[b] Slot = comparison with slotted retrofit to before retrofit; Bolts = comparison with slotted retrofit and bolts removed to before retrofit.
[c] Comparison of critical web plate stress at the top of the connection plate weld after retrofit comparing to stress at critical location before retrofit.

flange weld, and 66 percent for the weld stress. However, as shown in Table 25, the maximum single web plate stress range at the top of the 10 in. slotted connection plate weld was not below the previously defined fatigue limit of 10 ksi for the web plate. The maximum weld stress at the 10 in. slot location was reduced almost to the 6 ksi fatigue limit.

The weld stress effective stress range either equalled or exceeded the before retrofit magnitudes at the 6 in. slot location. As a result of the two retrofits at the 6 in. slot location, the reduction in effective stress range varied from 8 to 15 percent for the web plate at the outside web-flange weld and from 15 to 25 percent at the inside web-flange weld.

The effective stress ranges determined after retrofit represented somewhat less stress reduction than was noted for the static test truck results. This difference was due, in part, to the variation of random truck weights and axle spacings in the 250 trucks sampled during each respective test configuration. Still, the 10 in. slot outperformed the 6 in. slot through greater stress reductions relative to before retrofit stresses and, again, by producing overall after retrofit stress magnitudes that were lower than at the 6 in. slot, as seen in Table 25.

At the 10 in. slot location, the removal of the top three connection plate bolts produced equal or lower measured effective stress ranges than the fully bolted retrofitted connection, and hence greater apparent stress reductions. This was accomplished with relatively little increase in the out-of-plane displacements between the two trial retrofits tested at this connection. The removal of the top two connection plate bolts at the 6 in. slot location after retrofit produced greater measured effective stress ranges and maximum single stress ranges than with the connection plate fully bolted after retrofit. At the 6 in. slot location, a much greater variation in the effective stress range magnitudes at critical locations

between bolted and unbolted retrofit configurations was noted than at the 10 in. slot location. However, at both connections the noted stress range differences could be attributed to the variations in the test populations. In a later section, fast run test truck results are used to determine whether these noted differences are indicators of behavior changes, or if the differences represent primarily apparent changes due to the differences in the population of random trucks sampled for each retrofit study.

Stress Range Histograms

Stress ranges in the web plate at the outside web-flange weld toe of the 10 in. slotted connection produced by random truck crossings with the connection plate fully bolted appear in Figure 103 for the before retrofit status and Figure 104 for the after retrofit status. Similarly, the stress ranges at the web-flange weld toe of the 6 in. slotted connection appear in Figures 105 and 106 for the before and retrofit statuses, respectively. The superior performance of the 10 in. slot compared to the 6 in. slot is readily evident from these figures. Two locations that became significant in the after retrofit web gap geometry, the web plate at the top of the connection plate to web weld and the web plate at the side of that weld, experienced stress ranges for the 10 in. slot location that were lower than for the 6 in. slot location. Figures 107 through 110 display the random truck stress ranges for these critical locations for both slotted connections. The effective stress ranges calculated for these two critical locations (Table 25) also show lower magnitudes for the 10 in. slot than for the 6 in. slot.

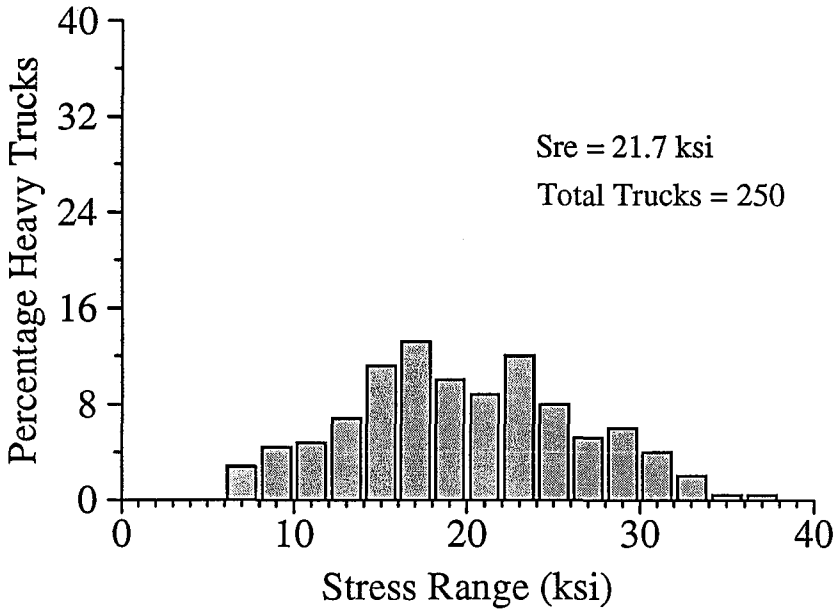

Figure 103. Web Plate Stress Ranges at the Outside Web-Flange Weld Toe at the 10 Inch Slotted Connection Before Retrofit

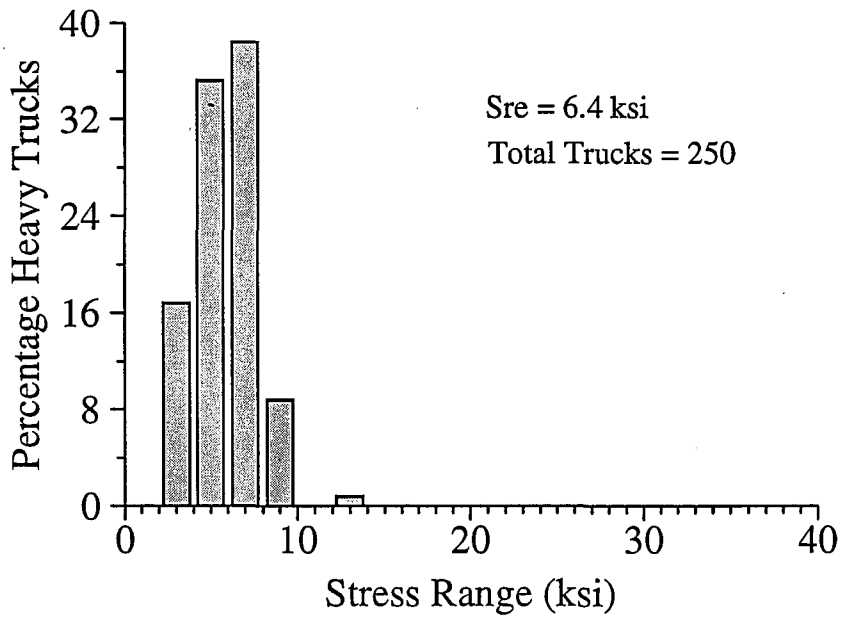

Figure 104. Web Plate Stress Ranges at the Outside Web-Flange Weld Toe at the 10 Inch Slotted Connection After Retrofit

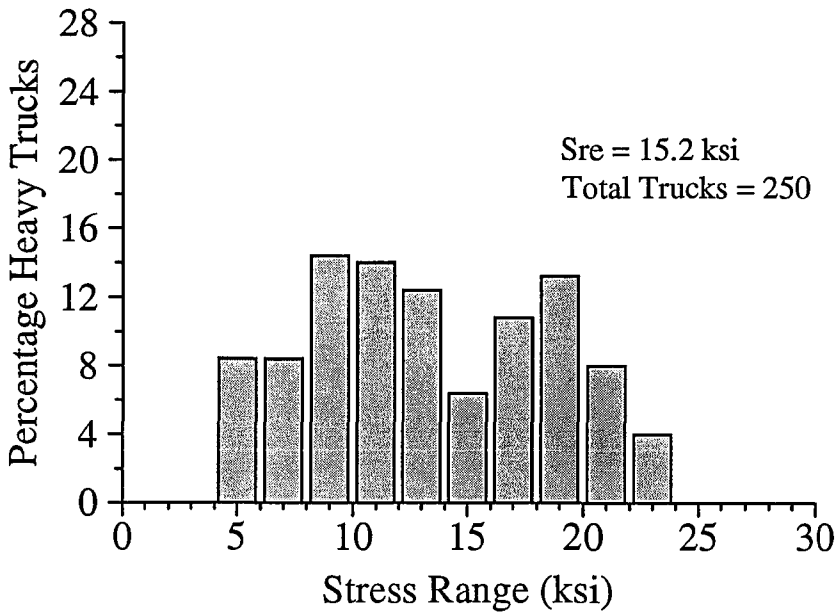

Figure 105. Web Plate Stress Ranges at the Outside Web-Flange Weld Toe at the 6 Inch Slotted Connection Before Retrofit

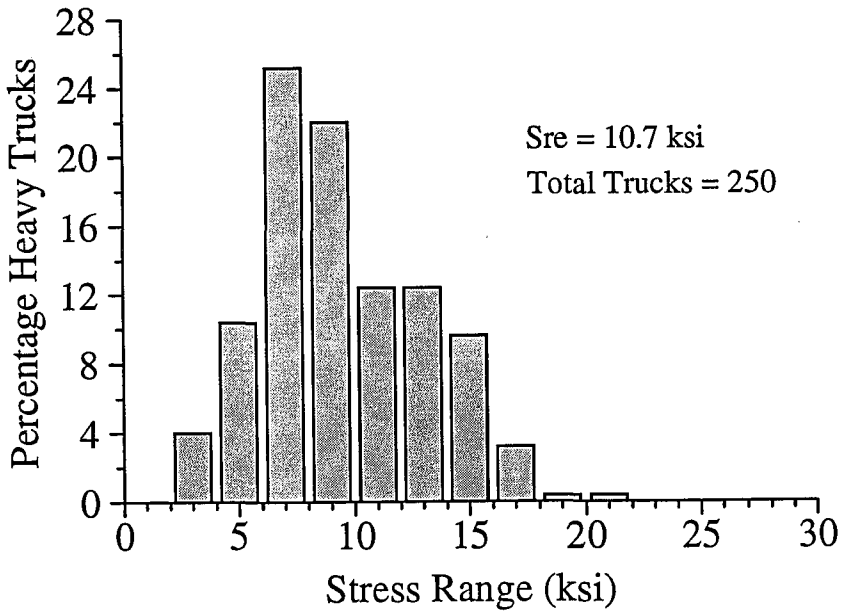

Figure 106. Web Plate Stress Ranges at the Outside Web-Flange Weld Toe at the 6 Inch Slotted Connection After Retrofit

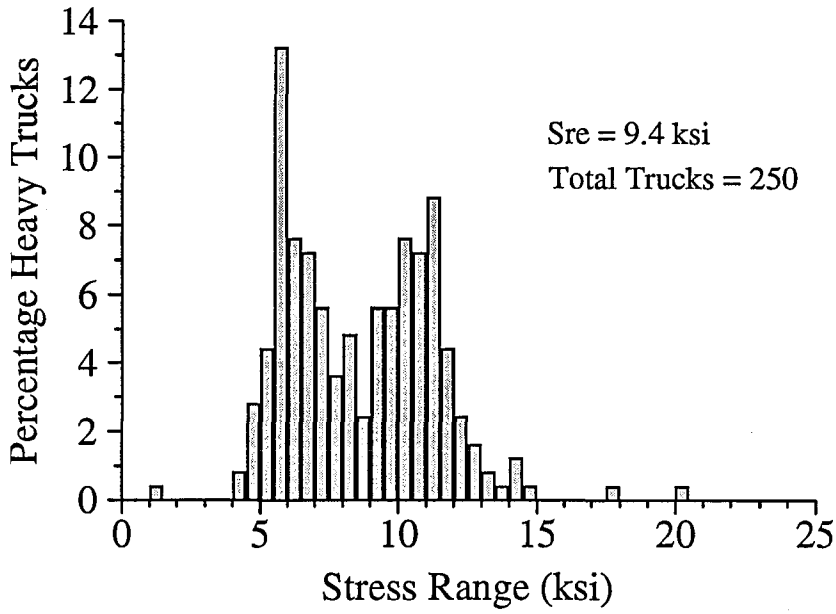

Figure 107. Web Plate Stress Ranges at the Top of the 10 Inch Slotted Connection Plate to Web Weld

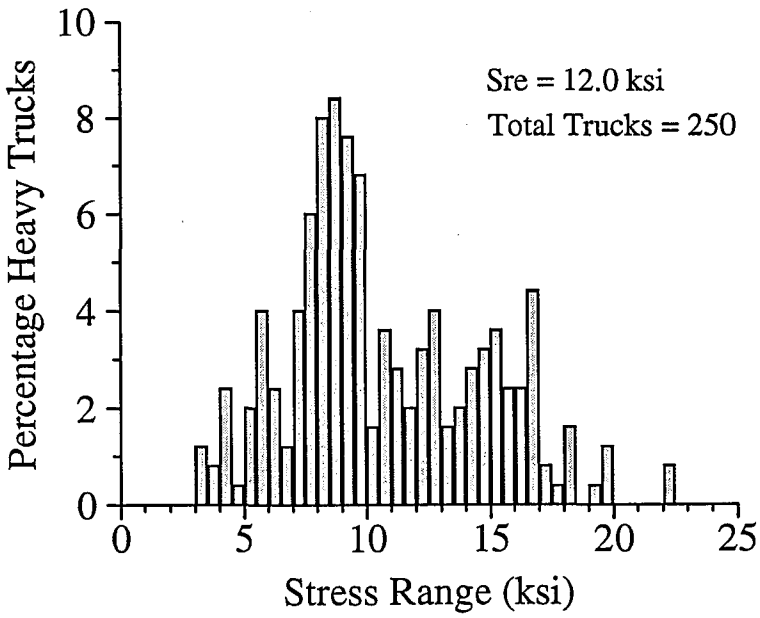

Figure 108. Web Plate Stress Ranges at the Top of the 6 Inch Slotted Connection Plate to Web Weld

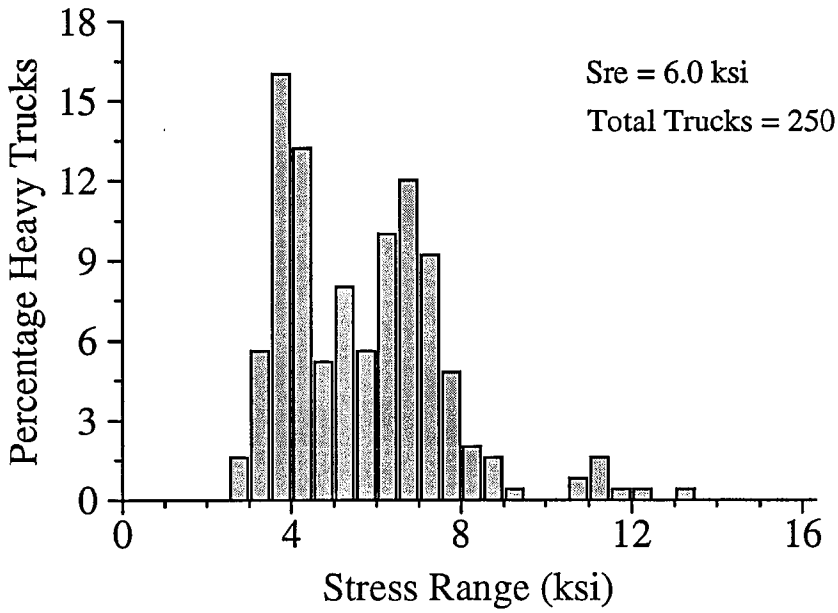

Figure 109. Web Plate Stress Ranges at the Side of the 10 Inch Slotted Connection Plate to Web Weld

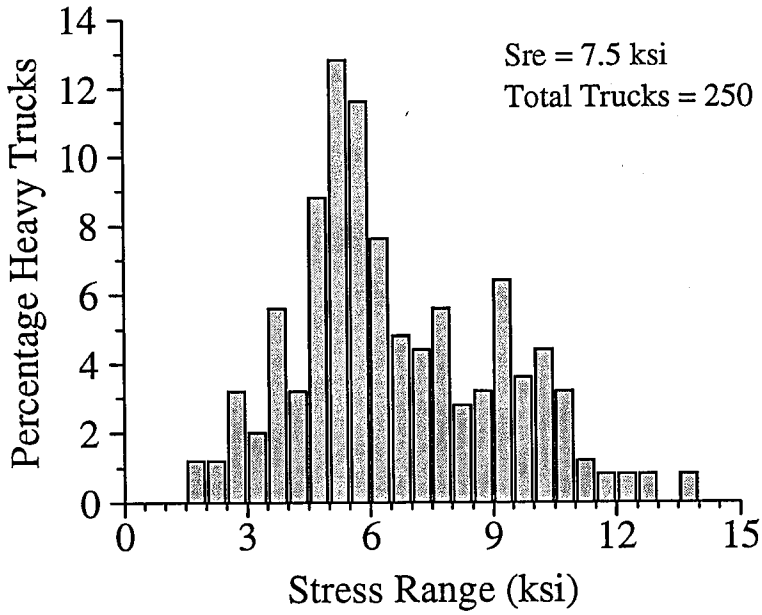

Figure 110. Web Plate Stress Ranges at the Side of the 6 Inch Slotted Connection Plate to Web Weld

Fast Run Test Truck Results at Critical Locations

The test truck fast runs were useful in providing a known loading which could be used for baseline comparisons between before and retrofit configurations and between fast runs and static runs (for determining impact effects). The fast run tests are also a tool for estimating the maximum load case that could be expected for these test locations.

The stress and displacement ranges experienced from test truck passes in the traffic lanes appear in Table 27 for the 10 in. slot location and in Table 28 for the 6 in. slot location. The percentage changes in stress and displacement ranges after the slotted retrofits were implemented appear in Table 29 and 30. Again, the 10 in. slot was found to reduce the stress ranges to a smaller magnitude than the stress ranges experienced at the 6 in. slot. The magnitudes of stress reductions were similar to those previously noted in this chapter. The results at the 10 in. slotted connection for dynamic loading (Table 27) produced stress and displacement ranges which exceeded the static loading (Table 21), as would be expected due to impact effects and some stress reversal as the test truck crossed the continuous span.

Comparison of results at the 6 in. slotted connection for dynamic and static loading (Tables 28 and 22) shows far less pronounced differences than for the 10 in. slotted connection. The static stresses at the 6 in. slotted connection were very close to the dynamic stress ranges and exceeded a few of the dynamic stress ranges before retrofit.

The weld stress range produced by test truck crossings at the 10 in. slotted connection (Table 27) was well below the 6 ksi fatigue limit, while at the 6 in. slotted connection the weld stress range (Table 28) was not below 6 ksi for any test truck crossing. The magnitudes of the displacement ranges at the 10 in. slotted connection exceed the

Table 27. Stress and Displacement Ranges at Critical Locations at the 10 Inch Slotted Connection for Test Truck Fast Runs, Before and After Retrofit

Truck	Lane	Retrofit Status[a]	Outside Web-Flange Weld Sr (ksi)	Inside Web-Flange Weld Sr (ksi)	Conn. Plate Weld B.R.[b] Sr (ksi)	Conn. Plate Weld A.R.[c] Sr (ksi)	Side of Conn. Plate Weld Sr (ksi)	Weld Stress Sr (ksi)	Displ. Near Top of Conn. Pl. (in.)
5-Axle	Slow	Before	+36	-32	+7.0	----	----	+11[n]	0.0083
5-Axle	Slow	Slot	+7.8	-7.3	-5.0	+11	+7.2	+3.9[s]	0.0224
5-Axle	Slow	Bolts	+8.5	-8.0	-5.5	+13	+8.1	+3.8[s]	0.0245
5-Axle	Fast	Before	+29	-26	+5.7	----	----	+9.0[n]	0.0067
5-Axle	Fast	Slot	+6.5	-6.3	-4.4	+9.5	+6.6	+2.6[s]	0.0193
5-Axle	Fast	Bolts	+6.7	-6.4	-4.4	+9.6	+6.5	+2.4[s]	0.0195
3-Axle	Slow	Before	+42	-37	+8.0	----	----	+12[n]	0.0096
3-Axle	Slow	Slot	+10	-9.6	-6.6	+15	+9.6	+4.6[s]	0.0294
3-Axle	Slow	Bolts	+10	-9.8	-6.7	+16	+9.9	+4.3[s]	0.0298
3-Axle	Fast	Before	+34	-30	+6.6	----	----	+11[n]	0.0079
3-Axle	Fast	Slot	+8.3	-7.9	-5.5	+12	+8.1	+3.3[s]	0.0244
3-Axle	Fast	Bolts	+8.1	-7.8	-5.4	+12	+8.0	+2.7[s]	0.0237

[a] Slot = with slot in connection plate; Bolts = after slotted retrofit and with the top three connection plate bolts removed.
[b] Location of critical web plate stress at the top of the connection plate weld before retrofit.
[c] Location of critical web plate stress at the top of the connection plate weld after retrofit.
[n] Weld stress on north side of the connection plate.
[s] Weld stress on south side of the connection plate.

Table 28. Stress and Displacement Ranges at Critical Locations at the 6 Inch Slotted Connection for Test Truck Fast Runs, Before and After Retrofit

Truck	Lane	Retrofit Status[a]	Outside Web-Flange Weld Sr (ksi)	Inside Web-Flange Weld Sr (ksi)	Conn. Plate Weld B.R.[b] Sr (ksi)	Conn. Plate Weld A.R.[c] Sr (ksi)	Side of Conn. Plate Weld Sr (ksi)	Weld Stress Sr (ksi)	Displ. Near Top of Conn. Pl. (in.)
5-Axle	Slow	Before	+17	-18	+4.8	----	----	$+6.3^{n}$	0.0048
5-Axle	Slow	Slot	+14	-13	-6.9	+15	+9.6	$+7.2^{s}$	0.0162
5-Axle	Slow	Bolts	+15	-14	-7.4	+17	+10	$+7.1^{s}$	0.0182
5-Axle	Fast	Before	+19	-20	+5.4	----	----	$+6.3^{n}$	0.0054
5-Axle	Fast	Slot	+15	-14	-7.9	+17	+11	$+6.7^{s}$	0.0181
5-Axle	Fast	Bolts	+15	-14	-7.6	+16	+11	$+6.1^{s}$	0.0184
3-Axle	Slow	Before	+24	-25	+7.0	----	----	$+8.6^{n}$	0.0068
3-Axle	Slow	Slot	+24	-22	-12	+27	+17	$+12^{s}$	0.0285
3-Axle	Slow	Bolts	+22	-20	-11	+25	+15	$+11^{s}$	0.0268
3-Axle	Fast	Before	+23	-25	+6.8	----	----	$+9.2^{n}$	0.0067
3-Axle	Fast	Slot	+18	-17	-9.4	+20	+13	$+8.3^{s}$	0.0217
3-Axle	Fast	Bolts	+22	-20	-11	+24	+16	$+9.2^{s}$	0.0267

[a] Slot = with slot in connection plate; Bolts = after slotted retrofit and with the top three connection plate bolts removed.
[b] Location of critical web plate stress at the top of the connection plate weld before retrofit.
[c] Location of critical web plate stress at the top of the connection plate weld after retrofit.
[n] Weld stress on north side of the connection plate.
[s] Weld stress on south side of the connection plate.

Table 29. Percentage Change[a] of Stress and Displacement Ranges at Critical Locations After Retrofit at the 10 Inch Slotted Connection for Test Truck Fast Runs

Truck	Lane	Retrofit Status[b]	Outside Web-Flange Weld (%)	Inside Web-Flange Weld (%)	Conn. Plate Weld A.R.[c] (%)	Weld Stress (%)	Displ. Near Top of Conn. Pl. (%)
5-Axle	Slow	Slot	-78	-77	+63	-64	+170
5-Axle	Slow	Bolts	-76	-75	+80	-65	+195
5-Axle	Fast	Slot	-78	-76	+67	-71	+188
5-Axle	Fast	Bolts	-77	-75	+68	-73	+191
3-Axle	Slow	Slot	-76	-74	+89	-61	+206
3-Axle	Slow	Bolts	-76	-74	+94	-64	+210
3-Axle	Fast	Slot	-76	-74	+80	-69	+209
3-Axle	Fast	Bolts	-76	-74	+77	-74	+200

[a] Negative values indicate a decrease, positive values indicate an increase.
[b] Slot = comparison with slotted retrofit to before retrofit; Bolts = comparison with slotted retrofit and bolts removed to before retrofit.
[c] Comparison of critical web plate stress at the top of the connection plate weld after retrofit comparing to stress at critical location before retrofit.

Table 30. Percentage Change[a] of Stress and Displacement Ranges at Critical Locations After Retrofit at the 6 Inch Slotted Connection for Test Truck Fast Runs

Truck	Lane	Retrofit Status[b]	Outside Web-Flange Weld (%)	Inside Web-Flange Weld (%)	Conn. Plate Weld A.R.[c] (%)	Weld Stress (%)	Displ. Near Top of Conn. Pl. (%)
5-Axle	Slow	Slot	-19	-29	+221	+14	+238
5-Axle	Slow	Bolts	-13	-24	+244	+13	+279
5-Axle	Fast	Slot	-19	-29	+211	+6	+235
5-Axle	Fast	Bolts	-21	-31	+200	-3	+241
3-Axle	Slow	Slot	0	-12	+290	+42	+319
3-Axle	Slow	Bolts	-8	-19	+253	+22	+294
3-Axle	Fast	Slot	-22	-32	+196	-10	+224
3-Axle	Fast	Bolts	-6	-19	+254	0	+299

[a] Negative values indicate a decrease, positive values indicate an increase.

[b] Slot = comparison with slotted retrofit to before retrofit; Bolts = comparison with slotted retrofit and bolts removed to before retrofit.

[c] Comparison of critical web plate stress at the top of the connection plate weld after retrofit comparing to stress at critical location before retrofit.

displacement ranges at the 6 in. slotted connection for all test runs, except the 3-axle truck in the inside lane after connection plate bolt removal. Yet, the 10 in. slotted connection produced much greater stress reductions than the 6 in. slotted connection. This corresponded to the fact that the percentage increases in displacement range between the before and after retrofitted configurations increased less at the 10 in. slotted connection (Table 28) than at the 6 in. slotted connection (Table 29). For the fast run tests the percentage increase in displacement ranges at the 10 in. slotted connection was between 170 and 210 percent greater than the before retrofit magnitudes. The 6 in. slotted connection experienced percentage increases between 220 and 320 percent relative to the before retrofit displacements.

In Chapter Seven it was determined that test truck stress ranges for a single pass in the traffic lanes were near the maximum recorded stress ranges for random trucks. However, the addition of stress ranges produced by a test truck pass in lane B (slow lane) with the stress ranges from the same test truck pass in lane C (fast lane) was considered to be a reasonable estimate of the maximum load case that could be expected on these bridges. The majority of trucks traveling the interstate in the bridge vicinity have a 5-axle configuration. Therefore, addition of results from loadings of the 5-axle test truck would seem to be a more probable estimate of the maximum load case than loadings of the 3-axle test truck. Side-by-side truck crossings of 3-axle trucks comparable to the test truck weight and axle spacings are possible, but not as probable.

The estimated maximum load case for side-by-side truck crossings (by adding lane B stress ranges to lane C stress ranges) at both slotted connections appears in Table 31 for each test truck. Most notable from Table 31 is the drastic reduction of the lane B+C stresses

Table 31. Stress and Displacement Ranges for Estimated Side-by-Side Test Truck Fast Runs at Critical Locations at the 10 and 6 Inch Slotted Connections with Fully Bolted Connection Plates

Truck	Lane	Outside Web-Flange Weld Sr (ksi)	Inside Web-Flange Weld Sr (ksi)	Conn. Plate Weld A.R.[a] Sr (ksi)	Side of Conn. Plate Weld Sr (ksi)	Weld Stress Sr (ksi)	Displ. Near Top of Conn. Pl. (in.)
10 Inch Slot: Pier S3-11, First Floortruss South, Outside Girder (106" Web)							
5-Axle	B	+7.8	-7.3	+11	+7.2	+3.9[s]	0.0224
5-Axle	C	+6.5	-6.3	+9.5	+6.6	+2.6[s]	0.0193
5-Axle	B+C	+14	-14	+21	+14	+6.5	0.0417
3-Axle	B	+10	-9.6	+15	+9.6	+4.6[s]	0.0294
3-Axle	C	+8.3	-7.9	+12	+8.1	+3.3[s]	0.0298
3-Axle	B+C	+18	-18	+27	+18	+7.9	0.0592
6 Inch Slot: Pier S3-4, Second Floortruss North, Outside Girder (126" Web)							
5-Axle	B	+14	-13	+15	+9.6	+7.2[s]	0.0162
5-Axle	C	+15	-14	+17	+11	+6.7[s]	0.0181
5-Axle	B+C	+29	-27	+32	+21	+14	0.0343
3-Axle	B	+24	-22	+27	+17	+12.2[s]	0.0285
3-Axle	C	+18	-17	+20	+13	+8.3[s]	0.0217
3-Axle	B+C	+42	-39	+47	+30	+21	0.0502

[a] Location of critical web plate stress at the top of the connection plate weld after retrofit.
[s] Weld stress on south side of the connection plate.

from the before retrofit levels noted in Tables 16 and 17 for the 10 in. slot location. Again the superior performance of the 10 in. slot is noted. The 10 in. slotted connection would experience stress ranges from lane B+C loading that would be less than the stress ranges at the 6 in. slotted connection for both test trucks. The lane B+C loading would produce displacement ranges at the 10 in. slotted connection which are greater than, but comparable to, the ranges at the 6 in. slotted connection. The comparison of the results in Table 31 with fatigue limits will be discussed later in the section "EFFECTIVENESS OF RETROFITS".

OUT-OF-PLANE DISPLACEMENTS

Table 32 presents the out-of-plane displacement range statistics from random trucks before and after the two retrofits were performed at each connection. The displacement range average, standard deviation, and maximum were highest for the 10 in. slotted connection for each respective test configuration. The increase in average displacement range magnitude due to the retrofit was 310 percent greater than the before retrofit magnitude for the 10 in. slotted connection and ranged from 330 to 360 percent greater than the before retrofit magnitude for the 6 in. slotted connection. This represented a lower relative increase in out-of-plane displacement ranges for random trucks at the 10 in. slotted connection than at the 6 in. slotted connection as a result of the retrofit, and with the 10 in. slotted connection also experiencing the greatest stress reduction. A similar result was noted for the displacements produced by the fast runs with the test trucks.

The displacement range histograms for the 10 in. slotted connection before and after retrofit with fully bolted connection plates appear in Figures 111 and 112. The before and

Table 32. Displacement Range Statistics at Test Locations Before and After Retrofit for Random Truck Data

Retrofit Status[a]	Average (in.)	Std. Dev. (in.)	Maximum (in.)
10 Inch Slot: Pier S3-11, First Floortruss South, Outside Girder			
Before	+0.0041	+0.0015	+0.0093
Slot	+0.0170	+0.0051	+0.0404
Bolts	+0.0171	+0.0051	+0.0372
6 Inch Slot: Pier S3-4, Second Floortruss North, Outside Girder			
Before	+0.0027	+0.0016	+0.0058
Slot	+0.0116	+0.0043	+0.0248
Bolts	+0.0125	+0.0046	+0.0303

[a] Slot = with slot in connection plate; Bolts = after slotted retrofit with the top connection plate bolts removed.

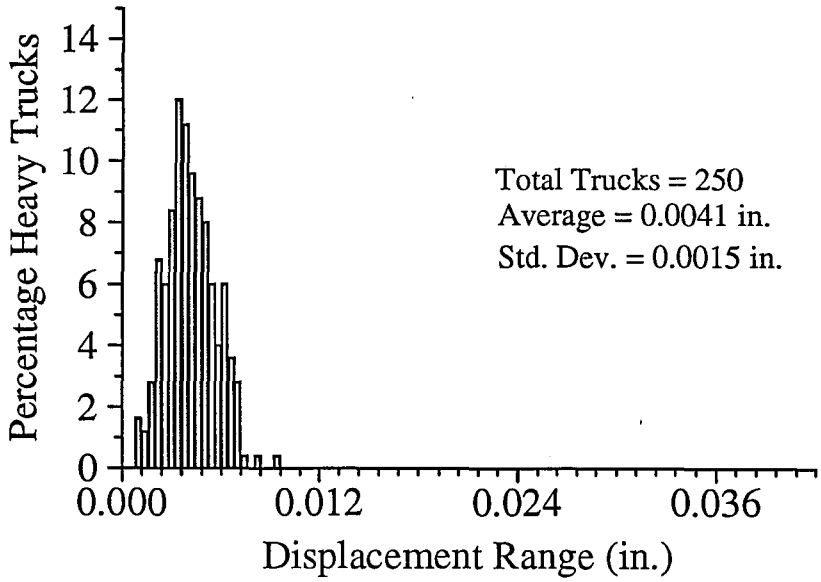

Figure 111. Out-of-Plane Displacement Ranges at the 10 Inch Slotted Connection Before Retrofit

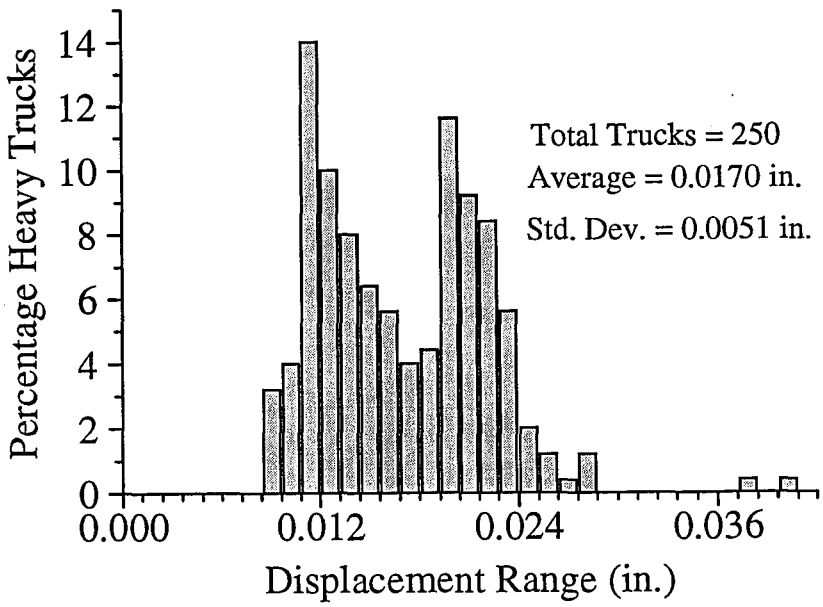

Figure 112. Out-of-Plane Displacement Ranges at the 10 Inch Slotted Connection After Retrofit

after retrofit displacement range histograms for the 6 in. slotted connection (with fully bolted connection plate) appear in Figures 113 and 114. These figures display similar displacement range increases from the before to the after retrofit configuration.

Critical Web Gap Location Stresses Versus Displacements

Plots of the stress range versus displacement range for the outside web-flange weld toe before and after the retrofit with the connection plate fully bolted appear in Figures 115 and 116 for the 10 in. slotted connection and the 6 in. slotted connection, respectively. These figures show the stress range reductions and the corresponding increases in out-of-plane displacement range after each slotted retrofit was performed. The superiority of the 10 in. slot over the 6 in. slot is evident at nearly equivalent out-of-plane displacement range magnitudes after retrofit. Plots of stress range versus displacement range for the web plate at the top and at the side of the slotted connection plate to web weld for fully bolted connection plates at the 10 in. slot and 6 in. slot connections appear in Figures 117 through 120. Table 33 illustrates through regression analyses the retrofit effects at each connection on the stress range versus displacement range relationships before and after retrofit for Figures 115 through 120. The plots for the 6 in. slotted connection show somewhat more scatter than for the 10 in. slots. Still, a high correlation was noted for all the figures. Therefore, the stress ranges and out-of-plane displacement ranges were well matched.

An important result was noted in the slopes (regression coefficients) and intercepts (regression constants) at the critical locations before and after retrofit. Before retrofit the slopes of the relationships between the stress range and displacement range at corresponding

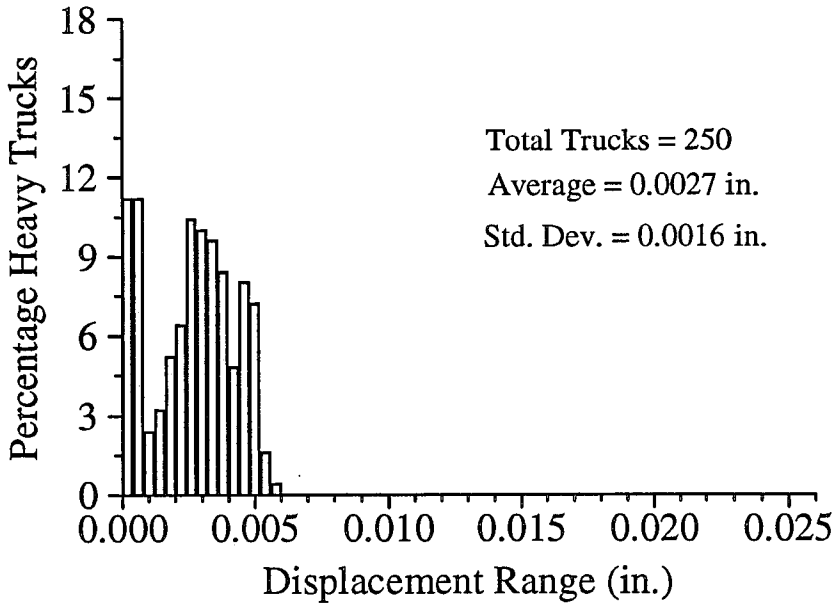

Figure 113. Out-of-Plane Displacement Ranges at the 6 Inch Slotted Connection Before Retrofit

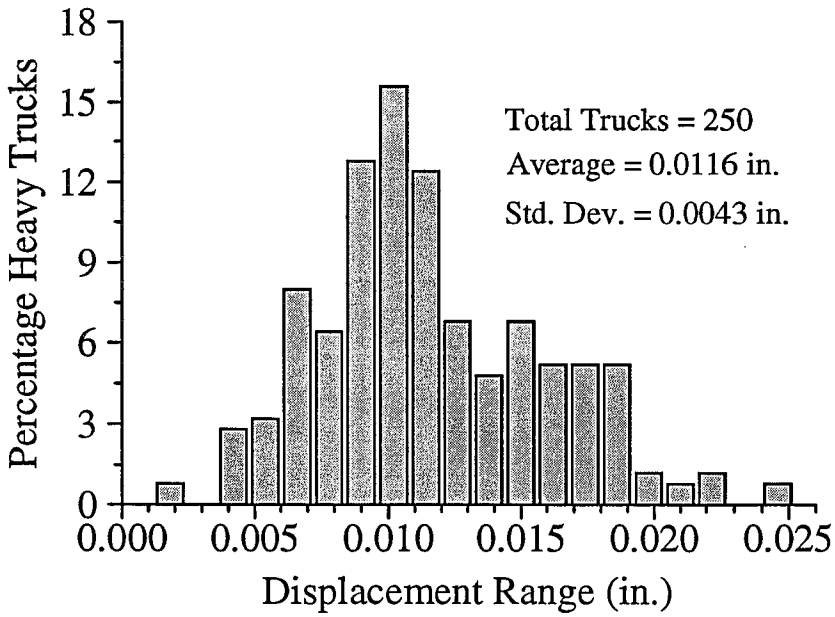

Figure 114. Out-of-Plane Displacement Ranges at the 6 Inch Slotted Connection After Retrofit

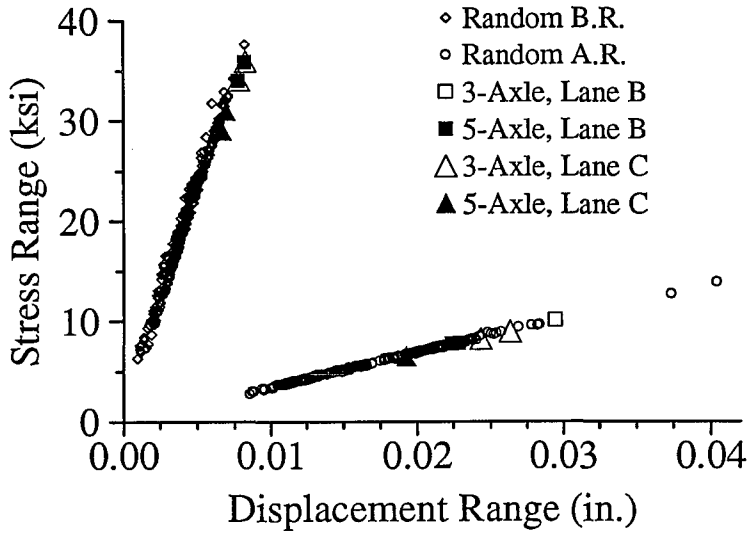

Figure 115. Web Plate Stress Range at the Outside Web-Flange Weld Toe Versus Out-of-Plane Displacement Range at the 10 Inch Slotted Connection After Retrofit

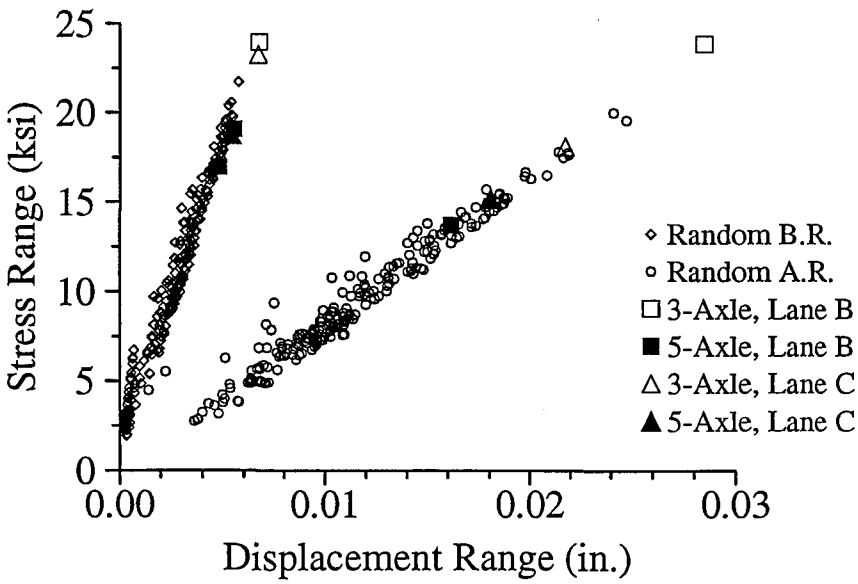

Figure 116. Web Plate Stress Range at the Ouside Web-Flange Weld Toe Versus Out-of-Plane Displacement Range at the 6 Inch Slotted Connection After Retrofit

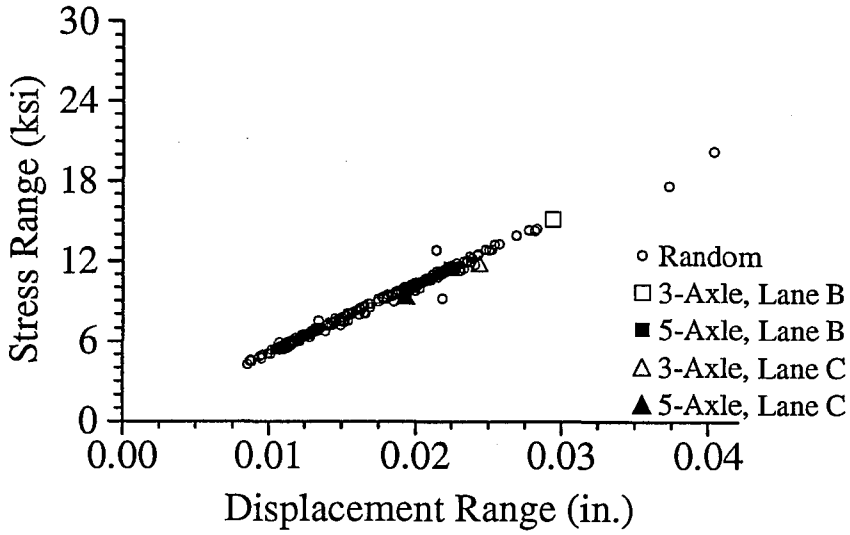

Figure 117. Web Plate Stress Range at the Top of the 10 Inch Slotted Connection Plate to Web Weld Versus Out-of-Plane Displacement Range After Retrofit

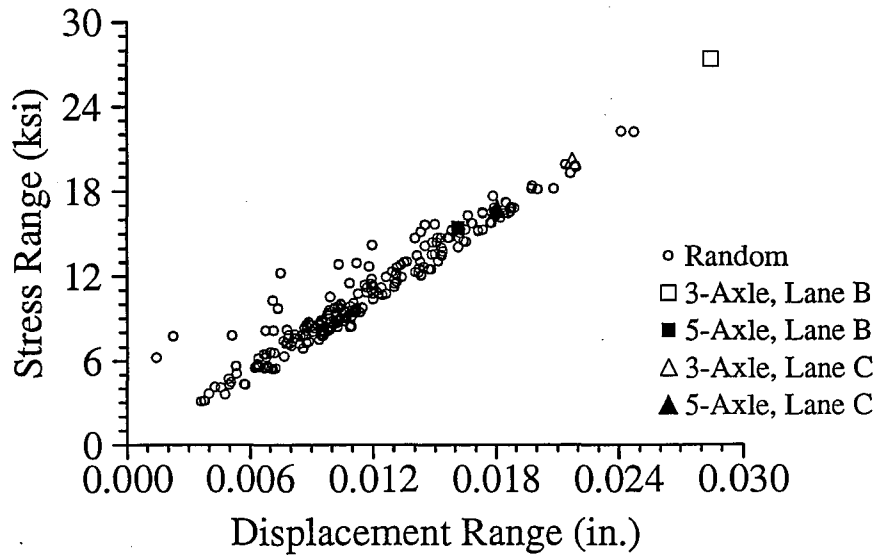

Figure 118. Web Plate Stress Range at the Top of the 6 Inch Slotted Connection Plate to Web Weld Versus Out-of-Plane Displacement Range After Retrofit

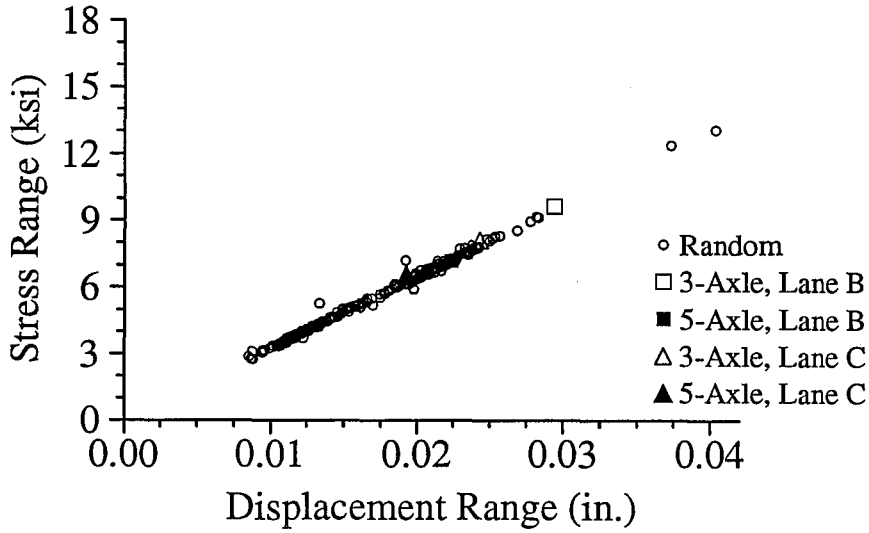

Figure 119. Web Plate Stress Range at the Side of the 10 Inch Slotted Connection Plate to Web Weld Versus Out-of-Plane Displacement Range After Retrofit

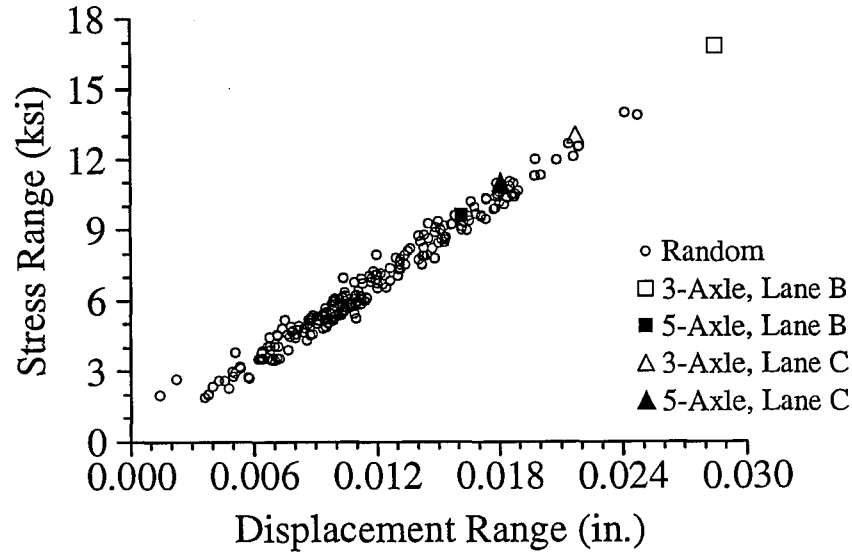

Figure 120. Web Plate Stress Range at the Top of the 6 Inch Slotted Connection Plate to Web Weld Versus Out-of-Plane Displacement Range After Retrofit

Table 33. Regression Analyses of Critical Location Stress Ranges Versus Displacement Ranges for Random Truck Data Before and After Retrofit

	Outside Web-Flange Weld			Top of Conn. Plate Weld[b]			Side of Conn. Plate Weld		
Retrofit Status[a]	Correlation Coefficient	Regression Coefficient (ksi/in.)	Regression Constant (ksi)	Correlation Coefficient	Regression Coefficient (ksi/in.)	Regression Constant (ksi)	Correlation Coefficient	Regression Coefficient (ksi/in.)	Regression Constant (ksi)
10 Inch Slot: Pier S3-11, First Floortruss South, Outside Girder (106" Web)									
Before	0.992	4430	1.6	0.975	975	0.8	------	------	------
Slot	0.999	345	0.0	0.995	504	0.1	0.997	320	0.1
6 Inch Slot: Pier S3-4, Second Floortruss North, Outside Girder (126" Web)									
Before	0.986	3280	1.9	0.921	970	1.2	------	------	------
Slot	0.979	807	0.1	0.967	887	0.4	0.988	576	-0.1

All regression statistics were obtained from data in Figures 77, 78, 85, 86, and 115 through 120.

[a] Slot = with slot in connection plate.

[b] Top of the connection plate weld before retrofit and the top of the slotted connection plate weld after retrofit.

critical locations were greater at the pier S3-11 connection than at the pier S3-4 connection. After the slotted retrofit with all connection plate bolts in place, however, the pier S3-11 connection (10 in. slot) had smaller slopes than those for the pier S3-4 connection (6 in. slot) for the corresponding critical locations. The intercepts were also lower for the 10 in. slotted connection than for the 6 in. slotted connection for all three of the relationships shown in Table 33, except for the web plate stress range at the side of the connection plate weld. For this exception the intercepts for both the 6 in. and 10 in. slotted connections were very small. Replacing the random data with the regression line as a predictor of stresses for given displacements would yield lines that, overall, have a higher y-intercept and greater slope for the 6 in. slotted connection (with the exception noted). The regression lines for the 6 in. slotted connection would not cross the corresponding lines for the 10 in. slotted connection, except for the web plate stress range at the side of the connection plate weld. For this exception the lines cross at very low stress ranges where the regression lines are subject to the greatest percent error. This suggests that, in spite of individually varying test results that may not correlate well with the regression lines, given a specific displacement range applied equally at both of these connections, the 10 in. slotted connection will be subjected to lower stress ranges at these three critical locations than the 6 in. slotted connection. This is a more generalized display of the greater success of the 10 in. slot length compared to the 6 in. slot length than comparisons of individual truck crossings.

Truss Force Components Versus Displacements

The vertical force component ranges for the end diagonal truss members were relatively unchanged by the retrofits as previously mentioned in this chapter. Plots of vertical force component range in the end diagonals versus out-of-plane displacement range appear in Figures 121 and 122 for the 10 in. and 6 in. slotted connections, respectively. Data is shown for before and after retrofit with all connection plate bolts in place. The plots were originally developed to determine whether the out-of-plane displacement was well matched to the vertical force applied to the connection by truck loading. However, as with before retrofit, the vertical force transferred to the connection was dependent on lane positions, as would be expected from an engineering statics analysis. The distributions of vertical force component ranges were relatively unchanged for both slotted connections, but the corresponding displacement ranges were greater for both slotted connections. This produced different slopes for the groups of before and after retrofit results at both connections.

Table 34 presents the statistics from the linear regression analyses performed from data in Figures 121 and 122. The vertical force and out-of-plane displacement were not well matched, but higher correlations after retrofit were noted at both connections. Once again the initially higher slope of the vertical force component range versus displacement range at the 10 in. slotted connection was reduced to below the 6 in. slotted connection results after retrofit. The y-intercept, regression constant, of the 10 in. slotted connection was also lower than the 6 in. slotted connection y-intercept. This means that lower out-of-plane displacement ranges could be expected at the 10 in. slotted connection than at the 6 in.

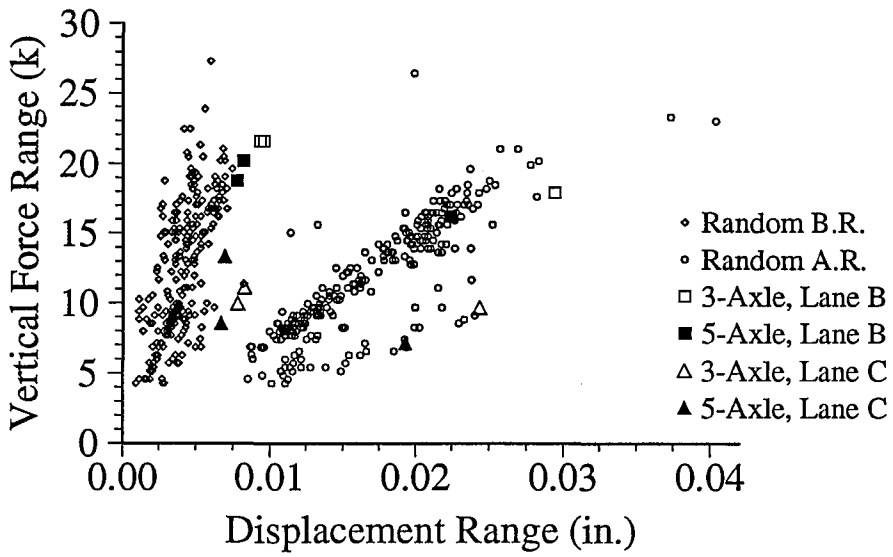

Figure 121. Vertical Force Component Range in the End Diagonal Versus Out-of-Plane Displacement Range at the 10 Inch Slotted Connection After Retrofit

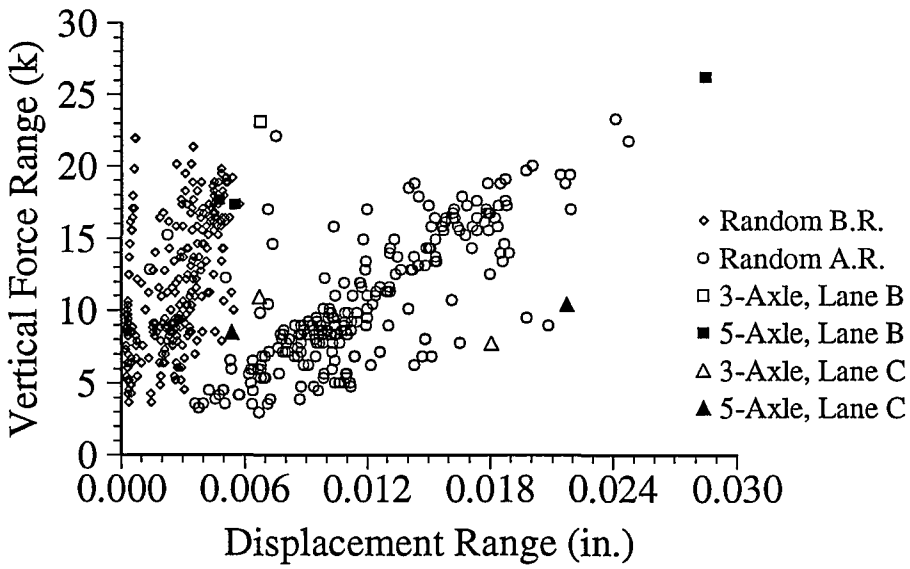

Figure 122. Vertical Force Component Range in the End Diagonal Versus Out-of-Plane Displacement Range at the 6 Inch Slotted Connection After Retrofit

Table 34. Regression Analyses of Vertical Force Ranges in End Diagonals Versus Displacement Ranges for Random Truck Data Before and After Retrofit

Vertical Force Ranges in End Diagonals		
Correlation Coefficient	Regression Coefficient (ksi/in.)	Regression Constant (ksi)
Pier S3-11: First Floortruss South, Outside Girder Before Retrofit		
0.660	2150	3.7
10 Inch Slotted Connection with Fully Bolted Connection Plate		
0.844	696	-0.0
Pier S3-4: Second Floortruss North, Outside Girder Before Retrofit		
0.542	1570	7.7
6 Inch Slotted Conection with Fully Bolted Connection Plate		
0.767	799	1.1

All regression statistics were obtained from Figures 90, 94, 121, and 122.

slotted connection from the same specified diagonal force ranges applied at these connections.

EFFECTIVENESS OF RETROFITS

An evaluation of the effectiveness of the retrofits requires a set of criteria or fatigue limits for comparison with fatigue stresses after the retrofit. Unfortunately, clear criteria are not available. For use in this report, fatigue limits at critical locations were estimated. A discussion of background information used to estimate fatigue limits follows.

Of all the solid-web floorbeam to girder connections for which comprehensive test information is available, only two projects employed use of a lengthened web gap retrofit. One investigation was field testing performed by Koob et al. (1985). The other lengthened web gap investigation involved laboratory studies performed by Fisher et al. (1990).

Koob et al. (1985) performed a number of loosening retrofits on a bridge complex in East St. Louis, Illinois at floorbeam-girder connections in which the entire upper connection plate and knee brace portion of the connection were removed. The results after retrofit included elevated stresses in the web gap at the web-flange weld toe and at the weld radius transition (top of connection plate weld after retrofit) due to stress concentrations. The maximum recorded stress ranges in that project after retrofit were 13.5 ksi at the web-flange weld toe and 19.8 ksi at the ground weld radius transition. The stress at the ground weld radius transition was the highest overall stress at each connection tested after retrofit. The lengthened web gap retrofits performed during that project were judged by Koob to be successful.

Koob also noted the maximum recorded out-of-plane displacement at a single floorbeam-girder connection was 0.050 in. after the lengthened web gap retrofits were performed during that project. It should be stressed that the out-of-plane displacements recorded after retrofit in Koob's tests were taken with the displacement monitoring device mounted at the ground weld radius transition. The LVDTs for the floortruss connections tested in this project were mounted near the top of the connection plate at the same point for before and after retrofit, since the entire connection plate was not removed during the retrofit. The LVDTs were mounted at the same point before and after retrofit so that a direct comparison of the displacements before and after retrofit could be made. The displacements measured in this project included the out-of-plane displacements of the girder web and any plate bending of the loosened, retrofitted connection plate.

Fisher et al. (1990) found a lengthened web gap retrofit to be successful in reducing crack growth rate in steel girders tested in the laboratory. As discussed in Chapter Seven, Fisher's results for un-retrofitted connections indicated that 10 ksi and 15 ksi were appropriate fatigue limits for the web plate at the end of the connection plate weld and at the web-flange weld toe, respectively. In evaluating the effectiveness of the slotted retrofit, the fatigue limit of 10 ksi will be used for comparison with the horizontal stress extrapolated to the side of the connection plate weld. The fatigue limit of 15 ksi will be used for stress ranges at the web-flange weld toe. Also as discussed in Chapter Seven, the AASHTO allowable fatigue stress range on the throat of the transversely loaded fillet welds between the connection plate and girder web will be used. That allowable stress range is 6 ksi.

The appropriate choice for a fatigue limit of stress ranges in the girder web at the top of the connection plate to web weld after slotted retrofit is the most difficult fatigue limit to establish. A slotted connection plate geometry of the type chosen for retrofit during this project had never been previously tested. The slotted connection geometry is unique, especially in the slotted connection plate weld transition. Qualitatively, the relative smoothness of the weld transition after the retrofit is predicted to be superior to the before retrofit geometry of the connection plate weld.

Hence, a fatigue limit between 10 and 15 ksi was estimated to be reasonable to use for the web plate fatigue stress range in the vertical direction at the top of the slotted connection plate to web weld. This range suggests that the fatigue performance at this critical location is better than at the original condition at the end of the weld, but no better than at the toe of the web-flange weld. The actual fatigue limit could even be higher. The 10 to 15 ksi range appears to be a reasonable engineering estimate, but it has not been verified by laboratory tests.

All information presented in this chapter was considered in evaluating the effectiveness of the retrofits. The fatigue limits at critical locations, the stress reductions produced by the retrofits, and the out-of-plane displacement levels after retrofit were three main points considered in the effectiveness determination.

Six Inch Slot

Overall, the 6 in. slot was judged to be ineffective. The 6 in. slot produced relatively small stress reductions and even some stress elevations at critical locations while increasing

the out-of-plane displacements to roughly 200 to 350 percent greater than (3 to 4.5 times) the original out-of-plane displacements. The percentage changes in the weld stress listed in Table 30 for the 6 in. slot show, for the most part, stress elevations in the welds which had a high potential for cracking before retrofit. The stress ranges at the top of the slotted connection plate also show a dramatic increase. However, even by considering that the before retrofit gage locations may have underestimated the actual stress ranges at the top of the connection plate weld before retrofit by a factor of 2 or 3, the stress ranges at the top of the slotted connection plate weld would still show an actual increase.

In Table 31 for the 6 in. slot, the lane B+C stress ranges for both test trucks were well above the fatigue limits for all critical locations. Some lane B+C stress ranges even approached the yield strength of the steel girder web. The 6 in. slot was judged to produce after retrofit stress levels that were too high. The large increases in out-of-plane displacement ranges with corresponding relatively small stress range reductions rendered the 6 in. slot retrofit ineffective. Use of the 6 in. slot will produce no significant benefit.

Ten Inch Slot

Overall, the 10 in. slot was judged to be effective because it will produce significant structural life improvements. However, the 10 in. slot will not eliminate the possibility of future fatigue cracking. Considering the estimated side-by-side truck loadings in Table 31, there is a possibility for future cracking. Table 31 also shows that the 10 in. slot retrofit did reduce the lane B+C stress ranges to levels that will not cause yielding of the girder web plate. This is a significant improvement from the before retrofit stress range conditions.

The 10 in. slot produced dramatic stress range reductions at critical locations while increasing the out-of-plane displacements for the test truck loadings by 170 to 210 percent more than the original out-of-plane displacements. The out-of-plane displacements were expected to rise after a lengthened web gap retrofit such as this, but there was a concern that the displacements might increase to unreasonable levels as a result of the retrofit. The increased displacements measured in the field tests are judged to be acceptable for slender floortruss-girder connections of this type. The overall maximum displacement of 0.0404 in. measured after retrofit for a truck in the normal traffic stream was less than the maximum of 0.050 in. noted by Koob et al. (1985) at floorbeam-girder type connections. However, Koob used side-by-side 5-axle trucks for loading. From Table 31 the maximum estimated displacement range for side-by-side 5-axle test truck crossings is 0.0417 in., which is still less than the maximum displacement noted by Koob. The maximum estimated displacement range for side-by-side 3-axle trucks is 0.0592 in. which is somewhat greater than the maximum value noted by Koob.

The results in Table 29 for test truck fast runs provide good comparisons of stress conditions before and after retrofit. The stress range reductions at the web-flange weld ranged from 74 to 78 percent for the inside and outside of the web plate. For simplicity, if a 75 percent stress range reduction is assumed, the remaining fatigue life of the web-flange weld detail would be increased to 64 times the fatigue life at the time of the retrofit implementation. This estimated fatigue life increase is based on the common slope parameter of 3.0 used for the stress-range-life relationships of all AASHTO fatigue life categories. The stress range reductions in the connection plate weld stress (Table 29) range from 61 to 74

percent. If a 67 percent weld stress range reduction is assumed, the connection plate weld fatigue life is estimated to increase by a factor of 27. Since the connection plate welds at floortruss-girder connections have a greater tendency for cracking than the web-flange welds, conservative considerations of improved fatigue life would be based on the weld stress range reductions.

Fatigue life for cracks includes crack initiation and propagation life. For fatigue cracks, such as those forming in these bridges, the majority of fatigue life discussion is concerned with crack initiation life. For instance if the current crack initiation life at an uncracked connection was 1 year, then a 10 in. slot would be expected to extend the initiation life to a minimum of 27 years (if all other factors remained unchanged and assuming the stress reductions noted during this project were repeatable).

Stress range reductions at any detail can improve fatigue life, but the reductions alone cannot prevent future fatigue crack formation. However, reduction of the applied stress range levels to below the fatigue limit produces a low probability of fatigue cracking. In Table 31 for the 10 in. slot, the lane B+C stress ranges at the web-flange weld (inside and outside) were slightly below the fatigue limit (15 ksi) for the 5-axle truck and slightly above the fatigue limit for the 3-axle truck. The lane B+C stress ranges for the web plate at both the top and the side of the connection plate weld exceeded the fatigue limits of 10 to 15 ksi in the vertical direction and 10 ksi in the horizontal direction, respectively. The lane B+C weld stress range exceeded the 6 ksi fatigue limit by 8 percent for the 5-axle truck and 32 percent for the 3-axle truck. The weld stress ranges on the north side welds were even smaller. Overall, the potential for cracking after the 10 in. slot implementation was not

eliminated. However, the probability of cracking was significantly reduced and the length of time required for cracking to occur was markedly increased.

Removal of Connection Plate Bolts

The removal of connection plate bolts as an extension of the lengthened web gap retrofits produced lower stresses for some specific tests. It also raised stresses for some test load cases. The test truck results were used to determine the effect of bolt removal on the slotted connection since those results were for a controlled loading. For the slot length judged to be effective, 10 in., the test truck fast runs in Table 27 are referenced here. The removal of connection plate bolts produced changes in the stress ranges at the critical locations that ranged from an 18 percent increase to an 18 percent decrease relative to those measured with all connection plate bolts in place. The majority of stress ranges at critical locations changed in a range of 6 percent increase or decrease as a result of bolt removal. One negative aspect of the removal of connection plate bolts is the increased bending effect of the connection plate about a vertical axis, as previously discussed in this chapter (Figures 98 and 100). Overall, the removal of connection plate bolts was judged to be ineffective despite producing some marginal stress reductions beyond the initial retrofit of cutting a slot in the connection plate.

CHAPTER NINE

CONCLUSIONS AND RECOMMENDATIONS

SUMMARY AND CONCLUSIONS

Determining the potential for cracking at floortruss-girder connections located away from piers of the I-65 Mobile Delta Crossing Bridges was one objective of the research that was accomplished through the field testing conducted. Stress and displacement measurements were taken at six floortruss-girder connection details located one and two floortrusses away from the pier locations at two different girder depths. Short cracks in the floortruss connection plate to girder web weld had previously been found by AHD bridge inspectors at three of the six connections tested in the research.

The field tests verified that the stress ranges occurring in the connection plate to web welds were high enough at the six connections tested to cause fatigue cracking. The field tests also revealed that all six floortruss-girder connections tested experienced distortion-induced stress ranges sufficient to cause fatigue cracking in the girder webs. Hence, based on the field test results, fatigue cracking in the connection plate to web welds and girder webs can be expected to eventually occur at a large percentage of floortruss-girder connections along the plate girder spans.

The maximum stress range measured was 58 ksi at the toe of the outside web-flange weld at a connection at the 106 in. deep plate girders. This stress range was measured for a

truck in the normal traffic stream. This measured stress range and estimates of stress ranges expected for side-by-side truck crossings made from calibration test results indicate that heavy side-by-side trucks might cause yielding of the web in the web gap at the floortruss-girder connections of the 106 in. girders.

Some significant variations in the stress conditions were found at the floortruss-girder connections tested. Overall the 106 in. deep girder connections consistently experienced more severe stress conditions than the 126 in. deep girder connections. Based on this result it is estimated that the stress conditions at the 146 in. deep girders are less severe than at these locations.

Another objective of the research was to determine effective retrofits for fatigue cracks that might occur at the floortruss-girder connections. After field tests of the floorbeam-girder connections in Volume I (Stallings et al. 1993), it was determined that a positive attachment retrofit would be an effective repair for distortion-induced fatigue cracking at the floorbeam-girder connections along the I-65 bridges. The positive attachment was made by rigidly bolting the connection plate to the girder tension flange. The rigid attachment retrofit should also be effective if implemented at the floortruss connections.

The relatively high cost of this retrofit prompted the development of a lengthened web gap retrofit which consisted primarily of cutting a slot in the connection plate. The retrofit was implemented and tested at two slot lengths, 6 in. and 10 in. The 10 in. slot retrofit was tested before and after retrofit at a connection that had weld cracks before retrofit. The 6 in. slot retrofit was tested before and after retrofit at a connection that did not have weld cracks before retrofit. In addition to cutting the slot, a variation of the repair method consisted of

removing some of the bolts from the floortruss-girder connection. The top three bolts were removed at the 10 in. slot, and the top two bolts were removed at the 6 in. slot. Both of these connections were tested after retrofitting with all the connection plate bolts in place and with the bolts removed.

The 6 in. slot retrofit was judged to be ineffective. The 6 in. slot produced only modest changes in the stress conditions with 224 to 319 percent increases in out-of-plane displacements for controlled loading tests with trucks of known weight. The removal of bolts from the connections was also found to be ineffective at both slot lengths. The removal of bolts produced both increases and decreases in stresses at various critical locations. In most cases the changes were less than 6 percent.

Overall, the 10 in. slot retrofit was judged to be successful. The 10 in. slot retrofit was effective in reducing the stress ranges at critical locations by approximately 50 to 75 percent while limiting the out-of-plane displacements to an acceptable level. The out-of-plane displacements at the 10 in. slot were found to increase by 170 to 210 percent above the before retrofit conditions for controlled loading tests. The 10 in. slot retrofit will not eliminate all possibility of fatigue cracking at the floortruss-girder connections. However, the reductions in stress ranges at the slot correspond to an increase in remaining fatigue life by factors of 27 to 64.

RECOMMENDATIONS

The field test results indicate that the distortion-induced stresses at the floortruss-girder connections are very high at the 106 in. girders. The use of a slotted retrofit similar

to the one tested in this project is recommended as a preventative maintenance measure at the floortruss-girder connections along the 106 in. girders. A slot of the type shown in Figure 15 with a total length of approximately 12 in. should be used at the floortruss-girder connections away from the piers in the negative moment regions. The slot will eliminate the possibility of yielding in the web gaps and will significantly increase the remaining fatigue life of the connections. Based on the less severe stress conditions measured at the 126 in. girders, the need for preventative measures at the 126 in. and 146 in. girders is not as great as at the 106 in. girders.

The stresses in the connection plate weld at the top of the connection plate were found to above the fatigue limit. Weld cracks of the type already found by AHD bridge inspectors can be expected in the future and will probably be common at all girder depths. As originally mentioned in the project proposal, simply grinding out the weld cracks is a viable repair. Although the repair will not be permanent, several years may pass before the weld cracks re-initiate. Considering the large distortion-induced stresses occurring at the floortruss-girder connections, the slotted connection plate retrofit is recommended instead of simply grinding out the weld cracks. This will provide a significant increase in fatigue life without significantly increasing the repair costs relative to grinding out the weld cracks.

The slotted connection plate retrofit in combination with drilling holes at the crack tips is recommended as a repair for distortion-induced web cracking at the floortruss-girder connections. For example, this combination should be used when web cracking occurs at connections where the slot was not used as a preventative measure. Although there is no

proof that this will provide a permanent repair, this method should prevent re-initiation of cracks for several years.

REFERENCES

American Association of State Highway and Transportation Officials. (1991). Interim Specifications - Bridges, Washington, D.C.

Clough, R.W. and Penzien, J. (1975). Dynamics of Structures, McGraw-Hill, Inc., New York, N.Y., 424-429.

Fisher, J.W. (1978). "Fatigue Cracking in Bridges from Out-of-Plane Displacements." Canadian Journal of Civil Engineering, 5(4), 542-556.

Fisher, J.W., Fisher, T. A., and Kostem, C.N. (1979). "Displacement Induced Fatigue Cracks." Engineering Structures, Oct: 252-7.

Fisher, J.W., Bathelemy, B.M., Mertz, D.R., and Edinger, J.A. (1980). "Fatigue Behavior of Full-Scale Welded Bridge Attachments." Transportation Research Record 227. National Research Council, Washington, D.C.

Fisher, J.W., Mertz, D.R., and Zhong, A. (1983). "Steel Bridge Members Under Variable Amplitude Long Life Fatigue Loading." Transportation Research Record 267, National Research Council, Washington, D.C.

Fisher, J.W., Yen, B.T., Wagner, D.C. (1987). "Review of Field Measurements for Distortion-Induced Fatigue Cracking in Steel Bridges." Transportation Research Record 1118, National Research Council, Washington, D.C., 49-55.

Fisher, J.W., Yen, B.T., and Wang, D., "Fatigue of Bridge Structures - A Commentary and Guide for Design, Evaluation, and Investigation of Cracking," ATLSS, Advanced Technology for Large Scale Structural Systems, Lehigh University, July 1989, 89-102.

Fisher, J.W., Jin, J., Wagner, D.C., and Yen, B.T. (1990). "Distortion Induced Cracking in Steel Bridge Members," Final Report. ATLSS No. 90-07. NCHRP No. 12-28 (6).

Galambos, C.F. and Heins, C.P. (1971). "Loading History of Highway Bridges, Comparison of Stress Range Histograms." Highway Research Record 354, 1-13.

Kachigan, S.K. (1982). Multivariate Statistical Analysis: A Conceptual Introduction, Radius Press, New York, N.Y.

Keating, P.B. and Fisher, J.W. (1986). "Evaluation of Fatigue Tests and Design Criteria on Welded Details." Transportation Research Record 286, National Research Council, Washington D.C., 6-16.

Keating, P.B. and Fisher, J.W. (1987). "Fatigue Behavior of Variable Loaded Bridge Details Near the Fatigue Limit." Transportation Research Record 1118, National Research Council, Washington, D.C., 56-64.

Koob, M.J., Frey, P.D., and Hanson, J.M. (1985). "Evaluation of Web Cracking at Floor Beam to Stiffener Connections of the Poplar Street Bridge Approaches, FAI Route 70, East St. Louis, St. Clair County, Illinois", Wiss, Janney, Elstner Associates for the Illinois Department of Transportation, Summarized in Transportation Research Record 1118 (1987).

Moses, F., Schilling, C.G., and Raju, K.S. (1987). "Fatigue Evaluation Procedures for Steel Bridges." Transportation Research Record 299, National Research Council, Washington, D.C., 25-31.

Schilling, C.G., Klippstein, K.H., Barsom, J.M., and Blake, G.T. (1978). "Fatigue of Welded Steel Bridge Members Under Variable-Amplitude Loadings." Transportation Research Record 188, National Research Council, Washington, D.C.

Stallings, J.M., Cousins, T.E., Rotto, R.K., and Reid, C.B. (1993). "Evaluation of Fatigue Cracking in I-65 Mobile Delta Crossing Bridges, Volume I: Floorbeam - Girder Connections," Final Report, Alabama Highway Department Research Project 2019-16, Highway Research Center, Auburn University, Alabama, 186 pages.

Stallings, J.M., Cousins, T.E., and Christopher, B.P. (1993). "Evaluation of Fatigue Cracking in I-65 Mobile Delta Crossing Bridges, Volume II: Filler Plate Weld Cracks," Final Report, Alabama Highway Department Research Project 2019-16, Highway Research Center, Auburn University, Alabama, 122 pages.

Technical Manual for the Megadac Series 3008AC - Release 3.2.0. (1991). Optim Corporation, Germantown, Maryland.

Yamada, K. and Albrecht, P. (1976). "Fatigue Design of Welded Bridge Details for Service Stresses." Transportation Research Record 607, National Research Council, Washington, D.C., 25-30.